THE JOURNAL
OF
CHEMICAL PHYSICS

VOLUME 17, NUMBER 8 AUGUST, 1949

Electron Deficient Compounds. II. Relative Energies of "Half-Bonds"*

R. E. RUNDLE
Department of Chemistry, Iowa State College, Ames, Iowa
(Received June 21, 1948)

It is suggested that the tendency to make use of all low energy orbitals is the underlying principle of electron-deficient bonding. Simple theoretical arguments, limited to the special case of two electrons and three orbitals, are given to show that this principle is a direct consequence of quantum-mechanical theories of valence.

Two half-bonds are shown to be of lower energy than a single bond plus an unused low energy orbital in most cases. The tendency to form half-bonds should be most important in symmetrical cases, and particularly where the electronegativities of all atoms involved are equal, e.g., the boron hydrides and H_3^+.

Certain consequences of the proposal to the fields of organo-metallic compounds, catalysis, and molecular rearrangements are pointed out. It is suggested that at low temperatures complexes may exist between molecules with excess orbitals and molecules with no unshared pairs.

IN recent papers structures of such diverse compounds as boron hydrides, trialkylaluminum dimers,[1] the tetramethylplatinum tetramer,[1,2] certain interstitial compounds,[1,3] and metallic hydrides[4] are discussed in terms of a bonding in which a non-metallic atom uses one orbital and one electron pair to form more than one interatomic link. Except in range of application the type of bonding suggested differs only in details from earlier suggestions,[5] but it is pointed out that common to all compounds in which this electron-deficient bonding occurs are a metal atom with more low energy orbitals than valence electrons combined with atoms or groups containing no unshared pairs. It has been suggested that the non-metal "overextends" the use of its orbitals in order to use effectively all the low energy orbitals of the metal.[1]

Electron-deficient bonding is not really rare in chemistry. It occurs quite generally where the above condition is fulfilled.[6] It would, therefore, be a serious fault in modern theories of valence if they were merely reconcilable with electron-deficient bonding.

In this paper it is pointed out that both the molecular orbital and Heitler-London theories of valence lead naturally to the conclusion that "normal" structures which leave low energy orbitals unused are unstable with respect to electron-deficient bonding in which all the low energy orbitals are used. The tendency to use all low energy orbitals is, in our view, the underlying principle of electron-deficient bonding.[7] Rather than

* Delivered before the Division of Phys. and Inorg. Chem. of the American Chemical Society Convention, April, 1947. Research supported in part by a grant from the Industrial Science Research Institute of the Iowa State College.

[1] R. E. Rundle, J. Am. Chem. Soc. **69**, 1327, 2075 (1947).

[2] R. E. Rundle and J. H. Sturdivant, J. Am. Chem. Soc. **69**, 1561 (1947).

[3] R. E. Rundle, Acta Crystallographica **1**, 180 (1948).

[4] R. E. Rundle, J. Am. Chem. Soc. **69**, 1719 (1947).

[5] See for example, B. Eistert, Zeits. f. physik. Chemie **B52**, 202 (1942); H. Longuet-Higgins and R. Bell, J. Chem. Soc. 250 (1943); K. Pitzer, J. Am. Chem. Soc. **67**, 1126 (1945); A. D. Walsh, J. Chem. Soc. 89 (1947); R. Mulliken, Chem. Rev. **41**, 207 (1947), and earlier works referred to in these papers. An entirely different proposal has been made by Pitzer and H. Gutowsky, J. Am. Chem. Soc. **68**, 2204 (1946).

[6] Further examples of electron-deficient bonding are discussed by H. Schlesinger and A. Burg, Chem. Rev. **31**, 1 (1942) and by S. Bauer, Chem. Rev. **31**, 43 (1942). Metals are examples of highly electron-deficient bonding, as discussed from several points of view. See Frederick Seitz, *Modern Theory of Solids* (McGraw-Hill Book Company, Inc., New York, 1940), Chapters VII–X, and L. Pauling, J. Am. Chem. Soc. **69**, 542 (1947).

[7] This principle has not been recognized. For example, predicted structures for tetramethylplatinum, and even trimethylplatinum chloride [L. C. Pauling (*The Nature of the Chemical Bond*, hereafter N.C.B., Cornell University Press., Ithaca, 1st Edition, 1939), p. 90; and E. Cox and K. Webster, Zeits. f. Krist. **90**, 561 (1935)] took no account of the fact that four normal bonds to platinum would leave two low energy platinum orbitals unused. Indeed, even after the structure was known, no immediate reason for the structure was apparent. See N.C.B., 2nd Edition (1940), p. 120.

Pitzer's suggestion (see reference 5) for the boron hydrides, though satisfactory for the lower hydrides, leaves low energy bonds orbitals unused for the higher hydrides, and hence is in

electron-deficient structures being exceptional, it is molecules of the trimethylboron type, which possess unused low energy orbitals that are exceptional. Presumably these molecules exist with apparently unused low energy orbitals only because an enhanced hyperconjugation *does* make use of the extra orbital,[8] and because polymerization through electron-deficient bonds is inhibited for steric reasons.[1]

The present discussion will be limited to the simple case in which the stability of a structure containing one normal bond and one excess orbital is compared with a structure consisting of two half-bonds (bonds containing half an electron pair, or of bond number $\frac{1}{2}$ in Pauling's nomenclature).[6] The reason for this limitation is first, one of simplicity. However, it has been shown that where the number of excess orbitals is relatively small, the resulting electron-deficient bonds can generally be discussed in terms of half-bonds.[1] This is the most localized type of electron-deficient bond and might well be expected to occur frequently. As in the case of ordinary structures, where added stability is to be gained by delocalization of bonds, or where resonance among several bond structures is a factor, localized single bonds are not sufficient to describe the system, so the picture presented below, limited to half-bonds, will sometimes be too simple for the description of electron deficient compounds, *e.g.*, the higher hydrides of boron, where the number of excess orbitals becomes relatively large.[9] We have already had to use a somewhat more complex discussion to arrive at bonds of number two-thirds in tetramethylplatinum and certain interstitial compounds.[1] In the case of metals, where the number of excess orbitals is large, the delocalization of bonds proceeds to such an extent that entirely different discussions are needed.[6]

A QUANTUM-MECHANICAL CONSIDERATION OF THE ENERGY OF HALF-BOND PAIRS

Half-bonds occur in pairs in electron-deficient (or, better, excess orbital) structures. The system, *A*—B—*A*, with one electron pair, may be thought of as resonating between the principal contributing structures I and II. This system, composed of two electrons with paired spins and three atomic orbitals, has frequently been suggested for this situation.[2,5] We shall inquire as to the relative energy of the resonating system as compared with I or II individually.

$$A\text{—B}\quad A' \quad \text{I} \qquad\qquad A\quad \text{B—}A' \quad \text{II}$$

Ignoring exchanges between A and A', and assuming equal exchanges between A and B and A' and B, a molecular orbital treatment gives the secular Eq. (1).[10] To make all the β's equal,

$$\begin{vmatrix} q_A-W & \beta & 0 \\ \beta & q_B & \beta \\ 0 & \beta & q_A-W \end{vmatrix}=0 \qquad (1)$$

the orbital which B uses in the half-bonding must be equally directed toward A and A'. This will generally require the use of a bidirectional orbital, such as a p-orbital, or a symmetrical orbital, such as an s orbital.[2] The use of an unidirectional orbital, such as a tetrahedral sp^3 orbital, would require that this orbital be directed symmetrically between A and A', and this would generally lead to poor overlap and poor binding to both A and A', although with a small bond angle, A—B—A', such binding may be possible.[9]

The solutions of Eq. (1) are

$$W=(q_A+q_B)/2\pm\sqrt{2}\beta+\Delta^2/8\sqrt{2}\beta, \qquad (2)$$

and

$$W=q_A \qquad (3)$$

where $\Delta=q_A-q_B$.

For a two-electron system, both electrons may be put in the lowest state, so that

$$W=q_A+q_B+2\sqrt{2}\beta+\Delta^2/4\sqrt{2}\beta. \qquad (4)$$

For structure I_A or II_A above,

$$W=q_A+q_B+2\beta. \qquad (5)$$

For the case that Δ is small, the resonance energy,

$$W_R=0.828\beta. \qquad (6)$$

An *HLSP*-type treatment, and various refinements of the simple treatment, have been made for H_3^+ by Hirschfelder, Eyring, and Rosen.[11] Their Wang-type treatment of the resonating system

$$\text{H—H H} \qquad\qquad \text{H H—H}$$

leads to a binding energy of about 130 kcal./mole, *versus* about 90 kcal. for the Wang treatment of H_2. This is about a 40 percent increase, in good agreement with the simple *MO* treatment above. If long bond and ionic terms

$$\overline{\text{H H H}}\ \text{III} \qquad \ddot{\text{H}}\,\text{H H}\ \text{IV} \qquad :\text{H H H}\ \text{V} \qquad \text{H H H:}\ \text{VI}$$

are included, the binding energy increases to 150 kcal./mole. In the later treatment III and IV are of more importance than V and VI, and the exchange integrals they introduce are much like the single electron exchange integrals encountered in H_2^+. The latter are

disagreement with the principle given above. Where all low energy orbitals are not used, Pitzer's suggested structures appear to be incorrect (see reference 9). His suggestions for the trialkyl-aluminum dimers makes no use of the fourth orbital of aluminum.

[8] See R. Mulliken, reference 5.

[9] S. Bauer, J. Am. Chem. Soc. **70**, 115 (1948); and J. Kasper, C. Lucht, and D. Harker, J. Am. Chem. Soc. **70**, 881 (1948).

[10] Here β and q are the usual exchange and Coulomb integrals respectively. The symbols used follow those of L. C. Pauling and E. B. Wilson, Jr., *Introduction to Quantum Mechanics* (McGraw-Hill Book Company, Inc., New York, 1935), p. 381 ff.

[11] J. Hirschfelder, H. Eyring, and N. Rosen, J. Chem. Phys. 4, 130 (1936).

important only if the electronegativities of the atoms involved are approximately equal. Consequently, in cases where electronegativities are unequal, the first approximation is probably a better estimate of the increased stabilization than the latter.

The most stable form of H_3^+ appears to be a triangle with two shorter and one longer sides.[12] This corresponds to further delocalization of the bonding and an increased bond energy of 20 kcal./mole. It seems likely that here the spherical symmetry of the *s* orbitals of hydrogen, which permit good overlap in all directions, aids in the further delocalization, but will be less important in most other cases.

If *A* and *A'* of I and II are not equivalent, and if the energy of a normal *A*—B bond is quite different from the *A'*—B bond energy, then only I *or* II will be important. In this case we should expect little stabilization by delocalization of the bonding.

From the above we should expect symmetrical cases with all atoms having equal electronegativities, e.g., H_3^+ and the boron hydrides, to be most favorable for half-bonds, but all symmetrical cases should be favorable. Unsymmetrical half-bonds are favorable only if the normal bonds *A*—B and B—*C* are not greatly different in bond energy.[13]

As noted, the fractional bonds in the proposed bridge structure for diborane should be especially strong. The bridge structure is now supported by the Raman spectrum interpretation of Bell and Longuet-Higgins,[14] by the infra-red study of Price,[15] by the electron diffraction of the presumably similar molecule, tetramethyldiborane,[16] and by the critical examination of other structural information by Pitzer.[5]

The heat of formation of BH_3 should be approximately zero, since the electronegativities of boron and hydrogen are essentially equal.[17] Hence, the heat of formation of B_2H_6 may be ascribed to the extra energy involved in forming the equivalent of two half-bond pairs. (The four-membered ring in B_2H_6 undoubtedly involves some further delocalization of the bonds, but for reasons previously noted,[18] it seems likely that the electron density is concentrated primarily in the B—H ligands, which are then approximately half-bonds.)

For the reaction

$$2B(s)+3H_2(g)=B_2H_6(g), \quad \Delta H=-44 \text{ kcal.}^{19}$$

The comparison should be made for single-bonded reactants as gases forming single-bonded products as gases, so that under these circumstances ΔH should be even more negative by about 8 kcal. Hence, the energy of the bridge system exceeds that of two ordinary B—H bonds by more than 50 kcal. Since a B—H bond must have a strength of the same order of magnitude as a C—H or an N—H bond, (70–80 kcal.), or perhaps less,[20] we may conclude that the half-bond pair is better than the single bond by nearly 30 percent, possibly more if the B—H bond is weak, as Walsh has suggested. This is close to the amount of added stabilization expected from the above calculations.

For less favorable, unsymmetrical *A*—B—*C* bonds, one can get some indication of strength from the fact that there are no known molecules whose parts are held together by one such bond. Since for gaseous molecules at room temperature, $T\Delta S^\circ$ of dimerization will be of the order of -10 to -15 kcal./mole, one may conclude that bonds of this type are stabilized by energies of less than that amount, leading to unfavorable free energies of dimerization. Since normal bonds have energies of the order of 40–90 kcal., the half-bond pair in this case does not exceed normal bonds by more than 15–25 percent. However, they are strong enough that asymmetric fractional bonds appear to exist in tetramethylplatinum.[1]

Though the data on strengths of half-bonds which can be presented are as yet meager, the above values of half-bond energies seem to substantiate the general deductions from the simple treatment presented above, *i.e.*, half-bond energies appear to be relatively greatest for symmetrical cases in which the electronegativities of the three elements in the half-bond pair are equal (the boron hydrides and H_3^+) and to be least for unsymmetrical half-bonds.

It is interesting to note the similarities and differences between electron-deficient bonding and ordinary, single bonds. If *A* and B each have a stable orbital, then by suitable combination of the two orbitals two new orbitals may be obtained, one of lower and one of higher energy than either of the original orbitals. If only two electrons are involved, *i.e.*, if the system is deficient two electrons under the four necessary to fill all orbitals, then it will be energetically advantageous for the electron pair to occupy the lower, combined orbital, or bonding orbital. In this sense, electron deficiency is necessary for any covalent bonding.

In a system of three atoms, each with an orbital, it is generally possible to obtain, by linear combination of three atomic orbitals, a bond orbital which is lower in

[12] J. Hirschfelder, J. Chem. Soc. **6**, 795 (1938).

[13] This point of view is somewhat different from that of A. D. Walsh (see reference 5) who suggested that weak bonds should be electron donors to good electron acceptors, which would seem to suggest electron-deficient bonds should result in cases where the normal bond *A*—B is weak and the bond B—*C* is strong. Actually asymmetric fractional bonds are almost unknown.

[14] R. Bell and H. Longuet-Higgins, Proc. Roy. Soc. **A183**, 357 (1945).

[15] W. C. Price, J. Chem. Phys. **15**, 614 (1947).

[16] W. Shand, J. Chem. Eng. News, **24**, 2950 (1946) has found that tetramethyldiborane has a bridge structure. Hence, at least for this molecule, the ethane structure is ruled out.

[17] See reference 10, Chapter II.

[18] See reference 1, p. 2075.

[19] Roth, Borger, and Bertrand, Ber. **70**, 971 (1937).

[20] See reference 13.

energy than any one of the atomic orbitals or any combination of only two. Of course, at the same time two other orbitals of higher energy are obtained. If the system has only two electrons, i.e., if there is a deficiency of four electrons, then it will be energetically advantageous for the system to use the linear combinations of three orbitals for the electron pair.

We might expect that in cases of greater electron deficiency, limited mainly to metals, four or five or more atomic orbitals may be combined to give a single-bond orbital of lower energy than any atomic orbital or any combination of fewer bond orbitals. In this case, if the electron deficiency is great enough, one electron pair may bond a large number of atoms together through this combination of orbitals. This is compatible with the point of view outlined both by Pauling, and by quantum-mechanical treatments of metals, where the "orbitals" belong to the metal aggregate as a whole.[6]

In any case, a localized bond point of view must be approximate, and it will not be surprising if in electron-deficient compounds, now described in terms of half-bonds, more complicated terms will have to be added. It is our feeling, however, that, as in the case of "normal" molecules, the localized picture of the bonding will serve as a close enough approximation to permit the drawing of conclusions concerning the molecules in which electron-deficient bonding is to be expected, the relative importance of this bonding, and, combined with the directional properties of orbitals, something about configurations in electron-deficient structures.

CONSEQUENCES OF THE PROPOSAL

It appears possible from the above discussion to predict that in nearly all symmetrical cases, and in some unsymmetrical cases, a half-bond pair is to be preferred to a single bond plus an unused low energy orbital. One can now hope to predict where other electron-deficient structures are to be found, and these predictions may be expected to furnish the severest tests of the present proposal.

The largest single field for electron-deficient structures is probably to be sought in organometallic compounds, since metals quite generally have more low energy orbitals than valence electrons, and organic groups have no unshared pairs. As an example, we may cite the case of trimethylgold which has recently been prepared, but whose structure is still unknown.[21] Trivalent gold has four stable bond orbitals, the dsp^2 orbitals, leading to four bonds directed toward the corners of a square. Trimethylgold must be expected to have a square configuration, with four interatomic links to gold, in spite of the fact that the "normal" compound would involve only three bonds. Possible structures, for example, include a tetramer, *A*, planar except for hydrogens, where one-third the methyl

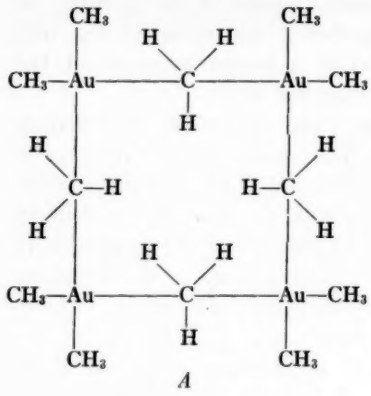

A

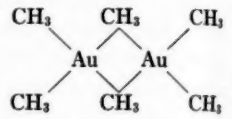

B

groups bridge gold atoms together, using a p orbital for the bridge. The bridging methyl group might then be planar, using sp^2 carbon orbitals for the three bonds to hydrogen. The methyl groups outside the ring should be normal. Alternately, a planar dimer, *B*, with more conventional methyl groups may exist.

It should be noted that low energy orbital is a relative term. It appears that if orbitals are of low enough energy to be used in accepting unshared pairs to form coordinate link bonds they may be low enough in energy to lead to the formation of electron-deficient bonds in most cases. It will not be surprising, however, if the exact limits do not coincide in the two instances, and, indeed, one might expect the requirements on the orbital to be more severe for the formation of electron-deficient bonds than for the formation of coordinate links.

One might now also expect certain molecules with excess orbitals, e.g., trimethylboron, boron trifluoride, to form complexes with certain molecules containing no unshared pairs. Since such complexes would generally contain unsymmetrical half-bonds, they may be expected only at low temperatures where entropy considerations are relatively unimportant. Since molecules which do not dimerize in spite of excess orbitals usually contain extra stabilization of one type or another (hyperconjugation in the case of trimethylboron, double-bond character of the B—F bonds in boron trifluoride), it may be difficult to demonstrate such complex molecules. Success may depend upon choosing molecules in which this excess stabilization is slight.

Complexes between molecules with excess orbitals and molecules with no unshared pairs are not of trivial interest. Catalysts are frequently metals or compounds with excess orbitals (BF_3, $AlCl_3$, etc.). It is well known that repulsive forces leading to high activation energies result from interactions of filled electron shells. Hence, compounds which may accept electrons should behave as catalysts. It is, of course, recognized in the case of compounds with unshared pairs that catalysts may operate by combining with reagent molecules through the unshared pairs. It would appear that they may act similarly on compounds with no unshared pairs.

[21] H. Gilman and L. Woods, J. Am. Chem. Soc. **70**, 550 (1948).

It is of interest that rearrangements of the hydrides of boron have already been compared with cracking and alkylations of hydrocarbons in the presence of $AlCl_3$.[22] The former contains its own excess orbitals, while the latter needs an outside agent. Moreover, the hydrides of boron react with Si_2H_6 to give SiH_4 and boron even at comparatively low temperatures (115°).[23] The breaking of an Si—Si bond at this temperature indicates a relatively low activation energy, and a half-bond intermediate appears to be an attractive possibility. Trimethylaluminum appears to react with saturated hydrocarbons (Apiezon grease),[24] and again, this reaction seems understandable if a molecule with no unshared pairs is able to form at least an unstable intermediate involving partial transfer of electrons to the excess orbital through the formation of fractional bonds.

Finally, the Whitmore mechanism for molecular rearrangement involves an intermediate with unused bond orbital. The intramolecular character of the migration and the preservation of optical activity centers during the migration suggest that the migrating group is bound to two atoms by one electron pair in the intermediate, rather than existing with an unused orbital. A similar situation obtains in *trans*-addition to a double bond, and here a form of electron-deficient bonding of the positive ion intermediate has already been suggested.[25] The present discussion would indicate that it is natural that the electron-deficient intermediate should somewhat stabilize itself by forming enough fractional bonds to use all low energy orbitals. In both addition and migration this can be accomplished by bonding one group by one electron pair to two other atoms.

ACKNOWLEDGMENT

The author wishes to express his appreciation to Dr. A. J. Stosick with whom he has discussed the major portion of this paper.

[22] H. I. Schlesinger and A. B. Burg, Chem. Rev. **31**, 4 (1942).
[23] A. Stock, *Hydrides of Boron and Silicon* (Cornell University Press, Ithaca, 1933), p. 150.
[24] N. Davidson and H. Brown, J. Am. Chem. Soc. **64**, 319 (1942).
[25] C. C. Price, *Reactions at Carbon-Carbon Double Bonds*, Interscience Publishers, Inc., New York, N. Y., 1946, Chapt. II. See also A. D. Walsh, J. Chem. Soc. 89 (1947) and M. Dewar, *ibid.*, 406 (1946) who express similar ideas concerning mechanisms of molecular rearrangements.

THE JOURNAL OF CHEMICAL PHYSICS VOLUME 17, NUMBER 8 AUGUST, 1949

The Relative Reaction Velocities of Isotopic Molecules

JACOB BIGELEISEN
Brookhaven National Laboratory, Upton, Long Island, New York
(Received October 22, 1948)

The rate constants for competitive reactions of isotopic molecules are considered from the theory of "absolute rates" and the collision theory. Formulas are derived for the ratio of the rate constants and the difference in the activation energies for reactions of isotopic molecules. The difficulties in the *a priori* calculation of relative rates are pointed out and discussed.

In general the rate constant for the light molecule will be greater than that of the heavy molecule. It is shown that the maximum ratio in the rates occurs when the isotopic atom is essentially free in the activated complex. The conditions for the rate constant of the heavy molecule to exceed that of the light one are formulated.

It is shown that the difference in activation energies covers the range from zero to the difference in the differences in the zero-point energies of the reacting molecules and their respective activated complexes.

INTRODUCTION

AMONG the interesting and important chemical differences between two isotopic atoms or molecules is their difference in reaction rates. One of the goals of any theory of reaction rates is to calculate these differences precisely. Experimental determination of relative reaction rates of isotopic molecules can aid in understanding the mechanism of a reaction and testing different approaches to the problem of reaction rates.

Eyring[1] and Evans and Polanyi[2] have treated the general problem of reaction rates from a statistical viewpoint. The method has come to be known as the "theory of absolute rates." The assumptions, applications and limitations of the theory have been discussed in detail.[3] Several of the early applications of the theory were to reactions involving hydrogen and deuterium atoms and molecules.[4–6] In these applications the rate constants of each reaction were calculated explicitly after an evaluation of the potential energy surface of

[1] Henry Eyring, J. Chem. Phys. **3**, 107 (1935).
[2] M. G. Evans and M. Polanyi, Trans. Farad. Soc. **31**, 875 (1935).
[3] See S. Glasstone, K. J. Laidler, and H. Eyring, *The Theory of Rate Processes* (McGraw-Hill Book Company, Inc., New York, 1941).
[4] L. Farkas and E. Wigner, Trans. Farad. Soc. **32**, 708 (1936).
[5] J. O. Hirschfelder, H. Eyring, and B. Topley, J. Chem. Phys. **4**, 170 (1936).
[6] A. Wheeler, B. Topley, and H. Eyring, J. Chem. Phys. **4**, 178 (1936).

the specific type of reaction. By the use of this method it is difficult to see what the important effects are contributing to the differences in rates.[1,4] In addition it is difficult to get any idea of how large these differences may be for isotopic compounds of elements of higher atomic number than hydrogen and even for hydrogen itself. In this paper formulas are derived which formally give the ratio of the rate constants for reactions of isotopic molecules.

DERIVATION

If we consider the reactions between A_1, B, $C\cdots$ to give P_1 and A_2, B, C to give P_2, where A_1 and A_2 are isotopic molecules, then the rate constants according to the Eyring[7] method will be

$$k_1=K_1\frac{C_1^{\ddagger}}{C_{A_1}C_B\cdots}\left(\frac{kT}{2\pi m_1^*}\right)^{\frac{1}{2}}\frac{1}{\delta_1}, \tag{1}$$

$$k_2=K_2\frac{C_2^{\ddagger}}{C_{A_2}C_B\cdots}\left(\frac{kT}{2\pi m_2^*}\right)^{\frac{1}{2}}\frac{1}{\delta_2}. \tag{2}$$

In Eqs. (1) and (2) K is the transmission coefficient, $C^{\ddagger}$ is the concentration of the activated complex, m^* is the effective mass of the complex along the coordinate of decomposition, and δ is the length of the top of the potential energy barrier, which the complex traverses. In Eqs. (1) and (2) we have neglected the contribution to the rate constants by tunneling through the barrier. We shall apply a correction for this effect later. Since the potential energy surfaces for isotopic molecules are the same to a high degree of approximation, δ_1 is equal to δ_2. Then

$$\frac{k_1}{k_2}=\frac{K_1}{K_2}\frac{C_1^{\ddagger}}{C_2^{\ddagger}}\frac{C_{A_2}}{C_{A_1}}\left(\frac{m_2^*}{m_1^*}\right)^{\frac{1}{2}}. \tag{3}$$

The ratios of the concentrations of the individual molecules in Eq. (3) can be replaced by the corresponding ratios of the partition functions and

$$\frac{k_1}{k_2}=\frac{K_1}{K_2}\frac{Q_1^{\ddagger}}{Q_2^{\ddagger}}\frac{Q_{A_2}}{Q_{A_1}}\left(\frac{m_2^*}{m_1^*}\right)^{\frac{1}{2}}. \tag{4}$$

The Q's in Eq. (4) are the complete partition functions. The zero of the energy scale for the normal molecules is best chosen as the minimum in the potential energy curve of the normal molecules. The minimum in the saddle of the potential energy surface of the activated complex is a suitable zero for the calculation of the ratio of the partition functions of the isotopic activated complexes.

Bigeleisen and Mayer[8] have shown that the ratio of the complete partition functions of two isotopic molecules can be expressed as a simple function of the vibrational energy levels of the two molecules.[9] Thus, Eq. (4) becomes

$$\frac{k_1}{k_2}=\frac{K_1}{K_2}\frac{f}{f^{\ddagger}}\left(\frac{m_2^*}{m_1^*}\right)^{\frac{1}{2}}, \tag{5}$$

where

$$f=\frac{Q_{A_2}}{Q_{A_1}}\pi_i\left(\frac{M_{i(1)}}{M_{i(2)}}\right)^{\frac{1}{2}}, \tag{6}$$

and the M_i's are the masses of the isotopic atoms in the isotopic molecules. The function f has been evaluated previously[8] and is equal to

$$f=\frac{s_1}{s_2}\prod_i^{3n-6}\frac{u_i}{u_i+\Delta u_i}e^{\Delta u_i/2}\frac{(1-e^{-(u_i+\Delta u_i)})}{(1-e^{-u_i})}, \tag{7}$$

where the s's are symmetry numbers, $u_i=h\nu_i/kT$, and $\Delta u_i=h/kT(\nu_{i(1)}-\nu_{i(2)})$. A relation similar to (7) holds for $f^{\ddagger}$. The various approximations given by Bigeleisen and Mayer[8] can be used to evaluate f and $f^{\ddagger}$.

For the case where Δu_i is small

$$\ln\frac{k_1}{k_2}\cdot\frac{s_2}{s_1}\cdot\frac{s_1^{\ddagger}}{s_2^{\ddagger}}=\ln\frac{K_1}{K_2}+\tfrac{1}{2}\ln\frac{m_2^*}{m_1^*}$$

$$+\sum_i^{3n-6}G(u_i)\Delta u_i-\sum_i^{3n'-6}G(u_i^{\ddagger})\Delta u_i^{\ddagger}, \tag{8}$$

or

$$\frac{k_1}{k_2}\cdot\frac{s_2}{s_1}\cdot\frac{s_1^{\ddagger}}{s_2^{\ddagger}}=\frac{K_1}{K_2}\left(\frac{m_2^*}{m_1^*}\right)^{\frac{1}{2}}$$

$$\times\left(1+\sum_i^{3n-6}G(u_i)\Delta u_i-\sum_i^{3n'-6}G(u_i^{\ddagger})\Delta u_i^{\ddagger}\right), \tag{8a}$$

where $G(u)=1/2-1/u+1/(e^u-1)$. $G(u)$ has been tabulated as a function of u in a form convenient for rapid calculation.[8]

Equations (5), (8), and (8a) must now be corrected for the "tunnel effect." Wigner[10] has shown that the rate constants in Eqs. (1) and (2) must be multiplied by a term of the form $(1-(u_L^2/24))$ where $u_L=h\nu_L/kT$. The frequency ν_L is the stretching vibration along the coordinate of decomposition and is an imaginary number. Thus, Eqs. (5), (8), and (8a) become, re-

[7] See reference 3, p. 187.
[8] J. Bigeleisen and M. G. Mayer, J. Chem. Phys. **15**, 261 (1947).
[9] For molecules whose rotation is not classical at the temperature of the reaction, the ratios of the partition functions must be corrected for a small isotope effect. This can be done following the method outlined in reference 8.
[10] E. P. Wigner, Zeits. f. physik. Chemie. **B19**, 203 (1932).

spectively,

$$\frac{k_1}{k_2}=\frac{K_1}{K_2}\frac{f}{f^\ddagger}\left(\frac{m_2^*}{m_1^*}\right)^{\frac{1}{2}}\frac{(1-(u^2_{L(1)}/24))}{(1-(u^2_{L(2)}/24))}, \tag{9}$$

$$\ln\frac{k_1}{k_2}\frac{s_2}{s_1}\frac{s_1^\ddagger}{s_2^\ddagger}=\ln\frac{K_1}{K_2}+\tfrac{1}{2}\ln\left(\frac{m_2^*}{m_1^*}\right)+\sum_i^{3n-6}G(u_i)\Delta u_i$$

$$-\sum_i^{3n'-6}G(u_i^\ddagger)\Delta u_i+\ln\left(1-\frac{u^2_{L(1)}}{24}\right)$$

$$-\ln\left(1-\frac{u^2_{L(2)}}{24}\right), \tag{10}$$

$$\frac{k_1}{k_2}\frac{s_2}{s_1}\frac{s_1^\ddagger}{s_2^\ddagger}=\frac{K_1}{K_2}\left(\frac{m_2^*}{m_1^*}\right)^{\frac{1}{2}}\left(1+\sum_i^{3n-6}G(u_i)\Delta u_i\right.$$

$$\left.-\sum_i^{3n'-6}G(u_i^\ddagger)\Delta u_i^\ddagger\right)\frac{(1-(u^2_{L(1)}/24))}{(1-(u^2_{L(2)}/24))}. \tag{10a}$$

Since the u_L's are small,

$$\frac{k_1}{k_2}=\frac{K_1}{K_2}\frac{f}{f^\ddagger}\left(\frac{m_2^*}{m_1^*}\right)^{\frac{1}{2}}\left(1+\frac{u^2_{L(2)}-u^2_{L(1)}}{24}\right), \tag{11}$$

$$\ln\frac{k_1}{k_2}\frac{s_2}{s_1}\frac{s_1^\ddagger}{s_2^\ddagger}=\ln\frac{K_1}{K_2}+\tfrac{1}{2}\ln\frac{m_2^*}{m_1^*}+\sum_i^{3n-6}G(u_i)\Delta u_i$$

$$-\sum_i^{3n'-6}G(u_i^\ddagger)\Delta u_i^\ddagger+\frac{u^2_{L(2)}-u^2_{L(1)}}{24}, \tag{12}$$

$$\frac{k_1}{k_2}\frac{s_2}{s_1}\frac{s_1^\ddagger}{s_2^\ddagger}=\frac{K_1}{K_2}\left(\frac{m_2^*}{m_1^*}\right)^{\frac{1}{2}}\left(1+\sum_i^{3n-6}G(u_i)\Delta u_i\right.$$

$$\left.-\sum_i^{3n'-6}G(u_i^\ddagger)\Delta u_i^\ddagger\right)\left(1+\frac{u^2_{L(2)}-u^2_{L(1)}}{24}\right). \tag{12a}$$

From Eqs. (11) and (12) we obtain the differences in the experimental activation energies.

$$(E_1-E_2/kT^2)=[d\ln(k_1/k_2)/dT]. \tag{13}$$

From (11)

$$\frac{E_1-E_2}{kT^2}=\frac{d\ln K_1/K_2}{dT}+\frac{u^2_{L(1)}-u^2_{L(2)}}{12T}$$

$$+\sum_i^{3n-6}\frac{1}{T}\left[\frac{u_ie^{u_i}(e^{\Delta u_i}-1)-\Delta u_i(e^{u_i}-1)}{(e^{u_i}-1)(e^{u_i+\Delta u_i}-1)}-\frac{\Delta u_i}{2}\right]-\sum_i^{3n'-6}\frac{1}{T}$$

$$\times\left[\frac{u_i^\ddagger e^{u_i^\ddagger}(e^{\Delta u_i^\ddagger}-1)-\Delta u_i^\ddagger(e^{u_i^\ddagger}-1)}{(e^{u_i^\ddagger}-1)(e^{u_i^\ddagger+\Delta u_i^\ddagger}-1)}-\frac{\Delta u_i^\ddagger}{2}\right], \tag{14}$$

and from (12)

$$\frac{E_1-E_2}{kT^2}=\frac{d\ln K_1/K_2}{dT}+\frac{u^2_{L(1)}-u^2_{L(2)}}{12T}$$

$$+\sum_i^{3n-6}\left[\frac{e^{u_i}(u_i-1)+1}{(e^{u_i}-1)^2}-\frac{1}{2}\right]\frac{\Delta u_i}{T}$$

$$-\sum_i^{3n'-6}\left[\frac{e^{u_i^\ddagger}(u_i^\ddagger-1)+1}{(e^{u_i^\ddagger}-1)^2}-\frac{1}{2}\right]\frac{\Delta u_i^\ddagger}{T}. \tag{15}$$

DISCUSSION

The difficulties in the *a priori* calculation of relative rates of reaction of isotopic molecules or the interpretation of experimental data by means of Eqs. (9)–(12a) are analogous to the problems in the direct applications of the Eyring method to the calculations of absolute rates. However, the above equations reduce to a minimum the number of properties of the activated complex which have to be evaluated. In many cases it is possible to get *a priori* qualitative answers about the relative rates and information about the mechanism of the reaction and the configuration of the activated complex from the experimentally determined relative rates.

In many reactions the transmission coefficients can be set equal to each other. Hirschfelder and Wigner[11] have made a theoretical study of the absolute value of the transmission coefficient and its dependence on the properties of the potential energy surface of the activated complex. They have also considered the possible differences in the transmission coefficients in reactions involving hydrogen and deuterium atoms. They conclude that there is very little difference in the transmission coefficients for systems which are above room temperature and have a distribution in the velocities of the reacting isotopic molecules.

Hirschfelder, Eyring, and Topley[5] as well as Farkas and Wigner[4] have calculated the absolute rates of the reactions of hydrogen and deuterium atoms with the isotopic hydrogen molecules. Both these authors use transmission coefficients of $\frac{1}{2}$ for the symmetrical reactions, *viz.*,

$$\mathrm{H+H_2=H_2+H}, \tag{16}$$

$$\mathrm{D+D_2=D_2+D}, \tag{17}$$

$$\mathrm{H+DH=HD+H}, \tag{18}$$

$$\mathrm{D+HD=DH+D}. \tag{19}$$

For the asymmetric reactions, *viz.*,

$$\mathrm{H+HD=H_2+D}, \tag{20}$$

$$\mathrm{D+H_2=DH+H}, \tag{21}$$

$$\mathrm{D+DH=D_2+H}, \tag{22}$$

$$\mathrm{H+D_2=HD+D}, \tag{23}$$

[11] J. O. Hirschfelder and E. P. Wigner, J. Chem. Phys. **7**, 616 (1939).

they use transmission coefficients which are either estimated[4] or calculated[5] from certain assumptions about the behavior of the three-atom system when it is in the energy basin at the top of the potential energy surface. When the transmission coefficients for reactions (20)–(23) are set equal to one another and one-half the agreement between theory and experiment for these reactions is equally as good as when the values estimated by Farkas and Wigner[4] and the ones calculated by Hirschfelder, Eyring, and Topley[5] are used. It would be desirable, indeed, to be able to calculate the ratio K_1/K_2 in Eqs. (9) and (10). However, in many cases a good approximation will be to replace the ratio, K_1/K_2, by unity.

If we approach the problem of relative rates of reaction of isotopic molecules from the viewpoint of the collision theory, we get a factor containing the ratio of the reduced masses of the two reacting molecules to the one-half power just as we do from the theory of absolute rates. The other terms in ratio of the rates calculated from the collision theory, $e^{(E_2-E_1)/RT}$, and P_1/P_2 cannot be calculated *a priori* from molecular data. E_1 and E_2 are the activation energies, and P_1 and P_2 are the steric factors for the reactions with the light and heavy isotopes, respectively.

From Eqs. (5) and (8) we can see that when the different isotopic atoms are chemically bound as molecules in the reacting species, the light molecule usually will have a greater rate constant than the heavy molecule. This results from the $(m_2^*/m_1^*)^{\frac{1}{2}}$ factor, which is always unity or larger, and the fact that the reacting molecule is in general more "tightly bound," i.e., $\sum_i^{3n-6}G(u_i)\Delta u_i > \sum_i^{3n'-6}G(u_i^\ddagger)\Delta u_i^\ddagger$, than the activated complex. If the activated complex is sufficiently "tightly bound" so that $\sum_i^{3n'-6}G(u_i^\ddagger)\Delta u_i^\ddagger > \sum_i^{3n-6}G(u_i)\Delta u_i + \frac{1}{2}\ln(m_2^*/m_1^*)$, the rate constant for the heavy molecule reaction will be greater than that of the light molecule, if we may neglect the "tunnel" effect.

The largest ratio in the rates occurs when the isotopic atoms are essentially free in the activated complex. Here $\sum_i^{3n-6}G(u_i^\ddagger)\Delta u_i^\ddagger$ is equal to zero. The individual terms $\sum_i^{3n-6}G(u_i)\Delta u_i$ and $\sum_i^{3n'-6}G(u_i^\ddagger)\Delta u_i^\ddagger$ are always positive.[8] If the isotopic atoms are free atoms in the initial state, then the rate constant for the heavy atom may be greater than that for the light atom. Here $\sum_i^{3n-6}G(u_i)\Delta u_i$ is zero. The condition for the rate constant for the heavy atom reaction to be greater than the light reaction is, neglecting the "tunnel" effect, $\sum_i^{3n'-6}G(u_i^\ddagger)\Delta u_i^\ddagger > \frac{1}{2}\ln(m_2^*/m_1^*)$ or $f^\ddagger > (m_2^*/m_1^*)^{\frac{1}{2}}$. This latter condition is easily fulfilled for the isotopes of hydrogen. Thus the order of the rate constants for reactions involving the isotopic hydrogen atoms as reactants will be $k_T > k_D > k_H$. This conclusion is in agreement with the argument advanced by Polanyi[12] based on a consideration of the effect of the zero-point energies of the initial state and the activated complex on the energy of activation. For isotopes of elements of higher atomic number than hydrogen the inequality $\sum_i^{3n'-6}G(u_i^\ddagger)\Delta u_i^\ddagger > \frac{1}{2}\ln(m_2^*/m_1^*)$ may not be fulfilled and the rate constant for the light atom reaction will be greater than the one for the heavy atom. Urey[13] has tabulated values of f, Eq. (7), for isotopic compounds of the elements of the first row of the periodic table as well as the halogens. The f values for different compounds of a given element are usually closely the same, excepting the compounds of hydrogen. From the magnitude of the f values for different compounds of the element and a knowledge of m_2^*/m_1^*, one can determine qualitatively whether $k_2 > k_1$.

From Eqs. (14) and (15) for the difference in the activation energies of the two isotopic molecules, we find the difference is not simply the difference in the zero-point energies of the two normal molecules and their respective activated complexes. The population of the vibrational levels other than the zero levels makes this difference in the experimental activation energies less than the difference in the difference of the zero-point energies. For low temperatures or high frequencies we find, neglecting the "tunnel" effect and the change in the ratio of the transmission coefficients with temperature, that the difference in the activation energies approaches the difference in the difference in zero-point energies. For high temperatures or low frequencies there is no difference in the activation energies.

[12] M. Polanyi, Nature **133**, 26 (1934).
[13] Harold C. Urey, J. Chem. Soc., 562 (1947).

Vibration Frequencies and Binding Forces in Some Silicate Groups

FRANK MATOSSI
Naval Ordnance Laboratory, Washington, D. C.
(Received September 10, 1948)

Frequency formulas for some atomic groups occurring in silicates (Si_2O_7, Si_3O_9 ring, SiO_3 chain, SiO_2 network) are computed, using simplified force systems, and force constants are calculated. The strong force between the O atoms connecting the SiO_4 groups of the Si_3O_9 ring is especially remarkable. Further observations are necessary to indicate the choice of less simple force systems.

I. INTRODUCTION

THE main structure elements in building the crystal lattice of silicates are tetrahedral SiO_4 groups, which may be either isolated as in the orthosilicates or connected with one another by common O atoms as in building an Si_2O_7 group from two connected tetrahedra. Connection at all corners will result in the structure found, for instance, in quartz, SiO_2. Connection of SiO_4 groups so as to form a ring of tetrahedra occurs in the crystals of benitoite ($BaTiSi_3O_9$) or beryl ($Al_2Be_3Si_6O_{18}$).

The infra-red reflection spectra of all silicates[1] contain two reflection maxima near 1000 and 500 cm^{-1}, which have been interpreted as the two active frequencies of a tetrahedral point group. In addition to these, there may occur other maxima corresponding to other particular features of the crystal lattice. Of special interest is the reflection band at 750–850 cm^{-1}—the so-called ring-band—which occurs whenever there is a ring-forming connection. This band has originally been interpreted as a pulsation vibration of the tetrahedron which somehow might have been activated in ring structures, while being inactive in a single tetrahedron.

Certain theoretical considerations[2] have indeed led to the prediction that connected SiO_4 groups should give two active frequencies at wave numbers near those of a single group. These same considerations, however, rule out the possibility of the activation of the pulsation vibration in symmetrical groups such as Si_6O_{18}, thus invalidating the above-mentioned interpretation of the ring-band as an activated pulsation.

One of the objects of the present investigation was to shed more light on the connection between the ring-band and ring-structure. To this end I have computed, as the most simple example, the vibrations of the Si_3O_9 group as found in benitoite. It will indeed be seen that a frequency at the observed wave numbers is to be expected; this frequency is dependent on the binding force between the connecting atoms in the ring. Also the spectrum of wollastonite ($CaSiO_3$) can be accounted for in terms of Si_3O_9 vibrations.

The vibrations of the Si_2O_7 group in thortveitite ($Sc_2Si_2O_7$) and those of a linear chain of SiO_4 groups, as it occurs, somewhat distorted, in silicates of the pyroxene type (e.g., diopside, $CaMgSi_2O_6$) are also calculated. For comparison, the vibrations of the isolated SiO_4 group (e.g., in zircone, $ZrSiO_4$) and those of quartz are considered.

In the following sections are presented the frequency formulas developed in this investigation.

The theory gives statements about the forces within the groups, but at present all such statements are of a qualitative character. For complete quantitative statements, we should have a complete set of binding forces; this is not possible, however, since observational data are not sufficient to determine the entire force system unambiguously. The calculations would, moreover, become extremely involved.

We have assumed a special central force system, retaining forces only between Si and the O atoms and, in some cases, between the connecting O atoms. Only for Si_2O_7 a valence-force system has been used. The general method need not be discussed here beyond the fact that group theoretical methods and symmetry coordinates have been used. Our symmetry coordinates are defined in a somewhat different manner from those of Howard and Wilson[3] who introduced symmetry coordinates first. Our coordinates are defined as

$$q=\sum_i (a_i x_i+b_i y_i+c_i z_i),$$

where x_i, y_i, z_i are "point-coordinates" described in the figures; the constants a_i etc., are determined in applying symmetry operations (linear transformations with coefficients given by group theoretical considerations). These coordinates are not necessarily normal coordinates, but those of one species are orthogonal to those of other species. They are similar to the coordinates of Bhagavantam,[4] but differ from them by a more consequent application of group theory and in not excluding translations and rotations, which is more convenient in the case of complicated molecules.

In general, the approximate character of the calculations suggests that we must not attach too great an importance to the special numerical values. As long as there are no more observations (Raman effect, separa-

[1] C. Schaefer, F. Matossi, and K. Wirtz, Zeits. f. Physik **89**, 210 (1934); F. Matossi and H. Krueger, *ibid.* **99**, 1 (1936); C. Schaefer and M. Schubert, Zeits. f. techn. Phys. **3**, 201 (1929).
[2] F. Matossi and R. Mayer, Naturwiss. **33**, 219 (1946).
[3] J. B. Howard and E. B. Wilson, Jr., J. Chem. Phys. **2**, 620 (1934).
[4] S. Bhagavantam and T. Venkatarayudu, Proc. Ind. Acad. Sci. **A9**, 224 (1939).

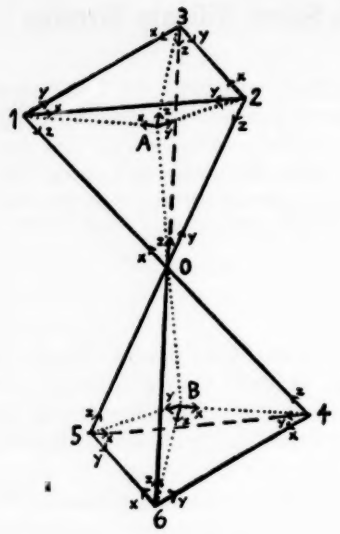

FIG. 1. Si_2O_7 group.
A, B = Si atoms at the centers } of regular tetrahedra;
$0, 1 \cdots 6$ = O atoms at the corners }
x, y, z = point coordinates.

tion of the different vibration directions in the infra-red spectrum), we cannot make a more definite statement about the forces in silicate-groups, and we must be content with the result that it is possible, even with simplified force assumptions, to obtain reasonable correspondence between observed and theoretical frequencies. As in many other cases where vibrational analysis does not or cannot furnish complete information, the data obtained should be considered more as the statement of a problem than as a result.

II. FREQUENCY FORMULAS

The force constants k_i are defined by the potential energy ϕ written as $\phi=\frac{1}{2}\Sigma k_i\Delta_i^2$ (Δ_i = distance changes) and are always designated in the following manner:

k_1 = force between Si and free O atoms,
k_2 = force between Si and connecting O atoms,
k' = force between connecting O atoms (in SiO_4, free O atoms);
d = bond-bending force at Si in Si_2O_7, assumed to be equal for all angles O−Si−O.

M is the mass of the Si atom, m is the mass of the O atoms; $\omega=2\pi\nu$, ν being the frequency.

a. Si_2O_7 Group, Symmetry Group D_{3d}

Species A_{1g} (inactive, polarized Raman lines):

$$\omega_1^2+\omega_2^2+\omega_3^2=(1/m+1/3M)k_1+k_2/M+(2/m+16/3M)d,$$

$$\omega_1^2\omega_2^2+\omega_2^2\omega_3^2+\omega_3^2\omega_1^2=k_1k_2/Mm+(2/m^2+6/Mm)k_1d+2k_2d/Mm,$$

$$\omega_1^2\omega_2^2\omega_3^2=2k_1k_2d/Mm^2.$$

Species A_{2u} (active with vibration parallel to threefold axis, no Raman lines):

$$\omega_6^2+\omega_7^2+\omega_8^2=(1/m+1/3M)k_1+(2/m+1/M)k_2+(2/m+16/3M)d,$$

$$\omega_6^2\omega_7^2+\omega_7^2\omega_8^2+\omega_8^2\omega_6^2=(2/m^2+5/3Mm)k_1k_2+(2/m^2+6/Mm)k_1d+(4/m^2+38/3Mm)k_2d,$$

$$\omega_6^2\omega_7^2\omega_8^2=(4/m^3+14/Mm^2)k_1k_2d.$$

Species E_g (inactive, depolarized Raman lines):

$$\omega_{10}^2+\omega_{11}^2+\omega_{12}^2=(1/m+4/3M)k_1+(7/2m+11/3M)d,$$

$$\omega_{10}^2\omega_{11}^2+\omega_{11}^2\omega_{12}^2+\omega_{12}^2\omega_{10}^2=(7/2m^2+8/Mm)k_1d+(9/4m^2+3/Mm)d^2,$$

$$\omega_{10}^2\omega_{11}^2\omega_{12}^2=(9/4m^3+6/Mm^2)k_1d^2.$$

Species E_u (active with vibration perpendicular to threefold axis, no Raman lines):

$$\omega_{14}^2+\omega_{15}^2+\omega_{16}^2=(1/m+4/3M)k_1+(13/2m+11/3M)d,$$

$$\omega_{14}^2\omega_{15}^2+\omega_{15}^2\omega_{16}^2+\omega_{16}^2\omega_{14}^2=(13/2m^2+12/Mm)k_1d+(39/4m^2+11/Mm)d^2,$$

$$\omega_{14}^2\omega_{15}^2\omega_{16}^2=(39/4m^3+24/Mm^2)k_1d^2.$$

All other frequencies are zero.

The oscillations are described by the following symmetry coordinates, expressed in the "point coordinates" of Fig. 1. The properties of the vibration patterns of any species are obtained in putting zero all coordinates not belonging to this species.

Species A_{1g}: $x_A+y_A+z_A+x_B+y_B+z_B$, $\sum_{i=1}^{6}(x_i+y_i)$, $\sum_{i=1}^{6} z_i$.

Species A_{1u}: $\sum_{i=1}^{6}(x_i-y_i)$.

Species A_{2g}: $\sum_{i=1}^{3}(x_i-y_i)-\sum_{i=4}^{6}(x_i-y_i)$.

Species A_{2u}: $x_0+y_0+z_0$, $x_A+y_A+z_A-x_B-y_B-z_B$,

$$\sum_{i=1}^{3}(x_i+y_i)-\sum_{i=4}^{6}(x_i+y_i),\quad \sum_{i=1}^{3} z_i-\sum_{i=4}^{6} z_i.$$

Species E_g (two sets):

$$q:\begin{cases}2x_A-y_A-z_A+2x_B-y_B-z_B, & x_1-x_3+x_4-x_5+y_1-y_2+y_4-y_6,\\ x_2-x_3-x_5+x_6-y_2+y_3+y_5-y_6, & 2z_1-z_2-z_3+2z_4-z_5-z_6;\end{cases}$$

$$q':\begin{cases}y_A-z_A+y_B-z_B, & x_1-x_3-x_4+x_5-y_1+y_2+y_4-y_6,\\ x_2-x_3+x_5-x_6+y_2-y_3+y_5-y_6, & z_2-z_3+z_5-z_6.\end{cases}$$

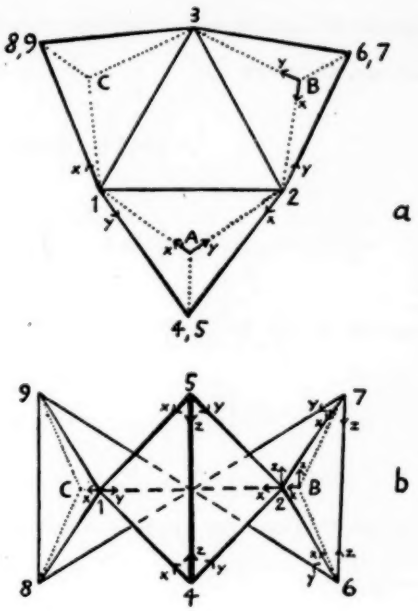

FIG. 2. Si_3O_9 group.
(a) view along the threefold axis;
(b) view along one twofold axis;
A, B, C=Si atoms; 1, 2 $\cdots$ 9=O atoms;
$<3B2=\psi(\cos\psi=-\frac{1}{3})$, $<32B=\chi=\frac{\pi}{2}-\frac{\psi}{2}$.

Species E_u (two sets):

$$q:\begin{cases}2x_0-y_0-z_0, & 2x_A-y_A-z_A-2x_B+y_B+z_B, & x_1-x_3-x_4+x_5+y_1-y_2-y_4+y_6,\\ x_2-x_3+x_5-x_6-y_2+y_3-y_5+y_6, & 2z_1-z_2-z_3-2z_4+z_5+z_6,\end{cases}$$

$$q':\begin{cases}y_0-z_0, & y_A-z_A-y_B+z_B, & x_1-x_3+x_4-x_5-y_1+y_2-y_4+y_6,\\ x_2-x_3-x_5+x_6+y_2-y_3-y_5+y_6, & z_2-z_3-z_5+z_6.\end{cases}$$

Only frequencies belonging to E_u and A_{2u} are observed, but these species could not be identified separately from the experiments.

b. Si_3O_9 Group, Symmetry Group D_{3h}

Species A_1' (inactive, polarized Raman lines):

ω_1, ω_2, ω_3 are given by

$$\begin{vmatrix}\alpha & \beta & \gamma\\ \beta & \delta & 0\\ \gamma & 0 & \epsilon\end{vmatrix}=0 \quad \text{with}$$

$$\alpha=-\tfrac{1}{2}M\omega^2+\tfrac{1}{3}(k_1+k_2),$$

$$\beta=\left(\frac{\sqrt{2}}{3}-\frac{\sqrt{3}}{4}\right)k_2,\quad \gamma=-(\tfrac{2}{3})^{\frac{1}{2}}k_1,$$

$$\delta=-\frac{3m}{4}(1-\cos\varphi)\omega^2+\frac{15-6(6)^{\frac{1}{2}}}{8}k'+\frac{59-4(6)^{\frac{1}{2}}}{8}k_2,$$

$$\epsilon=-2m\omega^2+2k_1,\quad \varphi=2\chi-\frac{\pi}{3},\quad \cos\chi=(\tfrac{2}{3})^{\frac{1}{2}}.$$

Species A_2' (inactive, no Raman lines):

$$\omega_6^2=(4/3M+32/9m[1+\cos\varphi])k_2.$$

Species A_2'' (active with vibration parallel to threefold axis, no Raman lines):

$$\omega_9^2=(1/m+4/3M)k_1.$$

Species E' (active with vibration in ring-plane, depolarized Raman lines):

ω_{13}, ω_{14} are given by

$$\begin{vmatrix} -3m(1+\cos\varphi)\omega^2+\left(\frac{59}{12}+2(6)^{\frac{1}{2}}\right)k_2+\frac{21+6(6)^{\frac{1}{2}}}{8}k' & -\left(\sqrt{3}+\frac{4\sqrt{2}}{3}\right)k_2 \\ -\left(\sqrt{3}+\frac{4\sqrt{2}}{3}\right)k_2 & -4M\omega^2+\frac{16}{3}k_2 \end{vmatrix}=0;$$

ω_{15}, ω_{16}, ω_{17} are given by

$$\begin{vmatrix} \alpha & -\beta & \gamma \\ -\beta & \eta & 0 \\ \gamma & 0 & \epsilon \end{vmatrix} \quad \text{with} \quad \eta=-3m(1-\cos\varphi)\omega^2+\left(\frac{59}{12}-2(6)^{\frac{1}{2}}\right)k_2+\frac{15-6(6)^{\frac{1}{2}}}{8}k',$$

Species E'' (inactive, depolarized Raman lines):

$$\omega_{20}^2=4k_1/3M.$$

All other frequencies are zero. E' is the only species to which observed frequencies belong in benitoite (Fig. 2).

The symmetry coordinates are:

Species A_1': $\sum_{i=1}^{3}(x_i+y_i)$, $\sum_{i=A}^{C}(x_i+y_i)$, $\sum_{i=4}^{9}(x_i+y_i)$, $\sum_{i=4}^{9}z_i$.

Species A_1'': $\sum_{i=2}^{4}[(x_{2i}-y_{2i})-(x_{2i+1}-y_{2i+1})]$.

Species A_2': $\sum_{i=1}^{3}(x_i-y_i)$, $\sum_{i=A}^{C}(x_i-y_i)$.

Species A_2'': $\sum_{i=2}^{4}[(x_{2i}+y_{2i})-(x_{2i+1}+y_{2i+1})]$, $\sum_{i=1}^{3}z_i$, $\sum_{i=A}^{C}z_i$, $\sum_{i=2}^{4}(z_{2i}-z_{2i+1})$.

Species E':

q: $\begin{cases} 2x_2-x_1-x_3, & 2y_2-y_1-y_3, & 2x_C-x_A-x_B, & 2y_C-y_A-y_B, \\ 2x_8+2x_9-x_4-x_6-x_5-x_7, & 2y_8+2y_9-y_4-y_6-y_5-y_7, & 2z_8+2z_9-z_4-z_6-z_5-z_7; \end{cases}$

q': $\begin{cases} x_1-x_3, & y_1-y_3, & x_A-x_B, & y_A-y_B, \\ x_4-x_6+x_5-x_7, & y_4-y_6+y_5-y_7, & z_4-z_6+z_5-z_7. \end{cases}$

Species E'':

q: $\begin{cases} 2z_2-z_1-z_3, & 2z_C-z_A-z_B, & 2x_8-2x_9-x_4-x_6+x_5+x_7, \\ 2y_8-2y_9-y_4-y_6+y_5+y_7, & 2z_8-2z_9-z_4-z_6+z_5+z_7; \end{cases}$

q': z_1-z_3, z_A-z_B, $x_4-x_6-x_5+x_7$, $y_4-y_6-y_5+y_7$, $z_4-z_6-z_5+z_7$.

c. Chain, Symmetry Group C_{2v}

The chain is treated as a crystal lattice of the symmetry group C_{2v} with a translation period in one direction only (Fig. 3).

Species A_1 (active with vibration parallel y_0, polarized Raman lines):

$$\omega_1^2=(1/m+4/3M)k_1,$$

$$\omega_2^2+\omega_3^2=(1/m+2/3M)k_1+(4/9m+2/3M)k_2,$$

$$\omega_2^2\omega_3^2=(4/9m^2+26/27Mm)k_1k_2.$$

Species A_2 (inactive, depolarized Raman lines):

$$\omega_8^2=(4/9m+4/3M)k_2.$$

Species B_1 (active, vibration parallel x_0, depolarized Raman lines):

$$\omega_{12}^2=\omega_1^2,$$

$$\omega_{13}^2+\omega_{14}^2+\omega_{15}^2=\left[\left(Mm-\frac{7}{12}m^2\right)k_1+\left(\frac{14}{9}Mm-m^2\right)k_2+(4Mm-3m^2)k'\right]\Big/(Mm^2-\tfrac{3}{4}m^3),$$

$$\omega_{13}^2\omega_{14}^2+\omega_{14}^2\omega_{15}^2+\omega_{15}^2\omega_{13}^2=\left[\left(\frac{14}{9}M-\frac{20}{27}m\right)k_1k_2+\left(4M-\frac{7}{3}m\right)k_1k'+\frac{8}{9}Mk_2k'\right]\Big/(Mm^2-\tfrac{3}{4}m^3),$$

$$\omega_{13}^2\omega_{14}^2\omega_{15}^2=28Mk_1k_2k'/27m(Mm^2-\tfrac{3}{4}m^3).$$

Species B_2 (active, vibration parallel z_0, depolarized Raman lines):

$$\omega_{20}^2=(14/9m+4/3M)k_2.$$

The observations do not allow to separate the active vibrations.

The symmetry coordinates are:

Species A_1: y_0+y_1, $x_a+x_b+y_a+y_b$, z_a+z_b, $x_3+x_5+y_3+y_5$, $x_2+x_4+y_2+y_4$, z_3+z_5, z_2+z_4.

Species A_2: y_0-y_1, $x_a+x_b-y_a-y_b$, $x_3+x_5-y_3-y_5$, $x_2+x_4-y_2-y_4$.

Species B_1: x_0-x_1, z_0+z_1, $x_a-x_b+y_a-y_b$, z_a-z_b, $x_2-x_4+y_2-y_4$, $x_3-x_5+y_3-y_5$, z_2-z_4, z_3-z_5.

Species B_2: x_0+x_1, z_0-z_1, $x_a-x_b-y_a+y_b$, $x_3-x_5-y_3+y_5$, $x_2-x_4-y_2+y_4$.

d. SiO_4 and SiO_2

The frequency formulas for the complicated SiO_2 structure are not computed with the general method.[5] For our purpose, the following approximation may be sufficient. If two atomic groups are connected by a common O atom which is an inversion center, then the frequency formulas for the connected system are the same as those of the single system, but in which the mass m' of the connecting atom is changed[2] successively to $m'/2$ and to ∞. Thus the frequency formulas for Si_2O_7 may be obtained from those for a Y_3XZ molecule. Now, in the case of quartz, we have not one but four points common to SiO_4 groups, and these connecting points are not inversion centers. Nevertheless, it has been considered a possible approximation to obtain the frequencies of quartz by substituting into the formulas of the isolated SiO_4 group first $m/2$ and then ∞ for m. This treatment cannot, of course, account for all observed frequencies.

For the frequencies of the SiO_4 group, we use the central-force formulas of Dennison-Schaefer,[6] in which k is an additional force constant related to linear terms of the potential energy. These formulas give the following frequencies:

Species A_1 (inactive, completely polarized Raman lines):

$$\omega_1^2=(1/m)k_1+(4/m)k'.$$

Species E (inactive, depolarized Raman lines):

$$\omega_2^2=(1/m)k'-(1/m)k.$$

Species F_2 (active, depolarized Raman lines):

$$\omega_3^2+\omega_4^2=\left(\frac{4}{3M}+\frac{1}{m}\right)k_1+\frac{2}{m}k'-\left(\frac{32}{3M}+\frac{2}{m}\right)k;$$

$$\omega_3^2\omega_4^2=\frac{8m+2M}{3Mm^2}(k_1k'-5k_1k-8k'k-8k^2).$$

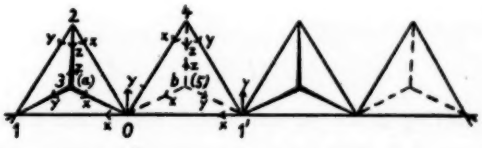

FIG. 3. Chain of SiO_4 groups.

a, b = Si atoms at the centers
0, 1 ··· 6 = O atoms at the corners
} of regular tetrahedra;

3 and a above
5 and b below
} drawing plane;

z coordinates of a and b are perpendicular to the drawing plane, directed to the points 3 and 5, respectively.

[5] For β-quartz, the calculation has been accomplished by J. Barriol, J. de phys. et rad. **7**, 209 (1946).

[6] D. M. Dennison, Astrophys. J. **62**, 84 (1925); C. Schaefer, Zeits. f. Physik **60**, 586 (1930).

TABLE I. Frequencies and binding forces for several silicate groups.

Group	Frequencies (cm^{-1}) (Observed = Infra-red reflection maxima, in parentheses: Raman effect data of zircone)							Force constants (10^5 dynes/cm) k_1	k_2	k' or d	k
SiO_4	obs.	944–894	770*	455(440)	300*(360)						
	calc.	924	770	450	260						
zircone		ω_3	ω_1	ω_4	ω_2			4.0	—	0.38	−0.26
	* calculated from combination bands										
Si_2O_7	obs.	980–860	587	486	435						
	calc.*	915	610	490				2.0	3.0	0	—
thortveitite		1190	750	585				3.0	5.0	0	—
		1110	760	585	425	290	200	3.0	4.0	0.2(d)	—
		ω_6	ω_{14}	ω_7	ω_{15}	ω_8	ω_{16}				
	* species A_{2u} and E_u										
Si_3O_9	obs.	1065–930		768	500–462		385				
	calc.*	1000		740	535		340	4.0	4.0	4.0	—
benitoite		ω_{13}		ω_{15}, ω_{16}	ω_{14}		ω_{17}				
		1080	870	770	565		355	5.0	4.5	5.4	—
		ω_{13}	ω_{15}	ω_{16}	ω_{14}		ω_{17}				
	* species E'										
Si_3O_9	obs.	1090	920	630	550						
	calc.*	970	900	635	510		255	5.0	4.0	3.0	—
wollastonite		ω_9, ω_{13}	ω_{15}	ω_{16}	ω_{14}		ω_{17}				
	* species A_2'' and E'										
SiO_3-chain	obs.	1120	970–930		565		520				
	calc.*	1050	1000	920	870	600	520	4.5	4.0	0	—
diopside		ω_{13}	ω_{20}	$\omega_{1,12}$	ω_2	ω_{14}	ω_3				
	* species A_1, B_1, B_2										
SiO_2	obs.	1200–1120	1015	800	690	480	385				
	calc.*	1100	1090		700	595	370	—	4.0	0.38	−0.26
quartz		ω_3'	ω_1'		ω_∞'	ω_4'	ω_2'				
	calc.**	1270 1215		817		538	382	—	4.5	0.7	—
	obs.		263		128						
	calc.**		292		216						
	* from zircone frequencies and forces ** according to Barriol (see reference 5)										

Substituting $m/2$ for m, we obtain

$$\omega_1'^2=2\omega_1^2, \quad \omega_2'^2=2\omega_2^2,$$

$$\omega_3'^2+\omega_4'^2=\left(\frac{4}{3M}+\frac{2}{m}\right)k_1+\frac{4}{m}k'-\left(\frac{32}{3M}+\frac{4}{m}\right)k;$$

$$\omega_3'^2\omega_4'^2=\frac{16m+8M}{3Mm^2}(k_1k'-5k_1k-8k'k-8k^2).$$

For $m=\infty$, we obtain

$$\omega_\infty'^2=(4/3M)k_1-(32/3M)k.$$

Neglecting k, we do not obtain consistent numerical results, and it may be asked, whether neglecting such terms may not involve essential discrepancies in the other cases too. It is not easy to give a reliable answer to this question; but it can be said that, according to experience, simpler force-systems always give good results with complicated molecules and bad ones for simple molecules.

III. BINDING FORCES

Comparison of calculated and observed frequencies will give the values of the force constants only if the interpretation of the observed spectra is correct. It is not possible, in certain cases, to obtain an unambiguous correspondence between observed and calculated frequencies, resulting in more than one possible solution for the force constants. The results of the comparison of calculated and observed frequencies are summarized in Table I.

It is seen that a reasonable interpretation of the spectra is possible by choosing the force constants so that at least one of the major forces k_1 or k_2 has the same value in all groups. But as mentioned before, the ambiguity of the results prevents a sure assertion. Sometimes, only the general structure of the spectrum is represented by the theoretical values, the actual values of the frequencies leading to impossible force constants. Improvements might be accomplished by introducing more complete force systems, but as long as new experiments do not give some indications for them,

it is virtually impossible to do this. Some remarks to the particular groups have to be made:

Si_2O_7

At first sight, the first solution seems to be the best one, but the force constants are unreasonably low compared with those of the other groups: In all other solutions there is no such good agreement between observed and calculated values. A not unreasonable substitute is the last combination of force constants which is not inconsistent with the observed spectrum although it is far from being ideal. The effect of the neglection of the bond-bending force is clearly seen in the second solution; cutting off the low frequencies and changing the remaining force constants.

Si_3O_9

The main feature of the proposed solutions is the large value of k'. It has been impossible to find solutions with substantially smaller forces k'. Which one of the two solutions should be preferred is hard to say. Regarding the desirable connection with the other groups, the first one should be selected, but the second one gives a better description of the higher frequencies. The observation of ω_9, which has not yet been made because of the crystallographic orientation of the benitoite sample, would at once give a decision and lead to further elucidation; it is to be expected at 865 or 970 cm^{-1} for $k_1=4$ or 5, respectively.

The large value of k' might be ascribed to the special structure of the group. It is not impossible that the formation of a ring may alter the binding forces considerably, or rather that ring-formation will occur only if there are such forces. Insofar as a frequency at about 750 appears within a considerable range of the force constants, it might be considered as characteristic of the structure itself and designated as ring-band as suggested before (of course, not every band at this frequency is a ring-band).

There are reasonable combinations of force constants that do not give a frequency near 750, e.g., the values $k_1=5.0$, $k_2=4.0$, $k'=3.0$ lead to the frequencies given in Table I for wollastonite. It is remarkable that wollastonite ($CaSiO_3=Ca_3Si_3O_9$) on the one side has Si_3O_9 rings but on the other side lacks the "ring-band" in the spectrum, if not the very weak band at 630 shall be acknowledged as this band. Our result for the just mentioned force constants shows that there need not be a contradiction of the wollastonite spectrum to our other interpretations. But there is no explanation for the change of k' in the wollastonite ring.

SiO_3 chain

With exception of ω_{13}, the frequency values are rigorously or practically independent of k'; therefore also larger k' values might be possible. But here as in Si_2O_7, the introduction of bond-bending forces might change some k values. Furthermore it must be realized that the chain of Fig. 3 is idealized, only more or less twisted chains occurring in the actual lattices.

SiO_2

Our approximation method does not claim to give unrefutable results for quartz, but nevertheless it is remarkable that it accounts reasonably well for the shift from ω_3 of SiO_4 to ω_3' of SiO_2; the vibration pattern of just this frequency approximately obeys the conditions for the applicability of our method. At present, we cannot decide which of the calculated frequencies corresponds to the observed one at 800 cm^{-1}. It may be that this frequency is not at all included in our treatment. The frequency values of Barriol, which are obtained from a more rigorous treatment similar to that used here for the other silicate groups, are not very satisfactory either although a frequency near 800 appears. Saksena[7] obtains different force constants for a valence force system from a computation of the totally symmetric vibrations. His values are: $k_2=5.065$, $d_{Si-O-Si}=0.512$, $d_{O-Si-O}=0.949$. The Raman-active species are calculated by Barriol with reasonable agreement with observation.

Finally, it must again be warned not to rely on the presented results as providing physical constants, because of the inherent incompleteness of this as every vibrational analysis of complicated molecules. However, it is my opinion that the results indeed show that a reasonable interpretation of the silicate spectra is possible even if simplified force systems are used and if it is assumed that the forces in the different groups are not quite independent of one another. But only further experiments can test the proposed solutions and lead to improvements and to indications whether the neglection of forces in some cases might have been too detrimental.

[7] B. D. Saksena, Proc. Ind. Acad. Sci. **A16**, 270 (1942).

Dielectric Relaxation of Molecules Containing Rotating Polar Groups*

A. BUDÓ
Department of Theoretical Physics, University of Debrecen, Debrecen, Hungary

(Received December 13, 1948)

Debye's theory of dielectric relaxation has been extended to molecules consisting of two similar polar groups, which cannot rotate freely relatively to one another owing to their mutual potential energy. As a result, the mean dipole moment of the molecule in the field $F_0 \exp(i\omega t)$ can be expressed by a sum of terms of Debye's type, namely $C_\lambda/(1+i\omega\tau_\lambda)$, where the relaxation times τ_λ and the constants C_λ are determined by an eigenvalue problem. τ_λ and C_λ are calculated in the case of the cosine coupling between the groups and in the case of the quasi-elastic bond. The results are compared with the experimental data for chloro-derivatives of diphenyl.

I

THE theory of dielectric relaxation, i.e., of anomalous dispersion and dielectric loss in liquids containing polar molecules, has been developed by Debye originally for spherical molecules with rigid dipole moments.[1] This theory has been extended, as regards the form and structure of the single molecule, on different lines. One of these generalizations refers to ellipsoidal molecules,[2] the other to certain simpler molecules which have a few freely rotating dipole groups,[3] and the third to non-rigid molecules of many internal degrees of freedom.[4]

Dielectric loss measurements on molecules consisting of two similar polar groups, especially measurements on *oo'*- and *mm'*-dichloro-diphenyl, show that when the groups cannot rotate freely relatively to one another, then the dielectric losses are different from that expected in the case of free rotation.[5] It seems, therefore, desirable to examine theoretically the influence on the relaxation phenomena of an intra-molecular potential which hinders the rotation of the groups.

We consider only the case in which the molecule consists of two groups of equal size with common rotational axis. In the following, denote the coefficient of friction of the molecule as a whole by ρ and that of one of the groups by ρ_1. (ρ refers to rotations about axes which are perpendicular to the axis of the groups, while ρ_1 refers to rotations about this axis.) Furthermore, denote by μ_1 and μ_2 the components of the dipole moments of the group 1 and 2, perpendicular to the molecular axis, and by μ_0 the sum of their parallel components. We consider first only the case of μ_0 being equal to zero.

In order to determine the mean dipole moment of the molecule in the field $F=F_0\exp(i\omega t)$, it is first necessary to find the differential equation for the distribution function f; $fd\Omega$ being the number of molecules the moments μ_1 and μ_2 of which are in the domain $d\Omega$ at the time t. The change of this number in the interval δt of time, formally expressed by $(\partial f/\partial t)\delta t d\Omega$, consists of two parts, ΔN_1 and ΔN_2, the first arising from the Brownian rotational movement of the molecule, and the other from the orientation of the dipoles by the external field and by the intra-molecular forces. To express the equation,

$$(\partial f/\partial t)d\Omega=(\Delta N_1/\delta t)+(\Delta N_2/\delta t), \tag{1}$$

in explicit form, let the position of the molecular axis and of the moments μ_1 and μ_2 be described by means of the angles ϑ, ψ, φ_1 and φ_2, relative to the direction of the external field F. (ϑ and ψ are the polar angles determining the position of the molecular axis; φ_1 and φ_2 are the azimutal angles of μ_1 and μ_2, measured from the plane containing F and the molecular axis. The distribution function f does not depend on the angle ψ owing to the rotational symmetry about the direction of F.) We obtain for the term $\Delta N_1/\delta t$ in Eq. (1) the expression[6]

$$\frac{\Delta N_1}{\delta t}=\frac{kT}{\rho}\left[\frac{\partial^2 f}{\partial\vartheta^2}+\operatorname{ctg}\vartheta\frac{\partial f}{\partial\vartheta}+\left(\operatorname{ctg}^2\vartheta+\frac{\rho}{\rho_1}\right)\times\left(\frac{\partial^2 f}{\partial\varphi_1^2}+\frac{\partial^2 f}{\partial\varphi_2^2}\right)+2\operatorname{ctg}^2\vartheta\frac{\partial^2 f}{\partial\varphi_1\partial\varphi_2}\right]d\Omega. \tag{2}$$

The term $\Delta N_2/\delta t$ in Eq. (1) is given formally by[7]

$$\frac{\Delta N_2}{\delta t}=-\left[\frac{\partial}{\partial\vartheta}\left(f\sin\vartheta\frac{\delta\vartheta}{\delta t}\right)+\frac{\partial}{\partial\varphi_1}\left(f\sin\vartheta\frac{\delta\varphi_1}{\delta t}\right)+\frac{\partial}{\partial\varphi_2}\left(f\sin\vartheta\frac{\delta\varphi_2}{\delta t}\right)\right]d\vartheta d\psi d\varphi_1 d\varphi_2, \tag{3}$$

where $\delta\vartheta/\delta t$, $\delta\varphi_1/\delta t$, and $\delta\varphi_2/\delta t$ are the changes of the corresponding angles per unit time, caused by the external field F and the intra-molecular forces. The part of these changes arising from the field are expressed in

* A preliminary report of a part of this work was given in Nature **161**, 133 (1948).

[1] P. Debye, *Polar Molecules* (Chemical Catalog Company, 1929).

[2] F. Perrin, J. Phys. (7) **5**, 497 (1934).

[3] A. Budó, Physik. Zeits. **39**, 706 (1938).

[4] J. G. Kirkwood and R. Fuoss, J. Chem. Phys. **9**, 329 (1941).

[5] E. Fischer, Physik. Zeits. **40**, 645 (1939); see p. 654.

[6] Cf. Eq. (2) and (14) of reference 3. (The notations χ, φ, μ_a, μ_b, ρ', and ρ'' of reference 3 must be replaced by φ_1, φ_2, μ_1, μ_2, ρ_1, and ρ_1.)

[7] Cf. Eq. (11) of reference 3.

Eq. (10) of reference 3. To obtain the other part, we introduce the mutual potential energy of the two groups. This potential energy will be a function of $\varphi_1-\varphi_2$ only and be denoted by $V(\varphi_1-\varphi_2)$. The moment of force, exerted by the dipole μ_2 on μ_1, is then $-V'(\varphi_1-\varphi_2)$, where the accent means differentiation with respect to the argument of V. Therefore, according to the usual assumption of proportionality between the angular velocity and the moment of force, the contribution of the intra-molecular forces in $\delta\varphi_1/\delta t$ is given by $-V'/\rho_1$ and, similarly, in $\delta\varphi_2/\delta t$ by $+V'/\rho_1$. Thus we have

$$\frac{\delta\vartheta}{\delta t}=-\frac{F}{\rho}\cos\vartheta(\mu_1\cos\varphi_1+\mu_2\cos\varphi_2),$$

$$\frac{\delta\varphi_1}{\delta t}=F\left[\frac{\cos^2\vartheta}{\rho\sin\vartheta}(\mu_1\sin\varphi_1+\mu_2\sin\varphi_2)+\frac{\mu_1}{\rho_1}\sin\vartheta\sin\varphi_1\right]-\frac{V'(\varphi_1-\varphi_2)}{\rho_1},$$

$$\frac{\delta\varphi_2}{\delta t}=F\left[\frac{\cos^2\vartheta}{\rho\sin\vartheta}(\mu_1\sin\varphi_1+\mu_2\sin\varphi_2)+\frac{\mu_2}{\rho_1}\sin\vartheta\sin\varphi_2\right]+\frac{V'(\varphi_1-\varphi_2)}{\rho_1}. \quad (4)$$

In the differential equation obtained from Eq. (1) by the substitutions Eq. (2)–Eq. (4) and $d\Omega=\sin\vartheta d\vartheta d\psi d\varphi_1 d\varphi_2$, we introduce instead of φ_1 and φ_2 the new variables,

$$\chi=(\varphi_1+\varphi_2)/2, \quad \eta=(\varphi_1-\varphi_2)/2. \quad (5)$$

Thus we get the equation

$$\frac{\partial f}{\partial t}=\frac{kT}{\rho}\left[\frac{\partial^2 f}{\partial\vartheta^2}+\operatorname{ctg}\vartheta\frac{\partial f}{\partial\vartheta}+\left(\operatorname{ctg}^2\vartheta+\frac{\rho}{2\rho_1}\right)\frac{\partial^2 f}{\partial\chi^2}+\frac{\rho}{2\rho_1}\frac{\partial^2 f}{\partial\eta^2}\right]+\frac{F}{\rho}\cos\vartheta[\mu_1\cos(\chi+\eta)+\mu_2\cos(\chi-\eta)]\frac{\partial f}{\partial\vartheta}$$

$$-F\left(\frac{\cos^2\vartheta}{\rho\sin\vartheta}+\frac{\sin\vartheta}{2\rho_1}\right)[\mu_1\sin(\chi+\eta)+\mu_2\sin(\chi-\eta)]\frac{\partial f}{\partial\chi}-\left\{\frac{F\sin\vartheta}{2\rho_1}[\mu_1\sin(\chi+\eta)-\mu_2\sin(\chi-\eta)]-\frac{V'(2\eta)}{\rho_1}\right\}\frac{\partial f}{\partial\eta}$$

$$-\left\{F\left(\frac{1}{\rho}+\frac{1}{\rho_1}\right)\sin\vartheta[\mu_1\cos(\chi+\eta)+\mu_2\cos(\chi-\eta)]-\frac{2}{\rho_1}V''(2\eta)\right\}f, \quad (6)$$

where $F=F_0\exp(i\omega t)$. If we assume a solution of the form

$$f=Ce^{-V(2\eta)/kT}\left\{1-\frac{F_0e^{i\omega t}}{kT}\sin\vartheta\times[(\mu_1+\mu_2)\cos\chi u(\eta)-(\mu_1-\mu_2)\sin\chi v(\eta)]\right\}, \quad (7)$$

and neglect second order terms in F_0, which is permitted in practically all the important cases, then we arrive at the following equations for u and v:

$$L(u)\equiv\frac{d^2u}{d\eta^2}-2\phi(\eta)\frac{du}{d\eta}-(a+i\omega b)u=2\phi(\eta)\sin\eta-(a+1)\cos\eta,$$

$$L(v)=-2\phi(\eta)\cos\eta-(a+1)\sin\eta, \quad (8)$$

with the abbreviations

$$\phi(\eta)=V'(2\eta)/kT, \quad a=1+2\rho_1/\rho, \quad b=2\rho_1/kT. \quad (9)$$

When the functions u and v are known, the mean moment $\bar{m}$ can be calculated from the expression[8]

$$\bar{m}=\frac{F_0e^{i\omega t}}{3kT}\frac{\int_{-\pi}^{\pi}e^{-V(2\eta)/kT}[(\mu_1+\mu_2)^2u\cos\eta+(\mu_1-\mu_2)^2v\sin\eta]d\eta}{\int_{-\pi}^{\pi}e^{-V(2\eta)/kT}d\eta}. \quad (10)$$

Let us suppose that the eigenvalues λ and eigenfunctions z_λ of the equation

$$(d^2z/d\eta^2)-2\phi(\eta)(dz/d\eta)+\lambda z=0, \quad (11)$$

are determined, and let us expand the functions u and v and the right hand sides of Eq. (8) with respect to the

[8] It is $\bar{m}=\int\mu_F f d\Omega/\int f d\Omega$, where μ_F, the sum of the components of μ_1 and μ_2 in the direction of the field, is given by $-F\sin\vartheta(\mu_1\cos\varphi_1+\mu_2\cos\varphi_2)$. Use of Eq. (5) and integration over ϑ, ψ, χ gives Eq. (10).

system of these eigenfunctions z_λ:

$$u=\sum_\lambda B_\lambda z_\lambda, \quad v=\sum_\lambda B_\lambda' z_\lambda,$$

$$2\phi(\eta)\sin\eta-(a+1)\cos\eta=\sum_\lambda A_\lambda z_\lambda,$$

$$-2\phi(\eta)\cos\eta-(a+1)\sin\eta=\sum_\lambda A_\lambda' z_\lambda. \qquad (12)$$

The eigenvalue problem Eq. (11) which must be solved in order to obtain λ, z_λ, and A_λ, can be transformed by the substitution $z=Z\exp(\int\phi(\eta)d\eta)$ into

$$(d^2Z/d\eta^2)+\{\lambda+\phi'(\eta)-[\phi(\eta)]^2\}Z=0, \qquad (16)$$

i.e., into an equation of Hill's type.[9]

In case of free rotation ($\phi(\eta)=0$), one finds for the mean moment

$$\bar m=\frac{F_0e^{i\omega t}}{3kT}\frac{\mu_1^2+\mu_2^2}{1+i\omega\tau_f} \quad \text{with} \quad \frac{1}{\tau_f}=kT\left(\frac{1}{\rho}+\frac{1}{\rho_1}\right), \qquad (17)$$

while for a rigid molecule, i.e., when the relative position of the groups is completely fixed (in equal or opposite direction of their moments), then one expects, on the base of Perrin's theory, the result

$$\bar m=\frac{F_0e^{i\omega t}}{3kT}\frac{(\mu_1\pm\mu_2)^2}{1+i\omega\tau_r} \quad \text{with} \quad \frac{1}{\tau_r}=kT\left(\frac{1}{\rho}+\frac{1}{2\rho_1}\right). \qquad (18)$$

The relaxation times τ_λ, which occur in the case of hindered rotation, therefore can be expressed also in the following way

$$\tau_\lambda=\frac{1+\rho_1/\rho}{1+\rho_1/\rho+(\lambda-1)/2}\tau_f,$$

or

$$\tau_\lambda=\frac{1+2\rho_1/\rho}{1+2\rho_1/\rho+\lambda}\tau_r. \qquad (19)$$

When μ_0 (the sum of the components of the groups, parallel to the molecular axis) is different from zero, then the formula Eq. (13) must be completed by the term

$$\frac{F_0e^{i\omega t}}{3kT}\frac{\mu_0^2}{1+i\omega\tau'}, \quad \tau'=\frac{\rho}{2kT}. \qquad (20)$$

[9] As the potential function $V(\varphi_1-\varphi_2)=V(2\eta)$ is periodic in η, the function $\phi(\eta)$ and therefore $\phi'(\eta)-[\phi(\eta)]^2$ are also periodic.

By substituting of these series in Eq. (8), we obtain the coefficients B_λ, B_λ' and thus we find, using Eq. (10), that the mean moment can be written in the form

$$\bar m=\frac{F_0e^{i\omega t}}{3kT}\sum_\lambda\frac{C_\lambda}{1+i\omega\tau_\lambda}, \qquad (13)$$

where the relaxation times τ_λ and the constants C_λ are given by

$$\frac{1}{\tau_\lambda}=kT\left(\frac{1}{\rho}+\frac{1+\lambda}{2\rho_1}\right), \qquad (14)$$

$$C_\lambda=-\frac{\int_{-\pi}^{\pi}e^{-V(2\eta)/kT}z_\lambda[A_\lambda(\mu_1+\mu_2)^2\cos\eta+A_\lambda'(\mu_1-\mu_2)^2\sin\eta]d\eta}{(\lambda+a)\int_{-\pi}^{\pi}e^{-V(2\eta)/kT}d\eta}. \qquad (15)$$

II

In order to have first information about the influence of the interaction between the groups, we shall examine two kinds of interaction, the cosine coupling and the quasi-elastic bond. In both kinds of the coupling we shall treat two cases in which the potential function $V(\varphi_1-\varphi_2)=V(2\eta)$ has its minimum in the equal or in the opposite directions of the moments μ_1 and μ_2 respectively. These two cases will be called shortly the *cis*- and the *trans*-case. In the following we measure η always from the position in which the potential has its minimum value. In such a manner we can obtain from the formulas for the *cis*-case those for the *trans*-case when we replace μ_2 by $-\mu_2$. For this reason, we shall put in all the following equations

$$\begin{aligned}&\mu_I=\mu_1+\mu_2, \quad \mu_{II}=\mu_1-\mu_2 \quad \text{in the } cis\text{-case,}\\ &\mu_I=\mu_1-\mu_2, \quad \mu_{II}=\mu_1+\mu_2 \quad \text{in the } trans\text{-case.}\end{aligned} \qquad (21)$$

(a) In the case of the *cosine coupling*, the potential has the form

$$V(\varphi_1-\varphi_2)=-E\cos(\varphi_1-\varphi_2),$$

or

$$V(2\eta)=-E\cos2\eta, \qquad (22)$$

where $2E$, the difference between the potential energies in the equal and opposite directions of the moments μ_1 and μ_2, is a measure of the interaction between the groups. Then we have in the Eqs. (8), (9), (11) and (12)

$$\phi(\eta)=q\sin2\eta, \quad q=E/kT. \qquad (23)$$

For small values of q, the solution of the eigenvalue

TABLE I. The "weights" C_m of the relaxation times τ_m, given as functions of the parameter $q=E/kT$ of the quasi-elastic bond between the two polar groups.*

q	C_0	C_2	C_4	C_6	C_8	C_{10}	C_1	C_3	C_5	C_7	C_9	C_{11}
0.125	0.056	0.126	0.141	0.105	0.058	0.026	0.051	0.114	0.127	0.095	0.052	0.023
0.25	0.198	0.203	0.103	0.034	0.009	0.002	0.165	0.167	0.084	0.028	0.007	0.001
0.5	0.388	0.167	0.034	0.005	0.001	—	0.271	0.113	0.022	0.002	—	—
1.0	0.574	0.089	0.006	—	—	—	0.289	0.038	0.002	—	—	—
2.0	0.739	0.034	0.001	—	—	—	0.221	0.006	—	—	—	—
4.0	0.858	0.010	—	—	—	—	0.132	0.001	—	—	—	—
8.0	0.932	0.002	—	—	—	—	0.071	—	—	—	—	—
16.0	0.962	0.001	—	—	—	—	0.037	—	—	—	—	—

* It is for $q=0.125$: $C_{12}=0.010$, $C_{14}=0.003$, $C_{16}=0.001$; $C_{13}=0.009$, $C_{15}=0.003$, $C_{17}=0.001$.

problem Eq. (11) can be expressed as a power series in q by means of an approximation method, using the well-known solutions of the problem $d^2z/d\eta^2+\lambda z=0$. When we take into account terms up to and including q^5, then we obtain on the base of the general theory given in Part I, after rather long calculations, the result

$$\bar{m}=\frac{F_0e^{i\omega t}}{3kT}\sum_{n=1}^{3}\left(\frac{\mu_I^2C_n^+}{1+i\omega\tau_n^+}+\frac{\mu_{II}^2C_n^-}{1+i\omega\tau_n^-}\right), \tag{24}$$

where (cf. Eqs. (17) and (21))[10]

$$\tau_1^\pm=\left(\frac{\rho_1}{\rho}+1\right)\left[\frac{\rho_1}{\rho}+1\mp\frac{1}{2}q+\frac{3}{16}q^2\mp\frac{3}{128}q^3-\frac{3}{2.8^3}q^4\pm\frac{5}{2.8^4}q^5\right]^{-1}\tau_f,$$

$$\tau_2^\pm=\left(\frac{\rho_1}{\rho}+1\right)\left[\frac{\rho_1}{\rho}+5+\frac{9}{32}q^2\pm\frac{3}{128}q^3+\frac{9}{2.8^4}q^4\mp\frac{15}{8^5}q^5\right]^{-1}\tau_f, \tag{25}$$

$$\tau_3^\pm=\left(\frac{\rho_1}{\rho}+1\right)\left[\frac{\rho_1}{\rho}+13+\frac{25}{96}q^2+\frac{125}{54.8^4}q^4\mp\frac{5}{8^5}q^5\right]^{-1}\tau_f,$$

and

$$2C_1^\pm=1\pm\frac{1}{2}q-\frac{1}{64}q^2\mp\frac{15}{256}q^3+\frac{17}{8^4}q^4\pm\frac{29}{6.8^3}q^5,$$

$$2C_2^\pm=\frac{1}{64}q^2\left(1\mp\frac{1}{4}q-\frac{69}{256}q^2\pm\frac{193}{6.8^3}q^3\right), \tag{26}$$

$$2C_3^\pm=\frac{1}{4.8^4}q^4\left(1\mp\frac{1}{12}q\right).$$

[10] This result gives probably a good approximation even if $q\approx1$. Namely, for $\omega=0$ one readily finds that in the expression (10) for the mean moment, the two factors containing integrals are:

$$\int_0^\pi e^{q\cos2\eta}\frac{\cos^2}{\sin^2}\eta d\eta\Big/\int_0^\pi e^{q\cos2\eta}d\eta=\frac{1}{2}\left[1\pm\int_0^{2\pi}\cos x e^{q\cos x}dx\Big/\int_0^{2\pi}e^{q\cos x}dx\right],$$

which can be evaluated exactly by means of Bessel functions. On the other hand, it follows for these factors from Eqs. (24) and (26) the evaluation

$$C_1^\pm+C_2^\pm+C_3^\pm=\frac{1}{2}\left[1\pm\left(\frac{1}{2}q-\frac{1}{16}q^3+\frac{1}{96}q^5\right)\right],$$

which differs, for $q<1$, from the exact values by less than 0.25 percent.

(b) We consider secondly the case of the *quasi-elastic bond* between the groups, with the potential

$$V(\varphi_1-\varphi_2)=\frac{2}{\pi^2}E(\varphi_1-\varphi_2)^2,\quad\text{or}\quad V(2\eta)=\frac{8}{\pi^2}E\eta^2, \tag{27}$$

$(-\pi/2\leq\eta\leq\pi/2)$.[11] Here is $2E$, again the difference between the potential energies in the equal and opposite directions of μ_1 and μ_2. Then we have in Eqs. (8), (9), (11) and (12)

$$\phi(\eta)=\alpha\eta\quad\text{with}\quad\alpha=(8/\pi^2)(E/kT)=(8/\pi^2)q, \tag{28}$$

and the eigenvalue problem (11) can be transformed by the substitution $x=\alpha^{\frac{1}{4}}\cdot\eta$ in Hermite's equation

$$(d^2z/dx^2)-2x(dz/dx)+(\lambda/\alpha)z=0. \tag{29}$$

With the eigenvalues and eigenfunctions

$$\lambda_n/\alpha=2n,\quad z_n=H_n(\alpha^{\frac{1}{4}}\eta), \tag{30}$$

where $H_n(x)$ are the Hermite polynomials, we obtain for the mean dipole moment the result

$$\bar{m}=\frac{F_0e^{i\omega t}}{3kT}\sum_{n=0,1,\cdots}\left(\frac{\mu_I^2C_{2n}^+}{1+i\omega\tau_{2n}}+\frac{\mu_{II}^2C_{2n+1}^-}{1+i\omega\tau_{2n+1}}\right). \tag{31}$$

The relaxation times τ_0, τ_1, $\cdots$ are given by (cf. Eqs. (14), (18))

$$\tau_m=\frac{2\rho_1}{kT(1+2\rho_1/\rho+2m\alpha)}=\frac{1+2\rho_1/\rho}{1+2\rho_1/\rho+2m\alpha}\tau_r,$$

$$(m=0,1,2,\cdots) \tag{32}$$

[11] For other values of η, let the potential be defined that $V(2\eta)$ is periodic in η with the period π.

TABLE II. The relaxation time τ, for long wave-lengths, as function of the parameter $q=E/kT$ of the quasi-elastic bond between the two polar groups.

	Cis-			*Trans-*		
		τ/τ_f			τ/τ_f	
q	μ^2/μ_f^2	$(\rho_1/\rho=0.5)$	$(\rho_1/\rho=0.25)$	μ^2/μ_f^2	$(\rho_1/\rho=0.5)$	$(\rho_1/\rho=0.25)$
0	1	1	1	1	1	1
0.125	1.050	1.076	1.105	0.950	1.001	1.010
0.25	1.099	1.143	1.201	0.901	0.980	0.995
0.5	1.187	1.249	1.348	0.813	0.924	0.914
1.0	1.341	1.366	1.503	0.659	0.780	0.751
2.0	1.546	1.449	1.606	0.454	0.564	0.519
4.0	1.735	1.485	1.649	0.265	0.353	0.312
8.0	1.857	1.496	1.662	0.143	0.200	0.173
16.0	1.926	1.499	1.665	0.074	0.107	0.091
∞	2.0	3/2	5/3	0	0	0

and the constants $C_0, C_1, \cdots$ by

$$C_{2n}^{+}=\frac{(-1)^n}{(2n)!(4\alpha)^n e^{1/4\alpha}} \times\int_0^{\pi/2} e^{-\alpha\eta^2}\cos\eta H_{2n}(\alpha^{\frac{1}{2}}\eta)d\eta \Big/ \int_0^{\pi/2} e^{-\alpha\eta^2}d\eta, \quad (33a)$$

$$C_{2n+1}^{-}=\frac{(-1)^n}{(2n+1)!(4\alpha)^{n+\frac{1}{2}} e^{1/4\alpha}} \times\int_0^{\pi/2} e^{-\alpha\eta^2}\sin\eta H_{2n+1}(\alpha^{\frac{1}{2}}\eta)d\eta \Big/ \int_0^{\pi/2} e^{-\alpha\eta^2}d\eta. \quad (33b)$$

Some values of these constants, as functions of the parameter α or q (cf. Eq. (28)) are collected in the Table I.[12]

The formulae (31)–(33) are valid for all values of the parameter q and so they describe the transition from the case of the free rotation to the case of the rigid molecule, as q increases from 0 to ∞. The result which appears for very small values of q in rather complicated form because of the many terms, reduces for middle q-values to a few terms, and for large q it consists practically of the single term with C_0 and τ_0.

(c) *For long wave-lengths*, that is, when $\omega\tau_m \ll 1$, the expressions (24) and (31) for the mean moment can be written as

$$\bar{m}=\frac{F_0 e^{i\omega t}}{3kT}\mu^2(1-i\omega\tau). \quad (34)$$

[12] The constants C_{2n} can be evaluated in the following manner. If we denote the quotient of the two integrals in Eq. (33a) by J_{2n}, then, as it can be proved

$$J_{2n}=\alpha^{-\frac{1}{2}}H_{2n-2}(x)\cdot\phi_1(x)/\phi(x)-\alpha^{-1}J_{2n-2},$$

where $x=(\pi/2)\alpha^{\frac{1}{2}}$, $\phi(x)$ is the error integral $(2/\pi^{\frac{1}{2}})\int^x e^{-t^2}dt$ and $\phi_1(x)$ is its derivative $(2/\pi^{\frac{1}{2}})e^{-x^2}$. The quotient

$$J_0=\int_0^{\pi/2} e^{-\alpha\eta^2}\cos\eta d\eta \Big/ \int_0^{\pi/2} e^{-\alpha\eta^2}d\eta$$

can be expressed, after expansion of $\cos\eta$, by the error integral and its derivatives. The constants C_{2n+1}^{-} are connected with C_{2n+2}^{+} by the relation $C_{2n+1}^{-}=4\alpha(n+1)C_{2n+2}^{+}$.

Here μ, the measurable dipole moment of the molecule and τ, the "relaxation time for long wave-lengths" are given by

$$\mu^2=\sum_m(\mu_I^2 C_m^{+}+\mu_{II}^2 C_m^{-}), \quad (35)$$

$$\mu^2\tau=\sum_m(\mu_I^2 C_m^{+}\tau_m^{+}+\mu_{II}^2 C_m^{-}\tau_m^{-}). \quad (36)$$

In particular, when the two moments μ_1 and μ_2 are equal (to μ_1, say), then one has by means of Eq. (21)

$$\mu^2=4\mu_1^2\sum_m C_m^{\pm}, \quad \tau=\sum_m C_m^{\pm}\tau_m^{\pm}/\sum_m C_m^{\pm}. \quad (37)$$

Comparing μ^2 and τ with the values of these quantities for the free rotation, i.e.; with $\mu_f^2=2\mu_1^2$ and with τ_f given in Eq. (17), we obtain from Eqs. (37), (25), and (26) *for the cosine coupling*, including the second order terms in q:

$$\mu^2/\mu_f^2=1\pm\tfrac{1}{2}q, \quad (38)$$

$$\tau/\tau_f=1\pm\frac{\beta}{2}q+\frac{\beta(4\beta^2-2\beta-1)}{16\beta+4}q^2, \quad (39)$$

where

$$\beta=(1+\rho_1/\rho)^{-1}, \quad (40)$$

and the upper and lower signs correspond to the *cis*- and *trans*-case, respectively.

For the quasi-elastic bond, some values of μ^2/μ_f^2 and τ/τ_f (calculated on the base of Eqs. (37), (32), (17) and Table I) are given in Table II, for two values of the ratio ρ_1/ρ.

III

Comparison with experiment. An influence of the coupling between the rotating groups on the relaxation time for long wave-lengths has been found in chloro-derivatives of the diphenyl.[5] The measurements give for the *mm'*-dichloro-diphenyl: $\mu=1.68$, $\tau=3.94\times10^{-11}$ sec. and for the *oo'*-dichloro-diphenyl: $\mu=1.75$, $\tau=4.68\times10^{-11}$ sec. If we assume that the rotation of the groups in *mm'*-dichloro-diphenyl, in which the dipoles are far enough apart, is free (that is, if we take $\mu_f=1.68$, $\tau_f=3.94\times10^{-11}$ sec), then the ratios obtained experimentally are

$$\mu^2/\mu_f^2=1.085, \quad \tau/\tau_f=1.19. \quad (41)$$

The accuracy of these values may be estimated to about 6–8 percent.

In order to compare the above values with the theoretical results given in Eqs. (38)–(40) and in Table II, we must know the ratio ρ_1/ρ. This can be estimated on the base of Perrin's theory.[2] We regard the molecules in question as rigid ellipsoids with the half principal axes $a=5.35$A, $b=3.2$A, $c=1.5$A, where a corresponds to the direction of the axis of the groups. Then it follows from Perrin's theory that the coefficients of friction ρ_a, ρ_b, and ρ_c, referring to the rotations about the respective

axes, are in the proportion $\rho_a:\rho_b:\rho_c=1.05:2.0:2.0$.[13] In our case in which the molecule consists of two rotating groups of equal size, we assume for ρ_1, which refers to rotation of one of the groups round the direction of a, the value $\rho_a/2$, while ρ, which refers to the molecule as a whole, will be identified with ρ_b or ρ_c. Thus we have $\rho_1/\rho\approx 0.25$.[14]

Assuming cosine coupling between the groups, formulas (38)–(40) give in the *cis*-case with $q=E/kT=0.25$, the ratios $\mu^2/\mu_f^2=1.12$ and $\tau/\tau_f=1.10$. And also assuming quasi-elastic bond, one obtains from Table II, again in the *cis*-case, for $q=0.25$: $\mu^2/\mu_f^2=1.10$, $\tau_1/\tau_f=1.20$; $q=0.23$ would give 1.09 and 1.19, in complete agreement with Eq. (41). With the *trans*-case the experimental data are incompatible. To the quantitative agreement, it is to attribute no extra meaning, partly because of the possible error of the experimental values, partly as the potential function is certainly more complicated than that we assumed, especially in the *oo'*-dichloro-diphenyl a steric hindrance can be present. We can state, however, on the base of the theory that the dielectric loss measurements confirm the conclusion drawn from the values of the dipole moments,[15] namely, that in *oo'*-dichloro-diphenyl there are influences which favor the *cis*-constellation.[16]

[13] These proportions can easily be calculated from the table given by A. Budó, E. Fischer and S. Miyamoto Physik. Zeits. **40**, 337 (1939).

[14] Another estimate can be obtained by regarding the groups as ellipsoids; then $\rho_1/\rho\approx 0.33$.

[15] A. Weissberger, R. Sängewald and G. C. Hampson, Trans. Farad. **30**, 884 (1934).

[16] The Coulomb-forces alone favor the *trans*-position.

THE JOURNAL OF CHEMICAL PHYSICS VOLUME 17, NUMBER 8 AUGUST, 1949

The Heats of Combustion of Polythene and Polyisobutylene

GEORGE S. PARKS AND JOHN R. MOSLEY
Department of Chemistry, Stanford University, California

(Received November 22, 1948)

Values, with uncertainties of about 0.03 percent, are here presented for the heats of combustion of polythene and polyisobutylene. The results for polythene indicate that this polymer is crystalline at least to the extent of about 50 percent at 25°C. The results for polyisobutylene are abnormally high and can be explained on the basis of a steric interference effect within the molecules of this liquid polymer.

INTRODUCTION

THE heats of combustion of two samples of polythene have been measured in the present investigation. Similarly, combustion values for two different samples of polyisobutylene were obtained in studies[1] which were carried out in this Laboratory several years ago. These have here been revised to bring them into accord with present-day standards.

The results for these two polymers are in marked contrast, and serve to throw light upon (1) the partial crystallization of polythene and (2) the steric interference effect within the polyisobutylene unit.

EXPERIMENTAL

Apparatus and Method

The apparatus and general method for measuring the heats of combustion of the polythene were essentially the same as those described previously by Parks[1] and collaborators. Two cylinders of oxygen were used in this investigation and with each a new series of calibrations, involving seven and five combustions, respectively, was carried out with standard benzoic acid (Sample 39f) supplied by the United States Bureau of Standards. For this sample Jessup[2] has reported a mean combustion value of 26,429.4 international joules (equal to 6317.8 cal.) per gram mass for the standard calorimetric conditions of Washburn,[3] which also approximated our own working conditions. The results obtained with our two calibrations agreed to within 0.003 percent.

The combustions were made with our Parr bomb (capacity 390 ml) filled with oxygen to a pressure of 30 atm. at 23° and with 1 ml of water initially in the bomb. In all cases most of the air originally in the bomb was washed out by two preliminary fillings with oxygen to a pressure of 5 atm. and thus the correction for nitric acid formation was kept down to less than 0.02 percent of the total heat involved. The magnitude of the thermal correction for this nitric acid was calculated on the basis of 14,340 cal. per mole of aqueous acid formed, in accordance with the recent study of Jessup. No tests for carbon monoxide were made in this work, but the high degree of concordance obtained in these and other sets of determinations really constitutes excellent evidence as to the completeness of the reported combustions.

[1] J. W. Richardson and G. S. Parks, J. Am. Chem. Soc. **61**, 3543 (1939); G. S. Parks, T. J. West, B. F. Naylor, P. S. Fujii and L. A. McClaine, *ibid.* **68**, 2524 (1946).

[2] R. S. Jessup, J. Research Nat. Bur. Standards **29**, 247 (1942); **36**, 421 (1946).

[3] E. W. Washburn, Bur. Standards J. Research **10**, 525 (1933).

TABLE I. Combustion data for polythene at 25.0°C.

Sample	$I(C_2H_4)_{700}$	$II(C_2H_4)_{700}$
No. of combustions	8	2
$-\Delta U_B/m$, cal. per g	11,095.1	11,093.1
Mean Δ, cal. per g	±1.2	±0.4
$-\Delta U_R$, cal. per C_2H_4 unit	311,162	311,106
$-\Delta H_R$, cal. per C_2H_4 unit	311,755	311,699
$-\Delta H_f°$, cal. per C_2H_4 unit	12,983	13,039

Units

The unit of energy used throughout this paper is the *defined* conventional calorie which has been derived from the international joule by dividing by the factor 4.1833. The unit of mass is the gram true mass which has been derived from the weight in air against brass weights by use of correction factors for buoyancy on the basis of 0.920 for the density of the polythene[4] samples and the respective values 0.907 and 0.915 for the polyisobutylene[5] Samples I and II. The weights of the C_2H_4 and C_4H_8 units in the polythene and polyisobutylene, respectively, have been taken as 28.052 and 56.104, based on the 1941 table of atomic weights.[6]

POLYMER MATERIALS

The polythene material was kindly given to us by the E. I. du Pont de Nemours Company. It was reported to be very pure, polymerized ethylene of about 18,000 to 20,000 molecular weight, and thus corresponded to the approximate formula $(C_2H_4)_{700}$. Our only treatment was to keep it in an evacuated desiccator over anhydrous magnesium perchlorate for a week or more prior to the combustion measurements. Sample I, described[4] as *microcrystalline*, had evidently been formed in sheets and then cut into small cubes of about 2 to 3 mm on an edge. The second sample consisted of similar material, which had been fabricated into tubing of about 5 mm diameter.

The two samples of the polyisobutylene were distinctly different. Sample I, prepared by the Shell Development Company, was a very viscous liquid with a molecular weight of about 4900. Sample II, prepared by the Standard Oil Development Company, was like crape rubber in appearance and was reported to approximate 200,000 in molecular weight. It yielded 0.033 percent ash, for which a correction was duly made in the combustion data. Neither of these samples showed any indication of even partial crystallinity, and polyisobutylene is generally considered as amorphous.

EXPERIMENTAL RESULTS

Our present experimental results for the combustions of these two samples of solid polythene to yield liquid water and gaseous carbon dioxide are summarized in the second and third columns of Table I. Here the first line of numerical values records the number of combustions carried out on each sample. The resulting mean values for the energy evolved in the isothermal bomb process per gram at 25.0°, represented by the term $-\Delta U_B/m$, and the mean deviations of the individual combustions from these mean values, represented by Δ, appear in the two succeeding lines. The values of the bomb process were then calculated per C_2H_4 unit and corrected to the standard constant-volume process where the reactants and products are each at 1 atm. by means of the equations of Washburn.[3] The energy evolved in this hypothetical process is designated in the table by the symbol $-\Delta U_R$. From this quantity $-\Delta H_R$, the heat evolved in the isobaric process at 1 atm., was obtained by addition of the proper work term. Finally, $-\Delta H_f°$, the heat of formation of a C_2H_4 unit of polymer from the elements (gaseous hydrogen and graphatic carbon), was calculated from $-\Delta H_R$ by use of 68,317.4 cal. and 94,051.8 cal.[7] for the heats of formation of water and carbon dioxide, respectively.

Table II contains similar thermochemical data which have been obtained from previous measurements by Parks and his collaborators[1] for the two different samples of polyisobutylene. In the present case, the data for Sample I as published in 1939 have been revised in terms of Jessup's newer combustion value[2] for the standard benzoic acid and the present-day atomic weights.

Following the procedures of Rossini[8] in considering the several sources of error, we now estimate 0.03 percent as the final uncertainty in these tabulated values of $-\Delta U_R$ and $-\Delta H_R$. As independent corroborative evidence on this accuracy question, it may also be noted here that our values for $-\Delta H_R$ for polythene are very close to a preliminary result (311.8 kcal. per C_2H_4 unit) obtained from two combustion experiments by Donald E. Roberts and recently quoted by Jessup.[9]

DISCUSSION

These combustion data provide a new method for estimating the degree of crystallinity of polythene.

TABLE II. Combustion data for polyisobutylene at 25°C.

Sample	$I(C_4H_8)_{87}$	$II(C_4H_8)_{3500}$
No. of combustions	6	3
$-\Delta U_B/m$, cal. per g	11,179.8	11,175.8
Mean Δ, cal. per g	±1.3	±2.0
$-\Delta U_R$, cal. per C_4H_8 unit	627,076	626,852
$-\Delta H_R$, cal. per C_4H_8 unit	628,298	628,037
$-\Delta H_f°$, cal. per C_4H_8 unit	21,179	21,440

[4] F. C. Hahn, M. L. Macht, and D. A. Fletcher, Ind. Eng. Chem. **37**, 526 (1945).
[5] J. D. Ferry and G. S. Parks, J. Chem. Phys. **4**, 70 (1936). The value for Sample II is an estimate.
[6] G. P. Baxter, M. Guichard, O. Hönigschmid, and R. Whytlaw-Gray, J. Am. Chem. Soc. **63**, 845 (1941).
[7] D. D. Wagman, J. E. Kilpatrick, W. J. Taylor, K. S. Pitzer, and F. D. Rossini, J. Research Nat. Bur. Standards **34**, 143 (1945).
[8] F. D. Rossini, Chem. Rev. **18**, 252 (1936).
[9] R. S. Jessup, J. Chem. Phys. **16**, 661 (1948).

From extensive studies pertaining to various series of hydrocarbons containing a normal paraffin chain, Rossini[10] and his co-workers have deduced a number of empirical equations of the type

$$-\Delta H_R = A + Bn \quad (1)$$

where $-\Delta H_R$ is the molal heat of combustion at 25°C, A is a constant dependent on the "end-group" involved in the particular hydrocarbon series, and B is a second constant (157,443±50 cal. for the gaseous state and 156,263±50 cal. for the liquid state) associated with the number of carbon atoms n in the molecule, where $n>5$. For the series of gaseous normal alkanes, liquid normal alkanes and gaseous normal 1-alkenes they have thus obtained the following equations:

Gaseous Alkanes: $-\Delta H_R = 57{,}909 + 157{,}443n$ (2)
Liquid Alkanes: $-\Delta H_R = 57{,}430 + 156{,}263n$ (3)
Gaseous 1-Alkenes: $-\Delta H_R = 19{,}592 + 157{,}443n$. (4)

For our present purposes we may correspondingly derive for the series of liquid normal 1-alkenes the equation

$$-\Delta H_R = 19{,}592 + 156{,}263n \quad (5)$$

by assuming the same "end-effect" constant as that used for the gaseous state. On the other hand, our present combustion data for Sample I of the polythene, when substituted in Eq. (5), yield 155,863 cal. for the constant B. This difference of 400 calories per CH_2 unit, or 28.5 calories per gram, can logically be attributed to partial, or localized, crystallization in the polymer. Thus the generally accepted picture[4,11] for a sample of polythene is that of numerous small regions of crystallized material, or crystallites, with amorphous material interspersed between these. A given macromolecule, in this case with the average formula $(C_2H_4)_{700}$, may accordingly participate in several of these crystallites, and exist partly in the crystallized form and partly in the amorphous, under-cooled liquid form. If a hypothetical heat of fusion value of 58.7 cal. per gram, as deduced by Parks and Rowe[12] for normal dotriacontane, be here assumed for a completely crystallized material, these data now yield 28.5/58.7×100 or 49 percent for the percentage crystallization in the polythene Sample I. Likewise, our values for Sample II yield 52 percent, indicating that a somewhat increased degree of crystallinity has been attained in the extrusion process for fabricating the polythene tubing.

Almost certainly, however, these estimates from combustion data are somewhat low, since they involve the assumption that the amorphous material in the polymer possesses the same heat of combustion as that found for normal 1-alkenes in the unstrained liquid state. Actually this amorphous material must be existing under a certain amount of strain, and in this condition, as in the case of the polyisobutylene to be discussed presently, it should have a somewhat higher combustion value. Our combustion method, therefore, probably gives a lower limit to the percentage of crystalline material but the correct value may easily be 10 or 15 percent higher than this.

Estimates for the percentage crystallization of similar polythene samples have been made by Hunter and Oakes[13] from density measurements, and by Raine, Richards, and Ryder[11] both by computation from enthalpy data for polythene in combination with a generalized specific heat equation for normal liquid paraffins and also by a simple extrapolation of the enthalpy data. For comparison these several results are now recorded in Table III. We have here revised the two estimates of Raine, Richards, and Ryder by using 58.7 cal. per gram for the hypothetical heat of fusion of a long-chain hydrocarbon, since the value of 56.5 originally employed by these authors was based on the pioneer work of Parks and Todd[14] and is undoubtedly somewhat low. In passing, it should be noted that the first of these estimates, which involves the combination of a general specific heat equation for liquid paraffins with the experimentally obtained enthalpy data, neglects any strain effects in the amorphous regions of the polythene and is therefore probably too high. For this reason the simple extrapolation of the enthalpy data appears to us more reliable. On the whole, considering the different nature of the measurements involved as well as the variety of polymer samples, we feel that the data of this table represent a reasonable degree of agreement on the partial crystallinity of polythene, and we now suggest 60 (±10) as our best estimate of this percentage.

TABLE III. Estimated crystallization of polythene at 25°C.

Method	Percentage crystallized
Heat of combustion data	49 to 52
Density measurements	55
Computation from enthalpy data	74
Extrapolation of enthalpy data	61
"Best" estimate	60(±10)

In the case of the C_4H_8 unit of liquid or amorphous polyisobutylene we might expect an approximate heat of combustion of 4×156,263 or 625,052 cal. plus the "end-group" contribution, if spatial factors were not to complicate the picture. We here estimate these end-group contributions as about 225 cal. and 6 cal., respectively, per C_4H_8 unit in the case of Samples I and II, on the assumption that the value 19,592 cal. in Eq. (5) can also be applied to branched alkenes. On

[10] E. J. Prosen and F. D. Rossini, J. Research Nat. Bur. Standards 34, 263 (1945); *ibid.* 36, 269 (1946); and E. J. Prosen, W. H. Johnson, and F. D. Rossini, *ibid.* 37, 51 (1946).
[11] H. C. Raine, R. B. Richards, and H. Ryder, Trans. Faraday Soc. 41, 56 (1945).
[12] G. S. Parks and R. D. Rowe, J. Chem. Phys. 14, 507 (1946).
[13] E. Hunter and W. G. Oakes, Trans. Faraday Soc. 41, 49 (1945).
[14] G. S. Parks and S. S. Todd, Ind. Eng. Chem. 21, 1235 (1929).

such a basis we might now expect resultant heats of combustion of 625,277 cal. and 625,058 cal. Actually, the heats of combustion of Samples I and II, respectively, are 3021 cal. and 2979 cal. greater than these expected figures; and these larger values can be most readily explained on the assumption that the pairs of methyl groups attached to alternate carbon atoms in the polyisobutylene chain are exerting very appreciable steric repulsion effects. Thus these repulsions would tend to loosen up or strain the molecule and might logically be reflected in larger than normal values for the heat of combustion. Indeed, such an explanation has been previously advanced by Evans and Polanyi[15] at a time when the quantitative data were less conclusive.

[15] A. G. Evans and M. Polanyi, Nature **152**, 738 (1943).

THE JOURNAL OF CHEMICAL PHYSICS VOLUME 17, NUMBER 8 AUGUST, 1949

Vibrational Spectrum and Infra-red Polarization Measurements for Malononitrile

FREDERICK HALVERSON AND RUDOLPH J. FRANCEL
Stamford Research Laboratories, American Cyanamid Company, Stamford, Connecticut
(Received December 1, 1948)

The infra-red spectra of gaseous, liquid, and solid malononitrile have been obtained using a spectrometer equipped with LiF, NaCl, and KBr prisms. Polarization measurements on a linearly oriented preparation of solid malononitrile using a transmission polarizer were of material assistance in the classification of absorption bands into their respective species. These data, together with the Raman data in the literature and a normal coordinate treatment, permitted a complete assignment of the fifteen fundamental frequencies and a determination of the force constants and thermodynamic functions for the molecule.

I. INTRODUCTION

PLANE polarized infra-red radiation has been suggested[1–6] as a valuable tool in the assignment of fundamental molecular vibrational frequencies and in the investigation of internal structure of crystals. Since vibrations with the same symmetry properties exhibit similar variations of absorption intensity as the plane of polarization is rotated with respect to the crystal, classification of vibrational frequencies is facilitated. In the ideal case where single crystals can be examined with several specified orientations of the axes, two approaches are apparent. If the internal structure of the crystal is known, sufficient information may be obtained to classify all the observed vibrational frequencies according to their symmetry species. On the other hand, if the vibrational species of certain absorption bands are known, the intensity variations with rotation of the plane of polarization indicate the spatial orientation of molecules in the crystal. In the present example, infra-red polarization measurements on a thin, linearly oriented preparation of malononitrile are used as a check on the vibrational frequency assignments.

Malononitrile (methylene cyanide) is a di-substituted methane with the formula

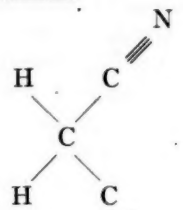

It melts at 32.1°C and boils at 219–220°C, so that infra-red spectra of the solid, liquid, and vapor phases may all be obtained for comparison. The Raman spectrum of molten malononitrile at 45°C has been reported by Kohlrausch and Ypsilanti[7] in the course of work on the free rotation of groups, but no infra-red or x-ray crystallographic data have been reported.

II. OBSERVED INFRA-RED SPECTRA

The malononitrile used was prepared in these laboratories by Mr. L. J. Hughes by the reaction of cyanoacetamide and phosphorus pentachloride.[8] The crude malononitrile obtained by distilling the reaction mixture was twice distilled at 2-mm pressure; the end fractions of each distillation were discarded. The product had a refractive index of $n_D^{34.2}=1.4139\pm.0002$ and a freezing point of 31.6°C.[9]

[1] R. S. Halford, J. Chem. Phys. **14**, 8 (1946).
[2] J. Mann and H. W. Thompson, Nature **160**, 17 (1947); Proc. Roy. Soc. **A192**, 489 (1948).
[3] D. A. Crooks, Nature **160**, 17 (1947).
[3a] C. J. Brown and D. E. C. Corbridge, Nature **162**, 72 (1948).
[4] G. B. B. M. Sutherland and V. A. Jones, Nature **160**, 567 (1948).
[5] A. Elliot, E. J. Ambrose, and R. B. Temple, J. Chem. Phys. **16**, 877 (1948).
[6] W. E. Keller, J. Chem. Phys. **16**, 1003 (1948).
[7] K. W. F. Kohlrausch and G. Prinz Ypsilanti, Zeits. f. physik. Chemie **B29**, 274 (1934).
[8] *Organic Syntheses* (John Wiley and Sons, Inc., New York, 1943), Coll. Vol. II, p. 379.
[9] Literature values are $n_D^{34.2}=1.41463$ and a melting point of 32.1°C given by Landolt-Börnstein, *Physikalisch-Chemische Tabellen* (Verlag Julius Springer, Berlin, 1923), Vol. I, p. 372 and Vol. II, p. 974.

All spectra were obtained with a Perkin-Elmer spectrometer Model 12A in an air-conditioned room (24° C) using LiF, NaCl, and KBr prisms. It is estimated that the reported frequencies are accurate to ± 2 cm^{-1}.

Vapor

The vapor spectrum was obtained using a multiple reflection cell with a variable path length of 1, 2, 3, or 4 meters. This cell was housed in an electrically heated furnace kept at 140°C. By interpolation of the boiling point data in the literature,[8,9] the vapor pressure of malononitrile was estimated to be 80 ± 20 mm at this temperature. Since it was found that malononitrile slowly decomposed at 140°C yielding ammonia, the following procedure was adopted to minimize the effects of decomposition. Several grams of liquid malononitrile were introduced into the cell and the pressure then reduced to promote the establishment of an equilibrium concentration of vapor. Spectral measurements were begun in about three minutes after the time of addition. Since the ammonia concentration increased rather gradually, it was possible to make measurements for one-half hour at a time without serious interference.

The spectrum of malononitrile vapor measured from 4000 to 650 cm^{-1} using a 2-meter optical path is shown in Fig. 1 with only the regions of absorption plotted. The observed bands, their relative intensities, and their corresponding type designations are given in Table I. Bands are termed type *B* or *C* depending upon whether the *Q* branch is absent or strong, respectively, relative to the *P* and *R* branches. An ambiguous band type is designated by a question mark. In cases where the *Q* branch is not observed, the band center is taken as the average of the *P* and *R* branch values.

The asymmetry on the low frequency side of the type *C* band at 2976 cm^{-1} is taken to indicate the presence of a weak type *B* band with *R* and *P* branches at 2958 and 2944 cm^{-1}, respectively. The absorption at 2623 cm^{-1} does not give the appearance of a clear-cut band type and is assumed to represent the superposition of two or more bands, one of which is probably type *C*.

TABLE I. Observed infra-red absorption bands of malononitrile vapor (140°C, 2-meter path length).

Frequency	Type	Int	Frequency	Type	Int
884 *P*					
892 *Av*	*B*	*S*	2333 *Q*?	*C*?	*W*
901 *R*					
			2623 ?	?	*M*
974 *P*					
982 *Av*	*B*	*S*	2730 *P*		
990 *R*			2739 *Av*	*B*	*W*
			2747 *R*		
1258 *P*					
1265 *Av*	*B*	*M*	2944? *P*		
1272 *R*			2951 *Av*	*B*	*W*
			2958 *R*		
1314 *P*					
1322 *Av*	*B*	*S*	2958? *P*		
1330 *R*			2976 *Q*	*C*	*M*
			2992 *R*		
1413 *P*					
1422 *Av*	*B*	*VS*	3159 *P*		
1432 *R*			3168 *Av*	*B*	*W*
			3177 *R*		
2265 ?					
2274 *Av*	?	*W*			
2283 ?					

Absorption of atmospheric carbon dioxide practically obscured the presence of a weak band at 2333 cm^{-1}, which may be type *C*. The absorption centered at 2274 cm^{-1} does not have a very definite band type, perhaps caused by a superposition of bands. Although the region from 1230 to 1020 cm^{-1} was carefully examined, no trace of absorption was found to match a band present in the solid spectrum at 1218 cm^{-1} or a band in the liquid at 1225 cm^{-1}.

Liquid

The spectrum of liquid malononitrile shown in Fig. 2 was obtained using a cell about 0.03 mm thick kept at *ca.* 40°C. The absorption bands and their relative intensities are given in Table II. Bands at 582, 936, and 2275 cm^{-1} appear to have unresolved absorption at slightly lower frequencies.

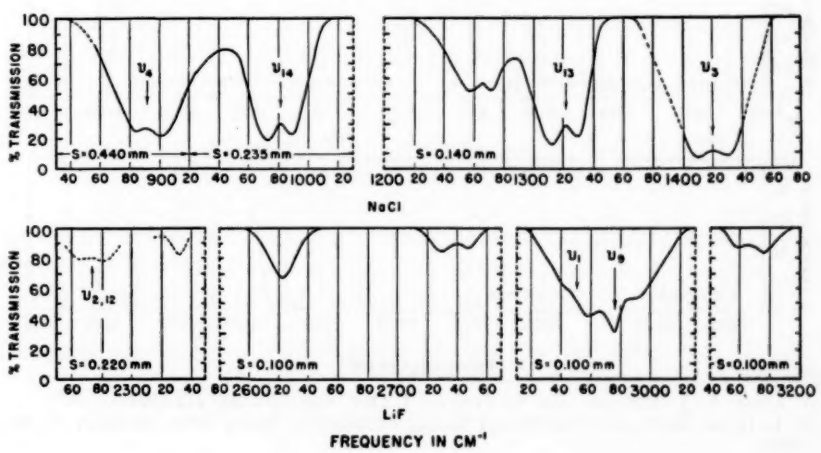

FIG. 1. Infra-red absorption spectrum of malononitrile vapor (140°C, 2-meter path length).

TABLE II. Observed infra-red absorption bands of liquid malononitrile (*ca.* 0.03 mm thick).

Frequency	Int	Frequency	Int
582	*M*	2207 ?	*VW*
702	*W*	2222	*VW*
728	*VW*	2275	*M*
874	*VW*	2297	*VW*
893	*S*	2603	*VW*
908	*VW*	2637	*W*
936	*M*	2848	*VW*
984	*S*	2935	*VS*
1225	*VW*	2968	*VS*
1263	*VW*	3168	*W*
1320	*W*	3243	*VW*
1395	*VS*		

Solid

Spectra of solid malononitrile were obtained using both a linearly oriented solid and a pulverized solid in the form of a "Nujol" (mineral oil) mull. In each case spectra were measured with polarized as well as unpolarized radiation. The polarizer used was of the type described by Elliot, Ambrose, and Temple[10] consisting of five selenium films inclined at an angle of *ca.* 25° to the spectrometer beam.

(*A*) *Linearly Oriented Solid*

The following procedure was used to prepare a linearly oriented solid.[11] A cell consisting of two KBr windows (about 2×5 cm) and a silver spacer (0.01 mm) was filled with liquid malononitrile and slowly heated to about 50°C on a small electric heater. The heater was then turned off and one end of the cell left in contact with the heater while the other end was placed on a water-cooled copper bar. Since the heater cooled rather slowly, a temperature gradient was set up along the length of the cell. As the cool end approached the freezing point, it was periodically seeded with some solid malononitrile until crystallization was induced. The crystals gradually grew along the length of the cell, and visual examination was used to determine the best oriented area to be placed in the spectrometer beam. This procedure was not consistently successful, but usually several attempts would produce a uniform orientation over a sufficiently large area. (Various compounds were found to respond to this method and its modifications with widely differing degrees of success.) Microscopic examination of such a malononitrile preparation indicated that the solid was in the form of elongated plates. A photomicrograph representing the approximate area of the spectrometer beam is shown in Fig. 3. The dark lines are parallel to the direction of growth and represent edges between the plates.

The spectra of the linearly oriented solid shown in Fig. 4 were obtained using unpolarized radiation and polarized radiation with the E vector successively parallel and perpendicular to the direction of crystal growth. In order to eliminate variations in sample thickness, the same preparation kept in a fixed position was used for these measurements. Although a 0.01-mm spacer was used in the cell, the sample was probably somewhat thicker. A comparison of the spectra in Fig. 4 shows that the intensities of most of the absorption bands are decidedly altered by rotation of the plane of polarization. Several absorption bands which were unresolved in the unpolarized spectrum were resolved into distinct bands in the polarized spectra. Not all preparations of malononitrile gave identical polarization differences, indicating that the orientation of the crystallographic axes with respect to the direction of growth was not always reproducible. The observed absorption bands, their relative intensities and their direction of polarization are given in Table III.

(*B*) *"Nujol" Mull*

A "Nujol" mull was prepared by placing a small portion (a few milligrams) of finely ground malono-

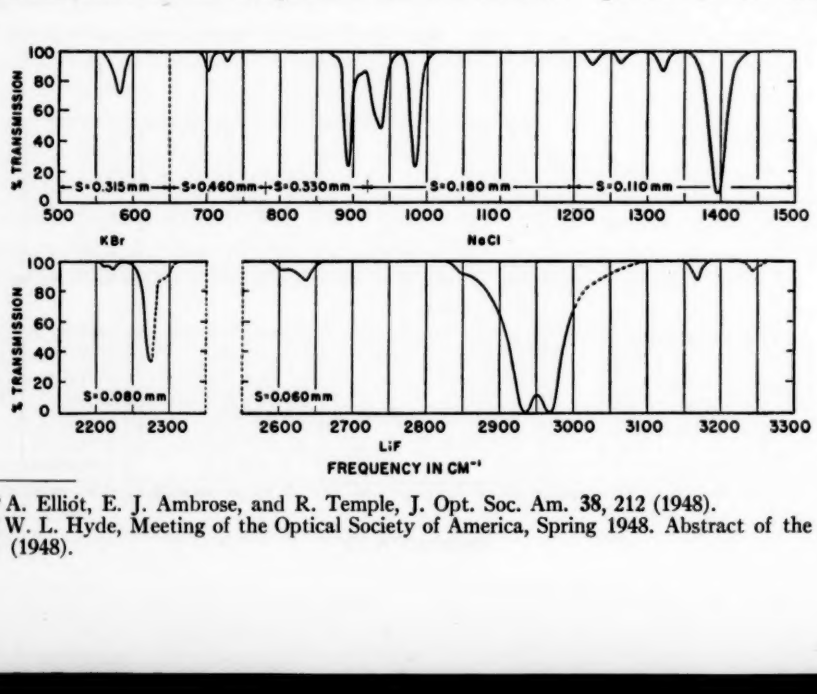

FIG. 2. Infra-red absorption spectrum of liquid malononitrile (*ca.* 0.03 mm thick).

[10] A. Elliot, E. J. Ambrose, and R. Temple, J. Opt. Soc. Am. **38**, 212 (1948).
[11] W. L. Hyde, Meeting of the Optical Society of America, Spring 1948. Abstract of the paper appeared in J. Opt. Soc. Am. **38**, 663 (1948).

nitrile on a KBr plate and adding enough "Nujol" to form a paste when mixed. A second KBr plate was placed on top of the first and the two plates ground together until a thin, uniform film resulted. It is likely that the crystals in such a preparation were non-oriented. The spectrum of the "Nujol" mull was independent of the plane of polarization and was identical with that obtained for the linearly oriented solid using unpolarized radiation (with the exception of the "Nujol" bands at 2970–2850, 1462, and 1380 cm^{-1}).

Solution

By the use of various solvents, the following absorption bands of malononitrile in solution were observed: 892, 931, 982, 1222, 1262, 1317, and 1400 cm^{-1}. In particular, the bands at 931 and 1222 cm^{-1} are comparable to those in the liquid at 936 and 1225 cm^{-1}, although analogous bands were not found in the vapor spectrum.

III. THEORETICAL CONSIDERATIONS

Vapor

The malononitrile molecule may be considered as being derived from methane by replacing two hydrogen atoms with nitrile (C≡N) groups. A diagram of its structure, together with some abbreviations for structural parameters, is given in Fig. 5. Its symmetry point group is C_{2v} with two mutually perpendicular planes of symmetry—one containing all the atoms except the hydrogens, bisecting the HCH angle, and the other bisecting the C—C—C angle, with a twofold symmetry axis along the line of intersection of the two planes. The reduced vibrational representation of this molecular point group is $\Gamma_{vib}=6A_1+2A_2+3B_1+4B_2$, where the symmetry species are taken as defined in Table IV. Selection rules for the molecule in free space permit all fifteen vibrations to be active in the Raman effect and thirteen to be active in infra-red absorption (species A_2 inactive).

Although no specific data are available for the molecular parameters, estimates can be made which will be useful for our discussion. We assume all angles at carbon atom 3 (Fig. 5) to be tetrahedral, r(C−H)=1.09A, r(C≡N)=1.17A, and r(C−C)=1.49A. These dimensions yield as principal moments of inertia $I_x \simeq 48$, $I_z \simeq 281$, and $I_y \simeq 321$ (in units of 10^{-40} g cm^2) about the axes designated in Fig. 5. A description of the band envelopes expected for this type of molecule in vapor phase infra-red absorption may be obtained from the computations of Badger and Zumwalt[12] on unsymmetrical rotator molecules. Vibrations in which the electric moment change (transition moment) is parallel to the x axis (transitions of species B_2) should give rise to type A bands with three peaks, the central one being weak relative to the other two. Vibrations in which the moment is parallel to the z axis (species A_1) should yield type B bands with two peaks and a minimum between them. Vibrations in which the moment is parallel to the y axis (species B_1) should yield type C bands with three peaks, the central one being strong relative to the other two. In the vapor spectrum shown in Fig. 1, type A and type B bands are indistinguishable since the weak central peak is not resolved.

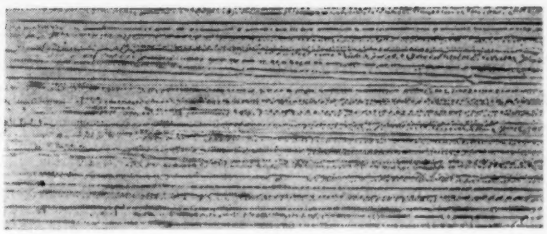

FIG. 3. Photomicrograph of linearly oriented solid malononitrile.

Wilson's technique[13] was used for setting up the secular equation. The various bending motions of the methylene group are described by changes in the following four coordinates: α, the HCH angle (deformation); ρ, the angle between the bisector of the HCH angle and the plane defined by the three carbon atoms (rocking); τ, the dihedral angle between the CH_2 plane and the carbon plane (twisting); and ω, the angle between the bisector of the C—C—C angle and the CH_2 plane (wagging). Additional coordinates are indicated in Fig. 5. Factoring of the secular equation is obtained by choosing the valence force symmetry coordinates (*VFSC*) given in Table V. For convenience, the *VFSC* are designated by S_1, S_2, $\cdots$, with a corresponding designation ν_1, ν_2, $\cdots$, for the vibrational frequencies, meaning that the vibration of frequency ν_1 involves coordinate S_1 primarily, etc.

The G matrix ($2T=\dot{S}'G^{-1}\dot{S}$) for the *VFSC* is given in Fig. 6. It contains the atomic masses, internuclear distances, and functions of the various bond angles. No relationship was assumed between the angles α and γ in calculating the matrix elements.

The F submatrices ($2V=S'FS$) used with the G matrix in obtaining the A_1 and B_2 factors of the secular equation ($|GF-\lambda E|=0$) for malononitrile molecules in the vapor state are given in Fig. 7. Certain types of interaction constants found important in investigations[14,15] of potential systems for groups of related molecules were included. Diagonal F submatrices ($F_i=\delta_{ij}F_{ij}$) were used for the A_2 and B_1 factors since the coordinates involved represented rather widely separated frequencies.

[12] R. M. Badger, and L. R. Zumwalt, J. Chem. Phys. **6**, 711 (1938).

[13] E. B. Wilson, J. Chem. Phys. **9**, 76 (1941).

[14] B. L. Crawford and S. R. Brinkley, J. Chem. Phys. **9**, 69 (1941).

[15] J. C. Decius, J. Chem. Phys. **16**, 214 (1948).

Solid

The problem of vibrations in molecular crystals has been discussed by a number of writers[1,16–20] and will be mentioned only briefly. The motions of the crystal are separated (approximately) into lattice modes and molecular modes. Intermolecular forces are assumed weak (relative to the normal covalent bond forces) so that from one point of view[1] each molecular mode is essentially multiply degenerate with a frequency nearly the same as for the free molecule. In the few cases where experimental data are available, the frequency values for the solid differ only slightly from those for the vapor. Furthermore, infra-red absorption bands of crystalline *molecular* solids are usually sharp (except for some cases of hydrogen bonding), and the number of strong bands is usually the same order of magnitude as the number of normal vibrations of the free molecule.

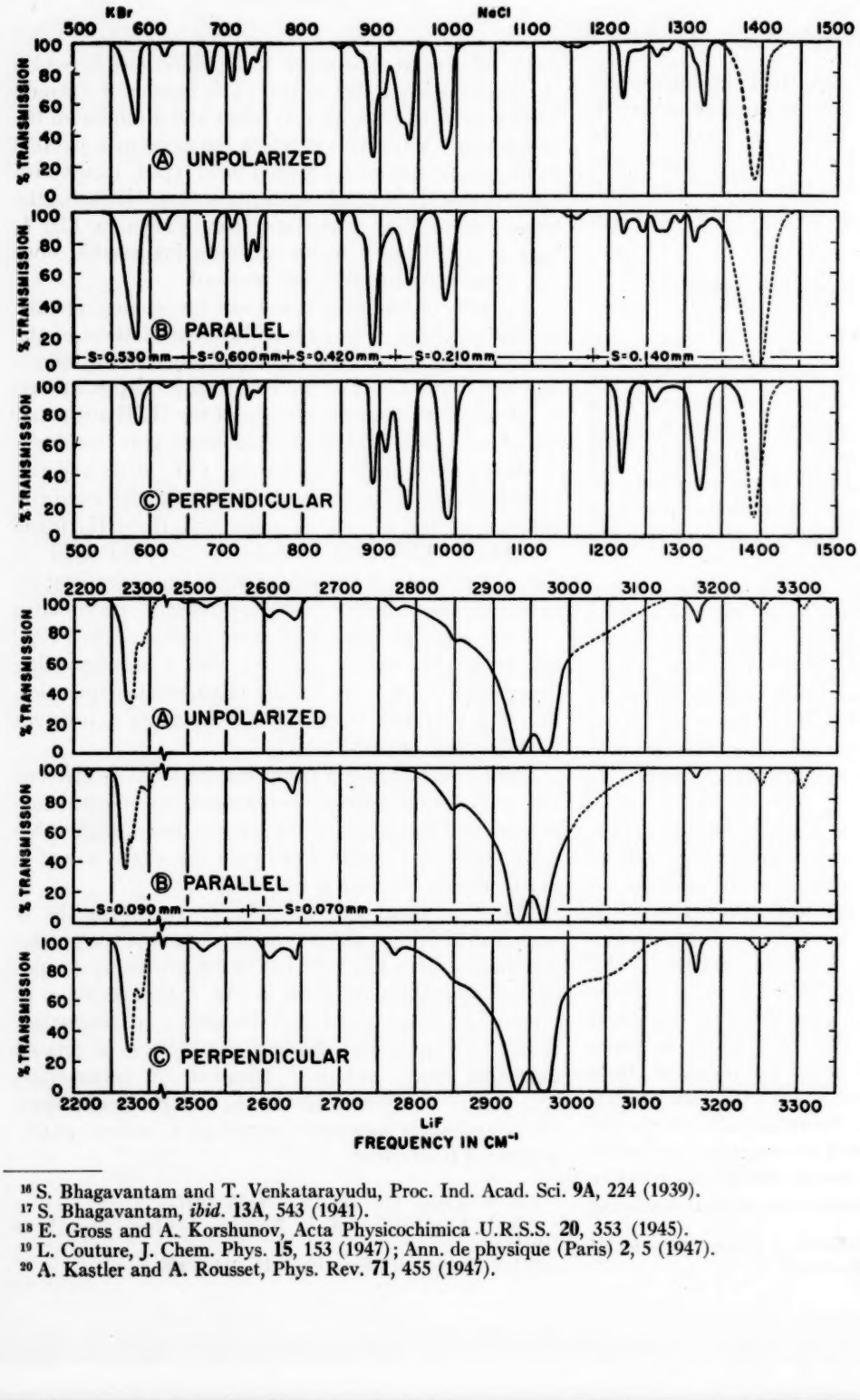

FIG. 4. Infra-red absorption spectra of linearly oriented solid malononitrile (*ca.* 0.01 mm thick) with incident radiation (*A*) unpolarized, (*B*) polarized with *E* vector parallel to direction of crystal growth, and (*C*) polarized with *E* vector perpendicular to direction of crystal growth.

[16] S. Bhagavantam and T. Venkatarayudu, Proc. Ind. Acad. Sci. **9A**, 224 (1939).
[17] S. Bhagavantam, *ibid.* **13A**, 543 (1941).
[18] E. Gross and A. Korshunov, Acta Physicochimica U.R.S.S. **20**, 353 (1945).
[19] L. Couture, J. Chem. Phys. **15**, 153 (1947); Ann. de physique (Paris) **2**, 5 (1947).
[20] A. Kastler and A. Rousset, Phys. Rev. **71**, 455 (1947).

TABLE III. Observed infra-red absorption bands of linearly oriented solid malononitrile (*ca.* 0.01 mm thick) using unpolarized and polarized radiation. Polarization is described by the orientation of the *E* vector with respect to the direction of crystal growth.

Unpolarized radiation	Polarized radiation Parallel	Perpendicular	Unpolarized radiation	Polarized radiation Parallel	Perpendicular
582 *M*	582† *S*	582 *W*			
618 *VW*	618† *W*	618 *VW*			
679 *W*	679† *W*	679 *VW*	1735* *VW*	1735* *VW*	1735†* *W*
710 *W*	710 *VW*	710† *M*	2220 *VW*	2220 *VW*	2220 *VW*
730 *W*	730† *M*	730 *W*	2268 *M*	2268† *M*	—
741 *W*	741† *W*	741 *VW*	2275 *M*	2275 *M*	2275† *S*
847 *VW*	847† *VW*	—	2290 *W*	—	2290† *M*
873 *VW*	873† *VW*	873 *VW*	2298 *VW*	2298† *W*	—
891 *S*	891† *S*	891 *M*	2495 *VW*	—	2495† *VW*
907 *W*	—	907† *M*	2523 *VW*	—	2523† *VW*
929 *M*	—	929† *M*	2608 *W*	2608 *VW*	2608† *W*
938 *M*	938 *M*	938† *S*	2639 *W*	2638† *W*	—
986 *M*	984† *M*	—		—	2642† *W*
	—	990† *S*	2770 *VW*	—	2770† *VW*
1145 *VW*	1145† *VW*	—	2849 *VW*	2849† *W*	2849 *VW*
1159 *VW*	1159† *VW*	—	2934 *VS*	2934† *VS*	2934 *VS*
1218 *M*	1218 *W*	1218† *M*	2968 *VS*	2968 *VS*	2968† *VS*
ca. 1243 *VW*	1243† *W*	—	*ca.* 3050 *VW*	—	*ca.* 3050† *W*
1263 *VW*	*ca.* 1263 *W*	1263 *W*	3165 *W*	3165 *VW*	3165† *W*
1277 *VW*	*ca.* 1277† *W*	—	3243 *VW*	—	3243† *VW*
1292 *VW*?	1292† *VW*	—	3251 *VW*	3251† *W*	3251 *VW*
1312 *VW*	1312† *W*	—	3306 *VW*	3306† *W*	3306 *VW*
1324 *M*	1324 *VW*	1324† *M*	3340 *VW*	—	3340† *VW*
1392 *S*	1392† *VS*	1392 *S*			

† Denotes polarization of bands—i.e., the orientation of the *E* vector showing the greater absorption intensity.
* These bands were not shown in Fig. 4 because of interference by atmospheric water vapor.

Consequently, the strong infra-red bands of crystalline malononitrile are correlated with the fundamental vibrational modes of the vapor molecules.

Intensities of bands appear to be more sensitive to the molecular environment than their frequencies so that relative absorption intensities of a solid and the corresponding vapor may differ considerably. Vibrations which are not infra-red active in the free molecule because of symmetry restrictions may become active in the solid if the effective molecular symmetry in the crystal (site symmetry) is lower than for the free molecule. Halford[1] has given a method for obtaining vibrational selection rules in crystals by considering the motions of one molecule moving in a potential field reflecting its environment.

A further point of interest in connection with the spectra of crystalline solids is the influence of molecular orientation. Since the molecules ordinarily are in fixed positions in the crystal, the orientation of a crystal (or crystals) with respect to the incident radiation will determine the orientation of the individual molecules. The intensity of a given spectral transition in infra-red absorption is determined, among other factors, by the component of the incident *E* vector along the transition moment of the molecule. (The transition moment may or may not be parallel to a certain chemical bond.) Thus, if the molecules are oriented in a specific direction with respect to the incident *E* vector, intensities of absorption bands may vary considerably from those for a random orientation. (Some bands may show a sharp increase in intensity while others decrease or even vanish.) Since this change is a function of spatial orientation, all transition moments with the same symmetry properties (i.e., of the same symmetry species) should behave in the same way. This behavior then is an aid in classifying the spectral transitions. If the molecular orientation is achieved by a single crystal, or by a similar orientation of several crystals, the symmetry species of the site group[1] (rather than of the molecular point group) should be used to classify the transition moments. In general, the site group species are combinations of the molecular point group species

TABLE IV. Symmetry species, characters, and selection rules for point group C_{2v}

C_{2v}	I	$C_2^{(z)}$	σ_{yz}	σ_{xz}	Selection rules R	IR
A_1	+1	+1	+1	+1	+	+
A_2	+1	+1	−1	−1	+	−
B_1	+1	−1	+1	−1	+	+
B_2	+1	−1	−1	+1	+	+

TABLE V. VFSC with symmetry designations

C_{2v}	*VFSC*	C_{2v}	VFSC
A_1	$S_1=2^{-\frac{1}{2}}(\Delta r_{13}+\Delta r_{23})$	B_1	$S_9=2^{-\frac{1}{2}}(\Delta r_{13}-\Delta r_{23})$
	$S_2=2^{-\frac{1}{2}}(\Delta r_{45}+\Delta r_{67})$		$S_{10}=\Delta\rho$
	$S_3=\Delta\alpha$		$S_{11}=2^{-\frac{1}{2}}(\Delta\phi_4+\Delta\phi_7)$
	$S_4=2^{-\frac{1}{2}}(\Delta r_{34}+\Delta r_{37})$		
	$S_5=\Delta\gamma$		
	$S_6=2^{-\frac{1}{2}}(\Delta\psi_4+\Delta\psi_7)$		$S_{12}=2^{-\frac{1}{2}}(\Delta r_{45}-\Delta r_{67})$
A_2	$S_7=\Delta\tau$	B_2	$S_{13}=\Delta\omega$
	$S_8=2^{-\frac{1}{2}}(\Delta\phi_4-\Delta\phi_7)$		$S_{14}=2^{-\frac{1}{2}}(\Delta r_{34}-\Delta r_{37})$
			$S_{15}=2^{-\frac{1}{2}}(\Delta\psi_4-\Delta\psi_7)$

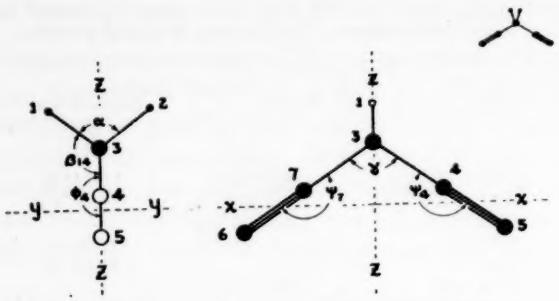

FIG. 5. Structural parameters for malononitrile.

resulting from symmetry restrictions imposed on the molecule by the surrounding crystal.

For a sufficiently fine powder mulled with "Nujol," a random orientation of crystals is expected. Consequently, no differences should appear in the infra-red spectrum whether polarized or unpolarized incident radiation is used, and the general selection rules[1] for the crystal should apply.

Liquid and Solution

Since molecules in the liquid state and in solution are assumed to have a random orientation in an environment with no specific symmetry, rigid selection rules do not apply. However, infra-red bands in the liquid arising from vibrations which are forbidden to absorb in the vapor will probably be weak (relative to active fundamentals).

IV. ASSIGNMENT OF OBSERVED FREQUENCIES

The C—H stretching vibrations $\nu_9(b_1)$* and $\nu_1(a_1)$ are assigned the values 2976 cm^{-1} (type *C* band) and 2951 cm^{-1} (type *B* band), respectively, from the vapor data. (Correlation of the vapor, liquid, and solid molecular vibrational frequencies is given in Table VI.) Both of the C≡N stretching vibrations $\nu_{12}(b_2)$ and $\nu_2(a_1)$ are believed to have the frequency 2274 cm^{-1} in the vapor, the superpositioning of the two bands accounting for the lack of clarity in the band contour. These two vibrational frequencies are not resolved in the liquid or solution spectra, but are definitely separated in the solid spectra using polarized incident infra-red radiation, with the band at 2275 cm^{-1} assigned to ν_{12} and the band at 2268 cm^{-1} assigned to ν_2 (based upon their behavior with respect to the plane of polarization).

The type *B* bands at 1422 cm^{-1} and 1322 cm^{-1} in

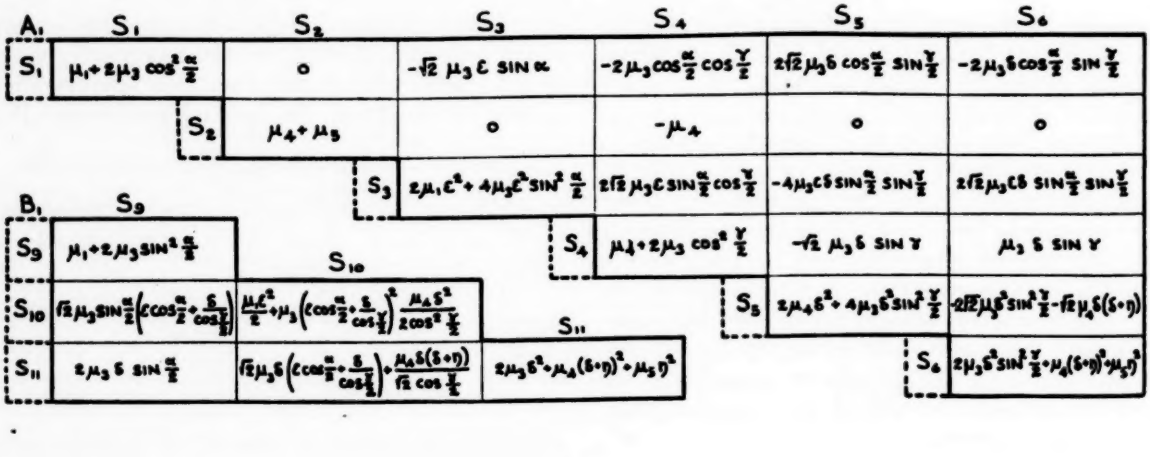

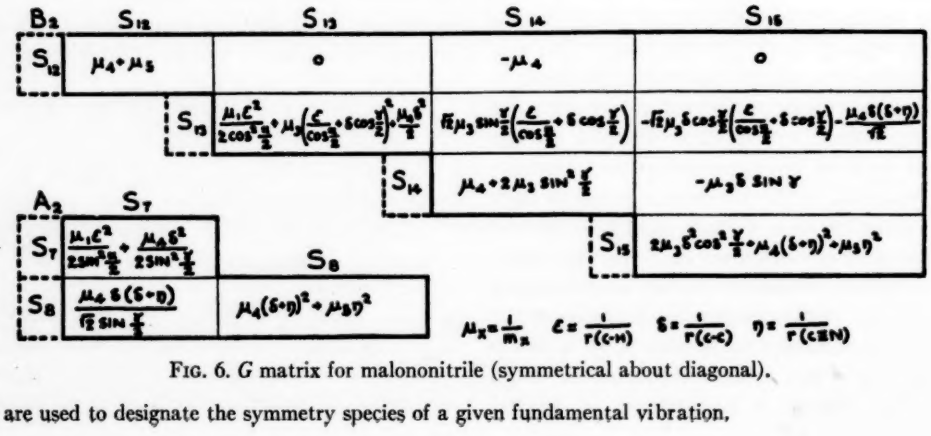

FIG. 6. *G* matrix for malononitrile (symmetrical about diagonal).

* Small letters are used to designate the symmetry species of a given fundamental vibration.

vapor phase infra-red absorption are assigned to methylene deformation, $\nu_3(a_1)$, and methylene wagging, $\nu_{13}(b_2)$, respectively, from considerations of intensities and frequency values in related molecules. Similarly, type B bands at 982 cm^{-1} and 892 cm^{-1} are assigned to $\nu_{14}(b_2)$ and $\nu_4(a_1)$, the antisymmetric and symmetric C−C stretching vibrations. Preliminary calculations using force constants from the literature[14,15] indicated that the methylene rocking frequency, $\nu_{10}(b_1)$, should have a value near 910 cm^{-1}. Since no type C band was found in this region of the vapor spectrum under the conditions of observation, the infra-red band appearing in the liquid at 936 cm^{-1} is assigned to ν_{10}.

Vapor phase measurements were not made at frequencies below 650 cm^{-1}, and so $\nu_5(a_1)$ is assigned the value 582 cm^{-1} from the infra-red data for the liquid, and $\nu_6(a_1)$ the value 167 cm^{-1} from the Raman data[7] for the liquid. There is considerable mixing of coordinates S_4, S_5, and S_6 in producing these low frequency vibrations, and no single coordinate may be associated with the individual frequencies. The three C−C≡N bending vibrations $\nu_8(a_2)$, $\nu_{11}(b_1)$, and $\nu_{15}(b_2)$ are assumed accidentally degenerate and assigned the value 367 cm^{-1} from the strong Raman line for the liquid.

Calculations indicated the methylene twisting vibration, $\nu_7(a_2)$, should have a frequency near 1240 cm^{-1}. Since this vibration is inactive in vapor phase infra-red absorption but should be Raman active, the line at 1214 cm^{-1} reported by Kohlrausch and Ypsilanti[7] for the liquid is assigned to ν_7. This Raman line is correlated with the weak infra-red absorption found in the liquid at 1225 cm^{-1} and with the stronger absorption found in the solid at 1218 cm^{-1}. (A round number value of 1220 cm^{-1} is assumed for the vapor.)

Comparison of the infra-red polarization characteristics of the fundamental absorption bands (Fig. 4) indicates that the transitions of species A_1 are polarized parallel, and species A_2, B_1, and B_2 perpendicular to the direction of crystal growth. In the case of species A_2, however, this direction of polarization is based only on the correlation between the solid absorption band at 1218 cm^{-1} and the liquid Raman line at 1214 cm^{-1} (ν_7).

Since all the fundamental vibrational frequencies have been assigned, the remaining infra-red bands must be the result of combinations. Assignment of combinations is facilitated by the consideration of both band contours in the vapor and band polarizations in the solid. For example, since the band at 3168 cm^{-1} in the vapor has a type B contour, the transition must be of species A_1 or B_2. However, the polarization of the corresponding band in the solid eliminates the possibility of the transition being of species A_1. Therefore, this band is assigned to the combination $\nu_4+\nu_{12}$ of species B_2.

In order to explain the contour of the infra-red vapor band at 2623 cm^{-1}, a superpositioning of a type C band with a type A and/or a type B band is assumed. These band types may be obtained from the following possible combinations: $\nu_2+\nu_{15}$ (type A band); $\nu_2+\nu_{11}$ and $\nu_{12}+\nu_8$ (type C bands); $\nu_{12}+\nu_{15}$ and $2\nu_{13}$ (type B bands). In the solid two slightly separated bands appear with opposite polarization characteristics, so that all these combinations have to be considered.

F	S_1	S_2	S_3	S_4	S_5	S_6	S_{12}	S_{13}	S_{14}	S_{15}
S_1	F_1	0	0	0	0	0	←(A_1)			
S_2	0	F_2	0	0	0	0				
S_3	0	0	F_3	$f_{3,4}$	$f_{3,5}$	0				
S_4	0	0	$f_{4,3}$	F_4	$f_{4,5}$	0				
S_5	0	0	$f_{5,3}$	$f_{5,4}$	F_5	0				
S_6	0	0	0	0	0	F_6				
S_{12}	(B_2)→						F_{12}	0	0	0
S_{13}							0	F_{13}	$f_{13,14}$	0
S_{14}							0	$f_{14,13}$	F_{14}	0
S_{15}							0	0	0	F_{15}

FIG. 7. Assumed F submatrices for A_1 and B_2 species of malononitrile.

Assignments for all except the very weak bands, together with the Raman data,[7] are given in Table VI.

V. FORCE CONSTANTS

In order to simplify calculation of force constants, carbon-hydrogen and carbon-nitrogen stretching coordinates were factored out of the secular equation using the method described by Wilson.[13] The error introduced by this approximation is believed to be no greater than that imposed by the nature of the potential function assumed. Structural parameters were assigned the same values as in the estimation of moments of inertia. The second-order determinants for species A_2 and B_1 were then investigated, and the diagonal force constants F_7 (methylene twisting), F_{10} (methylene rocking), and F_8, F_{11} (C−C≡N bending) evaluated. These values were used as guides for the determination of similar constants in the A_1 and B_2 factors. The values chosen as representing a reasonable set of force constants for malononitrile and a comparison of calculated and observed frequencies are given in Table VII. Since inclusion of the carbon-nitrogen stretching coordinate in the A_1 factor of the secular equation would be expected to shift the 1449-cm^{-1} frequency downward, a closer agreement than two percent above the observed value was not attempted (using the fourth-degree equation). Terms $f_{4,5}$ and $f_{13,14}$ (involving interactions between bending and stretching coordinates) were found necessarily large. The following relationships exist between the force constants: $F_1=K_H+k_H$; $F_9=K_H-k_H$; $F_4=K_C+k_C$; $F_{14}=K_C-k_C$; $F_2=K_N+k_N$; $F_{12}=K_N-k_N$; $F_6=K_\psi+k_\psi$; $F_{15}=K_\psi-k_\psi$; $F_8=K_\phi-k_\phi$; and

TABLE VI. Vibrational assignments for malononitrile.

Descriptive assignment	Gas	Infra-red Liquid	Solid	Raman* Liquid
$\nu_6(a_1)\psi$, γ	—	—	—	167 (10*b*)
$\nu_8(a_2)$	—	—	—	367 (10)
$\nu_{11}(b_1)$ C−C≡N bend	—	—	—	367 (10)
$\nu_{15}(b_2)$	—	—	—	367 (10)
$\nu_5(a_1)\gamma$, ψ	—	582 *M*	582 *M*	574 (3*b*)
$4\nu_9(A_1)$?	—	—	679 *W*	—
$2\nu_6+\nu_{11}(B_1)$	—	702 *W*	710 *W*	—
$2\nu_8(2\nu_{11}, 2\nu_{15})A_1$	—	728 *VW*	730 *W*	—
$\nu_5+\nu_9(A_1)$	—	—	741 *W*	—
$\nu_4(a_1)$C−C stretch	892 *S*	893 *S*	891 *S*	892 (5)
$\nu_8+\nu_9+\nu_{11}(B_2)$	—	908 *VW*	907 *W*	—
$\nu_5+\nu_{11}(B_1)$	—	—	929 *M*	—
$\nu_{10}(b_1)$CH$_2$ rock	—	936 *M*	938 *M*	—
$2\nu_5-\nu_6(A_1)$	—	?	984 *W*	—
$\nu_{14}(b_2)$C−C stretch	982 *S*	984 *S*	990 *M*	975 (1)
$\nu_6+\nu_{10}(B_1)$	—	—	—	1107 (1)
$\nu_7(a_2)$CH$_2$ twist	—	1225 *VW*	(1218 *M*)	1214 (3)
$\nu_4+\nu_{15}(B_2)$	1265 *M*	1263 *VW*	1263 *VW*	—
$\nu_{13}(b_2)$CH$_2$ wag	1322 *S*	1320 *W*	1324 *M*	1310 (2)
$\nu_3(a_1)$CH$_2$ deformation	1422 *VS*	1395 *VS*	1392 *S*	1386 (4)
$\nu_2(a_1)$C≡N stretch	2274 *W*	2275 *M*	2268 *M*	2263 (7)
$\nu_{12}(b_2)$C≡N stretch	2274 *W*	2275 *M*	2275 *M*	2263 (7)
$\nu_{10}+\nu_{14}+\nu_{15}(B_1)$	—	—	2290 W	—
$\nu_3+\nu_{10}(B_1)$	2333 *W*	—	—	—
$\nu_{12}+2\nu_9(B_2)$	—	2603 *VW*	2608 *W*	—
$2\nu_{13}(A_1)$ / $\nu_{12}+\nu_{15}(A_1)$	2623 *M*	2637 *W*	2638 *W*	—
$\nu_3+\nu_{15}(B_2)$ / $\nu_2+\nu_{11}(B_1)$	2623 *M*	2637 *W*	2642 *W*	—
$\nu_3+\nu_{13}(B_2)$	2739 *W*	—	—	—
$\nu_1(a_1)$C−H stretch	2951 *W*	2935 *VS*	2934 *VS*	2929 (5)
$\nu_9(b_1)$C−H stretch	2976 *M*	2968 *VS*	2968 *VS*	2960 (1)
$\nu_4+\nu_{13}(B_2)$	3168 *W*	3168 *W*	3165 *W*	—

* Raman data from Kohlrausch and Ypsilanti, reference 7.

$F_{11}=K_\phi+k_\phi$, where the small letters represent interaction terms between equivalent valence force coordinates and the capital letters represent diagonal terms.

A comparison between these constants and certain values found in the literature is given in Table VIII. Values reported by Crawford and Brinkley[14] are for methyl cyanide, and by Decius[15] are for methylene chloride. Substitution of nitrile groups by chlorine atoms does not appear to produce any marked changes in the methylene force constants. The transformation matrix used to correlate the potential functions, together with a general method for obtaining such matrices, is given in the Appendix.

VI. THERMODYNAMIC FUNCTIONS

Since the fundamental vibrational frequencies of the molecule have been determined and the moments of inertia have been estimated, the thermodynamic functions for the vapor may be calculated. Values obtained for the temperature range 298.16°–1000°K are given in Table IX in terms of calories per mole per degree. The translational and rotational contributions were obtained using the working equations given by Wagman *et al.*[21] and vibrational contributions using the tables given by Aston.[22] The set of frequencies used as best representing the free molecule are those given in the observed column of Table VII.

[21] D. Wagman, J. E. Kilpatrick, W. J. Taylor, K. S. Pitzer, and F. D. Rossini, J. Research Nat. Bur. of Stand. 34, 143 (1935).

[22] J. G. Aston, in Taylor and Glasstone, *Treatise on Physical Chemistry* (D. Van Nostrand Company, Inc., New York, 1942), Vol. 1, pp. 655–658.

ACKNOWLEDGMENTS

The authors wish to express their appreciation to Mr. L. J. Hughes for the preparation of the malononitrile, to Mr. E. J. Thomas for the photomicrograph in Fig. 3, and to Dr. R. C. Gore and Mr. M. C. Botty for the construction of the infra-red polarizer.

APPENDIX

In some cases it is convenient to use internal coordinates, q, other than the customary valence force coordinates, w, in setting up the secular equation, and it is desired to transform the one harmonic force constant system into the other. Since the net force acting on an atom in its equilibrium position is zero, the variations of the q's and w's are the coordinates actually used in treating small vibrations. If the n independent coordinates, q, are defined over the n dimensional configuration space R, and the k coordinates w are contained in R (the w's need not all be independent), the variations of the w's are given by

$$\delta w_m=\sum_{c=1}^{n}(\partial w_m/\partial q_c)_{\substack{q_i=\text{const}\\ i\neq c}}\delta q_c,\ m=1,\cdots,k \qquad \text{(a1)}$$

or in matrix form

$$\delta w=M\delta q, \qquad \text{(a2)}$$

where

$$[M]_{cd}=(\partial w_c/\partial q_d)_{\substack{q_i=\text{const.}\\ i\neq d}}$$

For these infinitesimal displacements the elements of M may be obtained from the expression

$$[M]_{cd}=\sum_i \mathbf{s}_{ci}\cdot\mathbf{t}_{id}, \qquad \text{(a3)}$$

where the sum is over all the atoms. (In practice one or both vectors will be zero for most atoms, so that only a few terms appear in (a3)). The $\mathbf{s}_{ci}$ are the vectors used by Wilson[13] for calculating the reciprocal kinetic energy matrix, G. The set of vectors $\mathbf{t}_{id}$

TABLE VII. Force constants and fundamental frequencies for malononitrile vapor.

C_{2v}	Force constants*	Coordinate descriptions	Frequencies Calculated	Frequencies Observed
A_1	F_1 = —	C−H stretch	—	2951
	F_2 = —	C≡N stretch	—	2274
	F_3 =0.670	CH$_2$ deformation	1449	1422
	F_4 =4.95	C−C stretch	878	892
	F_5 =1.25	C−C−C bend	582	582
	F_6 =0.350	C−C≡N bend	167	167†
A_2	F_7 =1.326	CH$_2$ twist	1220	(1220)‡
	F_8 =0.333	C−C≡N bend	366	367†
B_1	F_9 = —	C−H stretch	—	2976
	F_{10}=0.700	CH$_2$ rock	936	936
	F_{11}=0.349	C−C≡N bend	367	367†
B_2	F_{12}= —	C≡N stretch	—	2274
	F_{13}=0.663	CH$_2$ wag	1321	1322
	F_{14}=4.495	C−C stretch	982	982
	F_{15}=0.322	C−C≡N bend	366	367†
A_1	$f_{3,4}$=−0.080	Interaction		
	$f_{3,5}$=+0.160	Interaction		
	$f_{4,5}$=+0.372	Interaction		
B_2	$f_{13,14}$=−0.400	Interaction		

* Units of force constants are 10^5 dyne cm^{-1} for stretching coordinates, 10^{-11} dyne cm for bending coordinates, and 10^{-5} dyne for interaction of stretching and bending.
† Reference 7.
‡ Estimated.

TABLE VIII. Comparison of force constants with those for some related molecules.

Force constant	Present paper	Related molecules
F_3	0.670	0.679†
F_7	1.326	1.294†
F_{10}	0.700	0.764†
F_{13}	0.663	0.579†
$f_{3,5}$	0.160	0.149†
$\frac{1}{2}(F_4+F_{14})$	4.722	4.94*
$\frac{1}{4}(F_6+F_8+F_{11}+F_{15})$	0.339	0.344*

* Reference 14, for methyl cyanide.
† Reference 15, for methylene chloride.

are defined by the expression

$$\mathbf{t}_{ld}=(\partial\mathbf{r}_l/\partial q_d)_{q_i=\text{const},\, i\neq d},\quad l=1,\ 2,\ \text{etc.},\qquad \text{(a4)}$$

where $\mathbf{r}_l$ is the position vector of atom l with its origin arbitrarily fixed in the molecule. In general, this set of vectors will not be unique, but the value obtained for $[M]_{cd}$ is independent of the particular set chosen provided there is internal consistency. In order to determine such a set of vectors given by (a4), the coordinate q_d is permitted to increase from its equilibrium value by a small positive amount, keeping all other q's constant (and usually by moving as few atoms as are necessary). Then $\mathbf{t}_{ld}$ is a vector pointing in the direction in which the l'th atom started to move, and with a magnitude equal to the displacement of the l'th atom for a unit change in q_d. Its magnitude may be checked or determined from the condition that:

$$\sum_l \mathbf{s}_{dl}\cdot\mathbf{t}_{ld}=1.$$

TABLE IX. Thermodynamic functions for malononitrile vapor (cal. mole^{-1} deg.$^{-1}$).

Absolute temperature	$C_p°$	$\frac{(H°-H_0°)}{T}$	$-\frac{(F°-H_0°)}{T}$	$S°$
298.16	17.32	12.13	56.92	69.05
300	17.38	12.17	56.99	69.16
400	20.22	13.83	60.75	74.59
500	22.61	15.36	63.98	79.33
600	24.60	16.74	66.90	83.64
700	26.28	17.99	69.58	87.57
800	27.72	19.11	72.04	91.16
900	28.95	20.14	74.35	94.49
1000	30.00	21.07	76.53	97.61

Abbreviating the δw's and the δq's by W and Q, and using matrix notation,

$$2V=W'KW=Q'M'KMQ=Q'FQ,$$

where

$$F=M'KM \qquad \text{(a5)}$$

is the desired result. If the molecule possesses symmetry elements, they may be used to reduce the number of M matrix elements to be calculated.

The potential energy function for malononitrile expressed in terms of coordinates of the type used by Crawford and Brinkley[14] and by Decius[15] would be

$$\begin{aligned}2V=&K_\beta[(\Delta\beta_{14})^2+(\Delta\beta_{24})^2+(\Delta\beta_{17})^2+(\Delta\beta_{27})^2]\\&+2k_\beta{}^b[(\Delta\beta_{14})(\Delta\beta_{17})+(\Delta\beta_{24})(\Delta\beta_{27})]\\&+2k_\beta{}^c[(\Delta\beta_{14})(\Delta\beta_{24})+(\Delta\beta_{17})(\Delta\beta_{27})]\\&+2k_\beta{}^d[(\Delta\beta_{14})(\Delta\beta_{27})+(\Delta\beta_{17})(\Delta\beta_{24})]\\&+K_\alpha(\Delta\alpha)^2+K_\gamma(\Delta\gamma)^2+K_R[(\Delta r_{34})^2+(\Delta r_{37})^2]\\&+2k_R(\Delta r_{34})(\Delta r_{37})+2k_{R\gamma}(\Delta\gamma)[\Delta r_{34}+\Delta r_{37}]\\&+2k_{R\beta}{}^a[(\Delta r_{34})(\Delta\beta_{14}+\Delta\beta_{24})+(\Delta r_{37})(\Delta\beta_{17}+\Delta\beta_{27})]\\&+2k_{R\beta}{}^b[(\Delta r_{34})(\Delta\beta_{17}+\Delta\beta_{27})+(\Delta r_{37})(\Delta\beta_{14}+\Delta\beta_{24})]\\&+\{K_H[(\Delta r_{13})^2+(\Delta r_{23})^2]+2k_H(\Delta r_{13})(\Delta r_{23})\\&+K_N[(\Delta r_{45})^2+(\Delta r_{67})^2]+2k_N(\Delta r_{45})(\Delta r_{67})\\&+K_\phi[(\Delta\phi_4)^2+(\Delta\phi_7)^2]+2k_\phi(\Delta\phi_4)(\Delta\phi_7)\\&+K_\psi[(\Delta\psi_4)^2+(\Delta\psi_7)^2]+2k_\psi(\Delta\psi_4)(\Delta\psi_7)\},\end{aligned}\qquad \text{(a6)}$$

where the portion enclosed by braces is the same as in the present paper. The first eight coordinates used (seven of them being independent) are related to the other *VFSC* of Table V by the transformation matrix, M,

	$(\Delta\rho)$	$(\Delta\omega)$	$(\Delta\tau)$	$(\Delta\alpha)$	$(\Delta\gamma)$	(Δr^+)	(Δr^-)
M	S_{10}	S_{13}	S_7	S_3	S_5	S_4	S_{14}
$\Delta\beta_{14}$	$-A$	$-B$	$+C$	$+D$	$+D$	0	0
$\Delta\beta_{24}$	$+A$	$-B$	$-C$	$+D$	$+D$	0	0
$\Delta\beta_{17}$	$-A$	$+B$	$-C$	$+D$	$+D$	0	0
$\Delta\beta_{27}$	$+A$	$+B$	$+C$	$+D$	$+D$	0	0
$\Delta\alpha$	0	0	0	1	0	0	0
$\Delta\gamma$	0	0	0	0	1	0	0
Δr_{34}	0	0	0	0	0	$(2)^{-\frac{1}{2}}$	$(2)^{-\frac{1}{2}}$
Δr_{37}	0	0	0	0	0	$(2)^{-\frac{1}{2}}$	$-(2)^{-\frac{1}{2}}$

Elements A, B, C, and D are defined as follows:

$$A=2D=\cot\beta\,\tan\tfrac{1}{2}\alpha,$$
$$B=-\cot\beta\,\tan\tfrac{1}{2}\gamma,$$
$$C=\sin\tfrac{1}{2}\alpha\,\sin\tfrac{1}{2}\gamma\,\csc\beta.$$

Letting K represent the potential energy submatrix of (a6) relating to these eight coordinates, and $\mathfrak{F}$ the submatrix of F for the corresponding *VFSC*, the force constant transformation used in Table VIII is given by

$$\mathfrak{F}=M'KM.$$

Thermodynamics of Crystallization in High Polymers. VI. Incipient Crystallization in Stretched Vulcanized Rubber*,**

THOMAS G. FOX, JR.,*** PAUL J. FLORY,*** AND ROBERT E. MARSHALL
Goodyear Tire and Rubber Company, Research Laboratory, Akron, Ohio
(Received December 13, 1948)

Experimental determination of the elongation at which crystallization commences in vulcanized rubber has been attempted through measurement of density changes by a hydrostatic method. The critical elongation for incipient crystallization appears to depend on the temperature in approximate accordance with theoretical prediction. Crystallization sets in at an elongation well below that at which the stress-strain curve assumes a steep slope.

FROM consideration of the statistical thermodynamics of crystallization of rubber on stretching,[1] it has been shown that the temperature (T_m) of incipient crystallization, i.e., the highest temperature above which all crystallinity must disappear, should increase with the relative length α approximately in accordance with the relationship

$$1/T_m^0 - 1/T_m = (R/h_f)\phi(\alpha), \quad (1)$$

where

$$\phi(\alpha) = (6/\pi n)^{\frac{1}{2}}\alpha - \alpha^2/2n - 1/\alpha n. \quad (2)$$

Here T_m^0 is the crystallization temperature for the unstretched polymer ($\alpha=1$), h_f is the heat of fusion per polymer segment, R is the gas constant, and n represents the number of "statistical segments" per chain between cross linkages. With the object of establishing the dependence of T_m on α, we have measured the density of gum vulcanized rubber as a function of elongation at three temperatures, 20, 40, and 60°C, abrupt increase in density being used as the criterion for the onset of crystallization.[2] Experimental difficulties are formidable and they were not entirely overcome in the work reported here. Inasmuch as it has been necessary to abandon further work on this project, the significant results which have been obtained are set forth briefly below.

EXPERIMENTAL

Each of six molded rubber bands,[3] 0.1×1.0 cm in section and having a circumference of 10 cm, was marked at distances $L_0=3.00$ cm apart on its outer surface. The bands were evenly stretched about pairs of aluminum support rods $\frac{3}{16}''$ in diameter which were inserted through appropriately spaced holes drilled (perpendicular to the axis) through an aluminum tube 20″ long and $\frac{1}{2}''$ in diameter. The holes were so arranged as to provide relative lengths α from 1.0 to 10 in steps of 0.25. This assembly, suspended by a thin wire from one arm of an analytical balance, was immersed in water contained in a tall glass cylinder located in a water thermostat regulated to ±0.01°C. Weighings were accurate to the nearest milligram.

In carrying out an experiment, the unstretched bands were weighed in air and then in water at the temperature of the experiment. After stretching at room temperature to the desired elongation, they were held in water at a high temperature (either 70° or 90°) for ten minutes to melt crystallites which may have been formed. The bands were quickly transferred to the constant temperature bath and the weight determined after thirty minutes. On removal from the bath, the distances between the marks were measured first in the stretched condition (L_s) and then unstretched (L_0''). They were again stretched at room temperature and the cycle repeated.

RESULTS

The distance L_0'' between the marks on the bands on release of tension assumed successively larger values as the measurements proceeded from one elongation to the next, etc. This residual elongation was reduced slightly by immersion of the bands in petroleum ether (and drying in vacuo) and hence was due in part to slow elastic recovery. The remaining "permanent set" has been attributed[4] to a reversible breaking and reforming of chemical bonds between chains while the rubber is under tension. Upon release of tension the bonds which were formed while the sample was stretched oppose

* Contribution No. 158 from the Goodyear Tire and Rubber Company, Research Laboratory. The work presented in this paper comprises a part of a program of fundamental research on rubber and plastics carried out under contract between the ONR and the Goodyear Tire and Rubber Company.

** Paper V of this series, by R. D. Evans, H. R. Mighton, and P. J. Flory, was presented before the High Polymer Forum of the American Chemical Society, September, 1947, and will be published shortly. For Paper IV, see J. Chem. Phys. 17, 223 (1949).

*** Present address: Department of Chemistry, Cornell University, Ithaca, New York.

[1] Paper I of this series by P. J. Flory, J. Chem. Phys. 15, 397 (1947).

[2] W. L. Holt and A. T. McPherson, J. Research Nat. Bur. Stand. 17, 657 (1936).

[3] These bands were compounded according to the following formula, the relative amounts of the ingredients being given in parts by weight: Pale Crepe (100), zinc stearate (1), zinc oxide (2), mercaptobenzothiazole (0.5), phenyl β-Naphthylamine (1), and sulfur (2). The bands were cured for 30 min. at 287°F. Test sheets prepared in this way exhibited a tensile strength of 2200 lbs./in.² and an ultimate elongation of 820 percent.

[4] A. V. Tobolsky, I. B. Prettyman, and J. H. Dillon, J. App. Phys. 5, 380 (1944).

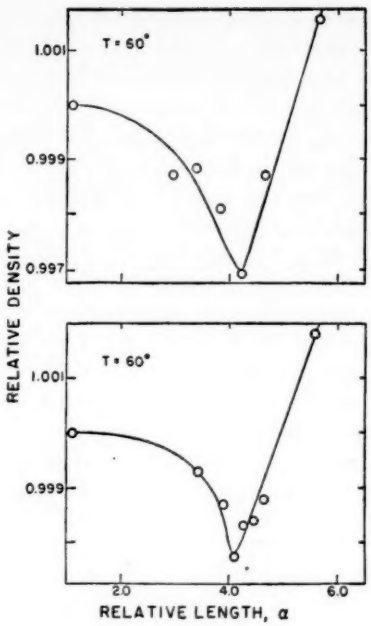

FIG. 1. Density-elongation curves obtained at 60° for two similar sets of bands.

contraction of the rubber.[5] The resulting increase in L_0 appears to be characteristic of the modified network structure and must therefore be accounted for in the calculation of the elongation. As an approximate corrective measure, α has been taken equal to L_s/L_0' where L_0' represents the distance between the marks after removal of the load and relaxation by solvent treatment. In practice L_0' was obtained from the observed values of L_0'' by means of a calibration curve relating the two lengths.

Density-time studies made at 40° indicated that although the major portion of the density change had occurred within thirty minutes, the time necessary to attain an apparent equilibrium varied from at least one hour at low elongation to at least ten hours at elongations above the crystallization point. In view of the occurrence of stress relaxation, such prolongation of the experiments obviously was impractical. While the equilibrium curve probably would differ from that reported here, the equilibrium elongation at which the density suddenly increases doubtless would occur near the position observed in these experiments. Hence, we believe that the present method yields a useful approximation to the equilibrium point for incipient crystallization.

The results of two experiments at 60° are shown in Fig. 1. The decrease in density with increasing α at low elongations is far greater than would be calculated from the compressibility.[6] This anomalous increase in volume may be due to the formation on stretching of vacuoles about solid vulcanization ingredients embedded in the rubber.[2,7] The elongation at the minimum point of the curve (α_c) is characteristic of the temperature and was taken as the point of incipient crystallization. The data are scattered and are not entirely reproducible for differ-

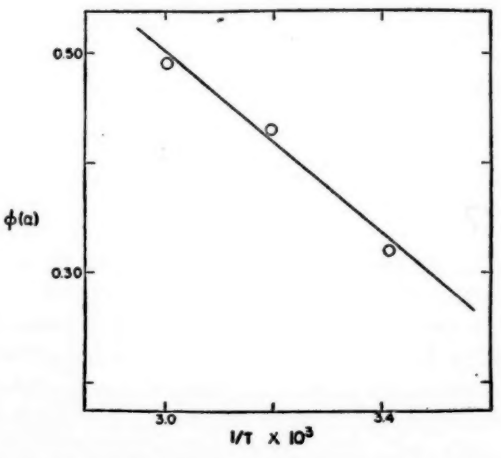

FIG. 2. The relation between the incipient crystallization temperature and the elongation, plotted as $1/T_m$ ($°A^{-1}$) *vs.* $\phi(\alpha)$.

[5] Immersion of these bands in boiling water (a treatment speeding up both viscous relaxation and chemical rupture of bonds) reduced the ratio L_s/L_0'' from 1.3 to 1.1 in four hours, with an indication that heating for longer periods would reduce the ratio further.

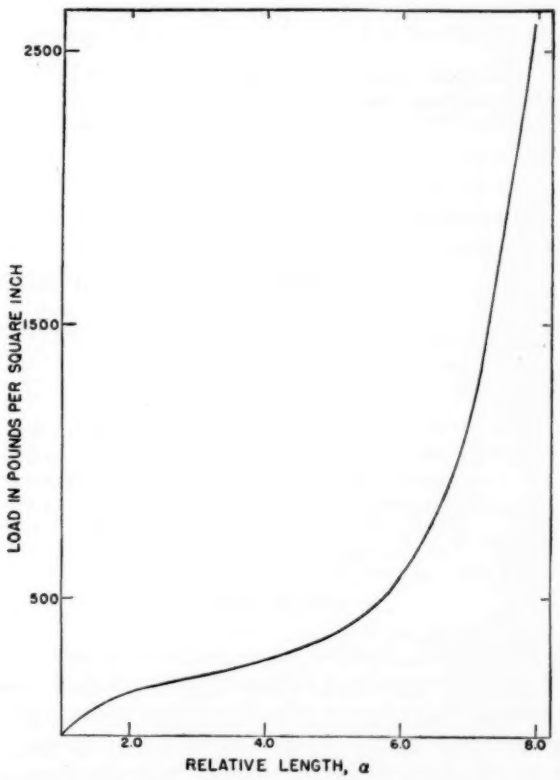

FIG. 3. The stress-strain curve for the rubber bands at room temperature.

[6] G. Gee, Trans. Faraday Soc. 42, 585 (1946).

[7] Dr. Gee and collaborators of the British Rubber Producers Research Association have independently observed a similar anomalous increase in volume, which they likewise attribute to vacuole formation. We are indebted to Dr. Gee for providing us with this unpublished information.

TABLE I. Incipient crystallization in vulcanized rubber.

T_m	$1/T_m$, °A^{-1}	α_c	$\phi(\alpha)$
60°	3.003×10^{-3}	4.10	0.48
40	3.195	3.60	0.43
20	3.413	2.50	0.31
		1	0.12

ent sets of bands. However, the values of α_c at 20, 40, and 60° (Table I) are probably accurate to ±0.20.

Values of $\phi(\alpha)$ (Table I) were calculated from these data by Eq. (2) assuming $n=100$. From the straight line drawn through the plot in Fig. 2 of $1/T_m$ *vs.* $\phi(\alpha)$, h_f and T_m^0 according to Eq. (1) were found to be 400 R cal. and -17°C, respectively. This value of h_f compares favorably with the estimate of 600 (±300) R suggested previously by one of the authors,[1] and with the value of 465 R recently deduced in a similar manner by Goppel[8] using incipient crystallization temperatures determined by Wildschut. While the true value of T_m^0 is probably above 0°C, the figure obtained here is similar to that (-20°C) employed by Goppel. The discrepancy may be due in part at least to the admitted failure of the theory at low elongations.[1]

The choice of n above is somewhat arbitrary. Fortunately the values of h_f and $1/T_m^0$ are rather insensitive to the choice of n. The equilibrium force of retraction at 100 percent elongation, 78 lbs./in.^{2}, is comparable to that obtained for a rubber vulcanizate known to contain on the average of 100 isoprene units between cross-linkages.[9] Hence, we conclude that the chains in this particular vulcanizate are about 100 *units* long. The configurational segment will not necessarily be identical with the structural unit, however.

From these data it is concluded that the theory predicts correctly the order of magnitude for the change in the incipient crystallization temperature with elongation. The experimental accuracy is not sufficient to determine the exact form of the relationship. Results of significantly greater accuracy are not to be expected from the present method.

A point of additional interest occurs in the relationship between the elongation for incipient crystallization and the shape of the stress-strain curve. Although under approximate equilibrium conditions at room temperature incipient crystallization occurs at $\alpha\cong3$, the stress-strain curve (Fig. 3) does not exhibit a sharp "break" until a relative length α of at least 5 has been reached. Obviously the "break" in this curve must not be identified with the elongation necessary for incipient crystallization. The "break" in the curve presumably represents the region in which the degree of crystallinity becomes large.

[8] J. M. Goppel, Paper presented at the Rubber Technology Conference, London, June 23–25, 1948. The authors are indebted to Dr. Goppel for providing them with a copy of this paper.

[9] P. J. Flory, N. Rabjohn, and M. C. Shaffer, forthcoming publication in J. Polymer Sci.

THE JOURNAL OF CHEMICAL PHYSICS VOLUME 17, NUMBER 8 AUGUST, 1949

Punched Card Calculation of Resonance Energies

MARGARET B. OAKLEY* AND GEORGE E. KIMBALL
Department of Chemistry, Columbia University, New York, New York
(Received December 21, 1948)

The calculation of resonance energies can be greatly simplified by using punched card machines. Two methods are developed. The first is easy to apply and works well for 8-, 10-, and 12-electron problems. This is used for naphthalene. The results lend themselves well to a bond probability calculation from which bond distances in good agreement with other methods are obtained. The second procedure is longer, but makes possible the calculation of anthracene and phenanthrene resonance energies. These are $-2.95_1\alpha$ and $-3.01_9\alpha$, respectively. Bond probabilities and lengths were also calculated from these data.

INTRODUCTION

AROMATIC hydrocarbons are more stable than would be predicted for any single method of drawing valence bonds by the rule of additive bond energies. This lowering of the energy, or resonance energy, is due to the freedom of the double bond electrons to move throughout the molecule instead of being localized in fixed double bonds. The magnitude of the resonance energy and the wave function of the electrons can be found by using quantum mechanics.

The valence electrons of each carbon atom are assumed to occupy one $2s$ and three $2p$ orbitals. The $2s$ and two of the $2p$ orbitals are used in forming single bonds to the adjacent hydrogen and carbon atoms. The remaining $2p$ function or π-orbital, which projects at right angles to the plane of the ring and is antisymmetric with regard to reflection in the plane of the ring, combines only with the corresponding functions on the other carbon atoms.

Two methods of attack which differ in the nature of further approximations have been devised.

Hückel[1] has proposed a molecular orbital method.

* Now Margaret Oakley Dayhoff, Rockefeller Institute for Medical Research, New York, New York.

[1] E. Hückel, Zeits. f. Physik **70**, 204 (1931); **72**, 310 (1931); **76**, 628 (1932).

By means of a Hartree type calculation, an atomic orbital is found for each π-electron. The blended effect of the other atoms and electrons is treated as a perturbation. The secular equation is of the same order as the number of free electrons. The resulting wave functions are linear combinations of the atomic orbitals. To obtain the lowest state of the molecule, two electrons of opposite spin are placed in each molecular orbital, beginning with the lowest energy orbital. The energy is the sum of the energies of each molecular orbital used and the energy of the rest of the molecule. The resonance energy is found by subtracting from this the energy of the molecule with fixed double bonds. Benzene,[1] naphthalene,[1] anthracene,[1] and phenanthrene[2] have all been treated in this manner. The ratios of the energies agree well with the experimental values. This method results in an extreme piling up of electrical charges in the molecule. For an appreciable part of the time all the electrons are located on the same carbon atom, as Van Vleck has pointed out.[3]

The other method of attack was developed originally by Slater,[4] and has been extended by Pauling,[5] Eyring,[6,7] Serber,[8] and many others. The zero-order functions for the perturbation calculation consist of a product of one atomic orbital and one spin function for each electron. For the ground state, only antisymmetrical sums of these, so-called Slater bond eigenfunctions, which are eigenfunctions of S_z of eigenvalue zero and of S^2 of eigenvalue zero, are considered. By a perturbation calculation that linear combination of bond eigenfunctions which leads to the lowest energy is found.

Serber[8] has treated this problem by means of matrix methods and has obtained results for six- and eight-electron problems.

The wave mechanical treatment was developed by Pauling, Eyring, and co-workers. Graphical methods were devised for obtaining the elements of the secular determinant.[5,6] Pauling and Wheland[9] treated the benzene molecule, and Sherman[10] treated naphthalene. Wheland[11] suggested a slightly different method of spin valence, which gives the same results from a different secular matrix. The secular equations are of order $(2N)!/N!(N+1)!$, where $2N$ is the number of free electrons. Thus, for six electrons the order is 5; for 8, 14; for 10, 42; for 12, 132; and for 14, 429. The determination of the elements soon becomes extremely laborious. Jonsson[12] has treated the fourteen-electron problems, anthracene and phenanthrene, by neglecting the contributions of many of the bond eigenfunctions. The ratios of the resonance energies again agree well with experiment.

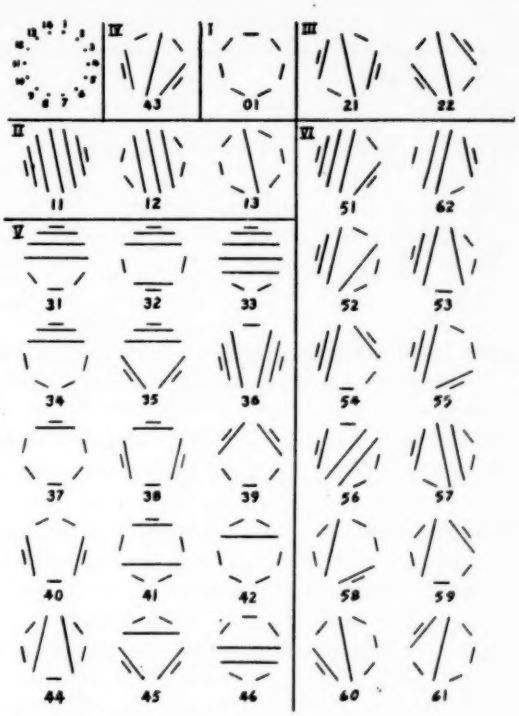

FIG. 1. The 34 types of circle diagrams for 14 electrons.

The bond eigenfunction method underestimates the possibility of more than one electron being near one carbon atom at the same time. This might be expected to be nearer the truth for aromatic hydrocarbons than the molecular orbital approximations.[2]

In the present paper, a punched card method is presented for the determination of the secular determinant elements for a Slater eigenfunction type calculation. This is then applied to the naphthalene molecule. The method is most useful for 8-, 10-, and 12-electron problems. For 14 electrons it becomes too unwieldy.

A second punched card method following Wheland's spin valence procedure is presented. This is used for a complete calculation of the anthracene and phenanthrene molecules.

A punched card iteration method for finding characteristic values and vectors of matrices has been described by Kimball.[13] This procedure was used for naphthalene, anthracene, and phenanthrene in a simplified manner, since all matrix elements and the roots are real.

SLATER EIGENFUNCTION METHOD

THEORY

The secular equations will be derived by the method of Eyring and Kimball,[6] using Slater eigenfunctions.

[2] G. W. Wheland, J. Chem. Phys. **2**, 474 (1934).
[3] J. H. Van Vleck, J. Chem. Phys. **1**, 177, 219 (1933).
[4] J. C. Slater, Phys. Rev. **38**, 1109 (1931).
[5] L. Pauling, J. Chem. Phys. **1**, 280 (1933).
[6] Eyring and G. E. Kimball, J. Chem. Phys. **1**, 239, 626 (1933).
[7] Taylor, Eyring, and Sherman, J. Chem. Phys. **1**, 68 (1933).
[8] R. Serber, J. Chem. Phys. **2**, 697 (1934).
[9] L. Pauling and G. W. Wheland, J. Chem. Phys. **1**, 362 (1933).
[10] J. Sherman, J. Chem. Phys. **2**, 488 (1934).
[11] G. W. Wheland, J. Chem. Phys. **3**, 230 (1935).
[12] C. V. Jonsson, Arkiv. Kemi Mineral. Geol. **15A**, No. 14, 1–9 (1942).
[13] Everett Kimball, Jr., *A Fundamental Punched Card Method for Technical Computations* (Bureau of the Census Memorandum).

TABLE I.

Type of symmetry	N	Anthracene	Phenanthrene
I	01	$n=1$	$n=1, 2$
II	11, 12, 13	$n=1$ to 4	$n=1$ to 4
III	21	$n=1$ to 7	$n=1$ to 7
IV	43	$n=2$ to 5	$n=2$ to 8
V	31 to 42 44 to 46	$n=2$ to 5	$n=1$ to 8
VI	51, 53, 55 57, 59, 61	$n=1$ to 7	$n=1$ to 14

Because the π-electrons and the others do not interact, the Hamiltonian operator is separable. Only the π-electrons will be considered.

Let the eigenfunctions of the carbon atoms be $a(x, y, z)$, $b(x, y, z)$, $\cdots$ and the coordinates of the electrons be $x_1, y_1, z_1, x_2, \cdots$ and set $a(x_n, y_n, z_n)=a(n)$. An approximate solution is the eigenfunction $a(1)b(2)\cdots$. Any function which permutes the electrons is equally good. A spin function α or β must be associated with each space function. Because of the Pauli exclusion principle, the complete eigenfunction must be antisymmetric with regard to electron interchanges. We will thus consider only linear combinations of the form

$$\phi=\begin{vmatrix} a(1)s_1(1) & b(1)s_2(1) & \cdots \\ a(2)s_1(2) & b(2)s_2(2) & \\ \vdots & & \end{vmatrix}.$$

$s_1, s_2, \cdots=\alpha$ or β. There must be equal numbers of α's and β's so that ϕ be an eigenfunction of S_z of value 0.

ϕ can be represented as $\begin{pmatrix} a & b & c & \cdots \\ s_1 & s_2 & s_3 & \cdots \end{pmatrix}$ or simply by the ordered set $(s_1 s_2 s_3 \cdots)$.

Using the ϕ-functions as a basis for the usual variational treatment, secular equations of the form

$$\sum_j H'_{ij}c_j - Wc_i\delta_{ij}=0, \quad H'_{ij}=\int \phi_i H \phi_j d\tau, \qquad (1)$$

$i=1, 2, \cdots 2N/(N!)^2$ (the number of π-electrons$=2N$), are obtained. W is the lowest average energy obtainable from a linear combination of ϕ-functions $\sum_j c_j\phi_j$. We will call such a linear combination a vector.

H'_{ij} is of the form $H'_{ij}=\alpha H_{ij}+Q\delta_{ij}$, where

$$\alpha=\int a(1)b(2)c(3)\cdots Hb(1)a(2)c(3)\cdots d\tau \qquad (2)$$

which is considered equivalent to any other single exchange integral between adjacent orbitals.

$$Q=\int a(1)b(2)\cdots Ha(1)b(2)\cdots d\tau,$$

the Coulomb integral. (3)

All other exchange integrals are neglected.

$$H_{ij}=0 \text{ or } 1.$$

The equations can then be expressed:

$$\sum_j H_{ij}c_j=[(W-Q)/\alpha]\cdot c_i, \quad i=1, 2, \cdots 2N/(N!)^2. \qquad (4)$$

It can be shown that the only H_{ij} which do not vanish are those for which ϕ_i can be made identical with ϕ_j by interchanging the spin functions associated with adjacent orbitals.

Since different orbital functions are never large in the same volume of space,

$$\int a(1)b(1)a(2)b(2)d\tau_1 d\tau_2 \ll \int |a(1)|^2|b(2)|^2 d\tau_1 d\tau_2$$

and the ϕ-functions are nearly orthogonal. We shall treat them as if they were exactly orthogonal.

SLATER EIGENFUNCTION METHOD PUNCHED CARD PROCEDURE

The matrix elements H_{ij} are very easily obtained. The representation of the ϕ's as an ordered set of α's and β's is used. This is put on $(2N)!/(N!)^2$ punched cards as an ordered set of 1's and 2's in the first $2N$ columns, followed by the subscript i of ϕ_i. This set is now reproduced once for each pair of adjacent orbitals with the two columns associated with the adjacent orbitals interchanged, and the rest of the card including the subscript i unchanged. Each resulting ϕ-function representation is then identified with the proper ϕ_j and the subscript j punched in the card. These reproduced cards are identical with the H_{ij} matrix, each containing an i and a j and considered of value 1. A matrix element of value n would appear as n identical cards. These can be replaced by one card containing an n instead of a 1 for its value, thus reducing the number of cards in the matrix substantially.

SPIN VALENCE METHOD THEORY

For 14 electrons, there are 3432 indepencent ϕ-functions. Because of the symmetry of the molecules, the number that need to be considered might be reduced to about 600 for anthracene and about 1000 for phenanthrene. The number of punched cards even in a 600th-order matrix would be far too large to make the calculation practical. Wheland's[11] method of spin valence, which is simpler in this case, will be followed.

We need not consider all the ϕ-functions for the lowest energy state, but only those sums which are eigenfunctions of S^2 of value 0. Rumer[14] has shown that a complete set of linearly independent functions, ψ_n, of this type is given by:

$$\psi_n=\sum_j(-1)^i P_j[a(1)b(2)\cdots k(k)\cdots n(n)\cdots] \times[\alpha(1)\beta(h)-\beta(1)\alpha(h)] \times\cdots[\alpha(k)\beta(n)-\alpha(n)\beta(k)], \qquad (5)$$

[14] G. Rumer, Nach. Ges. Wiss. Gott., M. P. Klasse, 1932, 337.

where P_j refers to permutations of the electrons. The numbers 1 to $2N$ are arranged on a circle and N lines which do not cross inside the circle are drawn between the points. To each possible circle diagram corresponds one and only one ψ_n of this linearly independent set such that if there is a line between k and n, $k<n$, then a factor of the type $[\alpha(k)\beta(n)-\beta(k)\alpha(n)]$ appears in ψ_n. ψ_n is a linear combination of only those ϕ's which have opposite spins in orbitals k and n. There are 429 independent ψ-functions for 14 electrons.

Circle diagrams with crossed lines also have corresponding ψ-functions, but these can be expressed as a sum of the linearly independent functions according to the rule:

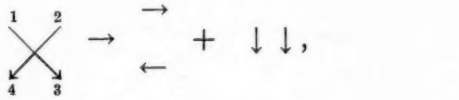

$$\psi_n=\sum_j(-1)^jP_juP_j\xi_n, \quad \text{where} \quad u=a(1)b(2)\cdots \tag{6}$$

$$\xi_n=\cdots[\alpha(k)\beta(n)-\beta(k)\alpha(n)]\cdots$$

the spin term of ψ_n.

Any other ψ can be expressed as

$$\psi_i=\sum_j(-1)^jP_juP_jP_i\xi_n=\sum_j(-1)^jP_juP_j\xi_i, \tag{7}$$

where

$$P_i\xi_n=\xi_i.$$

We seek a linear combination of the ψ's such that the average energy, W, is a minimum.

$$\psi=\sum_ic_i\psi_i, \quad W=\int\psi^*H\psi d\tau/\int\psi^*\psi d\tau. \tag{8}$$

By minimizing W, the usual Slater secular equations are obtained. The secular determinant contains W in every term. By adding rows, it is possible to confine W to the main diagonal. Using the spin valence method, this simpler determinant is obtained directly.

From first-order perturbation theory we get

$$\sum_i(H-W)c_i\psi_i=0. \tag{9}$$

Multiplying by u and integrating only over space coordinates:

$$\sum_i\int u(H-W)c_i\psi_i=\sum_{ij}c_iP_j\xi_i\int u(H-W)P_ju=0. \tag{10}$$

Setting

$$P_j\xi_i=\sum_kb_{ik}{}^j\xi_k,$$

then

$$\sum_{ijk}b_{ik}{}^jc_i\xi_k\int u(H-W)P_ju=0. \tag{11}$$

The ξ_k's are linearly independent and so their coefficients must vanish separately.

$$\sum_ib_{ik}{}^jc_i\int u(H-W)P_ju=0, \quad k=1, 2, \cdots. \tag{12}$$

TABLE II.

Iteration	$E=(W-Q)/\alpha$	Weight function b (Eq. 15)
1	2.0000	−2
2	3.3171	−2
3	3.7885	−2
4	3.9346	−8
5	4.0062	−10
6	4.0186	−6
·		
·		
·		
∞	4.0400	

Making the same assumptions regarding integrals as in Eqs. (3) and (4), this reduces to

$$\sum_ib_{ik}{}^jc_i=[(W-Q)/\alpha]c_k, \quad k=1, 2, \cdots. \tag{13}$$

The largest negative characteristic value of the matrix $|\sum_jb_{ik}{}^j|$ will be $E=(W-Q)/\alpha$ and the corresponding vector will be the ground state wave function.

In order to find $b_{ik}{}^j$, consider $P_j\xi_i=\sum_kb_{ik}{}^j\xi_k$. The circle diagram corresponding to ξ_i is drawn. $P_j\xi_i$ will

TABLE III.

Structure	Coefficient	Number of structures with this coefficient
1212121212	0.2373	2
1221212121	0.1141	8
1212112122	0.1088	4
1212122112	−0.0845	4
1121212122	0.0703	8
1212221211	−0.0627	2
1212212112	0.0564	8
1221121122	0.0556	4
1221221211	0.0551	8
1211212212	0.0542	8
1221112212	0.0539	4
1212211221	0.0471	4
1122112212	0.0446	8
1211221122	0.0369	8
1122212121	0.0290	4
1122122112	0.0281	2
1212112221	0.0267	8
1211221221	0.0256	4
1211222112	0.0223	8
1222121121	0.0186	8
1212222111	0.0182	4
1121121222	0.0174	8
1222121211	−0.0170	8
1211211222	0.0161	8
1222112112	0.0160	8
1221111222	0.0153	8
1122111222	0.0130	4
1121212221	0.0129	8
1112221122	0.0124	8
1121222121	0.0111	4
1112211222	0.0095	8
1112122212	−0.0089	4
1122222111	−0.0052	2
1112221221	0.0052	8
1112222112	0.0046	8
1112112222	0.0041	8
1211112222	0.0035	8
1111221222	0.0028	8
1111222212	0.0014	8
1222221111	0.0012	4
1111122222	0.0002	4

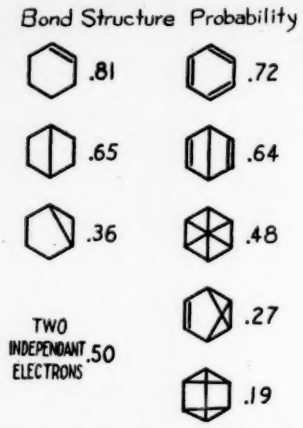

FIG. 2. Probability of finding opposite spins for the π-electrons in the positions joined by double bonds in the case of benzene.

be given by a permutation of bond ends and circle points corresponding to the permutation of electrons in orbitals. This new diagram can be expressed in terms of the uncrossed diagrams by the rule given above and these in turn translated back into ξ_k. All $b_{ik}{}^i(k=1, 2, \cdots)$ have the same sign.

Hückel[1] has shown that the lowest energy eigenfunction is symmetric with regard to reflections in planes of symmetry of the molecular frame perpendicular to the plane of the frame. Several ψ_n's may then have the same coefficient in the eigenfunction. Consider such a group $\psi_{a1}, \psi_{a2}, \cdots$ and the 429 equations for 14 electrons:

$$\sum_i(\sum_j b_{ik}{}^j)c_i=c_kE, \quad k=1, 2, \cdots.$$

Whenever $c_{a2}, c_{a3}, \cdots$ occur on the left, they are replaced by c_{a1} and similarly for all such groups. The equations for $k=a1, a2, a3, \cdots$ are identical and only one need be retained.

The new matrix for anthracene is of 126th order, and for phenanthrene, of 232nd order.

SPIN VALENCE METHOD PUNCHED CARD PROCEDURE

Only 34 circle diagrams can be drawn which cannot be made identical by a rotation of $(n/14)2\pi$ radians. Each of the 429 circle diagrams labeled $N-n$ is a rotation $(n/14)2\pi$ of one of these 34 types, N. The 34 circle types are shown in Fig. 1, each accompanied by the number N. The n label has the same position for all cycles, as shown at the upper left. It has been placed at the position which corresponds to orbital a. The orbitals for anthracene and phenanthrene are:

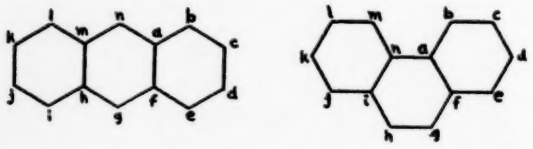

Thus 61–9 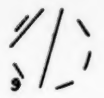 corresponds to

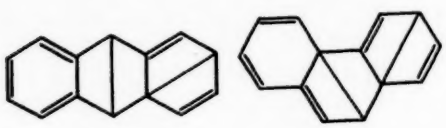

Six types of symmetry need to be distinguished in reducing the matrix order. Cycles of the same symmetry type are included in the same box of Fig. 1. The functions with distinct coefficients listed in Table I were used.

The P_j corresponding to adjacent interchanges about the outside of the ring were considered first. The $b_{ik}{}^i$ were found by hand for the 34 functions, $N-1$. This results in 289 elements, $N-1\rightarrow N'-n$, of value $+p$, $11>p>0$, which were then punched on cards.

If $N-1\rightarrow N'-n$, then $N-2\rightarrow N'-n+1$ provided $n+14\rightarrow n$. This addition process, yielding the rest of the uncrossing matrix, is easily performed by the punched card machines.

The interchange of electrons in orbitals a and f need also be considered, since these carbon atoms are also near neighbors. This is much more difficult than before, because now one structure may give as many as 122 others on uncrossing, instead of only two.

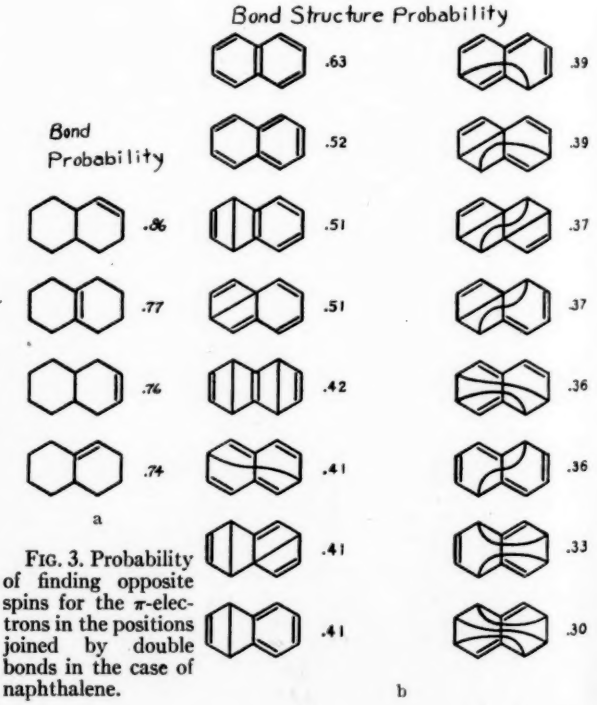

FIG. 3. Probability of finding opposite spins for the π-electrons in the positions joined by double bonds in the case of naphthalene.

The sign of $b_{ik}{}^{i}$ is determined from the bonds to positions 1 and 6 of structure i.

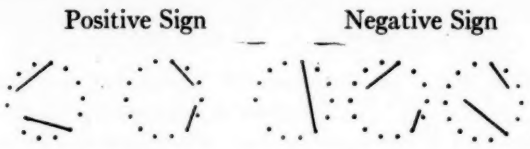

A negative sign is indicated by a punch in the x row of the card.

$N-n$, the sign of $b_{ik}{}^{i}$, its value, 1, and the bond configuration of each of the 429 functions was punched on a card. A bond was represented by the numbers of the two end positions punched in adjacent columns. An x punch in addition to the units digit was used for numbers greater than 9. The seven bond pairs were put in increasing order of the lowest number appearing. For example, the card for 53–8 contains

$$\begin{array}{rr} & x\quad\ x\ xxx \\ 538\ x1 & 14273645839012. \end{array}$$

The functions were sorted into 20 subclasses according to the configuration of the bonds ending on positions 1 to 6. Now, consider the two most complex subclasses:

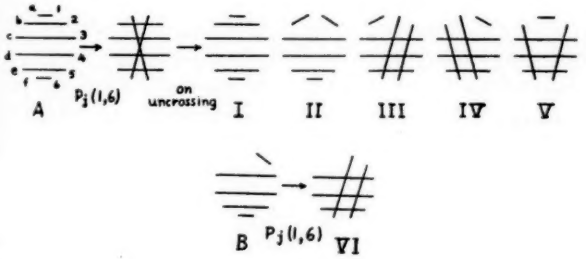

The crossed structures III, IV, V, and VI are of the same form. If corresponding bonds are punched in corresponding columns, these structures will continue to uncross in the same manner. Hence, the cards of subclass A were reproduced five times, permuting columns so that

$$\begin{aligned} 1a2b3c4d5e6fgh &\rightarrow 1a2b3c4d5e6fgh \\ &\quad\ 12ab3c4d5e6fgh \\ &\quad\ 1f263c4d5eabgh \\ &\quad\ bfa63c4d5e12gh \\ &\quad\ bf263c4d5e1agh. \end{aligned}$$

Structures of type B were permuted to give structure VI.

$$123a4b5c6dghij \rightarrow 1d263a4b5cghij.$$

The permuted cards also contain $N-n$ and $b_{ik}{}^{i}$ from the original cards.

The cards for structures III, IV, V, and VI were combined and further permutations carried out. Continuing to combine the subclasses and uncross by permutation, the uncrossed elements for all 429 structures were soon obtained. On the final cards, numbers in adjacent columns are bonded but the bond order is thoroughly scrambled. The cards were sorted and bonds punched in the proper order. They were then compared with a master set and the corresponding number $N-n$ punched in.

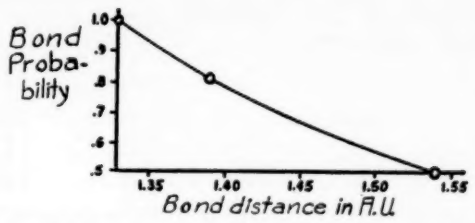

FIG. 4. Variation of carbon-carbon bond distance with bond probability as defined in the present article.

The matrix elements for an 8–13 or a 9–14 interchange can readily be obtained from the elements for a 1–6 interchange. If $N-n_j \rightarrow N'-n_k$ for a 1–6 interchange, then $N-n_{j+7} \rightarrow N'-n_{k+7}$ for an 8–13 interchange, used in the anthracene problem and $N-n_{j+6} \rightarrow N'-n_{k+6}$ for a 9–14 interchange, used in the phenanthrene problem. $(n_{j+14}=n_j)$.

We thus have all the $b_{ik}{}^{i}$ occuring in the anthracene and phenanthrene matrices. From the complete set of cards were sorted out only those needed to make up the reduced matrices by the aforementioned method.

There are 2096 non-vanishing elements in the anthracene matrix, and 4262 in the phenanthrene matrix.

SOLUTION OF THE SECULAR EQUATIONS

The largest negative characteristic value and the corresponding vector of a matrix H can be found by the process of iteration.[15] An arbitrary vector C is chosen. It can be expressed as the sum of the characteristic vectors of H, x_n.

$$C=\sum_n d_n x_n \quad \text{and} \quad Hx_n=E_n x_n.$$

Then

$$HC=\sum_n E_n d_n x_n$$

and

$$H^k C/E_1{}^k = d_1x_1+\sum_n (E_n/E_1)^k d_n x_n. \qquad (14)$$

These latter terms can be made arbitrarily small by increasing k providing $|E_n|<|E_1|$.

There may be a positive root larger than any negative one. However, a new matrix can be formed with the same characteristic vectors as the old one by adding a constant times the identity matrix to H. Then

$$(H-B)x_n=(E_n-b)x_n, \quad B=bI, \qquad (15)$$

$$(H-B)/(E_1-b)C=d_1x_1+\sum_n (E_n-b)/(E_1-b)d_n x_n.$$

The weight matrix B can be varied for successive iterations so that (E_n-b) is small for a number of E_n's while (E_1-b) is large.

[15] A. C. Aitken, Proc. Roy. Soc. Edinburgh **57**, 269 (1937).

TABLE IV.

Bond	I	II	III	Present method
A	1.43A	1.42A	1.41_7A	1.40_3A
B	1.41	1.40	1.40_2	1.41_3
C	1.37	1.38	1.37_7	1.37_4
D	1.40	1.40	1.40_0	1.40_7

The mth approximate eigenvalue E, given by the mth approximate vector C^m, $C^m=\sum_j c_j{}^m\phi_j$, is

$$E=\frac{\int C^{m*}HC^m d\tau}{\int |C^m|^2 d\tau}=\frac{\sum_j c_j{}^m c_j{}^{m+1}}{\sum_j (c_j{}^m)^2}. \quad (16)$$

TABLE V.

Iteration	E (Anthracene)	E (Phenanthrene)
8	5.4394	5.4583
9	5.4165	5.5022
10	5.4472	5.4905
11	5.4479	5.5098
11	$\Delta E=.017$	$\Delta E=.012$

James and Coolidge[16] have shown that when the vector space is orthogonal, as in the first method,

$$\delta^2=\frac{\int[(H-E)\psi]^2 d\tau}{\int |\psi|^2 d\tau}=\frac{\sum_n (c_n{}^{m+1}-Ec_n{}^m)^2}{\sum_n (c_n{}^m)^2}$$
$$\approx (E_1-E)(E_1-\bar{E}), \quad (17)$$

where $E_1<E_2<\cdots<\bar{E}<\cdots$. Thus an estimate of the error in the approximate E can be found. When E is sufficiently accurate, the iteration can be stopped.

In the second method, the ψ-functions are not orthogonal and this simple relationship is no longer valid. However, it may be expected to give a reasonable idea of the error.

$$E=\frac{\sum_n c_n{}^{m+1}c_n{}^m}{\sum_n (c_n{}^m)^2}. \quad (18)$$

TABLE VI.

Iteration	E' (Anthracene)	E' (Phenanthrene)
8	5.4594	5.5553
9	5.4351	5.5302
10	5.4563	5.5182
11	5.4541	5.5276

[16] James and Coolidge, J. Chem. Phys. **1**, 825 (1933).

The difference between the lowest root E_1, and E, ΔE, is given by

$$(\Delta E)^2\approx(\sum_n (C_n{}^{m+1}-EC_n{}^m)^2/\sum_n (C_n{}^m)^2). \quad (19)$$

The ratio of the sum of successive coefficients $(\sum_n |C_n{}^{m+1}|/\sum_n |C_n{}^m|)$ gives a measure of the lowest root, also. If the eigenfunction were expanded in terms of ϕ-functions, it would be very nearly the coefficient of the largest one, $\alpha\beta\alpha\beta\alpha\beta\alpha\beta\alpha\beta\alpha\beta$.

NAPHTHALENE SOLUTION

It is evident that a good initial approximation can shorten the iteration process. The bond eigenfunction corresponding to the structure 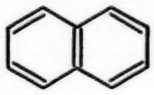 can be expressed as

$$\sum_n g_n\phi_n \quad \text{where} \quad g_n=\pm 1 \text{ or } 0.$$

For the initial approximation c_n was placed equal to g_n. This excludes the possibility of a solution which possesses reflection symmetry different from the lowest energy level.

For naphthalene, the H matrix is of order 252. This may be reduced to 126 using the fact that if $\phi_{i'}$ results from interchanging all five α's and β's of ϕ_i, then $-c_i=c_{i'}$. This reduction is accomplished very easily by using only the elements H_{jk} where s_1 of ϕ_k is α and then placing $H_{jk}=-H_{j'k}$ when s_1 of ϕ_j is β.

The matrix may be further reduced to order 41 if the reflection symmetry is taken into account. This adjustment is a little more tedious and may not be worth while if only a few iterations need be performed. The duplicate values serve as a partial check on the work.

NAPHTHALENE RESULTS

The iteration process converges rapidly, as shown by Table II. The error in the last energy value is about 0.5 percent.

The energy calculated for a single unexcited structure is $(Q-2\alpha)$. The difference, $(E-Q+2\alpha)=2.0400\alpha$, is the resonance energy.

Table III shows, for the sixth iteration, the 41 different coefficients, the number of times each occurs, and one of the functions possessing it. The function is represented by an ordered set of 1's and 2's corresponding to spins α and β in the order 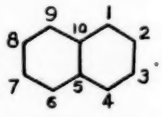

. The coefficients are normalized so that the sum of the squares of all 252 equals 1.

DOUBLE BOND PROBABILITY

The probability of finding electron 1 with spin α in the neighborhood of carbon atom a, and electron 2 with spin β in the neighborhood of carbon atom b can be found from the wave function. This quantity is not measurable. However, the probability that any two electrons be in the above state is just $2N(2N-1)$ times the probability that a specific two will be.

TABLE VII

Structure	Coefficient	Excitation	No. of structures with same coefficient
42–5	1.000	0	2
12–1	−0.748	1	1
1–1	0.625	0	2
59–2	−0.490	1	4
34–5	−0.451	1	2
44–2	0.440	1	4
41–5	−0.343	1	2
33–5	0.341	2	2
46–5	−0.331	1	2
42–2	0.244	1	4
13–3	−0.242	1	2
13–2	−0.240	1	2
37–4	−0.235	1	4
13–4	−0.234	1	2
37–3	−0.230	1	4
55–2	0.228	2	4
37–2	−0.211	1	4
53–2	−0.205	2	4
37–5	−0.199	1	2
42–4	0.189	1	4
53–1	−0.188	2	4
42–3	0.171	1	4
11–1	−0.156	3	1
32–5	0.155	2	2
13–1	−0.152	1	1
31–5	0.144	2	2
45–5	0.132	2	2
40–4	0.124	2	4
59–3	−0.113	2	4
41–3	−0.109	2	4
44–3	0.101	2	4
59–6	−0.0991	2	4
61–4	0.0980	2	4
61–1	0.0932	2	4
57–1	0.0907	2	4
36–2	0.0879	3	4
46–4	−0.0835	2	4
39–4	0.0833	2	4
61–3	0.0750	2	4
34–4	−0.0744	2	4
40–2	0.0698	2	4
41–2	−0.0686	2	4
40–3	0.0673	2	4
61–7	0.0641	2	4
35–5	−0.0632	3	2
55–1	0.0630	3	4
39–5	0.0613	2	2
53–3	−0.0592	3	4
59–5	−0.0576	2	4
21–7	−0.0543	3	2
39–2	0.0533	2	4
41–4	−0.0528	2	4
61–5	0.0517	2	4
57–7	0.0512	3	4
39–3	0.0507	2	4
61–2	0.0499	2	4
61–6	0.0496	2	4
38–4	−0.0486	3	4
34–2	−0.0483	2	4
12–2	−0.0475	3	2
45–4	0.0443	3	4
44–4	0.0402	2	4
21–3	−0.0396	3	2

TABLE VII.—*Continued.*

Structure	Coefficient	Excitation	No. of structures with same coefficient
31–4	0.0390	3	4
59–1	−0.0390	2	4
59–7	−0.0382	2	4
46–3	−0.0378	2	4
51–2	−0.0371	3	4
34–3	−0.0331	2	4
43–4	−0.0329	3	4
40–5	0.0314	2	2
51–1	−0.0283	4	4
33–4	0.0271	4	4
44–5	0.0258	2	2
21–2	−0.0257	3	2
35–4	−0.0253	4	4
43–3	−0.0245	3	4
21–1	−0.0242	3	2
55–5	0.0232	3	4
45–2	0.0225	3	4
32–3	0.0215	3	4
57–2	0.0215	3	4
53–7	−0.0208	3	4
57–3	0.0208	3	4
43–2	−0.0206	3	2
38–2	−0.0196	3	4
59–4	−0.0185	2	4
46–2	−0.0169	2	4
38–3	−0.0163	3	4
32–4	0.0163	3	4
11–2	−0.0161	5	2
43–5	−0.0134	3	4
21–6	−0.0132	3	2
55–6	0.0130	3	4
36–3	0.0129	4	4
55–3	0.0127	3	4
32–2	0.0108	3	4
21–4	−0.0106	3	2
53–4	−0.0097	3	4
31–3	0.0092	3	4
21–5	−0.0087	3	2
51–3	−0.0085	4	4
57–6	0.0070	3	4
35–2	−0.0063	4	4
55–4	0.0062	3	4
53–6	−0.0057	3	4
51–4	−0.0055	4	4
53–5	−0.0050	3	4
57–4	0.0043	3	4
12–3	−0.0037	3	2
57–5	0.0036	3	4
31–2	0.0028	3	4
55–7	0.0024	3	4
12–4	−0.0016	3	2
51–7	−0.0016	4	4
36–4	0.0015	4	4
38–5	−0.00127	3	2
33–3	0.00094	4	4
35–3	0.00089	4	4
51–5	−0.00078	4	4
36–5	0.00066	4	2
51–6	−0.00047	4	4
11–3	−0.00025	5	2
33–2	0.00020	4	4
45–3	−0.00029	3	4
11–4	−0.00003	5	2

TABLE VIII.

Structure	Coefficient	Excitation	No. of structures with same coefficient
44–01	1.000	0	1
42–04	0.765	0	2
1–01	0.452	0	1
53–01	−0.448	1	2
1–02	0.419	0	1
34–04	−0.366	1	2
59–09	−0.327	1	2
59–01	−0.319	1	2
41–05	−0.306	1	2
44–07	0.264	1	2
46–05	−0.260	1	2
37–01	−0.248	1	1
36–08	0.199	2	1
42–02	0.194	1	2
37–07	−0.181	1	2
37–06	−0.181	1	2
37–08	−0.177	1	1
42–08	0.172	1	1
13–04	−0.167	1	1
42–05	0.166	1	2
13–02	−0.159	1	2
13–03	−0.159	1	2
55–09	0.158	2	2
42–01	0.155	1	1
55–01	0.154	2	2
37–04	−0.152	1	2
32–04	0.149	2	2
42–06	0.142	1	2
37–02	−0.141	1	2
13–01	−0.137	1	2
37–05	−0.137	1	2
45–04	0.130	2	2
42–03	0.127	1	2
37–03	−0.125	1	2
53–09	−0.123	2	2
31–04	0.118	2	2
57–07	0.115	2	2
42–07	0.112	1	2
12–01	−0.108	2	2
39–03	0.097	2	2
61–14	0.085	2	2
46–06	−0.085	2	2
59–13	−0.077	2	2
41–02	−0.076	2	2
44–06	0.075	2	2
40–06	0.074	2	2
40–05	0.070	2	2
57–01	0.068	2	2
39–05	0.068	2	2
59–02	−0.068	2	2
41–06	−0.0678	2	2
59–05	−0.0668	2	2
46–04	−0.0665	2	2
61–08	0.0659	2	2
44–02	0.0644	2	2
41–08	−0.0639	2	1
34–05	−0.0628	2	2
61–11	0.0628	2	2
61–06	0.0627	2	2
34–08	−0.0624	2	1
40–03	0.0620	2	2
35–04	−0.0619	3	2
61–03	0.0585	2	2
39–08	0.0574	2	1
33–05	0.0571	3	2
39–06	0.0566	2	2
40–02	0.0554	2	2
53–07	−0.0530	2	2
41–07	−0.0523	2	2
34–03	−0.0514	2	2
39–07	0.0514	2	2

TABLE VIII.—*Continued.*

Structure	Coefficient	Excitation	No. of structures with same coefficient
40–08	0.0507	2	1
51–01	−0.0506	3	2
61–09	0.0504	2	2
41–03	−0.0499	2	2
41–04	−0.0496	2	2
59–08	−0.0491	2	2
33–04	0.0479	3	2
31–03	0.0461	3	2
61–07	0.0450	2	2
61–01	0.0430	2	2
59–11	−0.0428	2	2
53–10	−0.0422	3	2
59–03	−0.0414	2	2
44–08	0.0407	2	1
43–07	−0.0400	3	2
57–02	0.0397	3	2
38–01	−0.0395	3	1
41–01	−0.0394	2	1
39–04	0.0391	2	2
59–07	−0.0385	2	2
61–02	0.0378	2	2
34–02	−0.0376	2	2
55–08	0.0372	3	2
61–10	0.0370	2	2
53–02	−0.0368	3	2
59–12	−0.0363	2	2
61–12	0.0363	2	2
40–01	0.0357	2	1
31–05	0.0353	3	2
61–05	0.0351	2	2
61–04	0.0347	2	2
43–04	−0.0323	3	2
39–02	0.0323	2	2
40–04	0.0313	2	2
55–05	0.0313	3	2
46–03	−0.0305	2	2
51–09	−0.0304	3	2
40–07	0.0303	2	2
59–10	−0.0292	2	2
44–03	0.0292	2	2
61–13	0.0287	2	2
57–14	0.0272	3	2
59–14	−0.0267	2	2
38–05	−0.0266	3	2
21–07	−0.0262	3	2
44–04	0.0260	2	2
11–01	−0.0253	4	2
32–03	0.0251	3	2
36–02	0.0247	3	2
46–02	−0.0246	2	2
34–06	−0.0239	2	2
53–14	−0.0238	3	2
34–07	−0.0237	2	2
57–08	0.0234	3	2
34–01	−0.0231	2	1
43–02	−0.0226	3	2
38–03	−0.0220	3	2
57–06	0.0218	3	2
21–06	−0.0218	3	2
51–10	−0.0213	4	2
45–08	0.0210	3	1
44–05	0.0207	2	2
59–06	−0.0206	2	2
38–08	−0.0200	3	1
55–02	0.0197	3	2
38–07	−0.0186	3	2
38–06	−0.0181	3	2
55–11	0.0172	3	2
32–05	0.0172	3	2
53–08	−0.0169	2	2
45–05	0.0167	3	2

TABLE VIII.—*Continued.*

Structure	Coefficient	Excitation	No. of structures with same coefficient
45–02	0.0164	3	2
21–01	−0.0163	3	2
45–06	0.0154	3	2
51–08	−0.0147	4	2
32–07	0.0145	3	2
53–06	−0.0144	3	2
46–07	−0.0143	2	2
36–07	0.0140	4	2
57–10	0.0139	3	2
21–03	−0.0135	3	2
35–08	−0.0135	4	1
39–01	0.0127	2	1
57–13	0.0126	3	2
55–14	0.0125	3	2
21–02	−0.0124	3	2
12–02	−0.0122	3	2
46–01	−0.0121	2	1
43–08	−0.0120	3	2
51–14	−0.0119	4	2
59–04	−0.0116	2	2
51–02	−0.0115	4	2
46–08	−0.0115	2	1
43–03	−0.0113	3	2
55–10	0.0106	3	2
32–08	0.0103	3	1
55–13	0.0102	3	2
38–02	−0.0099	3	2
43–05	−0.0095	3	2
55–07	0.0093	3	2
35–05	−0.0089	4	2
32–02	0.0088	3	2
57–09	0.0087	3	2
45–01	0.0086	3	1
21–05	−0.0085	3	2
36–03	0.0085	4	2
36–01	0.0081	4	1
32–06	0.0077	3	2
32–01	0.0074	3	1
43–06	−0.0072	3	2
21–04	−0.0067	3	2
53–03	−0.0066	3	2
33–03	0.0064	4	2
31–06	0.0062	3	2
55–12	0.0061	3	2
53–04	−0.0060	3	2

TABLE VIII.—*Continued.*

Structure	Coefficient	Excitation	No. of structures with same coefficient
31–07	0.0058	3	2
53–05	−0.0051	3	2
55–03	0.0050	3	2
55–04	0.0047	3	2
35–02	−0.0046	4	2
53–11	−0.0045	3	2
53–13	−0.0045	3	2
57–12	0.0041	3	2
57–05	0.0041	3	2
57–03	0.0036	3	2
53–12	−0.0036	3	2
35–06	−0.0035	4	2
51–04	−0.0035	4	2
62–03	−0.0031	4	2
33–06	0.0031	4	2
57–11	0.0028	3	2
31–02	0.0028	3	2
57–04	0.0026	3	2
31–08	0.0023	3	1
35–03	0.0023	4	2
45–03	−0.0020	3	2
12–03	−0.0020	3	2
31–01	0.0020	3	1
55–06	0.0018	3	2
35–01	−0.0017	4	1
11–02	−0.0016	5	2
51–03	−0.0016	4	2
38–04	0.0016	3	2
12–04	−0.0012	3	1
36–06	0.0011	4	2
36–04	0.0010	4	2
45–07	−0.0010	3	2
51–13	−0.0008	4	2
51–11	−0.0007	4	2
35–07	0.0007	4	2
51–06	−0.0007	4	2
36–05	0.0006	4	2
51–05	−0.0006	4	2
33–02	0.0005	4	2
33–07	0.0004	4	2
51–12	−0.0004	4	2
33–08	0.0002	4	1
33–01	0.0001	4	1
11–03	−0.00006	5	2
11–04	−0.00003	5	1

Let Φ be the wave function. $\Phi=\sum c_n\phi_n$

$$\frac{P_{aa\beta\beta}}{2N(2N-1)}=\frac{\left[\sum_{\text{all spin coordinates except 1 and 2}}\int_{\text{space near } a}d\tau_1\int_{\text{space near } b}d\tau_2\int_{\text{all space}}\Phi^*\Phi d\tau_3 d\tau_4\cdots\right]_{\text{evaluated for } S_1=\alpha,\ S_2=\beta}}{\sum_{\text{all spin}}\int_{\text{all space}}\Phi^*\Phi d\tau}. \tag{20}$$

On assuming values for the following type integrals

$$\int_{\text{space near } a}|a(1)|^2 d\tau_1=1,\qquad \int_{\text{space near } a}a(1)^*b(1)d\tau_1=0,$$

substituting the analytical expressions for the ϕ's into Eq. (20), and integrating, one obtains:

$P_{aa\beta\beta}=(\sum_n c_n^2/\sum_j c_j^2)$ (n extends over all ϕ-functions with spin α associated with a, β with b) (j extends over all ϕ).

If the sum of $P_{aa\beta\beta}$ and $P_{a\beta ba}$ is taken as the criterian for a bond, the results shown in Fig. 3 are obtained.

Similarly, the probability that each of five pairs of orbitals be associated with opposite spins, which we will

TABLE IX.

Compound	$(W-W')$	Experimental resonance energy	α
Benzene	-1.106α	-1.71	1.55
Naphthalene	-2.040α	-3.24	1.59
Anthracene	$-2.95_{1}\alpha$	-4.54	1.54
Phenanthrene	$-3.01_{9}\alpha$	-4.78	1.59

call the probability of a bond structure, is:

$P_{\text{bond structure}}=(\sum_n c_n^2/\sum_j c_j^2)$($n$ extends over all ϕ-functions which have opposite spins in orbitals connected by bonds) (j extends over all ϕ).

The wave function obtained by Pauling and Wheland[9] for the benzene molecule using bond eigenfunctions was expanded in terms of Slater eigenfunctions and bond probability calculations were made. The results are shown in Figs. 2 and 3.

A number of attempts have been made to express the bonds of resonating systems as bonds of fractional order between 1 and 2. The carbon-carbon distances can then be correlated with this order. Points for single and double bonds are known. Some convention for a fractional bond order is established, and points for known symmetrical systems like benzene or graphite are filled in. A curve can then be drawn and used to find bond distances for other orders.

Following Penney,[17] we use 1.33A for the single bond distance, 1.54A for the double bond distance and 1.39A for the carbon-carbon distance in benzene. The graph obtained is shown in Fig. 4.

Naming the naphthalene bonds 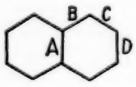

Fig. 4 gives

$$A=1.40_3,\quad C=1.37_4,$$
$$B=1.41_3,\quad D=1.40_7.$$

TABLE X.

Structure	Excitation	Coefficient (present investigation)	Coefficient (Jonsson)
(Anthracene)			
42–5	0	1.000	0.411
12–1	1	0.748	1.000
01–1	0	0.625	0.378
59–2	1	0.490	0.576
34–5	1	0.451	0.978
44–2	1	0.440	0.461
(Phenanthrene)			
44–1	0	1.000	0.430
42–4	0	0.765	0.477
01–1	0	0.452	0.510
53–1	1	0.448	1.000
01–2	0	0.419	0.280
34–4	1	0.366	0.963
59–9	1	0.327	0.606

[17] W. G. Penney, Proc. Roy. Soc. London **A158**, 306 (1937).

Pauling, Brockway, and Beach[18] formulated a convention on the basis of a bond eigenfunction calculation. The wave function is of the form

$$\Psi=\sum_n c_n\psi_n.$$

The probability of finding a bond between carbon atoms a and b, P_{ab}, is

$P_{ab}=(\sum_k c_k^2/\sum_n c_n^2)$($k$ ranges over all ψ_k which have a bond between a and b) (n ranges over all ψ_n).

Jonsson[12] has calculated relative strengths for naphthalene from this definition. These were normalized. Bond probabilities now range from 0 for a single bond to 1 for a double bond. Benzene gives a bond probability of 0.46. A graph similar to Fig. 4 was constructed and the bond distances for naphthalene determined. These are shown in Table IV, column I.

Penney[17] defined bond order on the basis of electron pairs and the vector model of Dirac. He obtained an expression for bond order in terms of resonance energy. By a bond eigenfunction type calculation, taking into account the small variations of the exchange integrals, he obtained the values for naphthalene shown in Table IV, column II.

Lennard-Jones and Coulson[19] have defined order as the probability of finding electrons on atoms a and b simultaneously, calculated from molecular orbital functions. This gives the values for naphthalene in Table IV, column III.

Lennard-Jones and Turkevich[20] found the bond lengths directly by including the bond distances as variables in a molecular orbital calculation. Only an approximate calculation was made for naphthalene assuming that bonds A and C had one length and B and D another. This gives values of 1.37 and 1.39, respectively.

The methods all agree on the prediction of the strongest double bond, C. The deviations of the other probabilities do not seem significant.

TABLE XI.

Anthracene	P	Bond length	Phenanthrene	P	Bond length
A	0.375	1.40A	A	0.136	1.47A
B	0.222	1.44	B	0.295	1.42
C	0.618	1.37	C	0.561	1.37
D	0.293	1.42	D	0.363	1.40
E	0.352	1.41	E	0.566	1.37
			F	0.279	1.43
			G	0.176	1.46
			H	0.710	1.36
			J	0.486	1.39

[18] L. Pauling, L. Brockway, and J. Beach, J. Am. Chem. Soc. **57**, 2705 (1935).

[19] J. E. Lennard-Jones and C. A. Coulson, Trans. Faraday Soc. **35**, 811 (1939).

[20] J. E. Lennard-Jones and J. Turkevich, Proc. Roy. Soc. London **A158**, 297 (1937).

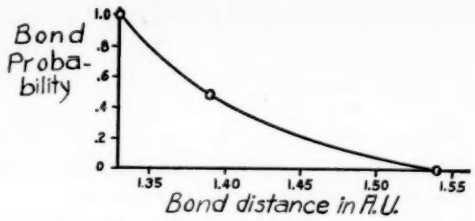

FIG. 5. Variation of carbon-carbon bond distance with bond probability using the convention of Pauling, Brockway, and Beach.

ANTHRACENE SOLUTION

The initial C vector was

$$c_n \text{ (both unexcited structures)} = 1,$$
$$c_n \text{ (all excited structures)} = 0.$$

The values added to the main diagonal on successive iterations were $-6, -6, -6, -6, -8, -8, -12, 0, 0, -10, -4$. The initial iteration gives about 0 for E. This rapidly improves so that in 5 iterations, and with only 851 matrix elements giving non-zero contributions, the energy is within 10 percent of the final value.

An error was found in the matrix after 11 iterations. Using C^{11} and the correct matrix, C^{12} was formed. This differed from C^{11} by about as much as C^5 differed from C^4. It is therefore assumed that C^{12} is about equivalent to C^5 with the correct matrix. The final answer is about what one would expect from 11 iterations with the correct matrix.

PHENANTHRENE SOLUTION

The initial C vector was

$$c_n \text{ (four unexcited structures)} = 1,$$
$$c_n \text{ (all excited structures)} = 0.$$

The values added to the main diagonal on successive iterations were $-7, -7, -7, -7, -14, -9, -9, 0, 0, -12, -4$. This converged in a manner very similar to anthracene. The same sort of error was made in the matrix. The final answer is equivalent to about 11 iterations with the correct matrix.

ANTHRACENE AND PHENANTHRENE RESULTS

Using Eqs. (18) and (19), the eigenvalues for the last four iterations and the error for the last one are listed in Table V.

The eigenvalues obtained from $E' = (\sum_n |c_n{}^{m+1}| / \sum_n |c_n{}^m|$ are shown in Table VI. The difference between the last approximate E's by the two methods is of the same order of magnitude as the ΔE listed above.

The average of the E's for iteration 11 will be used.

Tables VII and VIII give the coefficients of the structures of anthracene and phenanthrene, respectively. For anthracene the three most important types are:

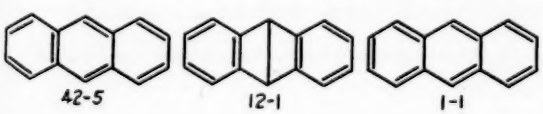

For phenanthrene the five most important ones are:

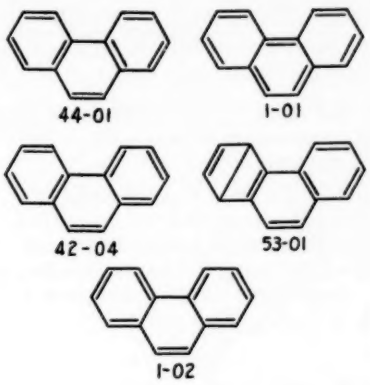

If the energy of the anthracene or phenanthrene molecule had been calculated on the assumption that only one unexcited bond structure described the situation, then $W' = Q - 2.5\alpha$. The resonance energy, $(W - W')$ is given in Table IX. Resonance energies for naphthalene, benzene, and all the experimental values are taken from Wheland.[2]

By the method of Pauling and Wheland,[9] neglecting all second, third, fourth, and fifth excited structures, Jonsson[12] calculated for the resonance energies—

$$\text{Anthracene:} \quad -2.823\alpha,$$
$$\text{Phenanthrene:} \quad -2.925\alpha.$$

These differ by 0.1 or about 3 percent from the values of the present treatment. The corresponding wave functions were considerably different, making the unexcited structures much less important than they really are. A comparison of the most important structures is made in Table X.

BOND PROBABILITIES

Using the method of Pauling for calculating bond probabilities, P_{ab}

$$P_{ab} = (\sum_n c_n{}^2 / \sum_j c_j{}^2) (n \text{ ranges over all structures with a bond between } a \text{ and } b) \ (j \text{ ranges over all structures}),$$

the probabilities shown in Table XI were found. Bonds are lettered in the following manner:

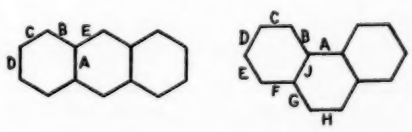

The bond lengths can be found using Fig. 5.

The probabilities calculated on the basis of Jonsson's approximate wave function show that the same bonds are very strong. The predicted lengths may differ by as much as 0.02A.

The Relative Rates of Photo-Chlorination of $CHCl_3$ and $CDCl_3$

T. W. NEWTON AND G. K. ROLLEFSON
Department of Chemistry, University of California, Berkeley, California

(Received December 27, 1948)

The relative rates of photo-chlorination of chloroform and deuterochloroform have been determined in the temperature range of $-20°$ to 180°C. The ratio of the rate constants for the two reactions can be fitted by the equation:

$$k_1/k_2 = 1.4 \pm 0.2 \exp(710 \mp 90/RT).$$

This result is discussed in terms of Eyring's absolute reaction rate theory and also in terms of an alternative mechanistic explanation. The observed difference in activation energy is accounted for in terms of the zero-point energies of the normal molecules and the activated complexes.

It was found that some deuterochloroform was produced when chloroform was chlorinated in the presence of deuterium chloride. This result indicates that the reaction

$$HCl + CCl_3 = CHCl_3 + Cl$$

must occur to some extent in the gas-phase chlorination of chloroform, contrary to the conclusions of Schumacher and Wolff. It was also found that appreciable amounts of hexachloroethane were formed in the reaction. Hence, it is concluded that the formation of this substance must be an important chain-terminating step in the reaction mechanism.

THE study of the relative rates of the photo-chlorination of chloroform and deuterochloroform was undertaken to obtain information concerning the effect of isotopic substitution on reaction rates. Such information is needed in order that experiments with isotopes, such as deuterium and tritium, in the study of the mechanisms of biological or other reactions, may be properly interpreted. Furthermore, studies of this kind afford a means of testing theories concerning reaction rates.

Some gas reactions which have been studied for the effect on the rate of substituting deuterium for hydrogen are as follows:

A. Chlorine with hydrogen and deuterium.[1,2]
B. Sodium with hydrogen chloride and deuterium chloride.[3]
C. Ethylene with hydrogen and deuterium.[4]
D. Decompositions of acetaldehyde and deuteroacetaldehyde.[5]
E. Decompositions of hydrogen iodide and deuterium iodide.[6]

Unfortunately, the data obtained in these experiments were not such as to be susceptible to precise theoretical interpretation. In A the observed difference in activation energy is not in disagreement with theory but the ratio of the collision numbers of hydrogen and deuterium is so large as to obscure any other sources of difference in the frequency factors. With reactions B and C the temperature coefficients were not determined, so it is impossible to separate the effects on the activation energy and those on the frequency factors on an experimental basis. C is also subject to the difficulty mentioned for A. The results for D are difficult to interpret because of uncertainties in the mechanism of the reaction. The data obtained for E are in fair numerical agreement with the calculations of Wheeler, Topley, and Eyring[7] at one temperature. This is rather surprising since the experimentally determined temperature coefficient of the ratio of the rate constants is opposite in sign to that predicted by the theoretical treatment.

The gas phase photo-chlorination of chloroform was chosen for our experiments because in this case we could hope to obtain reasonably accurate determinations of the ratio of the frequency factors and the difference in activation energies for the reaction with ordinary and deuterochloroform. This reaction has been studied with ordinary chloroform in the gas phase by Schumacher and Wolff[8] and in carbon tetrachloride solution by Schwab and Heyde.[9] Although the mechanisms which were proposed to account for the observed results differ somewhat in detail, they agree that hydrogen chloride is formed only by the reaction

$$Cl + CHCl_3 \rightarrow CCl_3 + HCl \quad k_1. \qquad (1)$$

Schumacher and Wolff found no evidence for the reverse of this reaction but Schwab and Heyde found it necessary to consider such a reaction in order to interpret their results.

In the work described in this paper, mixtures of chloroform and deuterochloroform were partially chlorinated. In this way a competition is set up between reaction (1) and

$$Cl + CDCl_3 \rightarrow CCl_3 + DCl \quad k_2. \qquad (2)$$

[1] G. K. Rollefson, J. Chem. Phys. **2**, 144 (1934).
[2] A. Farkas and L. Farkas, Naturwiss. **14**, 218 (1934).
[3] C. E. H. Bawn and A. G. Evans, Trans. Faraday Soc. **31**, 1392 (1935).
[4] A. Wheeler and R. N. Pease, J. Am. Chem. Soc. **58**, 1665 (1936).
[5] R. E. Smith, Trans. Faraday Soc. **35**, 1328 (1939).
[6] J. C. L. Blagg and G. M. Murphy, J. Chem. Phys. **4**, 631 (1936).
[7] A. Wheeler, B. Topley, and H. Eyring, J. Chem. Phys. **4**, 178 (1936).
[8] H. J. Schumacher and K. Wolff, Zeits. f. physik. Chemie **B25**, 161 (1934).
[9] G. M. Schwab and U. Heyde, Zeits. f. physik. Chemie **B8**, 147 (1930).

The ratio of the rate constants for these two reactions was determined from the relative amounts of hydrogen chloride and deuterium chloride produced. In addition, an exchange experiment was performed to determine whether or not the reverse processes were important under the conditions of the experiments.

MATERIALS

Chlorine.—Chlorine was taken from a cylinder obtained from the Matheson Company. It was purified on the vacuum line by distillation from a bulb at −78°C to one at −190°C; the last twenty percent from this distillation was discarded. The bulb was then evacuated at −130°C to remove the last traces of air and hydrogen chloride. The chlorine was stored in a bulb attached to the vacuum line.

Deuterium oxide.—The deuterium oxide was obtained in a ten-gram ampule from the California Isotope Company. The purity was quoted as 99.9 percent and the density as 1.1079 at 25°C. This material was degassed by several freezings and pumpings and convenient amounts were distilled into small ampules equipped with break-seals.

Chloroform.—Mallinckrodt analytical reagent chloroform was treated with anhydrous calcium chloride for about a week. Then it was distilled using a small Vigreux type column. The middle fraction which boiled from 61.1 to 61.2°C was used. This liquid was degassed by repeated freezing and pumping on the vacuum line. It was stored in a bulb arranged so that a ten-centimeter column of mercury stood between the chloroform and the stopcock.

Deuterochloroform.—A mixture of deuterochloroform and chloroform was prepared by the exchange between pure chloroform and an alkaline solution of deuterium oxide.[10] 1.38 g of anhydrous potassium carbonate, 12 g of chloroform, and about 2 g of deuterium oxide were sealed in a small Pyrex bomb in the absence of air. This bomb was held at a temperature of 100–105°C for thirteen days. The resulting mixture was distilled, dried, and distilled again; it was found that essentially all of it boiled at 61.0°C. The final product was degassed on the vacuum line and stored in the same manner as the chloroform. Two separate batches of deuterochloroform were prepared in this way at different times; one is referred to as batch *A*, the other as batch *B*.

Deuterium chloride.—Some isotopically impure deuterium chloride was prepared by the action of phosphorus trichloride on some deuterium oxide which had been recovered contaminated with water after another experiment. The product obtained was purified by distillation from a bulb at −78° to one at −195°C. Analysis showed the sample to be about 85 percent deuterium chloride, the rest being hydrogen chloride. It was stored at room temperature in a bulb sealed to the vacuum line.

[10] Z. Horiuti and Y. Sakemoto, Bull. Chem. Soc. Japan **11**, 627 (1936).

Hydrogen.—A three-liter storage bulb was filled with hydrogen from a tank and used without further purification. Some evidence of its purity is given by the fact that sharp explosions were observed in the hydrogen chloride photosynthesis runs described later. It is believed that traces of oxygen would have prevented such explosions.

APPARATUS AND PROCEDURE

Gas-handling apparatus.—This apparatus consisted of the storage bulbs for the various gases used and the two types of chloroform, a sulfuric acid manometer, and a standard bulb. This system could be evacuated to a pressure of 10^{-5} mm or less by means of a mercury vapor pump backed up by an oil pump. The amount of chlorine taken for a run was determined by measuring its pressure in the standard bulb and manometer at a known temperature. The chloroform was measured out by allowing it to fill a bulb of known volume to its vapor pressure at 0°C. This vapor was then condensed directly into the chlorination bulbs to prevent possible exchange with the manometer liquid. The volume of the bulb was determined by measuring the pressure produced in the standard bulb when such a dose was condensed in that bulb and then allowed to vaporize at a known temperature. Since absolute concentrations were not needed in our work, we have expressed our data in terms of units which correspond to a pressure of one centimeter of sulfuric acid in the standard bulb and manometer at 20°C.

Chlorination bulbs.—Because of the difficulty of finding a satisfactory stopcock lubricant for use with both chloroform and chlorine, the chlorinations were carried out in sealed bulbs equipped with break-seals. For most of the runs at room temperature and above the volume of these bulbs was 300 cc. The runs at −20° were carried out in two-liter bulbs in order to prevent the formation of a liquid phase during the experiments.

Illumination.—The details of the illumination procedure depended on the temperature used. Experiments at 180°C were carried out in a large beaker filled with a colorless oil. The light came in through the side of the beaker. For the temperatures of 90 and 20°C the procedure was the same except that the beaker was filled with water. Runs at −20°C were made in a large can filled with carbon tetrachloride. In this case the light came from above. In all experiments the temperature was controlled to within one degree either manually or by a de Khotinsky regulator. The light source for all of the experiments was an unfiltered General Electric AH4 mercury arc.

Reduction of the hydrogen chloride-deuterium chloride mixtures.—This process was carried out in a sealed tube equipped with a break-seal. Sodium amalgam was used for the reduction. Before use the sodium was melted in vacuum and triple-distilled through a series of small bulbs attached to the reduction vessel. As the distilla-

tion proceeded the empty bulbs were sealed off. The mercury was refluxed in vacuum before the sodium was distilled in to form the amalgam. About 7 g of mercury and 200 mg of sodium were used for the reduction of each sample. After distilling in the sample the tube was sealed off and heated to about 325°C for one hour. Preliminary attempts to reduce dry hydrogen chloride by less drastic means were unsuccessful. Heating with mercury, copper, or magnesium failed either as a result of the slowness of the reaction or of the formation of hydrides or solid solutions.

Chlorine analysis.—Unreacted chlorine was determined by light absorption. Two RCA 929 photo-tubes were used in a balanced circuit; one received light directly from the source while the other received light after it had passed through the cell which was fastened to the vacuum line. The source was a 500-watt G.E. projection bulb filtered through 8 mm of Corning 587 glass. The apparatus was calibrated empirically by the use of samples of chlorine measured with the manometer and standard bulb.

Isotopic analysis.—The isotopic composition of the mixtures of hydrogen and deuterium was determined by the thermal conductivity method. This method has been described in detail by many workers.[11] For our purposes the conductivity cell was constructed by mounting the filament, with its glass and wire supports, from an ordinary G.E. 15-watt light bulb in a Pyrex bulb which was sealed to the vacuum line. This filament was made one of the arms of a Wheatstone bridge. During operation a constant voltage was maintained across the entire bridge by manual variation of a resistance in the battery circuit. A voltage divider and a Leeds and Northrup Type K potentiometer were used to determine the magnitude of this voltage. The actual voltage used was 22.990±0.005 volts. With this voltage the current drawn from the battery was about 125 milliamperes. For convenience the amplification factor of the bridge was disregarded; thus in all cases the actual filament resistance was 0.1237 times the quoted resistance.

Relatively high pressures were used in the analysis; the pressure was usually 50 cm of sulfuric acid but occasionally was as low as 20 cm. In order to insure a constant temperature for the cell surroundings the cell was immersed in a mixture of ice and water which

TABLE I. Details of experimental results.

1 Run	2 $(Cl_2)_0$	3 $(Cl_2)_f$	4 Batch	5 $(CHCl_3)_0$	6 $(CHCl_3)_f$	7 $(CDCl_3)_0$	8 $(CDCl_3)_f$	9 $\log k_1/k_2$	10 R	11 T°K
9	78.4	43.3	*A*	24.9	8.9	53.5	34.4	0.368	0.289	453
10	76.0	54.5	*A*	24.7	13.7	53.4	42.9	0.431	0.165	453
11	75.1	43.2	*A*	25.0	9.9	53.9	37.1	0.396	0.269	453
12	80.4	47.6	*A*	24.9	9.3	53.5	36.3	0.404	0.256	453
13	69.7	30.9	*A*	24.8	6.6	53.4	32.8	0.434	0.386	363
15	42.7	1.0	*A*	24.9	5.1	53.6	31.7	0.478	0.955	363
16	75.0	40.7	*A*	24.8	7.8	53.5	36.2	0.472	0.297	363
19	101.0	76.4	*A*	24.7	11.5	53.4	42.0	0.503	0.139	363
21	93.6	77.4	*A*	24.8	16.1	53.5	46.0	0.456	0.095	363
27	29.6	0.4	*A*	24.9	13.0	53.6	36.3	0.222	0.974	363
33	71.0	54.5	*A*	51.3	36.7	27.1	25.2	0.6545	0.131	363
34	71.7	44.1	*A*	51.3	27.6	27.0	23.1	0.600	0.238	363
43	94.5	74.5	*B*	21.8	11.8	56.5	46.5	0.497	0.118	363
44	91.3	54.4	*B*	50.0	19.9	28.1	21.4	0.527	0.252	363
45	90.1	79.7	*B*	50.0	41.2	28.1	26.5	0.518	0.058	363
14	68.1	16.4	*A*	25.0	3.6	53.8	24.5	0.391	0.600	293
17	41.1	0.3	*A*	24.8	5.5	53.4	31.9	0.466	0.99	293
18	71.9	37.1	*A*	24.9	6.6	53.6	37.1	0.556	0.319	293
20	97.2	65.2	*A*	24.8	7.5	53.1	38.4	0.567	0.197	293
22	89.1	52.2	*A*	24.7	5.2	53.1	35.7	0.592	0.261	293
28	57.5	8.0	*A*	50.9	10.4	26.6	17.6	0.584	0.756	293
29	55.4	16.0	*A*	51.2	18.4	26.7	20.1	0.551	0.553	293
30	78.9	38.1	*A*	51.2	17 5	26.7	19.6	0.542	0.349	293
31	73.3	44.6	*A*	52.4	27.2	26.8	23.3	0.670	0.244	293
32	69.2	61.2	*A*	51.5	44.0	27.2	26.7	0.926	0.061	293
35	57.9	32.3	*B*	21.7	7.7	56.4	44.8	0.653	0.284	293
36	89.0	33.8	*B*	21.9	0.5	56.6	22.8	0.618	0.454	293
39	81.9	54.1	*B*	21.6	7.6	55.8	42.0	0.564	0.204	293
40	80.9	32.4	*B*	21.2	1.1	55.4	27.0	0.614	0.428	293
41	91.1	41.0	*B*	50.3	10.0	28.0	18.2	0.574	0.379	293
42	92.2	29.7	*B*	50.3	3.3	28.0	12.5	0.529	0.514	293
23	62.1	55.0	*A*	25.1	20.2	54.1	51.9	0.720	0.0605	253
24	71.0	35.6	*A*	24.7	6.7	53.4	36.0	0.520	0.332	253
25	66.0	30.3	*A*	24.8	7.0	53.5	35.6	0.492	0.371	253
26	63.2	44.6	*A*	24.9	13.4	53.7	46.7	0.646	0.173	253

[11] Farkas and Melville *Experimental Methods in Gas Reactions* (The Macmillan Company, New York, 1939), pp. 193 and 284.

was kept in a Dewar and stirred with a stream of air. It was estimated that the temperature of the filament was 120°C with hydrogen at a 50-cm pressure in the cell and 160°C with deuterium at the same pressure. This estimate was made by comparing the resistance of the filament under the ordinary operating conditions with its resistance at 0° and 25°C. These temperatures were obtained using a bridge current of only 3 milliamperes and the appropriate wall temperature.

No attempt was made to measure absolute conductivities; instead, the apparatus was calibrated with known mixtures of hydrogen and deuterium prepared by the reduction of mixtures of hydrogen chloride and deuterium chloride as previously described. By following this procedure we could be sure that the amount of hydrogen deuteride in the mixtures would correspond to that in the samples to be analyzed. The hydrogen chloride, deuterium chloride mixtures were prepared by the photo-chlorination of known mixtures of hydrogen and deuterium with excess chlorine present. The pure deuterium was prepared by the reduction of pure deuterium oxide by sodium amalgam.

Since it was not always possible to use a pressure of 50 cm in the cell, an empirical correction curve was constructed by running several of the samples at various pressures.

Typical run.—A chlorination bulb was fitted on to the line and pumped out while flaming it with a hand torch to aid in degassing. Two doses of the chloroform, deuterochloroform mixture were distilled in as previously described. Then the desired amount of chlorine was measured out by means of the standard bulb and the manometer. This was pumped at −190°C and then distilled into the chlorination bulb which was sealed off and stored in a dark cupboard until it was to be illuminated. The illumination was carried out as already described. After illumination the bulb was wrapped in towels to prevent further reaction, a glass enclosed iron rod was inserted above the break-seal, a ground joint sealed on and the bulb fitted onto the vacuum line. At the same time an amalgam reduction bulb was fitted onto the line and the amalgam prepared as described. Next the chlorination bulb was cooled to −80°C, the break-seal opened, and the mixture of excess chlorine, hydrogen chloride, and deuterium chloride distilled into the absorption cell. The other reaction products and excess chloroform remained in the chlorination bulb. The excess chlorine was determined by light absorption as already described. The absorption bulb was brought to a temperature of −132°C by a pentane bath and the hydrogen and deuterium chlorides distilled into the amalgam reduction bulb. Under these conditions the bulk of the excess chlorine and the last traces of chloroform are left in the absorption bulb. The reaction with the amalgam was carried out as described. Then a glass-enclosed iron rod was inserted above the break-seal and the bulb fitted back onto the vacuum line. The break-seal was opened and the gas passed back and forth, by means of a Toepler pump, through a trap surrounded by liquid nitrogen. This procedure removed the last traces of condensable vapors. Finally the sample was pumped into the thermal conductivity cell and its composition determined as previously described. Usually several samples were analyzed consecutively. Under these conditions a reading with pure hydrogen in the cell was made at the beginning and at the end of the series. The difference in these two readings rarely exceeded 0.5 ohm. In calculating the deuterium content of the mixture it was assumed that this variation was a linear function of the time.

The chlorination of chloroform in the presence of deuterium chloride.—Schumacher and Wolff[8] concluded that the reaction between HCl and the radical CCl_3 did not take place during the gas phase photo-chlorination of chloroform. This statement was based on the fact that within their experimental error no inhibition due to hydrogen chloride was observed. However, it was thought well to check this by an exchange experiment before the main series of experiments was begun. Mixtures of chloroform, chlorine, and deuterium chloride were illuminated at 85°C until essentially all the chlorine was gone. The mixture was then cooled with dry ice in acetone and pumped to remove hydrogen chloride and deuterium chloride. The completeness of this separation was checked by testing the remaining chloroform with a silver nitrate solution in another experiment. It was found that about 0.3 mole percent hydrogen chloride is left behind after such a separation. Excess chlorine was then added to the chloroform and it was illuminated until the chlorination was complete. The mixture was again cooled with dry ice and the evolved gas caught in an amalgam reduction tube. This tube was heated as described above and the gas formed analyzed as above. At the time this experiment was done the conductivity apparatus was not so highly refined and the difference in resistance of the filament with pure hydrogen and pure deuterium in the cell was only about 7.4 ohms. The results of these experiments are shown in the following table.

	Initial amounts			Resistance readings			
Run	$CHCl_3$	Cl_2	DCl	Sample	Pure H_2	Difference	%D
A	63.7 cm	29.6 cm	32.1 cm	718.4	718.0	0.4	5
B	64.1	30.7	33.1	718.8	718.4	0.4	5

It can be seen that a small amount of deuterochloroform was formed during the photo-chlorination of chloroform in the presence of deuterium chloride. This fact indicates that under these conditions some of the CCl_3 radicals have reacted with DCl and therefore some allowance for the processes which are the reverse of (1) and (2) must be made.

Thermal chlorination of chloroform at 180°C.—The thermal chlorination of chloroform has been studied by Taylor and Hanson.[12] Extrapolation of their data indi-

[12] H. A. Taylor and W. E. Hanson, J. Chem. Phys. 7, 418 (1939).

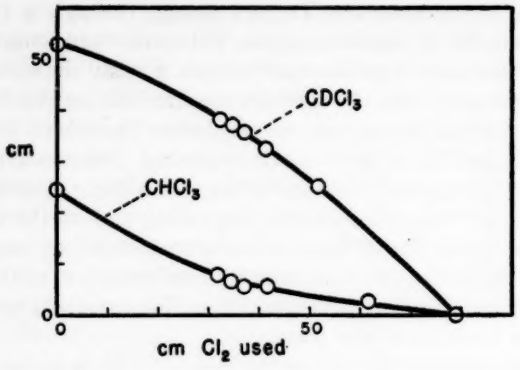

FIG. 1a. 20°C.

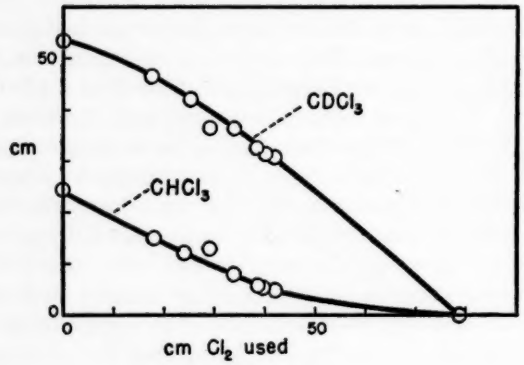

FIG. 1b. 90°C.

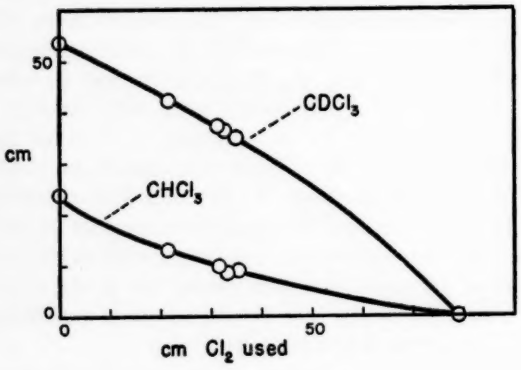

FIG. 1c. 180°C.

cates that only 0.03 percent of the chlorine would react per minute under the conditions used in our photochlorinations at this temperature. An experiment was performed to check this point and it was found that the amount of dark reaction was negligible in our experiments.

Isotopic analysis of the chloroform.—The procedure used to determine the deuterium content of the chloroform was similar to that described for a typical run. The only significant differences were that excess chlorine was used, illumination was for at least an hour, and the chlorine analysis was omitted. Six determinations were made on batch *A* and two on batch *B*. For *A* the average percent of deuterochloroform was 68.3, the maximum deviation being 0.6 percent and the mean deviation 0.3 percent. Both determinations on batch *B* gave a value of 72.1 percent deuterochloroform.

Formation of hexachloroethane.—At the end of most runs an appreciable amount of white volatile crystals was observed in the reaction bulb. A sample of these crystals was collected and they were identified by their melting point and odor as hexachloroethane.

RESULTS

The results of the relative rate experiments are given in Table I. The first column gives the run number, the second the initial amount of chlorine, the third the final amount of chlorine as determined by light absorption, the fourth shows whether the chloroform-deuterochloroform mixture used was from batch *A* or *B*. In some of the experiments the isotopic composition was varied by half of the chloroform from batch *A* or *B* and the other half from a sample of pure ordinary chloroform. The initial isotopic composition of a mixture is shown by the data in columns 5 and 7 which show the initial amounts of chloroform and deuterochloroform, respectively, for each experiment. The sixth column gives the amount of $CHCl_3$ after the reaction calculated from the expression

$$(CHCl_3)_f=(CHCl_3)_0-(1-F)[(Cl_2)_0-(Cl_2)_f],$$

in which F is the fraction of deuterium chloride in the hydrogen chloride-deuterium chloride mixture produced by the reaction. The eighth column gives the amount of deuterochloroform after the reaction calculated from the expression

$$(CDCl_3)_f=(CDCl_3)_0-F[(Cl_2)_0-(Cl_2)_f],$$

where F is defined as above. Column 9 gives the logarithm of the apparent ratio of the rate constants. Column 10 gives the quantity defined by the expression:

$$R=[(Cl_2)_0-(Cl_2)_f]/[(Cl_2)_0+(Cl_2)_f].$$

The significance of the results tabulated in columns 9 and 10 will be discussed further below. Column 11 gives the temperature at which each photo-chlorination was performed.

These data were plotted to show the course of the reaction of the two kinds of chloroform. In Figs. 1a, 1b, and 1c the amount of each species is plotted against the amount of chlorine used. Each of these plots shows the results of a series of runs using the same composition of starting material. Other compositions give the same sort of plots and are not shown. In principle slopes read from these plots could be used to evaluate the ratio of the rate constants for the two reactions:

(1) $CHCl_3+Cl=HCl+CCl_3$

and

(2) $CDCl_3+Cl=DCl+CCl_3$.

This procedure is not good in practice because the slopes cannot be determined with sufficient precision. Instead, the calculations were made on the basis of an

equation which is derived in the following way: Assuming that reactions (1) and (2) are the only ones in which molecules containing isotopes react, one can write:

$$-d(CHCl_3)/dt = k_1(CHCl_3)(Cl)$$

and

$$-d(CDCl_3)/dt = k_2(CDCl_3)(Cl);$$

dividing the first of these expressions by the second, one gets

$$d(CHCl_3)/(CHCl_3) = (k_1/k_2)d(CDCl_3)/(CDCl_3).$$

Integrating and taking limits one gets

$$k_1/k_2 = [\log(CHCl_3)_0 - \log(CHCl_3)]/[\log(CDCl_3)_0 - \log(CDCl_3)],$$

where the quantities with the subscript zero refer to the values at time zero and the quantities without subscript refer to the values at any time t. In practice the reaction was stopped before the chlorination was complete so that the quantities $(CHCl_3)$ and $(CDCl_3)$ could be determined. If one assumes in addition to reactions (1) and (2) the reverse of each, it is impossible to solve the resulting equation for k_1/k_2. Since the exchange experiment (see page 721) indicates that the reverses of reactions (1) and (2) do indeed take place, it is necessary to use an approximate method for evaluation of k_1/k_2. The method used was as follows. Apparent values of k_1/k_2 were calculated from the data of each run using the equation derived above. If the assumptions of the derivation are correct, the values of k_1/k_2 would be independent of the extent of the reaction. However, it was found that these apparent k_1/k_2 values were not independent of the extent of the reaction. For example, if the values from runs at a single temperature were plotted against the fraction of the available chlorine used, an appreciable downward trend is noticed. At the start of the reaction the reverses of reactions (1) and (2) cannot occur since there is no hydrogen chloride or deuterium chloride present. Thus if the apparent k_1/k_2 values can be extrapolated back to zero reaction, the true value of k_1/k_2 should be obtained. The reverses of reactions (1) and (2) compete with the reaction (3):

$$CCl_3 + Cl_2 = CCl_4 + Cl.$$

For this reason the function of the extent of reaction used was the average value of the sum of the amounts of hydrogen chloride and deuterium chloride divided by the average amount of chlorine present during the course of the reaction. It can be seen that the quantity R as defined for Table I is this function. Figure 2 shows all the apparent $\log(k_1/k_2)$ values plotted against the appropriate R value. It might be pointed out that the downward trend of the $\log(k_1/k_2)$ values is consistent with the fact that the reaction

$$HCl + CCl_3 = CHCl_3 + Cl \qquad (1')$$

is probably faster than

$$DCl + CCl_3 = CDCl_3 + Cl. \qquad (2')$$

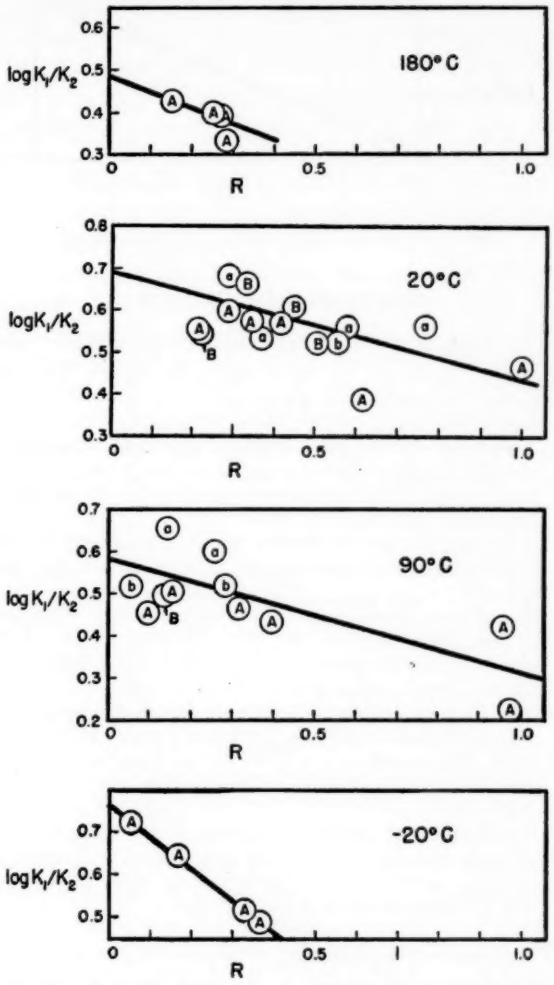

FIG. 2. Rate ratio as a function of extent of reaction. A batch A; a batch $A+CHCL_3$; B batch B; b batch $B+CHCL_3$.

It can be seen from Fig. 2 that the data scatter somewhat but that the extrapolation to the actual value of $\log(k_1/k_2)$ is fairly definite.

If one writes the usual expression for the specific rate constant for reaction (1) and for reaction (2) and divides the first by the second, he gets

$$k_1/k_2 = A_1/A_2 \exp(E_2 - E_1)/RT$$

or

$$\log(k_1/k_2) = \log(A_1/A_2) + (E_2 - E_1)/2.3RT,$$

where the subscript 1 refers to reaction (1) and the subscript 2 refers to reaction (2). Thus if the actual $\log(k_1/k_2)$ values are plotted against $1/T$ and a straight line drawn, $(E_2 - E_1)$ and A_1/A_2 may be evaluated. This plot is shown in Fig. 3. The best straight line gives the values $A_1/A_2 = 1.40$ and $(E_2 - E_1) = 714$ calories. Two nearby lines which just fit the data within the limit of error give values of 1.22 and 1.58 for A_1/A_2 and the values 800 and 621 calories, respectively, for $(E_2 - E_1)$. It is thus concluded that the data can be fitted by the equation

$$k_1/k_2 = 1.4 \pm 0.2 \exp(710 \mp 90)/RT.$$

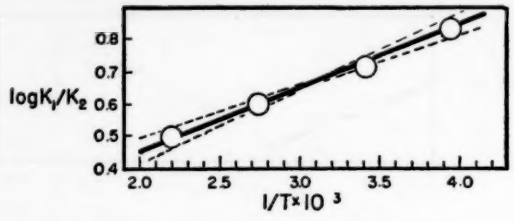

FIG. 3. Rate ratio as a function of temperature.

DISCUSSION OF ERRORS

Five experimentally determined quantities enter into the calculation of each $\log k_1/k_2$ value. The uncertainty in each will be discussed.

1. The initial amount of chloroform. The mean deviation on the dose size determination was 0.4 cm. Since two doses were used for each run, the uncertainty in the initial amount of chloroform was about 0.8 cm.
2. The initial amount of chlorine. This was measured with the manometer, so the uncertainty was probably not more than 0.1 cm.
3. The amount of chlorine at the end of the reaction. The spread of the points obtained for the calibration curve for the chlorine analysis apparatus was about 0.7 cm. This will be taken as the uncertainty.
4. The fraction deuterochloroform in the initial chloroform-deuterochloroform mixture. For batch A the mean devtiation of six determinations was 0.003 and the maximum deviation was 0.006. The uncertainty in this fraction will be taken as 0.005.
5. The fraction of deuterium chloride in the final hydrogen chloride-deuterium chloride mixture. The uncertainty in this quantity will be taken as 0.005 since it involved the same sort of measurement as discussed under 4.

The usual error formulas obtained by partial differentiation are not suitable in this case because the functions to be differentiated are too complicated. A more effective method is to recalculate the results of a particular run introducing errors of the magnitude indicated above. Run 18 will be taken as typical. The value for $\log k_1/k_2$ which appears in the table is 0.556. Table II shows how this value is affected by introducing errors of the magnitudes which have been indicated. In each case the column headed X gives the value from Table I and that headed X' is the value assumed in calculating the value of $\log k_1/k_2$ given in the next column. The final column shows the change in the value of $\log k_1/k_2$ caused by the indicated change in X. The effect of an error in the initial amount of chlorine is small compared to that caused by the error in the final amount of chlorine; therefore, it may be neglected. It is apparent that the principal errors in the list under consideration are the last two listed in Table II. The first of these is not an error that causes differences between individual experiments but rather affects the differences between the experiments run with the different batches of chloroform. Since the data as plotted in Fig. 2 show no tendency for the points to fall into groups determined by an error of this type, it can be concluded that the actual error must have been less than the indicated amount. The principal cause of variation from experiment to experiment is the determination of the fraction of deuterium chloride in the DCl-HCl mixture formed in the reaction. Corresponding to this fact the experimental values of $\log k_1/k_2$ have been plotted as circles with a radius of 0.026. Obviously, the other errors cannot be neglected but there seems to be no way of eliminating them or making an adequate allowance for them. The trends in the data are sufficiently definite so that we believe that the accuracy claimed for the data is reasonable.

DISCUSSION

It is of interest to compare the experimentally determined ratio of the rate constants with the value which can be calculated by applying the absolute reaction rate theory of Eyring. According to this theory the rate constant for a reaction is given by

$$k_1=\kappa(kT/h)(F'/F)\exp(-E/RT), \quad (1)$$

in which k_1 is the rate constant, κ the transmission coefficient, k the Boltzmann constant, T the temperature, h Planck's constant, F' is the total partition function of the activated complex except for the vibration frequency corresponding to the decomposition coordinate, F the total partition function for the reactants, E the activation energy, and R is the gas constant. If we write an equation of this form for the rate constant for the reaction of each type of chloroform, the ratio of the rate constants, k_1/k_2, is given by

$$k_1/k_2=(\kappa_1/\kappa_2)(F_1'/F_2')(F_2/F_1)\exp(E_2-E_1)/RT, \quad (2)$$

in which the subscripts 1 and 2 refer to the chloroform and deuterochloroform, respectively.

The total partition functions used in this equation are the products of four different partition functions F_t, F_r, F_v, and F_e corresponding to translation, rotation, vibration, and the electronic states of the system. Equation (2) may be rewritten as follows to show this fact:

$$k_1/k_2=(\kappa_1/\kappa_2)(F_1'F_2/F_1F_2')_t(F_1'F_2/F_1F_2')_r \times(F_1'F_2/F_1F_2')_v(F_1'F_2/F_1F_2')_e\exp(E_2-E_1)/RT. \quad (3)$$

The translational partition function for a molecule is given by $F_t=(2\ mkT)^{\frac{3}{2}}V/h^3$ in which m is the mass of the molecule and V is the volume of the system; the other symbols have the significance already given. Applying this to the system under consideration reduces the portion of Eq. (3) which pertains to translation to $(m_1'm_2/m_2'm_1)^{\frac{3}{2}}$ which is obviously nearly unity. The rotational partition function for a molecule is proportional to the square root of the product of the moments of inertia of the molecule; hence, the rotational part of Eq. (3) can be reduced to

$$(A_1'B_1'C_1'A_2B_2C_2/A_2'B_2'C_2'A_1B_1C_1)^{\frac{1}{2}}.$$

The value of this function must be nearly unity since the substitution of deuterium for the hydrogen in chloroform has very little effect on the moments of inertia. The electronic portion of the partition function is also unity since the fraction of the total number of

TABLE II. Effect of experimental errors on $\log k_1/k_2$.

Quantity varied	X	X'	$\log k_1/k_2$	Δ
Initial chloroform	78.5	79.3	0.551	0.005
Final chlorine	37.1	37.8	0.553	0.003
Fraction of $CDCl_3$ in the initial chloroform	0.683	0.678	0.538	0.018
Fraction of DCl in DCl-HCl	0.474	0.479	0.582	0.026

molecules in any particular electronic state will not be altered appreciably by substituting deuterium for hydrogen in a molecule as heavy as those under consideration.

The vibrational part of the partition function is given by the product over all vibrations of factors of the form $(1-\exp(-h\nu/kT))^{-1}$. The frequencies have been investigated for both chloroform and deuterochloroform[13] and it has been found that the only ones which differ by more than three percent are the C—H and C—D stretching and bending frequencies. However, these are of such a magnitude that the factors of the form indicated are essentially unity and, therefore, we see that the total partition function ratio in Eq. (2) (or Eq. (3)) reduces to unity. It follows that the only way that the non-exponential part of the expression for the ratio of the rate constants can differ from unity is for the ratio of the transmission coefficients to differ from that value. In view of the great similarity in the two reacting systems it seems unlikely that there would be any significant difference in these transmission coefficients. Therefore, we conclude that the probable value for the non-exponential part of the expression for the ratio of the rate constants is unity on the basis of this theory.

The difference in the activation energies for the two reactions is the difference in total zero-point energy in the initial molecules minus the difference in zero-point energy in the activated complexes. The simplest approximation to make for this calculation is to assume that the zero-point energies are the same in the normal state and the activated complex for all frequencies except the C—H and C—D stretching vibrations which are in the direction of the reaction coordinate. The difference in the zero-point energies for these vibrations is 1080 calories in the normal state. Therefore, as a first approximation we may write

$$k_1/k_2 = 1.00 \exp(1080/RT).$$

This is to be contrasted with the experimental result

$$k_1/k_2 = 1.4 \pm 0.2 \exp(714 \pm 90/RT).$$

It is possible to alter the model assumed for the activated complex so as to be able to calculate the correct activation energy difference. To do this it may be assumed that the frequency of the vibration of the H or D perpendicular to the line between the carbon and chlorine atoms is not the same as the bending frequency in the initial chloroform but instead is increased. If it is assumed that the ratio of these frequencies remains the same, we may choose 1720 cm^{-1} instead of 1215 for the C—H and 1284 instead of 908.3 cm^{-1} for C—D. With these values the calculated activation energy difference becomes 710 calories. Such a change has very little effect on the calculation of the frequency factor but we have calculated that factor under these conditions and find it to be 1.02 if it is assumed that the ratio of the transmission coefficients is unity.

The experimental value for the ratio of the non-exponential parts of the rate constant functions differs from the one calculated above by more than we believe to be a reasonable assignment of error to the data. It is, of course, possible to say that the discrepancy is due to the ratio of the transmission coefficients having a value other than unity but there is no means of calculating what such a value should be. On the other hand, if we adopt the relatively simple view that the ratio of the frequency factors is determined by the relative number of times that the H and D are moving in a direction favorable for reaction and that this ratio is given by the ratio of the C—H and C—D stretching frequencies, we calculate 1.33 which agrees with the experimental value well within the limits of error. This idea can be tested further when data on tritium containing compounds become available. A calculation similar to the one made above on the basis of the Eyring theory can be made for the tritium compound if we use the estimated values of 1840 and 741 cm^{-1} for the C—T stretching and bending frequencies, respectively, and assume 1100 cm^{-1} for the perpendicular vibration in the activated complex. The result is

$$k_1/k_2 = 1.06 \exp(1270/RT).$$

The non-exponential factor is again near unity whereas the ratio of the stretching frequencies is 1.63.

It should be pointed out that if the above expression is correct, the hydrogen-containing molecule should react 8.8 times as fast as the tritium-containing one if we use the factor 1.06 and over thirteen times as fast if the calculation is made using 1.63. It follows that tracer experiments using tritium containing compounds should be interpreted cautiously if rate phenomena are involved.

Incidental to the main purpose of this work, evidence has been obtained which casts doubt on the work of Schumacher and Wolff. Both the exchange experiment and the trend in the values of k_1/k_2 with the amount of reaction support the contention of Schwab and Heyde that the reaction

$$HCl + CCl_3 = CHCl_3 + Cl$$

must be included in the reaction mechanism. Furthermore, the formation of considerable amounts of hexachloroethane indicates that the probable chain terminating process must be the formation of this compound rather than the reaction

$$2CCl_3 + Cl_2 = 2CCl_4,$$

as was suggested by Schumacher and Wolff.

[13] G. Herzberg, *Infrared and Raman Spectra of Polyatomic Molecules* (D. Van Nostrand Publishing Company, Inc., New York, 1939). T. Y. Wu, *Vibrational Spectra and Structure of Polyatomic Molecules* (National University of Peking, Kun Ming, China, 1939).

Molecular Orbital Calculations of Vibrational Force Constants. II. The Ring-Twisting Constants of Benzene*

BRYCE L. CRAWFORD, JR. AND ROBERT G. PARR**
School of Chemistry, University of Minnesota, Minneapolis, Minnesota

(Received January 5, 1949)

Two out-of-plane bending force constants of the C_6 framework of benzene are calculated by the method of antisymmetric molecular orbitals, and the values obtained compared with those previously determined by Miller and Crawford from spectroscopic data.

RECENTLY[1] the Goeppert-Mayer-Sklar method of molecular orbitals[2] was adapted to the calculation of the electronic energy levels and twisting force constant of the ethylene molecule. The encouraging results obtained made it seem worth while to attempt the calculation of analogous force constants in other molecules. This will be done in the present paper for two ring-twisting force constants of benzene.

STATEMENT OF THE PROBLEM

The equilibrium configuration of benzene will be assumed to be the planar structure of D_{6h} symmetry, with[3]

C−C distance = 1.39A,
C−H distance = 1.08A,
CCC angle = HCC angle = 120°.

The nine non-planar vibrations of this model may be described conveniently by use of a set of *valence force coordinates* $r_0\gamma_i$ and $R_0\delta_i$, where

r_0 = equilibrium C−H distance,
R_0 = equilibrium C_1-C_2 distance,[4]
$r_0\gamma_i$ = perpendicular distance of the ith H atom from the plane defined by the two adjacent C−C bonds,
δ_i = angle between the planes defined by C_i, C_{i+1}, C_{i+2}, and C_{i-1}, C_i, C_{i+1}.

Miller and Crawford[5] have shown that the transformation

$$\begin{Bmatrix} S_4 \\ S_{16a} \\ S_{16b} \\ S_{11} \\ S_5 \\ S_{17a} \\ S_{17b} \\ S_{10a} \\ S_{10b} \end{Bmatrix} = \begin{Bmatrix} 6^{-\frac{1}{2}} & 6^{-\frac{1}{2}} & 6^{-\frac{1}{2}} & 6^{-\frac{1}{2}} & 6^{-\frac{1}{2}} & 6^{-\frac{1}{2}} \\ -12^{-\frac{1}{2}} & 3^{-\frac{1}{2}} & -12^{-\frac{1}{2}} & -12^{-\frac{1}{2}} & 3^{-\frac{1}{2}} & -12^{-\frac{1}{2}} \\ \frac{1}{2} & 0 & \frac{1}{2} & \frac{1}{2} & 0 & \frac{1}{2} \\ & & & & & \\ & & & & & \\ & & 0 & & & \\ & & & & & \\ & & & & & \end{Bmatrix} \begin{Bmatrix} R_0\delta_1 \\ R_0\delta_2 \\ R_0\delta_3 \\ R_0\delta_4 \\ R_0\delta_5 \\ R_0\delta_6 \end{Bmatrix}$$

$$\begin{Bmatrix} & & & & & \\ & & & & & \\ & & & & & \\ & & & & & \\ & & & & & \\ 6^{-\frac{1}{2}} & 6^{-\frac{1}{2}} & 6^{-\frac{1}{2}} & 6^{-\frac{1}{2}} & 6^{-\frac{1}{2}} & 6^{-\frac{1}{2}} \\ 6^{-\frac{1}{2}} & -6^{-\frac{1}{2}} & 6^{-\frac{1}{2}} & -6^{-\frac{1}{2}} & 6^{-\frac{1}{2}} & -6^{-\frac{1}{2}} \\ 0 & -\frac{1}{2} & \frac{1}{2} & 0 & -\frac{1}{2} & \frac{1}{2} \\ -3^{-\frac{1}{2}} & 12^{-\frac{1}{2}} & 12^{-\frac{1}{2}} & -3^{-\frac{1}{2}} & 12^{-\frac{1}{2}} & 12^{-\frac{1}{2}} \\ 0 & \frac{1}{2} & \frac{1}{2} & 0 & -\frac{1}{2} & -\frac{1}{2} \\ -3^{-\frac{1}{2}} & -12^{-\frac{1}{2}} & 12^{-\frac{1}{2}} & 3^{-\frac{1}{2}} & 12^{-\frac{1}{2}} & -12^{-\frac{1}{2}} \end{Bmatrix} \begin{Bmatrix} R_0\delta_1 \\ R_0\delta_2 \\ R_0\delta_3 \\ R_0\delta_4 \\ R_0\delta_5 \\ R_0\delta_6 \\ r_0\gamma_1 \\ r_0\gamma_2 \\ r_0\gamma_3 \\ r_0\gamma_4 \\ r_0\gamma_5 \\ r_0\gamma_6 \end{Bmatrix}, \quad (1)$$

gives *valence force symmetry coordinates* S_i, in terms of which the potential energy may be written

$$\begin{aligned} 2(V-V^0) = {} & \alpha S_{11}^2+\beta S_4^2+\epsilon S_5^2+\eta(S_4S_5+S_5S_4) \\ & +\theta(S_{16a}^2+S_{16b}^2)+\sigma(S_{17a}^2+S_{17b}^2) \\ & +\omega(S_{16a}S_{17a}+S_{17a}S_{16a} \\ & +S_{16b}S_{17b}+S_{17b}S_{16b})+\phi(S_{10a}^2+S_{10b}^2). \end{aligned} \quad (2)$$

It is the force constants β and θ which are analogous to the twisting force constant of ethylene and which will be the concern of this paper. The problem, then, is to obtain V as a function of S_4 and of S_{16a} (or S_{16b}) and to calculate β and θ from the formulas:

$$\begin{aligned} & \beta = (\partial^2 V/\partial S_4^2)_{S_4=0}, \\ & \theta = (\partial^2 V/\partial S_{16a}^2)_{S_{16a}=0} = (\partial^2 V/\partial S_{16b}^2)_{S_{16b}=0}. \end{aligned} \quad (3)$$

The results should provide independent support for one of the alternative sets of values for β and θ found by Miller and Crawford[5] from spectroscopic data.

Upon inverting (1) and setting all $S_i=0$ save the chosen one, one obtains

$$\begin{Bmatrix} R_0\delta_1 \\ R_0\delta_2 \\ R_0\delta_3 \\ R_0\delta_4 \\ R_0\delta_5 \\ R_0\delta_6 \end{Bmatrix}_{S_{16b}} = \begin{Bmatrix} (1/2)S_{16b} \\ 0 \\ -(1/2)S_{16b} \\ (1/2)S_{16b} \\ 0 \\ -(1/2)S_{16b} \end{Bmatrix}, \quad \begin{Bmatrix} R_0\delta_1 \\ R_0\delta_2 \\ R_0\delta_3 \\ R_0\delta_4 \\ R_0\delta_5 \\ R_0\delta_6 \end{Bmatrix}_{S_4} = \begin{Bmatrix} 6^{-\frac{1}{2}}\,S_4 \\ -6^{-\frac{1}{2}}\,S_4 \\ 6^{-\frac{1}{2}}\,S_4 \\ -6^{-\frac{1}{2}}\,S_4 \\ 6^{-\frac{1}{2}}\,S_4 \\ -6^{-\frac{1}{2}}\,S_4 \end{Bmatrix}. \quad (4)$$

* This paper is based partly on a thesis submitted by Robert G. Parr to the Graduate School of the University of Minnesota, August, 1947, in partial fulfillment of the requirements for the degree of Doctor of Philosophy, and partly on research supported by the Office of Naval Research, U. S. Navy, through Contract N5ori-147 with the University of Minnesota.

** Present address: Department of Chemistry, Carnegie Institute of Technology, Pittsburgh, Pennsylvania.

[1] R. G. Parr and B. L. Crawford, Jr., J. Chem. Phys. **16**, 526 (1948).

[2] M. Goeppert-Mayer and A. L. Sklar, J. Chem. Phys. **6**, 645 (1938).

[3] L. Pauling, *Nature of the Chemical Bond* (Cornell University Press, Ithaca, 1942), pp. 168, 172. Values of the angles are assumed.

[4] Here and later, i is to be understood reduced modulo 6, carbon atoms are numbered 1, 2, ···, 6 consecutively around the ring, and H_i is on C_i.

[5] F. A. Miller and B. L. Crawford, Jr., J. Chem. Phys. **14**, 282 (1946).

Consequently, S_{16b} and S_4 may be thought of as coordinates measuring distortions of the ring into "cradle" and "chair" forms, as shown in Fig. 1. In each case the amount of distortion is also completely specified by one angle φ. The energy, therefore, is also,

$$\begin{aligned} 2(V-V^0)s_{16b}&=k_{16b}\varphi_{16b}^2+\text{higher terms},\\ 2(V-V^0)s_4&=k_4\varphi_4^2+\text{higher terms}. \end{aligned} \tag{5}$$

β and θ are thus multiples of k_{16b} and k_4 respectively. Indeed, since geometry shows that for small distortions

$$\left.\begin{matrix}\delta\,1\\ \delta\,2\\ \delta\,3\\ \delta\,4\\ \delta\,5\\ \delta\,6\end{matrix}\right\}_{S_{16b}}=\begin{Bmatrix} 3^{-\frac{1}{2}}(2\varphi)\\ 0\\ -3^{-\frac{1}{2}}(2\varphi)\\ 3^{-\frac{1}{2}}(2\varphi)\\ 0\\ -3^{-\frac{1}{2}}(2\varphi)\end{Bmatrix},\quad \left.\begin{matrix}\delta_1\\ \delta_2\\ \delta_3\\ \delta_4\\ \delta_5\\ \delta_6\end{matrix}\right\}_{S_4}=\begin{Bmatrix} 3^{-\frac{1}{2}}(2\varphi)\\ -3^{-\frac{1}{2}}(2\varphi)\\ 3^{-\frac{1}{2}}(2\varphi)\\ -3^{-\frac{1}{2}}(2\varphi)\\ 3^{-\frac{1}{2}}(2\varphi)\\ -3^{-\frac{1}{2}}(2\varphi)\end{Bmatrix}; \tag{6}$$

one has, for small distortions,

$$\begin{aligned} S_4&=2^{\frac{1}{2}}(R_0\varphi_4),\\ S_{16b}&=(16/3)^{\frac{1}{2}}(R_6\varphi_{16b}); \end{aligned} \tag{7}$$

so that

$$\begin{aligned} \beta&=k_4/8R_0^2,\\ \theta&=3k_{16b}/16R_0^2. \end{aligned} \tag{8}$$

The problem is thus reduced to finding V as a function of φ_4 and φ_{16b}.

MOLECULAR ORBITALS

In the next section, the wave functions for the ground state of the distorted configurations will be built up as antisymmetrized products of one-electron molecular orbitals, which themselves are linear combinations of the $2p\pi$ atomic orbitals on the various carbon atoms.[6] In the present section symmetry will be used to determine these molecular orbitals; the different symmetries of the S_4 and S_{16b} configurations will lead to different linear combinations in the two cases.

Let the real, normalized $2p\pi$ wave function for the νth electron on carbon A_n be denoted by $\alpha_n(\nu)$. The problem is to find, by the method of variation of parameters,[7] the coefficients a_{nm} in the one-electron, normalized molecular orbitals

$$\phi_n=(6\sigma_n)^{-\frac{1}{2}}\sum_{m=1}^{6}a_{nm}\alpha_m,\quad n=1,2,\cdots,6, \tag{9}$$

where[8]

$$\sigma_n=(1/6)\sum_{m=1}^{6}\sum_{m'=1}^{6}a_{nm}{}^*a_{nm'}S_{\alpha_m\alpha_{m'}}, \tag{10}$$

$$S_{\alpha_m\alpha_{m'}}=\int\alpha_m\alpha_{m'}dv. \tag{11}$$

[6] The $2p\pi$ wave function on C_i is the $2p$ wave function on C_i whose principle axis of symmetry is perpendicular to the plane defined by C_{i-1}, C_i, C_{i+1} (and H_i).

[7] See Eyring, Walter, and Kimball, *Quantum Chemistry* (John Wiley and Sons, Inc., New York, 1944), pp. 99–101.

[8] $a_{nm}{}^*$ denotes the complex conjugate of a_{nm}.

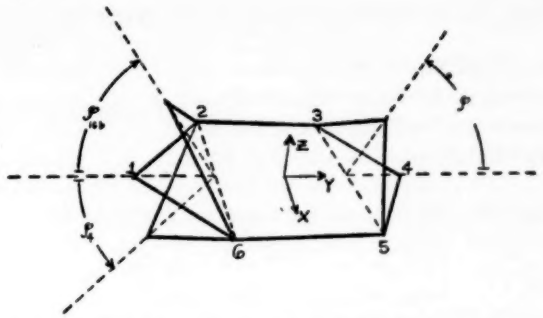

FIG. 1. Valence force symmetry coordinates S_4 and S_{16b}.

In general one would have to solve a sixth degree secular equation to obtain the coefficients, but symmetry helps here considerably—for the equilibrium and chair (S_4) forms the a_{nm} can be determined entirely by group theory; for the cradle (S_{16b}) form the problem can be reduced by group theory to the solution of two quadratics.

The character table for the groups D_{6h}, D_{3d}, and C_{2v}, to which the equilibrium, chair (S_4) and cradle (S_{16b}) configurations belong respectively, is given in Table I.[9] Here the twofold axes C_2' have been taken through opposite carbons (e.g., the y axis in Fig. 1), and C_2'' through opposite bonds (the x axis); the planes σ_v have been taken through bonds (the xz plane), and the σ_v' through carbons (the yz plane). The principal axis for the group D_{3d} is not the z axis in Fig. 1 but an axis in the yz plane tilted at a small angle to the z axis.

Taking the atomic orbitals α_n as basis for the reducible representation $\Gamma(\phi)$, one finds[9]

$$\begin{aligned}\Gamma(\phi)&=\Gamma_4+\Gamma_7+\Gamma_{10}+\Gamma_{11}\\ &=\begin{Bmatrix}\Gamma_{A_{2u}}+\Gamma_{B_{2g}}+\Gamma_{E_{2u}}+\Gamma_{E_{1g}}(D_{6h})\\ \Gamma_{A_{2u}}+\Gamma_{A_{1g}}+\Gamma_{E_u}+\Gamma_{E_g}(D_{3d})\\ \Gamma_{A_1}+\Gamma_{B_2}+\Gamma_{A_1}+\Gamma_{A_2}+\Gamma_{B_1}+\Gamma_{B_2}(C_{2v})\end{Bmatrix}.\end{aligned} \tag{12}$$

The proper molecular orbitals ϕ_n of (9) are bases for the irreducible representations appearing in (12) (these representations are *italicized* in Table I); one ϕ_n belongs to each non-degenerate representation, and two ϕ_n to each degenerate representation.

Completely orthonormal molecular orbitals for the several cases may now be found by the standard methods of group theory.[9] For the symmetries D_{6h} and D_{3d}, they are

$$\left.\begin{aligned}
&\phi_0=(6\sigma_0)^{-\frac{1}{2}}(\alpha_1+\alpha_2+\alpha_3+\alpha_4+\alpha_5+\alpha_6) && A_{2u}\\
&\phi_1=(12\sigma_1)^{-\frac{1}{2}}(2\alpha_1+\alpha_2-\alpha_3-2\alpha_4-\alpha_5+\alpha_6) &&\\
&\phi_{-1}=(4\sigma_{-1})^{-\frac{1}{2}}(\alpha_2+\alpha_3-\alpha_5-\alpha_6) && E_{1g}\text{ and }E_g\\
&\phi_2=(12\sigma_2)^{-\frac{1}{2}}(2\alpha_1-\alpha_2-\alpha_3+2\alpha_4-\alpha_5-\alpha_6) &&\\
&\phi_{-2}=(4\sigma_{-2})^{-\frac{1}{2}}(\alpha_2-\alpha_3+\alpha_5-\alpha_6) && E_{2u}\text{ and }E_u\\
&\phi_3=(6\sigma_3)^{-\frac{1}{2}}(\alpha_1-\alpha_2+\alpha_3-\alpha_4+\alpha_5-\alpha_6) && B_{2g}\text{ and }A_{1g}
\end{aligned}\right\}(D_{6h}\text{ and }D_{3d}), \tag{13}$$

[9] For group theoretical details, see reference 7, Chapters X and XIII and Appendix VII.

where the normalizing factors σ_n are given by

$$\left.\begin{aligned}\sigma_0&=1+2S_{\alpha_1\alpha_2}+2S_{\alpha_1\alpha_3}+S_{\alpha_1\alpha_4}\\ \sigma_1=\sigma_{-1}&=1+S_{\alpha_1\alpha_2}-S_{\alpha_1\alpha_3}-S_{\alpha_1\alpha_4}\\ \sigma_2=\sigma_{-2}&=1-S_{\alpha_1\alpha_2}-S_{\alpha_1\alpha_3}+S_{\alpha_1\alpha_4}\\ \sigma_3&=1-2S_{\alpha_1\alpha_2}+2S_{\alpha_1\alpha_3}-S_{\alpha_1\alpha_4}\end{aligned}\right\}(D_{6h}\text{ and }D_{3d}). \quad (14)$$

Similarly, the orbitals for the symmetry C_{2v} are

$$\left.\begin{aligned}\phi A_{1,1}&=(\sigma A_{1,1})^{-\frac{1}{2}}(\phi_0+\lambda_1\phi_2)\\ \phi A_{1,2}&=(\sigma A_{1,2})^{-\frac{1}{2}}(\phi_2+\lambda_2\phi_0)\\ \phi A_2&=\phi_{-2}\\ \phi B_1&=\phi_{-1}\\ \phi B_{2,1}&=(\sigma B_{2,1})^{-\frac{1}{2}}(\phi_1+\lambda_3\phi_3)\\ \phi B_{2,2}&=(\sigma B_{2,2})^{-\frac{1}{2}}(\phi_3+\lambda_4\phi_1)\end{aligned}\right\}(C_{2v}), \quad (15)$$

where the ϕ_n are given by expressions of the form (13), with

$$\left.\begin{aligned}\sigma_0&=(1/6)(6+8S_{\alpha_1\alpha_2}+4S_{\alpha_2\alpha_3}+8S_{\alpha_1\alpha_3}\\ &\quad+4S_{\alpha_3\alpha_5}+4S_{\alpha_2\alpha_5}+2S_{\alpha_1\alpha_4})\\ \sigma_1&=(1/3)(3+4S_{\alpha_1\alpha_2}-S_{\alpha_2\alpha_3}-4S_{\alpha_1\alpha_3}\\ &\quad+S_{\alpha_3\alpha_5}-S_{\alpha_2\alpha_5}-2S_{\alpha_1\alpha_4})\\ \sigma_{-1}&=(1+S_{\alpha_2\alpha_3}-S_{\alpha_3\alpha_5}-S_{\alpha_2\alpha_5})\\ \sigma_2&=(1/3)(3-4S_{\alpha_1\alpha_2}+S_{\alpha_2\alpha_3}-4S_{\alpha_1\alpha_3}\\ &\quad+S_{\alpha_3\alpha_5}+S_{\alpha_2\alpha_5}+2S_{\alpha_1\alpha_4})\\ \sigma_{-2}&=(1-S_{\alpha_2\alpha_3}-S_{\alpha_3\alpha_5}+S_{\alpha_2\alpha_5})\\ \sigma_3&=(1/6)(6-8S_{\alpha_1\alpha_2}-4S_{\alpha_2\alpha_3}+8S_{\alpha_1\alpha_3}\\ &\quad+4S_{\alpha_3\alpha_5}-4S_{\alpha_2\alpha_5}-2S_{\alpha_1\alpha_4})\end{aligned}\right\}(C_{2v}), \quad (16)$$

and the normalizing factors $\sigma A_{1,1}$, etc., are given by

$$\left.\begin{aligned}\sigma A_{1,1}&=1+2\lambda_1S_{\phi_0\phi_2}+\lambda_1^2\\ \sigma A_{1,2}&=1+2\lambda_2S_{\phi_0\phi_2}+\lambda_2^2\\ \sigma B_{2,1}&=1+2\lambda_3S_{\phi_1\phi_3}+\lambda_3^2\\ \sigma B_{2,2}&=1+2\lambda_4S_{\phi_1\phi_3}+\lambda_4^2\end{aligned}\right\}(C_{2v}), \quad (17)$$

where

$$\left.\begin{aligned}S_{\phi_0\phi_2}&=(2^{\frac{1}{2}}/3)(\sigma_0\sigma_2)^{-\frac{1}{2}}(S_{\alpha_1\alpha_2}-S_{\alpha_2\alpha_3}\\ &\quad+S_{\alpha_1\alpha_3}-S_{\alpha_3\alpha_5}-S_{\alpha_2\alpha_5}+S_{\alpha_1\alpha_4})\\ S_{\phi_1\phi_3}&=(2^{\frac{1}{2}}/3)(\sigma_1\sigma_3)^{-\frac{1}{2}}(-S_{\alpha_1\alpha_2}+S_{\alpha_2\alpha_3}\\ &\quad+S_{\alpha_1\alpha_3}-S_{\alpha_3\alpha_5}+S_{\alpha_2\alpha_5}-S_{\alpha_1\alpha_4})\end{aligned}\right\}(C_{2v}). \quad (18)$$

The parameters λ are functions of the amount of distortion from equilibrium which could be found by solution of second-order secular equations. As the distortion approaches zero the λ's approach zero.

ENERGY OF THE GROUND STATE IN TERMS OF INTEGRALS OVER MOLECULAR ORBITALS. FUNDAMENTAL SIMPLIFICATION THEOREM

In the general case of $2k$ electrons in $2k$ atomic orbitals, there are $2k$ one-electron molecular orbitals of the form

$$\phi_n=(2k\sigma_n)^{-\frac{1}{2}}\sum_{m=1}^{2k}a_{nm}\alpha_m,\ n=1, 2, \cdots, 2k, \quad (19)$$

where the σ_n are normalizing factors and the a_{nm} constants. Suppose that these orbitals are numbered in the order of increasing energy; i.e.,

$$\epsilon_1\leqslant\epsilon_2\leqslant\ldots\leqslant\epsilon_{2k}, \quad (20)$$

where the ϵ_n, given by

$$\epsilon_n=\int\phi_n^*(\mathbf{T}+\mathbf{H}_0)\phi_n dv, \quad (21)$$

are the one-electron energies—$\mathbf{T}$ and $\mathbf{H}_0$ are the kinetic and potential energy operators for a single electron in the field of the nuclear framework (the molecule minus

TABLE I. Character table for the groups D_{6h}, D_{3d}, and C_{2v}.

Representation	C_{2v}	D_{3d}	D_{6h}	Operation: E	C_2	—	—	—	—	—	—	—	—	σ_v	σ_v'
	Species			E	—	$2C_3$	—	—	$3C_2''$	iE	—	$2iC_3$	—	—	$3iC_2''$
				E	C_2	$2C_3$	$2C_6$	$3C_2'$	$3C_2''$	iE	iC_2	$2iC_3$	$2iC_6$	$3iC_2'$	$3iC_2''$
Γ_1	A_1	A_{1g}	A_{1g}	1	1	1	1	1	1	1	1	1	1	1	1
Γ_2	A_2	A_{1u}	A_{1u}	1	1	1	1	1	1	−1	−1	−1	−1	−1	−1
Γ_3	A_2	A_{2g}	A_{2g}	1	1	1	1	−1	−1	1	1	1	1	−1	−1
Γ_4	A_1	A_{2u}	A_{2u}	1	1	1	1	−1	−1	−1	−1	−1	−1	1	1
Γ_5	B_1	A_{2g}	B_{1g}	1	−1	1	−1	1	−1	1	−1	1	−1	1	−1
Γ_6	B_2	A_{2u}	B_{1u}	1	−1	1	−1	1	−1	−1	1	−1	1	−1	1
Γ_7	B_2	A_{1g}	B_{2g}	1	−1	1	−1	−1	1	1	−1	1	−1	−1	1
Γ_8	B_1	A_{1u}	B_{2u}	1	−1	1	−1	−1	1	−1	1	−1	1	1	−1
Γ_9	A_1+A_2	E_g	E_{2g}	2	2	−1	−1	0	0	2	2	−1	−1	0	0
Γ_{10}	A_1+A_2	E_u	E_{2u}	2	2	−1	−1	0	0	−2	−2	1	1	0	0
Γ_{11}	B_1+B_2	E_g	E_{1g}	2	−2	−1	1	0	0	2	−2	−1	1	0	0
Γ_{12}	B_1+B_2	E_u	E_{1u}	2	−2	−1	1	0	0	−2	2	1	−1	0	0

the $2k$ electrons being considered). The completely antisymmetric wave function for the ground state then is

$$\bar{\Psi}_0=(2k!)^{-\frac{1}{2}}\sum_{\mathbf{P}}(-1)^P\mathbf{P}(\psi_0X_0), \tag{22}$$

where the summation is over all permutations $\mathbf{P}$ of the electrons, $(-1)^P$ is 1 if $\mathbf{P}$ is even and -1 if $\mathbf{P}$ is odd;

$$\psi_0=\phi_1(1)\phi_1(2)\phi_2(3)\phi_2(4)\ldots\phi_k(2k-1)\phi_k(2k), \tag{23}$$

where $\phi_n(\nu)$ denotes the presence of electron ν in orbital ϕ_n; and

$$X_0=\delta_+(1)\delta_-(2)\delta_+(3)\delta_-(4)\ldots\delta_+(2k-1)\delta_-(2k), \tag{24}$$

where $\delta_+(\nu)$ and $\delta_-(\nu)$ are possible spin functions for the νth electron.

The complete $2k$-electron Hamiltonian in this case is

$$\mathbf{H}=\sum_{\nu=1}^{2k}[\mathbf{H}_0(\nu)+\mathbf{T}(\nu)]+\sum_{\mu,\nu}(e^2/r_{\mu\nu}), \tag{25}$$

where e is the charge on an electron and $r_{\mu\nu}$ is the distance between electrons μ and ν. Substituting this and (22) into the formula $E_0=\int\bar{\Psi}_0\mathbf{H}\bar{\Psi}_0d\nu$, one finds, after considerable use of orthogonality relations and simple properties of permutations,[10]

$$E_0=\sum_{n=1}^{k}[2\epsilon_n+\gamma_{nn}+4\sum_{m=1}^{n-1}\gamma_{mn}-2\sum_{m=1}^{n-1}\delta_{mn}], \tag{26}$$

where the inner sums are missing for $n=1$, and where

$$\gamma_{mn}=\int(e^2/r_{12})|\phi_m(1)|^2|\phi_n(2)|^2d\nu_1d\nu_2 \tag{27}$$

and

$$\delta_{mn}=\int(e^2/r_{12})[\phi_m(1)\phi_n(2)]^*\phi_n(1)\phi_m(2)d\nu_1d\nu_2 \tag{28}$$

are Coulomb and exchange integral respectively.

The molecular orbitals ϕ_n for the D_{3d} chair and D_{6h} equilibrium forms of benzene were given in (13). If one takes all the α_i positive on the same side of the benzene ring, one sees by examining the number of nodes that the energies of these orbitals should increase with $|n|$.[11] In the ground state there will therefore be two electrons in each of ϕ_0, ϕ_1, ϕ_{-1}:

$$\psi_0^{D_{3d}}=\phi_0(1)\phi_0(2)\phi_1(3)\phi_1(4)\phi_{-1}(5)\phi_{-1}(6). \tag{29}$$

By (26) adapted to this numbering, the ground state energy is

$$E_0^{D_{3d}}=2\epsilon_0+2\epsilon_1+2\epsilon_{-1}+\gamma_{00}+\gamma_{11}+\gamma_{-1-1}+4\gamma_{01}+4\gamma_{0-1}+4\gamma_{1-1}-2\delta_{01}-2\delta_{0-1}-2\delta_{1-1}, \tag{30}$$

where the ϵ_n, γ_{mn}, and δ_{mn} are defined by (21), (27), and (28).

The representations Γ_4 and Γ_{11} to which ϕ_0, ϕ_1, and ϕ_{-1} belong are given in bold face italics in Table I. As the D_{3d} chair configuration passes continuously into the C_{2v} cradle one, the orbitals ϕ_0, ϕ_1, ϕ_{-1} of (13) must change continuously into the orbitals $\phi_{A_1,1}$, $\phi_{B_2,1}$, ϕ_{B_1} of (15). The latter are therefore the lowest orbitals for the cradle form, and the wave function for its ground state will be

$$\begin{aligned}\psi_0^{C_{2v}}&=\phi_{A_1,1}(1)\phi_{A_1,1}(2)\phi_{B_2,1}(3)\phi_{B_2,1}(4)\phi_{B_1}(5)\phi_{B_1}(6)\\&=(1/\sigma_{A_1,1}\sigma_{B_2,1})[\phi_0(1)+\lambda_1\phi_2(1)]\\&\quad\times[\phi_0(2)+\lambda_1\phi_2(2)][\phi_1(3)+\lambda_3\phi_3(3)]\\&\quad\times[\phi_1(4)+\lambda_3\phi_3(4)]\phi_{-1}(5)\phi_{-1}(6).\end{aligned} \tag{31}$$

Now it is shown in the next paragraph that *for the purpose of obtaining $E_0^{C_{2v}}$ to the second power of the distortion φ_{16b}, the λ's may be completely neglected.* On account of this "fundamental simplification theorem," (31) may be replaced by

$$\psi_0^{C_{2v}}=\phi_0(1)\phi_0(2)\phi_1(3)\phi_1(4)\phi_{-1}(5)\phi_{-1}(6), \tag{32}$$

and the energy is

$$E_0^{C_{2v}}=2\epsilon_0+2\epsilon_1+2\epsilon_{-1}+\gamma_{00}+\gamma_{11}+\gamma_{-1-1}+4\gamma_{01}+4\gamma_{0-1}+4\gamma_{1-1}-2\delta_{01}-2\delta_{0-1}-2\delta_{1-1}, \tag{33}$$

just as before!

To prove this theorem, it will suffice to establish that

(*i*) Each λ may be written as an *even* power series in φ_{16b} with zero constant term.

(*ii*) In the expansion of the energy λ's always enter multiplied by integrals which are zero when $\varphi_{16b}=0$.

The vanishing of the λ's for $\varphi_{16b}=0$ follows from the group-theoretic result that as $\varphi_{16b}\to0$, $\phi_{A_1,1}\to\phi_0$ and $\phi_{B_2,1}\to\phi_1$. Evenness of the λ's could be demonstrated from the secular equations defining them, but can be proved in one fell swoop as follows. Under replacement of φ_{16b} by $-\varphi_{16b}$, the wave function (31) must transform into a wave function of the same energy and therefore into itself or its negative, since there are no wave functions degenerate with it. But (31) may be expanded in the form

$$\psi_0^{C_{2v}}=[\psi_0^{C_{2v}}]_{\varphi_{16b}=0}+A\varphi_{16b}+B\varphi_{16b}^2+\ldots, \tag{34}$$

where the constant term is not identically zero. If any of the λ's were not even, A would not be zero, which it must be in order for $\psi_0^{C_{2v}}$ to have the transformation property described above. Therefore all λ's are even, completing the proof of (*i*). To prove (*ii*), one need only note that the integrals $S_{\phi_0\phi_2}$ and

$$\int[\phi_0(1)\phi_0(2)\phi_1(3)\phi_1(4)\phi_{-1}(5)\phi_{-1}(6)]^*\mathbf{H}\times\phi_2(1)\phi_0(2)\phi_1(3)\phi_1(4)\phi_{-1}(5)\phi_{-1}(6)d\nu$$

[10] See reference 7, pp. 144 ff., for details of an analogous reduction.

[11] A. Wintner, J. Chem. Phys. **16**, 405 (1948), has recently proved, in the general three-dimensional case, that energy increases with the number of nodes of each type in the true wave function. This may not be true of an approximate wave function, but it would seem reasonable to assume it so.

are zero for $\varphi_{16b}=0$ because ϕ_0 and ϕ_2 belong to different symmetry classes for $\varphi_{16b}=0$; the integrals $S_{\phi_1\phi_3}$ and

$$\int[\phi_0(1)\phi_0(2)\phi_1(3)\phi_1(4)\phi_{-1}(5)\phi_{-1}(6)]^*\mathbf{H}\times\phi_0(1)\phi_0(2)\phi_2(3)\phi_1(4)\phi_{-1}(5)\phi_{-1}(6)dv$$

are zero for $\varphi_{16b}=0$ because ϕ_1 and ϕ_3 belong to different symmetry classes for $\varphi_{16b}=0$; etc.

ENERGY OF THE GROUND STATE IN TERMS OF INTEGRALS OVER ATOMIC ORBITALS

Reduction of the integrals γ_{mn} and δ_{mn} over molecular orbitals to linear combinations of integrals over atomic orbitals can be accomplished by substitution of (29) or (32) into (27) and (28); reduction of the ϵ_n to similar combinations can be accomplished by substitution of (29) or (32) into (21) and resolution of the one-electron Hamiltonian into parts. To the approximations that

(*i*) atomic integrals involving three or more distinct nuclei may be neglected,[12]

(*ii*) atomic integrals involving non-neighboring nuclei are negligible except the Coulomb ones (those of the form $(\alpha_p\alpha_p;\alpha_q\alpha_q)$ —see Eq. (38)),[13]

(*iii*) hydrogen atoms may be neglected—the potential on electron ν due to the nth CH group in the single-bonded C_6H_6 framework is the potential $\mathbf{H}_{A_n}^*(\nu)$ due to the neutral carbon atom C_n, minus the potential due to one electron in the orbital α_n,[14]

one obtains, for both chair (D_{3d}) and cradle (C_{2v}) configurations, the following formulas:

$$\begin{aligned}
3\sigma_0(W_{2p}-\epsilon_0)&=6(A_1{:}\,\alpha_2\alpha_2)+4(A_1{:}\,\alpha_1\alpha_2)\\
&\quad+2(A_2{:}\,\alpha_2\alpha_3)+4(\alpha_1\alpha_1;\,\alpha_1\alpha_2)+2(\alpha_2\alpha_2;\,\alpha_2\alpha_3)\\
&\quad+4(\alpha_1\alpha_1;\,\alpha_2\alpha_2)+2(\alpha_2\alpha_2;\,\alpha_3\alpha_3)+4(\alpha_1\alpha_1;\,\alpha_3\alpha_3)\\
&\quad+2(\alpha_3\alpha_3;\,\alpha_5\alpha_5)+(\alpha_1\alpha_1;\,\alpha_4\alpha_4)+2(\alpha_2\alpha_2;\,\alpha_5\alpha_5),\\
3\sigma_1(W_{2p}-\epsilon_1)&=6(A_1{:}\,\alpha_2\alpha_2)+4(A_1{:}\,\alpha_1\alpha_2)\\
&\quad-(A_2{:}\,\alpha_2\alpha_3)+4(\alpha_1\alpha_1;\,\alpha_1\alpha_2)-(\alpha_2\alpha_2;\,\alpha_2\alpha_3)\\
&\quad+5(\alpha_1\alpha_1;\,\alpha_2\alpha_2)+(\alpha_2\alpha_2;\,\alpha_3\alpha_3)+5(\alpha_1\alpha_1;\,\alpha_3\alpha_3)\\
&\quad+(\alpha_3\alpha_3;\,\alpha_5\alpha_5)+2(\alpha_1\alpha_1;\,\alpha_4\alpha_4)+(\alpha_2\alpha_2;\,\alpha_5\alpha_5),\\
\sigma_{-1}(W_{2p}-\epsilon_{-1})&=2(A_1{:}\,\alpha_2\alpha_2)+(A_2{:}\,\alpha_2\alpha_3)\\
&\quad+(\alpha_2\alpha_2;\,\alpha_2\alpha_3)+(\alpha_1\alpha_1;\,\alpha_2\alpha_2)+(\alpha_2\alpha_2;\,\alpha_3\alpha_3)\\
&\quad+(\alpha_1\alpha_1;\,\alpha_3\alpha_3)+(\alpha_3\alpha_3;\,\alpha_5\alpha_5)+(\alpha_2\alpha_2;\,\alpha_5\alpha_5);\\
18\sigma_0^2\gamma_{00}&=3(\alpha_1\alpha_1;\,\alpha_1\alpha_1)+8(\alpha_1\alpha_2;\,\alpha_1\alpha_2)\\
&\quad+4(\alpha_2\alpha_3;\,\alpha_2\alpha_3)+16(\alpha_1\alpha_1;\,\alpha_1\alpha_2)+8(\alpha_2\alpha_2;\,\alpha_2\alpha_3)\\
&\quad+4(\alpha_1\alpha_1;\,\alpha_2\alpha_2)+2(\alpha_2\alpha_2;\,\alpha_3\alpha_3)+4(\alpha_1\alpha_1;\,\alpha_3\alpha_3)\\
&\quad+2(\alpha_3\alpha_3;\,\alpha_5\alpha_5)+(\alpha_1\alpha_1;\,\alpha_4\alpha_4)+2(\alpha_2\alpha_2;\,\alpha_5\alpha_5),\\
36\sigma_1^2\gamma_{11}&=9(\alpha_1\alpha_1;\,\alpha_1\alpha_1)+16(\alpha_1\alpha_2;\,\alpha_1\alpha_2)\\
&\quad+2(\alpha_2\alpha_3;\,\alpha_2\alpha_3)+40(\alpha_1\alpha_1;\,\alpha_1\alpha_2)-4(\alpha_2\alpha_2;\,\alpha_2\alpha_3)\\
&\quad+8(\alpha_1\alpha_1;\,\alpha_2\alpha_2)+(\alpha_2\alpha_2;\,\alpha_3\alpha_3)+8(\alpha_1\alpha_1;\,\alpha_3\alpha_3)\\
&\quad+(\alpha_3\alpha_3;\,\alpha_5\alpha_5)+8(\alpha_1\alpha_1;\,\alpha_4\alpha_4)+(\alpha_2\alpha_2;\,\alpha_5\alpha_5),\\
4\sigma_{-1}^2\gamma_{-1-1}&=(\alpha_1\alpha_1;\,\alpha_1\alpha_1)+2(\alpha_2\alpha_3;\,\alpha_2\alpha_3)\\
&\quad+4(\alpha_2\alpha_2;\,\alpha_2\alpha_3)+(\alpha_2\alpha_2;\,\alpha_3\alpha_3)+(\alpha_3\alpha_3;\,\alpha_5\alpha_5)\\
&\quad+(\alpha_2\alpha_2;\,\alpha_5\alpha_5);
\end{aligned}\tag{35}$$

$$\begin{aligned}
6\sigma_1\sigma_{-1}(4\gamma_{1-1}-2\delta_{1-1})&=(\alpha_1\alpha_1;\,\alpha_1\alpha_1)\\
&\quad-4(\alpha_1\alpha_2;\,\alpha_1\alpha_2)-4(\alpha_2\alpha_3;\,\alpha_2\alpha_3)+4(\alpha_1\alpha_1;\,\alpha_1\alpha_2)\\
&\quad+8(\alpha_1\alpha_1;\,\alpha_2\alpha_2)+3(\alpha_2\alpha_2;\,\alpha_3\alpha_3)+8(\alpha_1\alpha_1;\,\alpha_3\alpha_3)\\
&\quad+3(\alpha_3\alpha_3;\,\alpha_5\alpha_5)+(\alpha_2\alpha_2;\,\alpha_5\alpha_5),\\
9\sigma_0\sigma_1(4\gamma_{01}-2\delta_{01})&=3(\alpha_1\alpha_1;\,\alpha_1\alpha_1)+7(\alpha_1\alpha_2;\,\alpha_1\alpha_2)\\
&\quad-4(\alpha_2\alpha_3;\,\alpha_2\alpha_3)+18(\alpha_1\alpha_1;\,\alpha_1\alpha_2)+6(\alpha_1\alpha_1;\,\alpha_2\alpha_2)\\
&\quad+3(\alpha_2\alpha_2;\,\alpha_3\alpha_3)+14(\alpha_1\alpha_1;\,\alpha_3\alpha_3)+(\alpha_3\alpha_3;\,\alpha_5\alpha_5)\\
&\quad+6(\alpha_1\alpha_1;\,\alpha_4\alpha_4)+3(\alpha_2\alpha_2;\,\alpha_5\alpha_5),\\
3\sigma_0\sigma_{-1}(4\gamma_{0-1}-2\delta_{0-1})&=(\alpha_1\alpha_1;\,\alpha_1\alpha_1)-(\alpha_1\alpha_2;\,\alpha_1\alpha_2)\\
&\quad+2(\alpha_2\alpha_3;\,\alpha_2\alpha_3)+2(\alpha_1\alpha_1;\,\alpha_1\alpha_2)+4(\alpha_2\alpha_2;\,\alpha_2\alpha_3)\\
&\quad+2(\alpha_1\alpha_1;\,\alpha_2\alpha_2)+(\alpha_2\alpha_2;\,\alpha_3\alpha_3)+2(\alpha_1\alpha_1;\,\alpha_3\alpha_3)\\
&\quad+3(\alpha_3\alpha_3;\,\alpha_5\alpha_5)+3(\alpha_2\alpha_2;\,\alpha_5\alpha_5).
\end{aligned}\tag{37}$$

Here W_{2p} is the energy of a 2_{2p} orbital of carbon in its valence state,

$$(\alpha_p\alpha_{p'};\,\alpha_q\alpha_{q'})=\int\alpha_p(1)\alpha_q(2)(e^2/r_{12})\alpha_{p'}(1)\alpha_{q'}(2)dv_1dv_2,\tag{38}$$

and

$$(A_q{:}\,\alpha_p\alpha_{p'})=-\int\mathbf{H}_{A_q}^*(1)\alpha_p(1)\alpha_{p'}(1)dv_1.\tag{39}$$

In the chair case, one has also the following identities:

$$\left.\begin{aligned}
S_{\alpha_2\alpha_3}&=S_{\alpha_1\alpha_2}\\
S_{\alpha_3\alpha_5}&=S_{\alpha_1\alpha_3}\\
S_{\alpha_2\alpha_5}&=S_{\alpha_1\alpha_4}\\
(\alpha_2\alpha_2;\,\alpha_3\alpha_3)&=(\alpha_1\alpha_1;\,\alpha_2\alpha_2)\\
(\alpha_3\alpha_3;\,\alpha_5\alpha_5)&=(\alpha_1\alpha_1;\,\alpha_3\alpha_3)\\
(\alpha_2\alpha_2;\,\alpha_5\alpha_5)&=(\alpha_1\alpha_1;\,\alpha_4\alpha_4)\\
(\alpha_2\alpha_3;\,\alpha_2\alpha_3)&=(\alpha_1\alpha_2;\,\alpha_1\alpha_2)\\
(A_2{:}\,\alpha_2\alpha_3)&=(A_1{:}\,\alpha_1\alpha_2)
\end{aligned}\right\}(D_{3d}).\tag{40}$$

FORCE CONSTANTS IN THE GROUND STATE

The dependence of the various atomic integrals on the angles φ must now be made explicit. This may be accomplished through the use of the vector property of p orbitals and the geometrical results expressed in Eq. (6). The procedure entails writing integrals over the α_i in terms of integrals over $2p$ orbitals with fixed orientation: a_i, a_{is}, a_{ir}, where the major axes of a_i and a_j are perpendicular to the $i-j$ internuclear axis and parallel to each other, the major axes of a_{is} and a_{js} are perpendicular to the $i-j$ axis and to the major axes of a_i and a_j, and the major axes of a_{ir} and a_{jr} are collinear with the $i-j$ axis.

Integrals which involve orbitals on the same nucleus or on neighboring nuclei may be written down immediately by direct analogy with the ethylene case,[1] for according to (6), for small φ (assumed henceforth) orbitals on neighboring nuclei are either parallel (but not coaxial) [α_2 and α_3, α_5 and α_6 in S_{16b}] or make the angle $3^{-\frac{1}{2}}(2\varphi)$ with each other [all other cases] in just the way α_1 and α_2 made the angle φ in ethylene.[1] Thus

[12] This assumption has been made by most authors employing this method, but has never been truly justified. There is even definite evidence that it is grossly wrong (see infra).

[13] Examination of numerical values (reference 16) justifies this assumption.

[14] See reference 2 for details.

one has:

$$\left.\begin{aligned}
&S_{\alpha_1\alpha_2}=[1-(2\varphi^2/3)]S_{a_1a_2}\\
&S_{\alpha_2\alpha_3}=S_{a_1a_2}\\
&(\alpha_1\alpha_1;\ \alpha_1\alpha_1)=(a_1a_1;\ a_1a_1)\\
&(\alpha_1\alpha_1;\ \alpha_2\alpha_2)=[1-(4\varphi^2/3)](a_1a_1;\ a_2a_2)\\
&\qquad\qquad+[4\varphi^2/3](a_1a_1;\ a_{2s}a_{2s})\\
&(\alpha_2\alpha_2;\ \alpha_3\alpha_3)=(a_1a_1;\ a_2a_2)\\
&(\alpha_1\alpha_1;\ \alpha_1\alpha_2)=[1-(2\varphi^2/3)](a_1a_1;\ a_1a_2)\\
&(\alpha_2\alpha_2;\ \alpha_2\alpha_3)=(a_1a_1;\ a_1a_2)\\
&(\alpha_1\alpha_2;\ \alpha_1\alpha_2)=[1-(4\varphi^2/3)](a_1a_2;\ a_1a_2)\\
&\qquad\qquad+[4\varphi^2/3](a_1a_{2s};\ a_1a_{2s})\\
&(\alpha_2\alpha_3;\ \alpha_2\alpha_3)=(a_1a_2;\ a_1a_2)\\
&(A_1{:}\,\alpha_2\alpha_2)=(A_1{:}\,a_2a_2)\\
&(A_1{:}\,\alpha_1\alpha_2)=[1-(2\varphi^2/3)](A_1{:}\,a_1a_2)\\
&(A_2{:}\,\alpha_2\alpha_3)=(A_1{:}\,a_1a_2)
\end{aligned}\right\}. \quad (41)$$

These formulas hold for both chair (D_{3d}) and cradle (C_{2v}) configurations, provided that in the former case Eq. (40) is given precedence.

The integrals which involve orbitals on non-neighboring nuclei are given as functions of φ by the following expressions:

$$\left.\begin{aligned}
&S_{\alpha_1\alpha_3}=S_{\alpha_3\alpha_5}=[1-(\varphi^2/3)]S_{a_1a_3}\\
&\qquad\qquad-[\varphi^2/3]S_{a_1r a_3r}\\
&S_{\alpha_1\alpha_4}=S_{\alpha_2\alpha_5}=S_{a_1a_4}\\
&(\alpha_1\alpha_1;\ \alpha_3\alpha_3)=(\alpha_3\alpha_3;\ \alpha_5\alpha_5)\\
&\qquad=[1-(2\varphi^2/3)](a_1a_1;\ a_3a_3)\\
&\qquad+[2\varphi^2/3](a_1a_1;\ a_{3r}a_{3r})\\
&\qquad\qquad-[4\varphi^2/3](a_1a_{1r};\ a_3a_{3r})\\
&(\alpha_1\alpha_1;\ \alpha_4\alpha_4)=(\alpha_2\alpha_2;\ \alpha_5\alpha_5)=(a_1a_1;\ a_4a_4)
\end{aligned}\right\}(D_{3d});\quad (42)$$

$$\left.\begin{aligned}
&S_{\alpha_1\alpha_3}=[1-(11\varphi^2/12)]S_{a_1a_3}\\
&\qquad\qquad+[\varphi^2/4]S_{a_1r a_3r}\\
&S_{\alpha_3\alpha_5}=[1-(\varphi^2/3)]S_{a_1a_3}\\
&\qquad\qquad-[\varphi^2/3]S_{a_1r a_3r}\\
&S_{\alpha_2\alpha_5}=[1-(5\varphi^2/12)]S_{a_1a_4}\\
&\qquad\qquad-[\varphi^2/4]S_{a_1r a_4r}\\
&S_{\alpha_1\alpha_4}=[1-\varphi^2]S_{a_1a_4}-[\varphi^2]S_{a_1r a_4r}\\
&(\alpha_1\alpha_1;\ \alpha_3\alpha_3)=[1-(4\varphi^2/3)](a_1a_1;\ a_3a_3)\\
&\qquad+[\varphi^2/2](a_1a_1;\ a_{3s}a_{3s})\\
&\qquad+[5\varphi^2/6](a_1a_1;\ a_{3r}a_{3r})\\
&\qquad-[\varphi^2](a_1a_{1s};\ a_3a_{3s})\\
&\qquad\qquad+[\varphi^2](a_1a_{1r};\ a_3a_{3r})\\
&(\alpha_3\alpha_3;\ \alpha_5\alpha_5)=[1-(2\varphi^2/3)](a_1a_1;\ a_3a_3)\\
&\qquad+[2\varphi^2/3](a_1a_1;\ a_{3r}a_{3r})\\
&\qquad\qquad-[4\varphi^2/3](a_1a_{1r};\ a_3a_{3r})\\
&(\alpha_1\alpha_1;\ \alpha_4\alpha_4)=[1-2\varphi^2](a_1a_1;\ a_4a_4)\\
&\qquad\qquad+[2\varphi^2](a_1a_1;\ a_{4r}a_{4r})\\
&\qquad\qquad\qquad-[4\varphi^2](a_1a_{1r};\ a_4a_{4r})\\
&(\alpha_2\alpha_2;\ \alpha_5\alpha_5)=[1-(2\varphi^2/3)](a_1a_1;\ a_4a_4)\\
&\qquad\qquad+[\varphi^2/6](a_1a_1;\ a_{4s}a_{4s})\\
&\qquad\qquad+[\varphi^2/2](a_1a_1;\ a_{4r}a_{4r})\\
&\qquad\qquad-[\varphi^2/3](a_1a_{1s};\ a_4a_{4s})\\
&\qquad\qquad\qquad-[\varphi^2](a_1a_{1r};\ a_4a_{4r})
\end{aligned}\right\}(C_{2v}).\quad (43)$$

These formulas can all be derived from appropriate resolutions of the α_i. (42) and part of (43) can for example be demonstrated from the resolution of the α_i along the x, y, and z axes of Fig. 1:

$$\left.\begin{aligned}
\alpha_1&=[\pm\varphi]a_{1y}+[1-(\varphi^2/2)]a_{1z}\\
\alpha_2&=[\mp 3^{-\frac{1}{2}}\varphi]a_{2x}+[1-(\varphi^2/6)]a_{2z}\\
\alpha_3&=[-3^{-\frac{1}{2}}\varphi]a_{3x}+[1-(\varphi^2/6)a_{3z}\\
\alpha_4&=[-\varphi]a_{4y}+[1-(\varphi^2/2)]a_{4z}\\
\alpha_5&=[3^{-\frac{1}{2}}\varphi]a_{5x}+[1-(\varphi^2/6)a_{5z}\\
\alpha_6&=[\pm 3^{-\frac{1}{2}}\varphi]a_{6x}+[1-(\varphi^2/6)]a_{6z}
\end{aligned}\right\}\begin{matrix}(\text{Upper sign}\\ C_{2v},\ \text{lower}\\ \text{sign } D_{3d}).\end{matrix}\quad (44)$$

Here a_{1z}, say, is a $2p$ orbital on atom 1 whose major axis is parallel to the z axis.

The ground state energies $E_0{}^{D_{3d}}$ and $E_0{}^{C_{2v}}$ are determined by Eqs. (30), and (33), Eqs. (35) to (37) and Eqs. (41) to (43) as functions of the angles φ and certain integrals over atomic orbitals. The force constants k_4 and k_{16b} are determined by Eq. (5) as functions of the same atomic integrals; *viz.*:[15]

$$\begin{aligned}
k_4&=[d^2E_0{}^{D_{3d}}/d\varphi^2]_{\varphi=0}=[2\epsilon_0''+2\epsilon_1''+2\epsilon_{-1}''\\
&\quad+\gamma_{00}''+\gamma_{11}''+\gamma''_{-1-1}+(4\gamma_{1-1}-2\delta_{1-1})''\\
&\quad+(4\gamma_{01}-2\delta_{01})''+(4\gamma_{0-1}-2\delta_{0-1})'']_{D_{3d}},\\
k_{16b}&=[d^2E_0{}^{C_{2v}}/d\varphi^2]_{\varphi=0}=[2\epsilon_0''+2\epsilon_1''+2\epsilon_{-1}''\\
&\quad+\gamma_{00}''+\gamma_{11}''+\gamma''_{1-1}+(4\gamma_{1-1}-2\delta_{1-1})''\\
&\quad+(4\gamma_{01}-2\delta_{01})''+(4\gamma_{0-1}-2\delta_{0-1})'']_{C_{2v}}.
\end{aligned}\quad (45)$$

Here ϵ_0'', for example, denotes the second derivative of ϵ_0 with respect to φ, evaluated at $\varphi=0$.

It will now be assumed that the integrals over the a_i, a_{is}, a_{ir} do not depend on the angles φ but only on *equi-*

TABLE II. $\varphi=0$ values of some integrals and their second derivatives (atomic units[a]). $Z=3.18$.

Integral	Value	Value of 2nd Derivative Chair (D_{3d})	Chair (C_{2v})
$-(2/3\sigma_0)$	−0.41266	−0.13799	−0.13818
$-(2/3\sigma_1)$	−0.55411	−0.19485	−0.15869
$-(2/\sigma_{-1})$	−1.66232	−0.58456	−0.14679
$(1/18\sigma_0{}^2)$	0.02129	0.01424	0.01426
$(1/36\sigma_1{}^2)$	0.01919	0.01350	0.01099
$(1/4\sigma_{-1}{}^2)$	0.17271	0.12147	0.03050
$(1/6\sigma_1\sigma_{-1})$	0.11514	0.08098	0.04314
$(1/9\sigma_0\sigma_1)$	0.05716	0.03922	0.03551
$(1/3\sigma_0\sigma_{-1})$	0.17149	0.11765	0.07257
$(\alpha_1\alpha_1;\ \alpha_1\alpha_t)$	1.2447	0	0
$(\alpha_2\alpha_2;\ \alpha_1\alpha_1)$	0.6633	−0.0424	−0.0424
$(\alpha_3\alpha_3;\ \alpha_2\alpha_2)$	0.6633	−0.0424	0
$(\alpha_3\alpha_3;\ \alpha_1\alpha_1)$	0.4166	0.0448	0.0192
$(\alpha_5\alpha_5;\ \alpha_3\alpha_3)$	0.4166	0.0448	0.0448
$(\alpha_4\alpha_4;\ \alpha_1\alpha_1)$	0.3657	0	0.0996
$(\alpha_5\alpha_5;\ \alpha_2\alpha_2)$	0.3657	0	0.0232
$(\alpha_2\alpha_2;\ \alpha_2\alpha_1)$	0.2436	−0.3248	−0.3248
$(\alpha_3\alpha_3;\ \alpha_3\alpha_2)$	0.2436	−0.3248	0
$(\alpha_2\alpha_1;\ \alpha_2\alpha_1)$	0.0700	−0.1765	−0.1765
$(\alpha_3\alpha_2;\ \alpha_3\alpha_2)$	0.0700	−0.1765	0
$(A_1{:}\,\alpha_2\alpha_2)$	0.0628	0	0
$(A_1{:}\,\alpha_2\alpha_1)$	0.1388	−0.1851	−0.1851
$(A_2{:}\,\alpha_3\alpha_2)$	0.1388	−0.1851	0

[a] See reference 17.

[15] The total electronic energies E_0 are (to the Born-Oppenheimer approximation) the potential energies V for the vibrational motion.

TABLE III. $\varphi=0$ values of second derivatives of integrals over molecular orbitals (atomic units[a]). $Z=3.18$.

2nd Derivative	Chair (D_{3d})	Cradle (C_{2v})
$2\epsilon_0''$	−0.1575	−0.6333
$2\epsilon_1''$	−0.9336	−0.3978
$2\epsilon_{-1}''$	−0.9336	−0.4679
γ_{00}''	0.0455	0.1189
γ_{11}''	0.1772	0.0859
γ''_{-1-1}	0.1772	0.1278
$(4\gamma_{1-1}-2\delta_{1-1})''$	1.1419	0.5283
$(4\gamma_{01}-2\delta_{01})''$	0.5870	0.4833
$(4\gamma_{0-1}-2\delta_{0-1})''$	0.5870	0.5225

[a] See reference 17.

librium molecular dimensions. This amounts to assuming that the 120° angle is preferred in the C−C=C situation even in acyclic structures and that the changes in distance between *opposite* carbon atoms across the ring may be neglected, and allows the quick determination of the second derivatives which appear in (45). Values for the integrals over the a_i, a_{is}, a_{ir} (assumed hydrogen-like) have been given elsewhere.[16] For

$$C_1-C_2 \text{ distance}=R_0=8.37 \text{ atomic units},^{17}$$
$$C_1-C_3 \text{ distance}=3^{\frac{1}{2}}R_0=14.5 \text{ atomic units},$$
$$C_1-C_4 \text{ distance}=2R_0=16.7 \text{ atomic units},$$
$$Z=\text{effective nuclear charge}=3.18,$$

these lead to the $\varphi=0$ values of the integrals over the α_i and their second derivatives which are listed in Table II. These in turn lead[18] to the $\varphi=0$ values of the second derivatives of integrals over molecular orbitals which are given in Table III, and from there immediately to

$$k_4=0.6911 \text{ atomic unit},$$
$$k_{16b}=0.3677 \text{ atomic unit};$$

and [by Eq. (8)]

$$\beta=0.098\times10^5 \text{ dynes/cm},$$
$$\theta=0.078\times10^5 \text{ dynes/cm}.$$

These "calculated" values of β and θ are compared in Table IV to "observed" values. The latter were found by Miller and Crawford[5] from a normal coordinate treatment of the out-of-plane vibrations of the molecule—i.e., from observed spectroscopic data. Their analysis led to alternative rather than unique values for the force constants—the several possibilities are included in the table. The computed and observed values of the force constants are not in particularly good agreement, but that could hardly be expected. Probably more significant than the calculated absolute values of the constants is their ratio; it appears that interaction between non-neighboring atoms causes the ratio β/θ to be increased slightly above the value 1 it would have if non-neighbors had no effect on one another.[19] This would seem to rule out the 0.757 value for θ and favor the smaller values of β.

FORCE CONSTANTS IN THE LOWEST EXCITED SINGLET STATES

The method of the preceding sections may be applied to the determination of the force constants β and θ in those excited states of the benzene molecule which arise from excitation of one or more of the six unsaturation electrons. The procedure will be illustrated in the present section by the calculation of β for the two lowest singlet excited states.

The symmetry properties of the excited states can be determined by group theory.[2] The lowest singly excited states arise from excitation of one electron from an orbital belonging to the representation Γ_{11} to an orbital belong to Γ_{10}. These excited states are eight in number, four singlet and four triplet, and because $\Gamma_{10}\times\Gamma_{11}=\Gamma_6+\Gamma_8+\Gamma_{12}$, one each of the singlet and triplet states has the symmetry Γ_6, one the symmetry Γ_8, and two the (degenerate) symmetry Γ_{12}. The wave functions for these states can be written down, and the energies calculated. This has been done by Goeppert-Mayer and Sklar[2] for the equilibrium (and hence chair) configuration; suffice it here to quote their result: the lowest singly excited singlet state has the symmetry Γ_8, and the excess of its energy $E_{2s}{}^{D_{3d}}$ over the energy $E_0{}^{D_{3d}}$ of the ground state is given by the formula[20]

$$\begin{aligned}E_{2s}{}^{D_{3d}}-E_0{}^{D_{3d}}=&[(1/\sigma_2)-(1/\sigma_1)][-2(A_1:\alpha_2\alpha_2)\\&-2(\alpha_1\alpha_1;\alpha_2\alpha_2)-2(\alpha_1\alpha_1;\alpha_3\alpha_3)-(\alpha_1\alpha_1;\alpha_4\alpha_4)]\\&+[(1/\sigma_2)+(1/\sigma_1)][A_1:\alpha_1\alpha_2)+(\alpha_1\alpha_1;\alpha_1\alpha_2)]\\&+[-(1/6\sigma_0\sigma_1)+(1/6\sigma_0\sigma_2)-(1/3\sigma_1\sigma_1)\\&+(1/3\sigma_1\sigma_2)](\alpha_1\alpha_1;\alpha_1\alpha_1)+[-(1/2\sigma_0\sigma_1)\\&+(5/6\sigma_0\sigma_2)-(7/6\sigma_1\sigma_1)+(1/\sigma_1\sigma_2)](\alpha_1\alpha_1;\alpha_2\alpha_2)\\&+[-(5/6\sigma_0\sigma_1)+(5/6\sigma_0\sigma_2)-(7/6\sigma_1\sigma_1)\\&+(2/3\sigma_1\sigma_2)](\alpha_1\alpha_1;\alpha_3\alpha_3)+[-(1/2\sigma_0\sigma_1)\\&+(1/6\sigma_0\sigma_2)-(1/3\sigma_1\sigma_1)+(1/\sigma_1\sigma_2)](\alpha_1\alpha_1;\alpha_4\alpha_4)\\&+[-(1/\sigma_0\sigma_1)+(1/3\sigma_0\sigma_2)\\&-(4/3\sigma_1\sigma_1)](\alpha_1\alpha_1;\alpha_1\alpha_2)+[-(1/6\sigma_0\sigma_1)\\&-(5/6\sigma_0\sigma_2)+(1/6\sigma_1\sigma_1)\\&+(1/3\sigma_1\sigma_2)](\alpha_1\alpha_2;\alpha_1\alpha_2).\end{aligned}\tag{46}$$

If it is assumed for simplicity that R_0 and Z have the same value in the excited state as in the ground state (R_0 is actually about 2 percent larger in the excited state[21]), the energy increment

$$E_{2s}-E_0=(E_{2s}{}^{D_{3d}}-E_0{}^{D_{3d}})_{\varphi=0},\tag{47}$$

[16] R. G. Parr and B. L. Crawford, Jr., J. Chem. Phys. **16**, 1049 (1948).

[17] Distances in units of 0.5292A, energies in units of 2.1792×10^{-11} erg.

[18] First derivatives with respect to φ of all integrals over the α_i, evaluated at $\varphi=0$, are zero.

[19] If interactions between non-neighbors could be neglected, k_4/k_{16b} would have the value $6/4=3/2$, for at equal φ, the distortions S_4 and S_{16b} correspond to equal torsions of 6 and 4 carbon-carbon bonds respectively. Under these conditions, therefore, $\beta/\theta=(2/3)(k_4/k_{16b})$ would be unity. This result depends in no way on the manner in which k_4 and k_{16b} are calculated.

[20] The formula for $E_{2s}-E_0$ quoted by V. Griffing [J. Chem. Phys. **15**, 421 (1947), Eq. (16)] is really an expression for $E_{1s}-E_0$.

[21] Sponer, Nordheim, Sklar, and Teller, J. Chem. Phys. **7**, 207 (1939); F. Garforth, J. de Chim. Phys. **45**, 6 (1948).

and force constant increment

$$\beta_{2s}-\beta=(1/8)[d^2(E_{2s}{}^{D_{3d}}-E_0{}^{D_{3d}})/d\varphi^2]_{\varphi=0} \quad (48)$$

can be computed from integrals of the sort tabulated in Table III. One finds

$$E_{2s}-E_0=3.7 \text{ electron volts}$$

and

$$\beta_{2s}-\beta=-0.034\times10^5 \text{ dynes/cm.}$$

The 3.7 volt excitation energy may be compared to Goeppert-Mayer and Sklar's 5.0 volt[2] and the experimental 4.7 volt.[2] The present calculation being merely a repetition of Goeppert-Mayer and Sklar's using improved values for the integrals, the agreement with experiment at this approximation must now be considered destroyed.[22]

The calculated value of β_{2s} is given in Table IV together with alternative observed values computed[23] by the method of Miller and Crawford[5] from experimental data of Ingold and Leeke.[24] Alternative observed values of θ_{2s} are also included in the table. Though the quantitative agreement between the calculated value 0.063 and observed value 0.061 for β_{2s} is certainly fortuitous, the 0.061 value for β_{2s} and 0.057 value for θ_{2s} would seem to be favored.

A similar computation for the singlet excited state of symmetry Γ_6 yields for its energy relative to the ground state

$$E_{1s}-E_0=4.2 \text{ electron volts,}$$

and for the force constant β_{1s} the value listed in Table IV.

θ_{2s} and θ_{1s} could be calculated by this same means (though with more algebraic difficulty).

DISCUSSION

In principle one could compute the effects on energies and force constants of perturbations due to excited states of appropriate symmetry, but the labor involved would be almost prohibitive.

More important, one should investigate the effects on energies and force constants of inclusion of three-center integrals. Using Sklar and Lyddane's[25] values for the various integrals, London[26] showed that Goeppert-Mayer and Sklar's energy increments were *increased* by about 3 ev (for example, $E_{2s}-E_0$ according to London is 7.3, not 5.0 ev) when three-center integrals were taken into account. The results obtained above indicate that use of improved values for the integrals *decreases* Goeppert-Mayer and Sklar's energy increments. It is quite possible that a combination of these factors may leave Goeppert-Mayer and Sklar's energies more or less unchanged, preserving the agreement with experiment!

Further indication that inclusion of three-center integrals is imperative is provided by the observation[27] that the one-electron energies are in the wrong order[11] when three-center integrals are neglected but (probably) in the right order when they are included. Thus the present authors find, using improved values for two-center integrals but neglecting three-center integrals,

$$\epsilon_2-\epsilon_1=-8.6 \text{ ev,}$$

whereas London[26] found,[28] using old values for two-center integrals but including three-center integrals.

$$\epsilon_2-\epsilon_1=+8.2 \text{ ev.}$$

These considerations, plus the fact that the computed force constants are low rather than high (the latter would be naively expected on the grounds that the assumed model for the molecule is a constrained form of the actual molecule), imply that the conclusions drawn from the present calculations must be regarded as tentative. Revised results will be presented at a later date.

TABLE IV. Calculated and observed values of the force constants β and θ for the ground state and two excited states of benzene (10^5 dynes/cm).

State	Force constant	Alternative observed values	Calculated value
Ground	β	0.203, 0.205, 0.339, 0.367	0.098
	θ	0.157, 0.757	0.078
First singlet excited state	β_{2s}	0.061, 0.212	0.063
	θ_{2s}	0.057, 0.416	—
Second singlet excited state	β_{1s}	—	0.101

[22] See the next section for further discussion of this point.

[23] An 0.777 C−H/C−C bond length ratio is assumed for the excited molecule.

[24] C. K. Ingold and F. M. Leeke, Nature **157**, 46 (1946).

[25] A. L. Sklar and R. H. Lyddane, J. Chem. Phys. **7**, 374 (1939).

[26] A. London, J. Chem. Phys. **13**, 396 (1945).

[27] Professor R. S. Mulliken (private communication) first explicitly advanced this resolution of the "$\epsilon_2-\epsilon_1$ difficulty."

[28] Private communication from A. London to J. Duffie, March 23, 1948 (copy kindly furnished by Dr. London).

The Normal Vibrations of Polyatomic Molecules as Calculated by Urey-Bradley Field. II. Vibrations of Polythene, Ethane, and Their Deuterium Compounds

TAKEHIKO SIMANOUTI
Chemical Institute, Faculty of Science, Tokyo University, Tokyo, Japan
(Received December 27, 1948)

Assuming the Urey-Bradley field as the type of intramolecular potential equations to calculate five optically active frequencies of polythene molecule were derived. If we assume as force constants $K_{CH}=4.2$, $H_{HCH}=0.15$, $F_{HH}=0.1$, $F_{HC}=0.4$, $F_{HH'}=0$ and $F_{HC'}=-0.05$ (10^5 dynes/cm), the observed frequencies of $(CH_2)_n$ and $(CD_2)_n$ as well as those of CH_4, CD_4, C_2H_6, C_2D_6, etc., were explained satisfactorily.

INTRODUCTION

In the preceding paper[1] which dealt with the calculation of the vibration frequencies of methane and its derivatives, it was concluded that repulsive forces between atoms which are not bonded directly cannot be neglected, as compared with stretching and bending forces of bonds, and that, therefore, the Urey-Bradley field is the most adequate type of potential energy for the normal coordinate treatment of these molecules.

The object of the present work is to determine whether this type of potential field is adequate in the case of polythene, $(CH_2)_n$, ethane, C_2H_6, and fully deuterated polythene, $(CD_2)_n$, and ethane, C_2D_6. Polythene is an interesting molecule because it gives a strikingly simple spectrum and one of its CH deformation frequencies is found to be extraordinarily low.[2] Whitcomb, Nielsen, and Thomas[3] have already developed the normal coordinate treatment of this type of molecule. But either the potential energy resulting from central forces they used or that caused by simple valence forces seems to be incapable of accounting for this frequency.

THE POTENTIAL ENERGY OF POLYTHENE MOLECULE

The model used for the structures of polythene and deuteropolythene is shown in Fig. 1. Since we assume the Urey-Bradley field, the terms in the potential energy involving the coordinates of the hth CH_2 group are taken to be

$$\begin{aligned}V_h=&K'_{CH}a(\Delta r_h+\Delta r_h')+\tfrac{1}{2}K_{CH}\{(\Delta r_h)^2+(\Delta r_h')^2\}\\&+K'_{CC}b(\Delta R_h)+\tfrac{1}{2}K_{CC}(\Delta R_h)^2\\&+H'_{HCH}a^2(\Delta\theta_h)+\tfrac{1}{2}H_{HCH}a^2(\Delta\theta_h)^2\\&+H'_{CCC}b^2(\Delta\Theta_h)+\tfrac{1}{2}H_{CCC}b^2(\Delta\Theta_h)^2\\&+H'_{HCC}ab(\Delta\varphi_h+\Delta\varphi_h'+\Delta\varphi_h''+\Delta\varphi_h''')\\&+\tfrac{1}{2}H_{HCC}ab\{(\Delta\varphi_h)^2+(\Delta\varphi_h')^2+(\Delta\varphi_h'')^2+(\Delta\varphi_h''')^2\}\\&+F'_{HH}(2a\sin\alpha)\Delta q_h+\tfrac{1}{2}F_{HH}(\Delta q_h)^2\\&+F'_{CC}(2b\sin\alpha)\Delta Q_h+\tfrac{1}{2}F_{CC}(\Delta Q_h)^2\\&+F'_{CH}\alpha(\Delta p_h+\Delta p_h'+\Delta p_h''+\Delta p_h''')\\&+\tfrac{1}{2}F_{CH}\{(\Delta p_h)^2+(\Delta p_h')^2+(\Delta p_h'')^2+(\Delta p_h''')^2\},\end{aligned}\quad(1)$$

where internal coordinates R_h, r_h, etc., denote the distances and angles, respectively, with equilibrium values as indicated in parentheses.

$$\begin{aligned}&R_h(C_h-C_{h+1}=b),\\&r_h(C_h-H_h=a), && r_h'(C_h-H_h'=a),\\&\Theta_h(\angle C_{h+1}-C_h-C_{h-1}=2\beta), && Q_h(C_{h-1}\cdots C_{h+1}=2b\sin\beta),\\&\theta_h(\angle H_h-C_h-H_h'=2\alpha), && q_h(H_h\cdots H_h'=2a\sin\alpha),\\&\varphi_h(\angle H_h-C_h-C_{h+1}=2\gamma), && p_h(H_h\cdots C_{h+1}=\alpha),\\&\varphi_h'(\angle H_h'-C_h-C_{h+1}=2\gamma), && p_h'(H_h'\cdots C_{h+1}=\alpha),\\&\varphi_h''(\angle H_h-C_h-C_{h-1}=2\gamma), && p_h''(H_h\cdots C_{h-1}=\alpha),\\&\varphi_h'''(\angle H_h'-C_h-C_{h-1}=2\gamma), && p_h'''(H_h'\cdots C_{h-1}=\alpha).\end{aligned}\quad(2)$$

Here

$$\alpha^2=a^2+b^2-2ab\cos2\gamma,\quad(3)$$

$$\cos2\gamma=-\cos\alpha\cos\beta.\quad(4)$$

Since the coordinates Q_h, q_h, p_h, p_h', p_h'', and p_h''', which denote elongations of distances between atoms not bonded directly, are expressed in terms of the other coordinates as shown in the preceding paper,[1] the potential energy is given by

$$\begin{aligned}2V_h=&K_1\{(\Delta r_h)^2+(\Delta r_h')^2\}+K_2(\Delta R_h)^2\\&+H_1(a\Delta\theta_h)^2+H_2(b\Delta\Theta_h)^2\\&+H_3ab\{(\Delta\varphi_h)^2+(\Delta\varphi_h')^2+(\Delta\varphi_h'')^2+(\Delta\varphi_h''')^2\}\\&+2K_{11}(\Delta r_h)(\Delta r_h')+2K_{22}(\Delta R_h)(\Delta R_{h-1})\\&+2K_{12}\{(\Delta r_h)(\Delta R_h)+(\Delta r_h')(\Delta R_h)\\&\qquad+(\Delta r_h)(\Delta R_{h-1})+(\Delta r_h')(\Delta R_{h-1})\}\\&+2F_{11}(a\Delta\theta_h)(\Delta r_h+\Delta r_h')\\&\qquad+2F_{22}(b\Delta\Theta_h)(\Delta R_h+\Delta R_{h-1})\\&+2F_{13}(ab)^{\frac{1}{2}}\{(\Delta r_h)(\Delta\varphi_h)+(\Delta r_h')(\Delta\varphi_h')\\&\qquad+(\Delta r_h)(\Delta\varphi_h'')+(\Delta r_h')(\Delta\varphi_h''')\}\\&+2F_{23}(ab)^{\frac{1}{2}}\{(\Delta R_h)(\Delta\varphi_h)+(\Delta R_h)(\Delta\varphi_h')\\&\qquad+(\Delta R_{h-1})(\Delta\varphi_h'')+(\Delta R_{h-1})(\Delta\varphi_h''')\}\\&+2H_{13}a(ab)^{\frac{1}{2}}\{(\Delta\theta_h)(\Delta\varphi_h)+(\Delta\theta_h)(\Delta\varphi_h')\\&\qquad+(\Delta\theta_h)(\Delta\varphi_h'')+(\Delta\theta_h)(\Delta\varphi_h''')\}\\&+2H_{23}b(ab)^{\frac{1}{2}}\{(\Delta\Theta_h)(\Delta\varphi_h)+(\Delta\Theta_h)(\Delta\varphi_h')\\&\qquad+(\Delta\Theta_h)(\Delta\varphi_h'')+(\Delta\Theta_h)(\Delta\varphi_h''')\}\\&+2H_{33}ab\{(\Delta\varphi_h)(\Delta\varphi_h')+(\Delta\varphi_h)(\Delta\varphi_h'')\\&\qquad+(\Delta\varphi_h')(\Delta\varphi_h''')+(\Delta\varphi_h'')(\Delta\varphi_h''')\},\end{aligned}\quad(5)$$

where, with the abbreviations

$$\begin{aligned}&s_1=\sin\alpha, \quad s_2=\sin\beta, \quad s_3=(a-b\cos2\gamma)/\alpha,\\&\qquad\qquad\qquad\qquad\qquad s_4=(b-a\cos2\gamma)/\alpha,\\&t_1=\cos\alpha, \quad t_2=\cos\beta, \quad t_3=b\sin2\gamma/\alpha,\\&\qquad\qquad\qquad\qquad\qquad t_4=a\sin2\gamma/\alpha,\end{aligned}$$

[1] Takehiko Simanouti, J. Chem. Phys. **17**, 245 (1949).
[2] N. Sheppard and G. B. B. M. Sutherland, Nature **159**, 739 (1947).
[3] S. E. Whitcomb, H. H. Nielsen, and L. H. Thomas, J. Chem. Phys. **8**, 143 (1940).

and intramolecular tension κ, we have

$$
\begin{aligned}
K_1&=K_{CH}+t_1^2F'_{HH}+s_1^2F_{HH}+2t_3^2F'_{HC}+2s_3^2F_{HC},\\
K_2&=K_{CC}+2t_2^2F'_{CC}+2s_2^2F_{CC}+4t_4^2F'_{HC}+4s_4^2F_{HC},\\
H_1&=H_{HCH}-s_1^2F'_{HH}+t_1^2F_{HH}+(3\kappa/8^{\frac{1}{2}}a^2),\\
H_2&=H_{CCC}-s_2^2F'_{CC}+t_2^2F_{CC}+(3\kappa/8^{\frac{1}{2}}b^2),\\
H_3&=H_{HCC}-s_3s_4F'_{HC}+t_3t_4F_{HC}+(3\kappa/8^{\frac{1}{2}}ab),\\
K_{11}&=-t_1^2F'_{HH}+s_1^2F_{HH},\\
K_{22}&=-t_2^2F'_{CC}+s_2^2F_{CC},\\
K_{12}&=-t_3t_4F'_{HC}+s_3s_4F_{HC},\\
F_{11}&=t_1s_1(F'_{HH}+F_{HH}),\\
F_{22}&=t_2s_2(F'_{CC}+F_{CC}),\\
F_{13}&=(b/a)^{\frac{1}{2}}(t_3s_4F'_{HC}+s_3t_4F_{HC}),\\
F_{23}&=(a/b)^{\frac{1}{2}}(t_4s_3F'_{HC}+s_4t_3F_{HC}),\\
H_{13}&=\kappa/a(2ab)^{\frac{1}{2}},\\
H_{23}&=\kappa/f(2ab)^{\frac{1}{2}},\\
H_{33}&=\kappa/2^{\frac{1}{2}}ab. \qquad (6)
\end{aligned}
$$

EQUATIONS FOR THE OPTICALLY ACTIVE VIBRATIONS

The same method as developed by Whitcomb, Nielsen, and Thomas[3] is applicable even when we assume Eq. (5) for the potential energy. In this case the following equations are obtained for all the optically active chain vibrations with the designations used by Whitcomb and others.

For $\nu_2(0\pi)$, i.e., CH_2 bending vibration parallel to chain axis, denoting $4\pi^2c^2\nu^2$ by λ, the reciprocal of the mass of a carbon atom by μ_0, and that of a hydrogen atom by μ, we have

$$
\begin{aligned}
\lambda=2(2\mu_0+\mu)(b\sin^2\beta/a\sin^2 2\gamma)\{&H_{HCC}-s_3s_4F'_{HC}\\
&+t_3t_4F_{HC}+(3\kappa/8^{\frac{1}{2}}ab)\}. \qquad (7)
\end{aligned}
$$

For $\nu_3(\pi\sigma)$ and $\nu_4(\pi\sigma)$, i.e., symmetric CH stretching and HCH deformation vibrations, respectively, both having the change of dipole moment in the plane of CCC$\cdots$zigzag chain and perpendicular to the chain axis,

$$
\begin{vmatrix}
\mu B-\lambda, & \{\mu(2\mu_0+\mu)\}^{\frac{1}{2}}C\\
\{\mu(2\mu_0+\mu)\}^{\frac{1}{2}}C, & (2\mu_0+\mu)A-\lambda
\end{vmatrix}=0, \qquad (8)
$$

where

$$
\begin{aligned}
A=s_1^2K_{CH}&+2s_5^2H_{HCC}+2s_1^2t_1^2F'_{HH}\\
&+\{2t_3^2s_1^2-4(b/a)^{\frac{1}{2}}t_3s_4s_1s_5-2s_3s_4s_5^2\}F'_{HC}\\
&+2s_6^2F_{HC}+(3s_5^2/2^{\frac{1}{2}}ab)\kappa,\\
B=t_1^2K_{CH}&+2t_5^2H_{HCC}+2t_1^4F'_{HH}\\
&+\{2t_3^2t_1^2+4(b/a)^{\frac{1}{2}}t_3s_4t_1t_5-2s_3s_4t_5^2\}F'_{HC}\\
&+2t_6^2F_{HC}+(3t_5^2/2^{\frac{1}{2}}ab)\kappa,\\
C=s_1t_1K_{CH}&-2s_5t_5H_{HCC}+2s_1t_1^3F'_{HH}\\
&+\{2t_3^2s_1t_1+2(b/a)^{\frac{1}{2}}t_3s_4(s_1t_5-t_1s_5)+2s_3s_4s_5t_5\}F'_{HC}\\
&+2s_6t_6F_{HC}-(3s_5t_5/2^{\frac{1}{2}}ab)\kappa,
\end{aligned}
$$

with the abbreviations

$$
\begin{aligned}
s_5&=(b/a)^{\frac{1}{2}}\sin\alpha\cos\alpha\cos\beta/\sin 2\gamma, & s_6&=a\sin\alpha/d,\\
t_5&=(b/a)^{\frac{1}{2}}\sin^2\alpha\cos\beta/\sin 2\gamma, & t_6&=(a\cos\alpha+b\cos\beta)/d.
\end{aligned}
$$

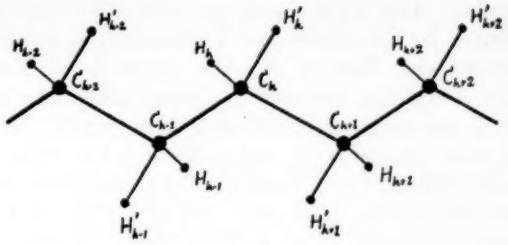

FIG. 1.

For $\nu_7(\pi\sigma)$ and $\nu_6(\pi\sigma)$, i.e., the antisymmetric CH stretching and CH_2 rocking vibrations, respectively, both having the change of dipole moment perpendicular to the plane of the CCC$\cdots$zigzag chain,

$$
\begin{vmatrix}
\mu B'-\lambda, & \{\mu(2\mu_0+\mu)\}^{\frac{1}{2}}C'\\
\{\mu(2\mu_0+\mu)\}^{\frac{1}{2}}C', & (2\mu_0+\mu)A'-\lambda
\end{vmatrix}=0, \qquad (9)
$$

where

$$
\begin{aligned}
A'=B&+2s_1^2H_{HCH}-2F'_{HH}\\
&+\{3bs_1^2-8(ab)^{\frac{1}{2}}s_1t_5+4at_5^2\}(\kappa/2^{\frac{1}{2}}a^2b),\\
B'=A&+2t_1^2H_{HCH}+2F_{HH}\\
&+\{3bt_1^2-8(ab)^{\frac{1}{2}}t_1s_5+4as_5^2\}(\kappa/2^{\frac{1}{2}}a^2b),\\
C'=C&-2s_1t_1H_{HCH}\\
&-\{3bt_1s_1-8(ab)^{\frac{1}{2}}s_1s_5+4at_5s_5\}(\kappa/2^{\frac{1}{2}}a^2b).*
\end{aligned}
$$

OBSERVED FREQUENCIES OF $(CH_2)_n$ AND $(CD_2)_n$

Investigations of the spectrum of polythene were carried out by Fox and Martin,[4] Thompson and Torkington,[5] Glatt and Ellis,[6] and Elliott, Ambrose, and Temple.[7] The writer also measured the spectrum of this substance and the results are in good agreement with those observations. The spectrum of $(CD_2)_n$ has recently been investigated by Sheppard and Sutherland.[2] The results of these spectra can be summarized as follows:

$(CH_2)_n$	$(CD_2)_n$	
728 cm^{-1}	520 cm^{-1}	(perpendicular to the chain axis)
1375	1060	(parallel to the chain axis)
1475	1100	(perpendicular to the chain axis)
2853	—	
2926	—	

The 1475- and 728-cm^{-1} vibrations have often been observed to be doublets, but it is most probable that this splitting is due to perturbation of neighboring

* For $\nu_9(0\pi)$, which was expected to be optically active by Whitcomb, Nielsen, and Thomas, we have

$$\lambda=2\mu(b\sin^2\beta/a\sin^2 2\gamma)\{H_{HCC}-s_3s_4F'_{HC}+t_3t_4F_{HC}-(\kappa/8^{\frac{1}{2}}ab)\};$$

but we can understand from Fig. 4 in their paper that this vibration is optically inactive according to the symmetry property of this molecule. In the case of $(CXY)_n$ molecule instead of $(CX_2)_n$ this vibration becomes optically active.

[4] J. J. Fox and A. E. Martin, Proc. Roy. Soc. **A157**, 961 (1940).
[5] H. W. Thompson and P. Torkington, Proc. Roy. Soc. **A184**, 3 (1945).
[6] L. Glatt and J. W. Ellis, J. Chem. Phys. **15**, 880 (1947).
[7] A. Elliott, E. J. Ambrose, and R. B. Temple, J. Chem. Phys. **16**, 877 (1948).

molecules.[7] The weak band at 1375 cm^{-1} has been attributed by Thompson and Torkington,[5] and Elliott, Ambrose, and Temple[7] to the presence of methyl groups. Certainly the methyl group gives the symmetrical deformation vibration in this region, but its absorption intensity is ordinarily weaker than degenerate deformation vibration which should be found in the region 800∼1000 cm^{-1}. We could not find any definite absorption band in this region; hence, it is natural to consider that this 1375-cm^{-1} frequency is due to methylene groups.

ASSIGNMENT AND CALCULATION

When we compare the five observed frequencies with the five optically active vibrations given in Eqs. (7), (8), and (9), it leads at once to the following assignment.

		$(CH_2)_n$	$(CD_2)_n$
$\nu_2(0\pi)$	=	1375 cm^{-1}	1060 cm^{-1}
$\nu_4(\pi\sigma)$	=	1475	1100
$\nu_3(\pi\sigma)$	=	2853	—
$\nu_6(\pi\sigma)$	=	728	520
$\nu_7(\pi\sigma)$	=	2926	—

To calculate these frequencies theoretically from Eqs. (7)–(9), seven force constants, K_{CH}, H_{HCH}, H_{HCC}, F_{HH}, F_{HC}, F'_{HH}, and F'_{HC}, and an intramolecular tension κ are necessary. Four of these constants, however, can be obtained directly from similar bond structures in methane and its derivatives which were treated in the preceding paper.[1]

$K_{CH}=4.2$, $H_{HCH}=0.4$, $F'_{HH}=0$, $F_{HH}=0.1$ (10^5 dynes/cm).

As the other constants we take the following values so as to give the best fit with the observed ν_2, ν_6, and ν_7.

$H_{HCC}=0.15$, $F'_{HC}=-0.05$, $F_{HC}=0.4$ (10^5 dynes/cm), $\kappa=0.2$ (10^{-11} dyne·cm).

The equilibrium bond distances are assumed to be: C—H 1.09, C—C, 1.54A, with tetrahedral angles for carbon atoms. Then from Eqs. (7)–(9) we obtain the calculated frequencies:

		$(CH_2)_n$	$(CD_2)_n$
$\nu_2(0\pi)$	=	1349 cm^{-1}	1020 cm^{-1}
$\nu_4(\pi\sigma)$	=	1474	1083
$\nu_3(\pi\sigma)$	=	2906	2117
$\nu_6(\pi\sigma)$	=	733	530
$\nu_7(\pi\sigma)$	=	2928	2169

TABLE I. The fundamental frequencies of ethane in cm^{-1}.

	C_2H_6			C_2D_6		
	Obs.[10]	Calc.*	Diff. %	Obs.[10]	Calc.*	Diff. %
A_{1g}	993	1005	1.2	852	821	3.6
	1375	1369	0.4	1158	1171	1.1
	2925	2916	0.3	2115	2086	1.4
A_{2u}	1380	1400	1.4	1072	1073	0.1
	2925	2938	0.4	2100	2103	0.1
E_u	827	825	0.2	601	596	0.8
	1465	1457	0.5	1102	1053	4.4
	2980	2984	0.1	2237	2215	1.0
E_g	1170	997**	14.8	970	789**	18.6
	1460	1438	1.5	1055	1039	1.5
	2960	2973	0.4	2225	2206	0.9

* The equilibrium distances were assumed to be: C—H, 1.09, C—C, 1.54A, with tetrahedral angles.

** This is the only calculated frequency differing by much more than four percent from the observed value. But it was shown by F. Stitt [J. Chem. Phys. 7, 297 (1939)] that inclusion of the interaction terms between the two methyl groups led to higher calculated value for this frequency without destroying the agreement of the other calculated and observed frequencies.

TABLE II. Force constants and intramolecular tensions.

Force constants (10^5 dynes/cm)

K Bond	Value	Molecule calculated
C—H(CH_4)	4.8	CH_4, CH_3D, CH_2D_2, CHD_3, CD_4
(CH_3—)	4.5	CH_3Cl, CD_3Cl, C_2H_6, C_2D_6
(CH_2—)	4.2	CH_2Cl_2, $(CH_2)_n$, $(CD_2)_n$
(CH—)	3.9	$CHCl_3$, $CDCl_3$
C—C	2.8	C_2H_6, C_2D_6
C—Cl	1.75	CCl_4, $CHCl_3$, CH_2Cl_2, CH_3Cl, $CDCl_3$, CD_3Cl, CCl_3Br, CCl_2Br_2, $CClBr_3$
C—Br	1.45	CBr_4, $CClBr_3$, CCl_2Br_2, CCl_3Br
H Bond Angle	Value	Molecule calculated
H—C—H	0.4	CH_4∼CD_4, C_2H_6, C_2D_6, $(CH_2)_n$, $(CD_2)_n$, CH_3Cl, CH_2Cl_2, CD_3Cl
Cl—C—Cl	0.1	CCl_4, CCl_3H, CCl_2H_2, $CDCl_3$, CCl_3Br, CCl_2Br_2
Br—C—Br	0.05	CBr_4, $CClBr_3$, CCl_2Br_2
H—C—C	0.15	C_2H_6, C_2D_6, $(CH_2)_n$, $(CD_2)_n$
H—C—Cl	0.05	$CHCl_3$, CH_2Cl_2, CH_3Cl, $CDCl_3$, CD_3Cl
Cl—C—Br	0.05	CCl_3Br, CCl_2Br_2, $CClBr_3$
F' Interacting Atoms	Value	Molecule calculated
H...H	0	CH_4∼CD_4, CH_3Cl, CD_3Cl, CH_2Cl_2, C_2H_6, C_2D_6, $(CH_2)_n$, $(CD_2)_n$
Cl...Cl	−0.1	CCl_4, CCl_3H, CCl_2H_2, CCl_3D, CCl_2Br_2, CCl_3Br
Br...Br	−0.1	CBr_4, $CClBr_3$, CCl_2Br_2
H...C	−0.05	C_2H_6, C_2D_6, $(CH_2)_n$, $(CD_2)_n$
H...Cl	−0.05	CCl_3H, CCl_2H_2, CCl_3D, $CClH_3$, $CClD_3$
Cl...Br	−0.1	$CClBr_3$, CCl_2Br_2, CCl_3Br
F Interacting Atoms	Value	Molecule calculated
H...H	0.1	CH_4∼CD_4, CH_3Cl, CD_3Cl, CH_2Cl_2, C_2H_6, C_2D_6, $(CH_2)_n$, $(CD_2)_n$
Cl...Cl	0.65	CCl_4, $CHCl_3$, $CDCl_3$, CCl_2H_2, $CClBr_2$, CCl_3Br
Br...Br	0.5	CBr_4, $CClBr_3$, CCl_2Br_2
H...C	0.4	C_2H_6, C_2D_6, $(CH_2)_n$, $(CD_2)_n$
H...Cl	0.8	$CHCl_3$, $CDCl_3$, CCl_2H_2, CH_3Cl, CD_3Cl
Cl...Br	0.55	$CClBr_3$, CCl_2Br_2, CCl_3Br

Intramolecular tensions (10^{-11} dyne·cm)

Molecule	κ	Molecule	κ	Molecule	κ
CH_4∼CD_4	0			CCl_4	0.3
CH_3Cl	0.05	C_2H_6, C_2D_6	0.05	CCl_3Br	0.3
CH_2Cl_2	0.1	$(CH_2)_n$, $(CD_2)_n$	0.2	CCl_2Br_2	0.3
$CHCl_3$	0.2			$CClBr_3$	0.3
				CBr_4	0.3

The calculated values are in good agreement with the observed ones. The average difference is 1.5 percent and the maximum difference 3.9 percent. The magnitude of the values of force constants and the intramolecular tension arbitrarily chosen in the calculation are also reasonable as compared with those obtained in the case of methane derivatives[1] (see Table II). Accordingly, there is little doubt that the Urey-Bradley field is adequate in the case of these molecules. To confirm this conclusion an attempt was made to calculate the vibration frequencies of ethane and deuteroethane using these force constants.

THE CALCULATION OF NORMAL VIBRATIONS OF ETHANE AND DEUTEROETHANE

The normal coordinate treatment was carried out according to the method of Wilson.[8] If we assume that the Urey-Bradley field as the intramolecular potential and interaction between the two methyl groups is neglected, eight force constants, K_{CC}, K_{CH}, H_{HCH}, H_{HCC}, F_{HH}, F_{HC}, F'_{HH}, and F'_{HC}, and an intramolecular tension κ are necessary. Seven of these constants have already been obtained as shown in the case of polythene.** As the two remaining constants we take the following values:

$$K_{CC}=2.8\times10^{5}\ \text{dynes/cm},^{***}$$
$$\kappa=0.05\times10^{-11}\ \text{dyne}\cdot\text{cm}.$$

The frequencies calculated in this way are compared with the observed values in Table I. The agreement is good, when it is considered that all were obtained purely from bond structure considerations except two constants. Hence it may be concluded in this case that the Urey-Bradley field is an adequate type of potential energy.

Table II gives the summary of the force constants and the intramolecular tension which have been obtained in this series of research.

The author wishes to express his sincere thanks to Professor San-ichiro Mizushima for suggesting this work and for many helpful discussions.

[8] E. B. Wilson, J. Chem. Phys. **7**, 1047 (1939); **9**, 76 (1941).

** K_{CH} is obtained from CH_3Cl (see Table II).

*** From this value we can calculate the force constant $K(CH_2—CH_2)$:

$$K(CH_2—CH_2)=K_{CC}+4t_4^2F'_{HC}+4s_4^2F_{HC},$$
$$=4.0\ (10^5\ \text{dynes/cm}).$$

This is in agreement with the force constant K which was obtained when we calculated the skeletal vibrations of normal paraffins. (S. Mizushima and T. Simanouti, accepted for publication for J. Am. Chem. Soc.)

Comparison of Relations between Covalent Bond Order, Energy, and Interatomic Distance for Carbon-Carbon Bonds

J. L. KAVANAU
University of California, Los Angeles, California
(Received December 21, 1948)

The results given by the relations of Bernstein, Gordy, and the author between interatomic distance and energy and order are compared for carbon-carbon bonds. The predictions of these relations for the benzene and graphite bond orders are compared with the results given by quantum mechanical calculations, while those for the energies are compared with experimental values.

DURING the last several years a number of empirical relations between covalent bond order, energy and interatomic distance have been proposed. It seems desirable to compare the values given by these relations for carbon-carbon bonds.

The author[1] has advanced the relation between bond order N, and the interatomic distance R,

$$R=a+b\left(\frac{n_1+n_2-1}{n_1+n_2+1}\right)^N, \tag{1}$$

where n_1 and n_2 are the principal quantum numbers of the valence electrons of the bonded atoms and a and b are constants. Lagemann[2] proposed a generalized modification of (1) by setting $a=k_1/(Z_1+Z_2)$, $b=k_2(Z_1+Z_2)$. k_1 and k_2 are constants for atom pairs having the same values of n_1 and n_2, and Z_1 and Z_2 are the atomic numbers of the bonded atoms. A simplified relation of similar form recently proposed by Bernstein[3] for symmetric bonds is

$$R=R_1\left[c+(1-c)\left(\frac{n-1}{n+1}\right)^{(N-1)/2}\right]. \tag{2}$$

R_1 is the single bond distance.

Of these equations involving N as an exponent, (2) with $c=\frac{2}{3}$ is used to prepare Tables I and II.

A relation recently proposed by Gordy[4] is

$$N=dR^{-2}+e. \tag{3}$$

A least squares determination of d and e using the C−C, C=C, and C≡C distances (Table I) gives $d=7.475$, $e=-2.179$.*

A parabolic relation proposed by the author[5] is

$$(1-N/4)^2=f(R-g), \tag{4}$$

where $f=1.488$ and $g=1.162$.

In Table I the distances given by (2), (3), and (4) are tabulated together with the percent *MD* (mean deviation) of these values from the experimental values.

Using the *AO* (atomic orbital) treatment, Penney[6] has calculated the benzene and graphite carbon-carbon bond orders to be 1.623 and 1.45, respectively. Using the *MO* (molecular orbital) method Coulson[7] obtained the values 1.667 and 1.53, respectively. In Table II the values predicted by (2), (3), and (4) for these bond orders are compared with the above values ($R_{\text{benzene}}=1.39$A, $R_{\text{graphite}}=1.42$A).[8]

The author[9] has proposed the parabolic-type relation

$$(1-N/4)^m=1-(E/q). \tag{5}$$

E is the energy of the bond of order N. Using the single, double and triple carbon-carbon bond energy values (Table III) calculated by Pitzer[10] upon the basis of the newly determined heat of atomization of carbon,[11,12] $m=\frac{3}{2}$, $q=225.8$. (4) and (5) give

$$(1-E/225.8)^{4/3}=1.488(R-1.162). \tag{6}$$

Bernstein[13] has proposed the relation

$$E=E_1N\left[1-s\left(\frac{R_1}{R}\right)^2\left(\frac{R_1-R}{R_1}\right)\right]. \tag{7}$$

E_1 and R_1 are the C−C bond energy and distance and $s=0.492$.

Gordy[4] has proposed the relation

$$E=tR^{-2}+u. \tag{8}$$

$t=441.9$, $u=-106$.

In Table III the carbon-carbon single, double and triple bond energies given by (6), (7), and (8) are

[1] J. Lee Kavanau, J. Chem. Phys. **12**, 467 (1944).
[2] Robert T. Lagemann, J. Chem. Phys. **14**, 743 (1946).
[3] H. J. Bernstein, J. Chem. Phys. **15**, 284 (1947).
[4] Walter Gordy, J. Chem. Phys. **15**, 305 (1947).
* All the constants used, except $c=\frac{2}{3}$, were evaluated by the author using the method of least squares and the single, double and triple bond data. The calculations are given to four figures for comparative purposes.
[5] J. Lee Kavanau, J. Am. Chem. Soc. **69**, 1827 (1947).
[6] W. G. Penney, Proc. Roy. Soc. **A158**, 306 (1937).
[7] C. A. Coulson, Proc. Roy. Soc. **A169**, 413 (1939).
[8] L. Pauling, *The Nature of the Chemical Bond* (Cornell University Press, Ithaca, New York, 1948).
[9] J. Lee Kavanau, J. Chem. Phys. **15**, 77 (1947).
[10] K. S. Pitzer, J. Am. Chem. Soc. **70**, 2140 (1948).
[11] L. Brewer, P. W. Gilles, and F. A. Jenkins, J. Chem. Phys. **16**, 797 (1948).
[12] L. Gerö, J. Chem. Phys. **16**, 1011 (1948).
[13] H. J. Bernstein, J. Chem. Phys. **15**, 339 (1947).

given together with those predicted for benzene and graphite.

Using the *MO* method and allowing for hyperconjugation, Mulliken *et al.*[14] have found $N_{\text{benzene}}=1.77$, $N_{\text{graphite}}=1.65$. For a pure single, double and triple bond the distances of Table IV have been proposed. Using the latter values in (2), (3), (4) gives $c=0.6466$, $d=6.93$, $e=-1.777$, $f=1.330$, $g=1.159$, with the results given in Table IV.

Because of the magnitude of the experimental error, (2), (3), (4), (6), (7), (8) may all be said to fit the single-, double-, and triple-bond data quite well. Bernstein's relation (2), since it involves the single bond distance as a parameter, requires the determination of but one constant (c). Upon the basis of the model used by Bernstein in arriving at (2) the value $c=\frac{2}{3}$ is taken for all symmetric bonds. The essential significance of this is that in any given row of the periodic table the single, double and triple bond distances bear a constant ratio to one another. (2) has the possible disadvantage of leading to benzene and graphite bond order values somewhat below those of the *MO* treatment (which is probably to be preferred to the *AO* method). Bernstein's relation (7), since it involves the bond order and the single bond distance, also requires the determination of but one constant (s). This relation gives values for the benzene and graphite bond energies in good agreement with the experimental values.

Gordy's relations (3) and (8) give good agreement with both the benzene and graphite experimental bond energies and *MO* orders. However, (8)+(3) give a zero order bond an energy of 23 kcal./mole, whereas the curves of (7) and (5) pass through the point $(E, N)=(0, 0)$. This is because Gordy has assumed a linear relation between E and N after the linear Coulson-Lennard-Jones relation between E and p, the mobile bond order. Such a relation fits the data with the rather large *MD* of 2 percent. Since the plot of the energy values against the bond order indicates a non-linear curve passing through the origin, this is possibly a disadvantage of the Gordy relations.

The author's relations (4), (5), (6) maximize the energy and minimize the interatomic distance for a hypothetical quadruple bond. (4) gives the best agreement with the benzene and graphite *MO* bond orders, and leads to the simple relation $3R_1+5R_3=8R_2$ for all bonds. (6) has the possible disadvantage of leading to values of the energy of the benzene and graphite bonds which are 4.2 percent and 2 percent greater than the experimental values. It should be pointed out, however, that a second method of calculating the energy of the benzene bonds gives larger values than the method utilizing the energy of formation of benzene from atoms. Thus, the *MO* or *AO* method may be used, after the treatment discussed by Pauling.[8] If α is the resonance energy associated with the interchange of two electrons between two p_z orbitals and β is the resonance energy of one electron between two p_z orbitals, then $\beta\cong 0.59\alpha$. If α is taken to be $E_{C=C}-E_{C-C}=65$ kcal./mole, the two treatments give the benzene bond an energy of 125.2 and 124.5 kcal./mole, respectively. If the interchange energy α is taken to be 80–90 percent of $E_{C=C}-E_{C-C}$ the values are reduced by 1.3–2.6 kcal./mole.

TABLE I. Comparison of the interatomic distance-order relations.

	C–C	C=C	C≡C	%*MD*
Experimental[a] interatomic distance	1.54A	1.33A	1.204A	—
Equation (4)	1.540	1.330	1.2040	0.00
Equation (2)	1.540	1.323	1.198	0.34
Equation (3)	1.533	1.337	1.201	0.41

[a] See Reference 8 of text.

TABLE II. Comparison of the carbon-carbon bond orders predicted for benzene and graphite.

	N_{benzene}	N_{graphite}
Penney	1.623	1.45
Coulson	1.667	1.53
Equation (4)	1.670	1.522
Equation (3)	1.686	1.528
Equation (2)	1.629	1.481

TABLE III. Comparison of the interatomic distance-energy relations.

		E_1	E_2	E_3	%*MD*	E_{benzene}	E_{graphite}
Experimental	$\left(\frac{\text{kcal.}}{\text{mole}}\right)$	80[a]	145[a]	198[a]	—	120.2[b]	113.6[c]
Equation (7)+(2)		80.00	145.6	197.8	0.17	122.6	113.1
Equation (8)		80.33	143.9	198.8	0.52	122.7	113.1
Equation (6)		79.14	146.0	197.6	0.66	125.2	115.7

[a] See reference 10 of text.
[b] Calculated from the energy of formation of benzene from atoms using the new energy values (see references 10 and 11).
[c] Two-thirds of the heat of atomization of graphite (170.39, see reference 11).

TABLE IV. Comparison of the interatomic distance order relations in the Mulliken-Rieke-Brown system.

	Distances				Orders		
	C–C	C=C	C≡C	%*MD*	Benzene	Graphite	%*MD*
Mulliken *et al.*	1.58A	1.35A	1.204A	—	1.77	1.65	—
Equation (3)	1.578	1.353	1.203	0.14	1.801	1.651	0.91
Equation (4)	1.581	1.347	1.206	0.15	1.780	1.641	0.55
Equation (2)	1.580	1.344	1.208	0.26	1.758	1.616	1.48

[14] R. S. Mulliken, C. A. Rieke, and W. G. Brown, J. Am. Chem. Soc. **63**, 41 (1941).

Letters to the Editor

THIS section will accept reports of new work, provided these are terse and contain few figures, and especially few halftone cuts. The Editorial Board will not hold itself responsible for opinions expressed by the correspondents. Contributions to this section should not exceed 600 words in length and must reach the office of the Managing Editor not later than the 15th of the month preceding that of the issue in which the letter is to appear. No proof will be sent to the authors. The usual publication charge ($4.00 per page) will not be made and no reprints will be furnished free.

Differential Diffusion Coefficients of Sodium Ion in Sodium Chloride Solutions

ARTHUR W. ADAMSON, JAMES W. COBBLE, AND JULIAN M. NIELSEN
Chemical Laboratories, University of Southern California, Los Angeles, California
June 13, 1949

A SERIES of investigations are being carried out in this laboratory on the determination of differential or self-diffusion coefficients of radioactive ions in aqueous solutions. Previous results published by one of us[1] on the differential diffusion coefficients of Na^+ in NaI solutions disagreed with the limiting value given by the Nernst equation, and the present work was undertaken to determine whether similar deviations occurred for Na^+ in NaCl solutions.

The limiting law equations for self diffusion are:[1]

$$D(\text{cm}^2/\text{day}) = 7.75\times10^{-5}\lambda + T(1+c(\partial \ln r/\partial c)), \quad (1)$$

or, for Na^+ in aqueous solutions,

$$\text{at } 25°\text{C}: D = D^0(1-1.41c^{\frac{1}{2}}), \quad \text{where } D^0 = 1.15 \text{ cm}^2/\text{day}, \quad (2)$$
$$\text{at } 35°\text{C}: D = D^0(1-1.43c^{\frac{1}{2}}), \quad \text{where } D^0 = 1.47 \text{ cm}^2/\text{day}. \quad (3)$$

The McBain-Northrop[2] technique has been used in obtaining the diffusion constants. (The apparatus employed consisted of a double ended glass diaphragm cell which could be suspended horizontally in a thermostat and rotated about its central axis. By means of an automatic reversing mechanism, the direction of rotation was changed every half-minute, and the eddy currents produced inside the compartments were sufficient to keep the solutions adequately stirred during the run. This method avoided the undesirable practice of introducing glass spheres, rods, etc., inside the compartments.)

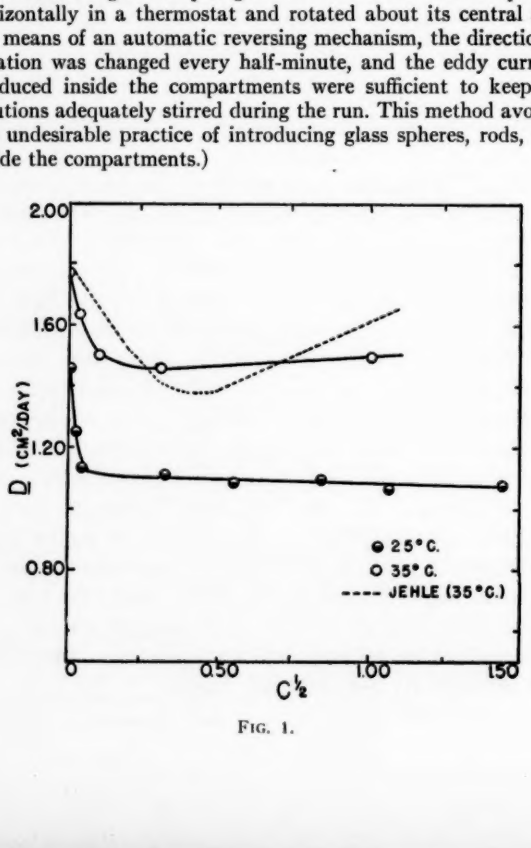

FIG. 1.

The cells were calibrated by using the standard calibration procedure recommended by Gordon,[3] using 0.1N KCl diffusing into water, and a mean diffusion coefficient of 1.58 cm²/day. The radioactive isotopes[4] employed were Na^{22} (3-yr.) and Na^{24} (14.8-hr.). No differences in diffusion behavior due to isotopic mass effects were observed. The change in concentration of the radioisotope in each compartment was determined by means of a solution counter and scaling circuit, and from this the diffusion constants were calculated by means of the standard equation.[2] The diffusion times were such as to allow approximately 25 percent changes in concentration, and the calculated D values were precise to about 1 percent.

The experimental results obtained at both 25°C and 35°C are plotted in the figure, and the limiting behavior is approximated by the equations below:

$$\text{at } 25°\text{C}: D = D^0(1-6.64c^{\frac{1}{2}}), \quad \text{where } D^0 = 1.46 \text{ cm}^2/\text{day}, \quad (4)$$
$$\text{at } 35°\text{C}: D = D^0(1-3.00c^{\frac{1}{2}}), \quad \text{where } D^0 = 1.80 \text{ cm}^2/\text{day}. \quad (5)$$

Comparison of Eqs. (2)–(5) shows that our results, although reproducible and consistent in themselves, do not agree with the limiting law demanded by present theory. On the other hand, Harned and Nuttall[5] have recently published values for the mean diffusion coefficients of KCl which are in excellent agreement with the Onsager-Fuoss limiting law. If this can be considered to be a general confirmation of present theory, then, clearly, the glass diaphragm technique must give spurious results, at least in dilute solutions. This conclusion is strengthened by comparing our results at 35°C with those of Jehle[6] (see Fig. 1) which were obtained by means of free diffusion studies.

We are now examining in some detail the ability of the diaphragm cell technique to give accurate diffusion data, and find that an important systematic error arises from surface diffusion of ions adsorbed on the walls of the diaphragm pores. These surface effects were reported by Mysels and McBain,[7] who observed that the glass membranes show an anomalously high conductance in dilute solution, as would be expected if surface transport were involved. The diffusion coefficients should be similarly affected. The conductance effect has been confirmed in our laboratories for sodium sulfate solutions more dilute than 0.01M and this study will be extended to NaCl solutions. Since an effective cell constant can be calculated from such conductance measurements, a subsequent correction of our diffusion data for surface conduction may bring them into agreement with theory.

The need for such corrections throws doubt on the validity of diffusion coefficient values in the literature obtained for dilute solutions by means of the glass diaphragm method, and in general can be expected to limit the advantages which this method has so far appeared to enjoy.

The authors wish to acknowledge the support of these studies by a grant-in-aid from the Research Corporation.

[1] A. W. Adamson, J. Chem. Phys. **15**, 762 (1947).
[2] J. W. McBain and T. H. Liu, J. Am. Chem. Soc. **53**, 59 (1931).
[3] A. R. Gordon, Ann. N. Y. Acad. Sci. **46**, 285 (1945).
[4] The Na^{22} was supplied by the Carnegie Institute of Terrestial Magnetism; the Na^{24} by the Atomic Energy Commission.
[5] H. S. Harned and R. L. Nuttall, J. Am. Chem. Soc. **71**, 1460 (1949).
[6] L. P. Jehle, Ph.D. Thesis (Univ. of California at Berkeley, 1938).
[7] K. J. Mysels and J. W. McBain, J. Coll. Sci. **3**, 45 (1948); we are indebted to Professor Mysels for calling our attention to this effect as a possible source of error.

The Vibrational Frequencies of $CF_2=CH_2$

WALTER F. EDGELL AND WILLIS E. BYRD
Department of Chemistry, State University of Iowa, Iowa City, Iowa
June 8, 1949

THE nature of the intramolecular forces, molecular structure and dimensions in fluorine containing molecules is of much interest. In particular, molecules which are intermediate between hydrocarbons and fluorocarbons should yield much information

TABLE I. The Raman spectrum of vinylidene fluoride.

	Line	Intensity*	ρ**	Assignment
1.	439 cm^{-1}	*M*	*D*	B_1; CF_2 rocking
2.	549	*M*	*P*?	A_1; CF_2 deformation
3.	603	*S*	*D*	B_2; CF_2 wagging
4.	714	*VW*		A_2; torsion?
5.	810	*M*	*D*	B_2; CH wagging
6.	915	*VS*	*P*	A_1; C−F stretching
7.	949	*W*	*D*	B_1; CH_2 rocking
8.	1212	*VW*		2×603
9.	1280	*W*		B_1; C−F stretching
10.	1359	*M*	*P*?	*A*; CH_2 deformation
11.	1389	*VW*		439+949
12.	1433	*VW*		2×714?; 2×439+549
13.	1472	*VW*		549+915
14.	1619	*VW*		2×810
15.	1718	*W*	*P*	A_1; C^{13}=C stretching
16.	1728	*VS*	*P*	A_1; C=C stretching
17.	1790	*VW*		439+1359
18.	1893	*VW*		2×949
19.	3101	*VW*	*P*	A_1; C−H stretching
20.	3171	*VW*	*D*	B_1; C−H stretching

* *VS*=very strong; *S*=strong; *M*=medium; *W*=weak, *VW*=very weak.
** *P*=polarized; *D*=depolarized.

which can form a sound basis for the treatment of the latter type of molecule. Consequently, a study of the rotational and vibrational spectrum of vinylidene fluoride has been undertaken in this laboratory. This note is a preliminary report on the Raman effect and related work; the microwave studies are reported separately.[1]

The Raman effect was studied in the liquid state at −100 to −125°C with a Lane-Wells spectrograph having a camera aperture of *F*/3. Filters were used to reduce general scattering and to eliminate Raman excitation from the mercury lines of the 4046A group. Qualitative polarization runs were made with Polaroid cylinders. The results are listed in Table I together with the assignment. The line at 714 cm^{-1} was observed only on the best films. Besides those listed, weak lines appeared shifted 857 and 1667 cm^{-1} from 4358A. These are believed to be the fundamentals 915 and 1728 cm^{-1} excited by 4348A.

Dr. George Evans of this laboratory made preliminary observations of the infra-red spectrum with a Perkin-Elmer spectrograph. For the most part the experimental results were essentially in agreement with the earlier work of Torkington and Thompson.[2]

The assignment of Table I was made on the basis of the polarization data, the expected magnitude of the fundamentals, and the infra-red data for this and the related olefins studied by Torkington and Thompson.[2] The torsional frequency is uncertain. One is led to expect it between 600 and 900 cm^{-1}. A much less satisfactory way would be to assign the line at 857 cm^{-1} to it; then 1667 becomes 857+810.

A normal coordinate treatment has been carried out using a *simple* valency force field (no interaction terms) as a basis and with one additional term $-kR^2$. Here R is the change in the distance between fluorine atoms. This latter term is an attempt to approximate the combined effect of the repulsions between the two fluorine atoms and between each fluorine atom and the π-electrons of the double bond. Force constants pertaining to the motion of the CH_2 group and the stretching of the C=C bond were given values essentially the same as in ethylene and those pertaining to the motions of the CF_2 group were evaluated from the experimental results. This procedure resulted in good quantitative agreement between the calculated and the experimental values for all frequencies and provided a substantial number of independent checks. It is worth while noting that the value obtained for the C—F bond stretching constant, 3.8×10^5 dynes/cm, seems more satisfactory for a single bond than the extremely high ("double bond") value of 9.15×10^5 dynes/cm obtained for several fluorocarbons using another type of potential function.[3]

The considerable importance of the repulsions in these molecules is indicated by the value for k of 1.17×10^5 dynes/cm—nearly one-third as large as the C—F stretching constant. And this one constant adequately replaces several valency type interaction constants otherwise required.

A full report on this work will be published soon.

One of us (W. F. E.) wishes to express his gratitude to the Research Corporation for a grant which made the purchase of the Lane-Wells spectrograph possible. Thanks are also due to Dr. George Evans for making his infra-red data available.

[1] A. Roberts and Walter F. Edgell, J. Chem. Phys. (to be published).
[2] P. Torkington and H. W. Thompson, Trans. Faraday Soc. **41**, 236 (1945).
[3] E. L. Pace, J. Chem. Phys. **16**, 74 (1948).

Decomposition of Benzoyl Peroxide in a Magnetic Field

J. E. LEFFLER*
Baker Laboratory of Chemistry, Cornell University, Ithaca, New York
June 13, 1949

THE decomposition of benzoyl peroxide is analogous to the polymerization of styrene in that both are radical chain reactions. In view of the reported effect of an external magnetic field on the rate of styrene polymerization,[1] it was decided to look for a similar effect on the rate of decomposition of benzoyl peroxide. The reaction was carried out in benzene under a nitrogen atmosphere and the peroxide content of the solutions determined by the method of Nozaki.[2] In each run one ampoule was between the poles of a 7518 gauss Alnico magnet and the control ampoule was in a remote part of the same thermostat, at 35.00 ±0.01°.

Run I, 102 hours		Run II, 766 hours	
Magnet	Control	Magnet	Control
20.53 cc*	20.28 cc	17.04 cc	16.88 cc
20.52	20.30	17.05	17.12
20.66	20.27	17.02	17.20
Av. 20.57	20.28	17.04	17.07

* Cc. of 0.00544 N sodium thiosulfate solution for each 1 cc aliquot. The initial titer was 20.72 cc.

There appears to be no significant difference between the magnetic and the control reaction rates. The author has received a private communication from Dr. J. W. Breitenbach reporting similarly negative results in an attempt to repeat the observation of Schmid on styrene polymerization.[3]

* du Pont Post-Doctoral Fellow, 1948–1949.
[1] Schmid, Muhr, and Marek, Zeits. f. Elektrochemie **51**, 37 (1945). For a theoretical discussion of such phenomena see J. E. Leffler and M. J. Sienko, J. Chem. Phys. **17**, 215 (1949).
[2] K. Nozaki, Anal. Chem. **18**, 583 (1946).
[3] To appear in Monatshefte.

Spectral Resemblances of Cata-Condensed Hydrocarbons

E. CLAR
Chemistry Department, University of Glasgow, Scotland
June 14, 1949

IN 1936 I introduced for the first time the comparative method in the study of the absorption spectra of polynuclear aromatic hydrocarbons and called it the anellation method,[1] which attributes bands of similar intensity and general character to similar origin. This method was applied systematically in numerous papers and reviewed in my book.[2] In this way I obtained three classes of bands:

(1) Para-bands, which shift most strongly with linear anellation to the red, and less strongly on angular anellation to the violet. These are, e.g., the long wave bands in anthracene and in the higher acenes and the second group of bands in benzene and naphthalene

(2) α-bands, less intense, shifting to the red on linear and angular anellation and hidden or partly hidden in the more intense para-bands in the higher acenes beginning with anthracene.[3]

(3) β-bands, the most intense, showing the same anellation effect and in a fixed ratio to the α-bands, lying more in the ultraviolet.

Recently H. B. Klevens and J. R. Platt,[4] in a paper of the above title described the same classes of bands and regularities calling them, however, (1) L_a-, (2) L_b- and (3) B_b-bands respectively. Although the authors take the details of 8 absorption spectra out of my book and quote them as such, no reference is made to the fact that these spectral regularities are already described quantitatively in my papers and my book.[1,2] Thus they claim in Section III:

"The preceding discussion has imputed properties to levels of a given type, which they retain from compound to compound and which make possible unambiguous identification according to the type. That states in compounds so diverse as benzene and benzanthracene should have so much in common seems to be *a novel idea*. To date, theory has offered no prediction of such result and indeed has sometimes denied the likelihood of it. We should therefore state this doctrine of types explicitly and summarize the evidence for it.

(1) Levels of a given type have unambiguous identifying characteristics, which do not change from compound to compound.

(2) Levels of a given type move in a systematic way from compound to compound."

As can be seen from the references given these results do not represent at all a novel idea, but have been worked out quantitatively in detail in my publications. The theoretical implications of these empirical regularities need not to be discussed here.

[1] E. Clar, Ber. **69**, 607, 1671 (1936); Atti d.X. Congresso Intern. d. Chimica, Roma **II**, 213 (1938); Ber. **72**, 1819 (1939); Ber. **73**, 81, 104, 596 (1940); Ber. **76**, 149, 257, 328, 458, 609 (1943); Chem. Ber. **81**, 52, 63, 163 (1948).
[2] E. Clar, *Aromatische Kohlenwasserstoffe* (Springer-Verlag, Berlin, 1941), p. 20.
[3] See reference 2, p. 26.
[4] H. B. Klevens and J. R. Platt, J. Chem. Phys. **17**, 470 (1949); J. R. Platt, J. Chem. Phys. **17**, 484 (1949).

Spectral Resemblances of Cata-Condensed Hydrocarbons

H. B. Klevens and J. R. Platt
Division of Agricultural Biochemistry, University of Minnesota, St. Paul, Minnesota, and
Department of Physics, University of Chicago, Chicago, Illinois
June 30, 1949

In a recent letter[1] Clar has criticized statements made in our earlier papers[2] which did not do adequate justice to his priority on the idea of spectral resemblances in condensed-ring systems.[3]

We made these statements because we had found the following difficulties in his scheme of resemblances and numerical relations as developed in his articles and book:

(1) He related the α-bands[1] (our ^1L_b bands) to bands of ethane and ethylene,[4] which seemed unreasonable.

(2) The α-bands were identified in only 3 out of the 15 3-ring, 4-ring, and 5-ring spectra.[4]

(3) The β-bands (our ^1B_b bands) were derived from an admittedly non-existent strong allowed band in benzene which he predicted should be at about 2000A.[5]

(4) Even after he had revised his numerical parameters completely from the integers and half-integers with which he started, there remained four cases[6] of serious disagreement with experiment in his plotted comparisons.

(5) He made no comparisons at all for two of the five 4-ring spectra (3,4-benzphenanthrene and triphenylene).

(6) His resemblances were, in various contexts, related to the Balmer series,[5] to the Moseley and Rydberg laws,[7] and to the existence of Kékulé and Dewar structures in benzene;[4] and indeed particular types of bands were assigned to particular types of resonance structures; and so on with several relations so difficult to fit into a rational quantum-theoretical account of the spectra that one is inclined to regard them as accidental.

As a result, since we sought a quantum-mechanical explanation of these spectra, we dismissed Clar's general correlations along with his unsatisfactory numerical formulae. We were not alone in this error. For instance, the longest wave-length bands of naphthalene have only within the past year been generally accepted as belonging to *two* electronic transitions,[2] although Clar clearly postulated this as long ago as 1939. We therefore began a fresh search in the original spectra for more acceptable and comprehensive relations which would omit no observed bands. The results were given in reference 2. Until Clar's letter was brought to our attention we overlooked the fact that we had come back to some of Clar's original correlations.

On reading his book and articles it is clear that he indeed must be credited with the idea of the resemblances and with the correlation of the β- and para-bands in most of the compounds and of the α-bands in several of them. Our new contribution was to eliminate the discrepancies of points 1 and 3 above; to extend his correlation to the bands he omitted, as mentioned in points 2 and 5; to make new correlations for the triplet bands and for the shorter wave-length bands which he did not know; and to make an interpretation of these levels and regularities on a quantum-mechanical basis, relating it to other theoretical work. Our statement quoted by Clar would perhaps be correct if it were amended to read, "That states in compounds so diverse as benzene and benzanthracene should have so much in common seems to be a novel idea *in the quantum-mechanical treatment of these molecules*."

Our objections concerning Clar's numerical relations do not diminish our admiration for his labors in obtaining and organizing the data on these compounds.

[1] E. Clar, J. Chem. Phys. **17**, 741 (1949).
[2] H. B. Klevens and J. R. Platt, J. Chem. Phys. **17**, 470, 484 (1949).
[3] E. Clar, *Aromatische Kohlenwasserstoffe* (Verlag. Julius Springer, Berlin, 1941) and articles.
[4] See reference 3, p. 24.
[5] See reference 3, p. 26.
[6] See reference 3, pp. 26, 33.
[7] See reference 3, p. 23.

The Microwave Spectrum of $CF_2=CH_2$

A. Roberts
Department of Physics
and
Walter F. Edgell
Department of Chemistry
State University of Iowa, Iowa City, Iowa
June 8, 1949

The microwave spectrum of $CF_2{=}CH_2$ has been studied in the region between 22,000 and 29,000 mc using a Stark effect sweep spectrometer of the Hughes-Wilson type.[1] Over eighty lines were observed with an intensity of ten times noise or greater; lines of lesser intensity were not recorded at this time since it was not likely that they would enter critically into the analysis.

All strong and moderately strong lines were examined to see whether their Stark patterns could be resolved. For most weak lines (10 to 20 times noise), and for many stronger ones, no definite Stark pattern could be seen; there were too many com-

TABLE I. The Lines of the $Q_{0\bar{1}}$* band-head.

Initial state	Final state	Calc.	Obs.
3_{-2}	3_{-1}	26,648 mc	26,649 mc
4_{-1}	4_0	26,328	26,329
5_0	5_1	25,729	25,729
6_1	6_2	24,770	24,770
7_2	7_3	23,434	23,433
8_3	8_4	21,735	21,734

TABLE II. Molecular constants of $CF_2=CH_2$.

$\kappa=0.7973$
$(a-c)=5{,}656.2$ mc
$(a+c)=16{,}347.4$ mc
$I_a=76.257\times10^{-40}$ g cm^2
$I_b=80.450\times10^{-40}$ g cm^2
$I_c=156.946\times10^{-40}$ g cm^2
$\mu=1.366\pm0.02$ debye

ponents, identifying the line with high J values. For some lines resolution of Stark components was incomplete even at the highest fields available, about 3000 volts per cm. Well-resolved Stark components were found for about fifteen lines, and the transitions giving rise to them were eventually identified.

On the basis of reasonable structural parameters, this molecule would approximate an oblate symmetric top. The figure axis might be either the axis of least moment of inertia or the axis of intermediate moment of inertia, only small changes in the parameters separating the two cases. Qualitatively the main features of the spectrum would be the same in either case, and consist of two Q sub-branches ($J\geqslant3$) having their band-heads at about 26,700 mc, one extending to lower and the other to higher frequencies. In addition one $R(J=1\rightarrow J=2)$ transition should be found in the region of each Q sub-branch near the band-head. Moreover, the general region would be covered with transitions involving high J values and belonging to other Q sub-branches having their band-heads outside the region of observation. The experimental results are in agreement with these expectations.

So far it has been impossible to obtain quantitative agreement between the calculated and observed spectrum on the assumption that the figure axis is the axis of intermediate moment of inertia. On the other hand if one assumes the figure axis to be that of least moment of inertia, all lines with resolvable Stark patterns are quantitatively accounted for. Table I gives a comparison between the observed frequencies of the $Q_{0\bar{1}}$* (i.e. band-head at $J=3$) subband and those calculated by interpolation in the tables of King, Hainer and Cross.[2] Two parameters, $(a-c)$ and κ* are required for the calculation, which gives excellent results for all six lines.

Equally good agreement was found for 5 lines of the $Q_{2\bar{1}}$* sub-branch expected in this region, as well as for two lines of the $Q_{2\bar{1}}{}^2$ sub-branch and three $R_{0\bar{1}}$ lines of the $J=1$ to $J=2$ transition.

The dipole moment was measured from the Stark effect of the $1_0\rightarrow2_{-1}$ and $1_{-1}\rightarrow2_{-2}$ transition.

The values of the spectroscopic parameters and the moments of inertia obtained from them are found in Table II. While it is not possible to determine uniquely the five structural parameters from these data, it is interesting to note that with C−F=1.32A, C=C=1.31A, C−H=1.07A and LFCF=LHCH=110°,

$$I_a=76.34\times10^{-40}$$
$$I_b=80.60\times10^{-40}$$
$$I_c=156.94\times10^{-40}\text{ g cm}^2$$

The presence of transitions due to isotopic modifications is now being investigated. A more detailed report on this work will appear shortly.

This research was supported in part by ONR under contract N8ori-79400.

[1] R. H. Hughes and E. B. Wilson, Jr., Phys. Rev. **71**, 562 (1947).
[2] King, Hainer, and Cross, J. Chem. Phys. **11**, 27 (1943).
* The nomenclature is that of reference 2.

Light Scattering from Solutions of Charged Macromolecules

PAUL DOTY AND ROBERT F. STEINER
Gibbs Memorial Laboratory, Harvard University, Cambridge, Massachusetts
June 27, 1949

IN the conventional theory of light scattering from dilute solutions the basic assumption is made that the fluctuations in solute concentration in neighboring volume elements are independent.[1] However, in view of the long range repulsive forces that are operative between similarly charged proteins or polymeric electrolytes in solutions of very low ionic strength it would appear that such an assumption is invalid. We have therefore considered the theory for such solutions from the point of view of the diminution of scattering per molecule as a result of intermolecular interference. In this approach the form of the radial distribution function must be selected. The Debye-Huckel approximation is not generally applicable because the potential energy is greater than the thermal energy. Of the several other choices available the simplest is that of characterizing the molecular interactions by a distance of closest approach thereupon imposing the hard sphere approximation. A general expression is then readily derived, the calculation being analogous to the solution of the problem of x-ray diffraction in monoatomic gases.[2] For the intensity of light scattered per unit volume of illuminated solution viewed, as a function of the angle of observation, in excess of that scattered by the solvent, when the incident light is vertically polarized and the scattered light is observed in the plane perpendicular to the electric vector, we obtain:

$$i=KMcP\{1-(\psi/V)\Phi(\kappa sd)\}.$$

The constant, $K=2n_0{}^2I_0(dn/dc)^2/(N_0\lambda^4r^2)$, where n_0 is the refractive index of the solvent; I_0, the intensity of the incident light of wave-length λ; dn/dc, the refractive index increment based on the weight concentration c; N_0, Avogadro's number; r, the distance from the scattering solution to the detector. The molecular weight of the solute is represented by M and the internal interference function, which is unity when the solute molecules are small relative to the wave-length, by P. The ratio ψ/V denotes the ratio of the excluded volume to the volume of the solution, its value has the limits of zero and unity. The function $\Phi(x)=3x^{-3}(\sin x-x\cos x)$. In the argument, $x=\kappa sd$, κ is the phase difference, $2\pi/\lambda$, $s=2\sin(\theta/2)$ where θ is the angle of observation and d is the distance of closest approach.

This equation predicts that when d is of the order of hundreds of angstroms i/c will fall rapidly from its infinite dilution value and become approximately constant at concentrations of the order of 1 g/liter. At higher concentrations the value of d must diminish for the excluded volume has attained its maximum value. Furthermore, if P is unity or if the data are corrected to this basis, the intensity of light scattered in backward directions will exceed that scattered in the corresponding forward directions; this would be a new experimental effect. Moreover, the ratio of the intensities of the forward and backward scattered light should with increasing concentration diminish from unity at infinite dilution, pass through a minimum and finally return to a value of unity as d diminishes to negligible values.

We have observed this behavior in solutions of several macromolecular electrolytes, data obtained for salt-free solutions of bovine serum albumin are summarized in the following table. These molecules are so small that the value of P may be taken as unity. Titration data indicate that under these conditions the albumin molecules carry net charges of about fifty protons. The consequence of intermolecular interference is clearly evident both in the absolute intensity of scattering per molecule and in the reduction of the dissymmetry, i_{45}/i_{135}. A value of d can be calculated from either effect. For the former we can set $(1-i/KMc)$ equal to ψ/V and proceed to solve the relation $\psi=4\pi d^3VN_0c/3M$ for d. This result is only approximate for it assumes that there is no interpenetration of the excluded volume spheres of radius d.

TABLE I.

pH	c(g/liter)	i_{90}/KMc	i_{45}/i_{135}	d_ψ	d_z	d_m
3.12	0.161	0.695	0.890	380A	590A	900A
	0.294	0.605	0.865	335	540	735
	0.408	0.500	0.845	325	460	660
3.20	0.690	0.485	0.830	275	470	555
	1.15	0.388	0.830	250	380	465
3.29	1.72	0.300	0.835	225	300	410
	1.87	0.280	0.870	225	240	395
	2.19	0.255	0.890	210	230	375
	2.62	0.230	0.910	200	180	355
	3.28	0.215	0.935	185	160	330
	7.00	0.164	1.00	82	—	255

Corrections for this effect would lead to somewhat larger values; however, this first approximation is entered in the table as d_z. On the other hand, the value of d as defined by the hard sphere approximation is obtained at once by fitting the dissymmetry data to the foregoing equation. These values of d are entered in the table as d_z, and as anticipated are seen to be generally larger than d_ψ. As a reference, the mean intermolecular distance d_m is given in the last column: this represents the upper limit to which d could approach. It thus appears that an approximate means has been found to represent the distribution of charged macromolecules in solution in addition to explaining the unusual light scattering data.

As expected the addition of a salt greatly diminishes these effects: both i/KMc and the dissymmetry approach unity at molalities of a few thousandths. When the dissymmetry has become unity, the downward curvature of the plot of Kc/i (or Hc/τ) against c disappears and the conditions required for the application of the fluctuation theory seem to be reinstated.

It is of interest to notice that if the value of d were of the order of thousands of Angstroms rather than hundreds and if the scattering could be observed at much lower concentrations the appearance of maxima in the angular intensity data would be expected. In this event it would then be practical to carry out a Fourier inversion and so arrive for the first time at the detailed radial distribution of charged macromolecules in solution. Solutions of some virus molecules provide these conditions and the possibilities thus offered are being explored.

[1] A. Einstein, Ann. d. Physik **33**, 1275 (1910).
[2] P. Debye, Physik. Zeits. **28**, 135 (1927).

Exchange of Ions between the Surface of Crystals and Solutions

R. M. STOW AND J. W. T. SPINKS
University of Saskatchewan, Saskatoon, Canada
June 20, 1949

THE exchange of ions between the surfaces of crystals and solutions has been used as the basis for a radioactive method for determining the active surface area of a precipitate.[1] While the active surface area is not necessarily the same as the geometric surface area, there is no doubt that the active surface area, as measured by exchange, is a characteristic property of the crystals which could be of considerable interest and importance.

In the so called, direct method, the exchange is measured with the help of a radioactive ion, isotopic with one of those in the precipitate and it should, in principle, be possible to use either the anion or the cation, or both, as tracers. We have now used both anion and cation to measure the area of crystals of strontium sulphate. The crystals, prepared by the addition of excess sulphuric acid to strontium chloride solution, were washed repeatedly with water and then aged for two years in contact with saturated strontium sulphate solution at room temperature.

Using a shaking time of ten minutes:

Active area, using $^{90}Sr^{++}$, $=14.9\times10^3$ sq. cm per gram;[2]
Active area, using $^{35}SO_4^{--}$, $=8.3\times10^3$ sq. cm per gram.[3]

The over-all precision of the measurements is thought to be about 4 percent.

The difference in areas as measured by Sr^{90} and S^{35} is quite beyond the limits of experimental error and would seem to be of considerable interest. It may be connected with the fact that excess sulphuric acid was used in preparing the strontium sulphate and experiments are being carried out to test this point. Alternatively, it may be related to the differing radii of the ions and to differing surface activity coefficients (see Coryell in reference 1.)

[1] F. A. Paneth, J. de Chim. Phys. **45**, 205 (1948).
[2] R. H. Singleton and J. W. T. Spinks, Can. J. Res. **27B**, 238 (1949).
[3] R. M. Stow, Thesis, University of Saskatchewan, Saskatoon, Canada (1949).

Determination of the Dissociation Energy of the C—Br Bond by Pyrolysis

M. SZWARC AND B. N. GHOSH
Chemistry Department, University of Manchester, Manchester, England
June 27, 1949

AN estimation of the dissociation energies of the C—Br bonds of various organic bromides should be of great interest, since knowledge of these dissociation energies, combined with the heats of formation of the relevant bromides in the gaseous state, makes it possible to determine the heats of formation of various organic radicals, and subsequently to calculate the various C—H dissociation energies, the resonance energies of these radicals, and related quantities.

The C—Br dissociation energy of an organic bromide can be estimated by investigating its pyrolysis in a stream of toluene used as a carrier gas. It was shown in previous communications that toluene is very effective in removing various radicals[1] which react with it according to Eq. (1).

$$C_6H_5\cdot CH_3+R\rightarrow C_6H_5\cdot CH_2+RH. \qquad (1)$$

Benzyl radicals produced in this process dimerise, forming dibenzyl which appears as one of the products of pyrolysis.

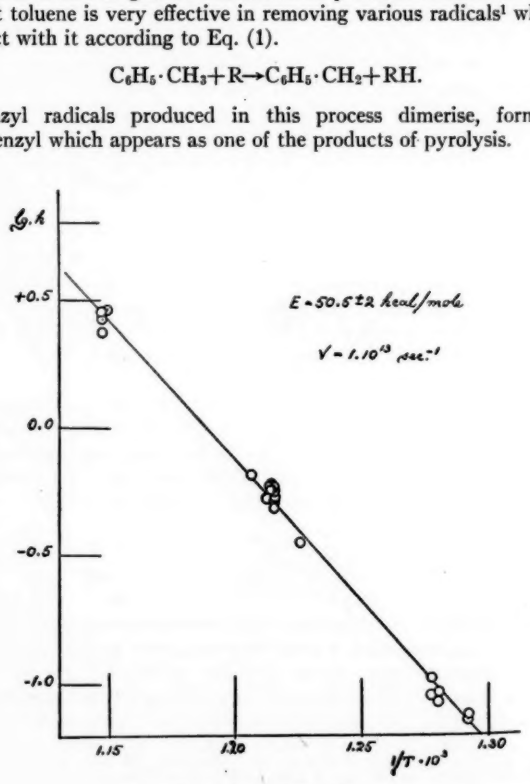

FIG. 1. Benzyl bromide.

We might expect that pyrolysis of an organic bromide RBr would result in a splitting of its molecule into a radical R and a Br atom. If toluene is used as a carrier gas then both fragments can react with it, and according to Eq. (1) each decomposed molecule of RBr would produce one molecule of HBr, one of RH and one of dibenzyl. Therefore, if this scheme applies, the rate of decomposition of bromide might be measured by the rate of formation of HBr, RH, or dibenzyl.

It is possible, however, that a molecule of organic bromide would decompose into HBr and the corresponding olefin.[2] This case can be easily distinguished from the former one, for although HBr would again be a product of pyrolysis, no dibenzyl would be produced. Hence, using toluene as a carrier gas one should be able to measure for an organic bromide both the rate of decomposition into radicals according to Eq. (2)

$$\mathrm{RBr} \rightarrow \mathrm{R} + \mathrm{Br}, \qquad (2)$$

and into HBr and olefin according to Eq. (3)

$$\mathrm{RBr} \rightarrow \mathrm{RBr} + \text{olefin}, \qquad (3)$$

even if these reactions occur simultaneously. The rate of reaction (2) would be measured by the rate of formation of dibenzyl, while the sum of the rates of both reactions (2) and (3) would be measured by the rate of formation of HBr.

Having described in general terms the principles of our method of pyrolysis of organic bromides we report now briefly the results obtained for benzyl bromide and allyl bromide. The apparatus used for these investigations as well as the experimental technique have been described previously.[1a,1c] An extra liquid air trap to collect the HBr was added before the first mercury vapor pump.

The rate of decomposition of benzyl bromide was measured by the rate of formation of either HBr or dibenzyl. It was shown that, within the experimental error, the molar ratio of dibenzyl to HBr was 1:1. Variation of the partial pressure of benzyl bromide (by a factor of 200) and of the time of contact (by a factor 3) demonstrated that the kinetics of the decomposition obeyed a first-order law. Variation of the partial pressure of toluene proved that the rate of decomposition of benzyl bromide was independent of the toluene pressure. Plot of the lg of unimolecular rate constant against $1/T$ for the temperature range 500°C to 600°C is shown in Fig. 1. The straight line corresponds to an activation energy of 50.5±2 kcal/mole and a frequency factor of 1.10^{13} sec.$^{-1}$. The numerical value of the latter is an indication that the decomposition is indeed a unimolecular process.

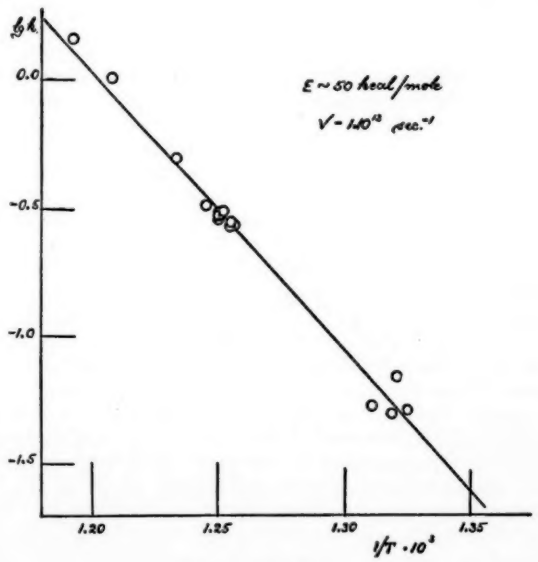

FIG. 2. Allyl bromide.

Assuming that the recombination of benzyl radicals and bromine atoms does not involve any activation energy, we conclude that the dissociation energy of the C−Br bond in benzyl-bromide is equal to the observed activation energy of the decomposition process, i.e., to 50.5±2 kcal/mole. This conclusion may be checked in the following way. The dissociation energy of the C−H bond in toluene was determined at 77.5±1.3 kcal/mole.[3] The difference between this dissociation energy and that of the C−Br bond in benzyl bromide was estimated calorimetrically at 29±3 kcal,[4] while the dissociation energies directly estimated by pyrolysis differ by 27±3.3 kcal. We see, therefore, that the agreement is very satisfactory.

A similar study of the pyrolysis of allyl-bromide leads to a value of about 50 kcal/mole for the dissociation energy of the C−Br bond in this compound. The plot of lg$k$ against $1/T$ is given in Fig. 2. The kinetics of the decomposition of allyl-bromide shows some peculiarities. The allyl radical, being very stable (probably as stable as the benzyl radical), does not react only with toluene but partially dimerises or associates with benzyl radicals. Therefore, the amount of dibenzyl formed in the pyrolysis of allyl-bromide is much lower than the amount of HBr, and it cannot be taken as a measure of decomposition.

A full account of these investigations is in course of publication.

[1] (a) M. Szwarc, Removing of CH_3 radical in the decomposition of ethylbenzene, J. Chem. Phys. **17**, 431 (1949). (b) M. Szwarc, Removing of NH_2 radical in the decomposition of hydrazine and benzylamine, J. Chem. Phys. **17**, 505 (1949). (c) M. Szwarc, Proc. Roy. Soc. (to be published).

[2] See, for example, E. T. Lessig, J. Phys. Chem. **36**, 2335 (1932); E. L. Vernon and F. Daniels, J. Am. Chem. Soc. **55**, 922 (1933); P. Fugassi and F. Daniels, J. Am. Chem. Soc. **60**, 771 (1938); F. Daniels and P. L. Veltmen, J. Chem. Phys. **7**, 756 (1939).

[3] M. Szwarc, Nature **160**, 403 (1947); J. Chem. Phys. **16**, 128 (1948).

[4] O. H. Gelner and H. A. Skinner, J. Chem. Soc. in press (1949).

Anomalous Mobility of H^+ and OH^- Ions

A. GIERER AND K. WIRTZ
Max Planck-Institut für Physik, Güttingen, Germany
June 25, 1949

THE mobility of H^+ and OH^- ions in water is much higher than that of other ions; its dependency on temperature and pressure is anomalous. If we assume that these ions are small complex hydrates, e.g., H_3O^+, we may expect mobilities of usual magnitude which are comparable to those of the Na^+ and Cl^- ions. Hence we may define excess mobilities $u^+ = u_{H^+} - u_{Na^+}$ and $u^- = u_{OH^-} - u_{Cl^-}$ due to special elementary processes. We postulate that these elementary processes behave "normally," i.e., that the dependence of their number per second (frequency) on temperature is of the form const. $\exp-(q/kT)$. The deviations of u^+ and u^- from this dependence on temperature are supposed to be due to structural changes of the water and will be taken into account by means of a factor $f(T)$.

So we put $u^+ = u_0^+ \cdot f^+(T) \cdot \exp-(q^+/kT)$ and $u^- = u_0^- \cdot f^-(T) \cdot \exp-(q^-/kT)$; the factor $f(T)$ is to be determined independently.

Eucken[1] tentatively expressed the anomalies of the volume and the specific heat of water by introducing mole fractions $\gamma_1, \gamma_2, \gamma_3, \gamma_4$ of different forms of association of water, γ_4 referring to the association form of larger volume, like ice. Eucken supposes that these association forms are cyclic ones.

We find that $f(T)$ can be derived from these values of γ_i when we assume that the icy association forms do not participate in the excess conductivity. We obtain the result that $f(T)$ means the number of H bridges per molecule H_2O in the non-icy association forms according to the formula $f^+(T) = f^-(T) = \frac{1}{2}\gamma_2 + \frac{3}{4}\gamma_3$ (see Table I). Also u_0 is equal for the H^+ and the OH^- ions. From the quotients $u^+/f(T)$ and $u^-/f(T)$ we obtain $q^+ = 2{,}4$ kcal/mole and $q^- = 3{,}0$ kcal/mole, both values being constant between 0° and 306°C. The value of u_0 can be calculated according to the theories of exchange of places.[2]

TABLE I. Analytic molar fractions of the non-icy association complexes, according to Eucken.

T°C	0°	20°	40°	60°	80°
γ_2	0.35	0.43	0.49	0.53	0.54
γ_3	0.30	0.31	0.29	0.26	0.22
T°C	100°	120°	160°	200°	374°
γ_2	0.54	0.53	0.49	0.43	0.22
γ_3	0.18	0.15	0.09	0.06	0.01

The mechanism of the excess mobility, therefore, consists of two processes: (1) association of a water molecule to one of the three H bonds of the H_3O^+ or OH^- ions, (2) transition of a proton over the hydrogen bridge. The slower of both processes is decisive for the velocity. The transitions of the protons preferably occur in the direction of the electric field applied to the system. Thus we have $u_0=\frac{1}{6}js^2\cdot e/kT$. With $s=2.76$A (distance of $0\cdots0$ in the H bridge) and $e=$electronic charge, we obtain $j=2700$ cm^{-1}.

If the transition of the protons over the H bridges is decisive for the velocity, $q^{\pm}$ would represent the activation to be overcome by the proton during the transition, and j would equal the frequency of the protons in the bridge. If, on the other hand, the formation of the H bridges is decisive for the velocity, q would represent the activation necessary for the dissociation of the bridge, and j would denote twice the frequency of the (hindered) rotation of the water molecules. The value of j resulting from our theory would fit both assumptions as is shown by a comparison to the measured Raman frequencies. Hence, which process is decisive for the velocity, cannot be decided in this way. Both possibilities are compatible with the fact that the u^+ of H^+ is $\sqrt{2}$ times greater than the u^+ of D^+.

Eucken published the dependency of the γ_i on pressures up to 10,000 atmos. Basing on these data we can interpret the anomalous increase with pressure of the excess mobility. We conclude that it is due to a diminution of the more voluminous icy association complexes in favor of the non-icy ones, in other words γ_2 and γ_3 increase with pressure.

According to our theory the elementary process of the excess mobility which is decisive for the velocity is proportional to the number of the H bridges in the non-icy association complexes of water. Our theory also renders from the experiments the quantities j and q. The number of the H bridges can be derived from the anomalies of water, according to Eucken. The transition of protons over the H bridges from a H_3O^+ ion to an associate H_2O molecule, or from a H_2O molecule to an OH^- ion, preferably occurring in the direction of an electric field, is the cause of the transition of a charge. The disturbed orientation of the remaining water molecules is re-established by the motion due to temperature.

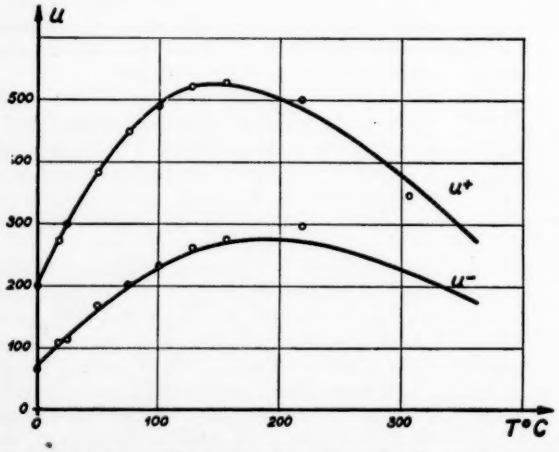

FIG. 1. Excess mobilities of the hydrogen ion (u^+) and the hydroxyl ion (u^-) as a function of temperature. The curve shows the theoretical response; the plots are experimentally gained.

A detailed paper will be published in a German journal. Therein previous theories will be discussed,[3] and the reasons of the non-participation of the icy structure and the question of the inner electric field[4] will be investigated.

[1] A. Eucken, Zeits. f. Elektrochemie **52**, 255 (1948); Göttinger Nachrichten 38 (1946).
[2] K. Wirtz, Zeits. Naturf. **3a**, 672 (1948).
[3] E. Hückel, Zeits. Elektrochemie **34**, 546 (1928). J. D. Bernal and R. H. Fowler, J. Chem. Phys. **1**, 515 (1933). G. Wannier, Ann. d. Physik (5) **24**, 545 (1925). M. L. Huggins, J. Phys. Chem. **40**, 723 (1936). P. Wulff and H. Hartmann, Zeits. f. Elektrochemie **47**, 858 (1941).
[4] L. Onsager, J. Am. Chem. Soc. **58**, 1486 (1936).

Photoelectric Measurements on Cool Flames

LUDOVIC OUELLET, EDOUARD LEGER, AND CYRIAS OUELLET
Département de Chimie, Université Laval, Québec, Canada
June 28, 1949

THIS is a preliminary report on what we believe to be the first photoelectric study of cool flames. Static, uniform glows were obtained by rushing the gaseous mixture into a preheated Pyrex cylinder. The intensity of the luminescence was measured by means of a multiplier phototube and recorded against the time on a single-sweep cathode-ray oscillograph. By this method, the cool flame of diethylether-oxygen mixtures has been studied over a wide range of conditions. A description of the apparatus and an analysis of the results will be published soon.[1] A few detached observations are described in this note.

Representative oscillograms are shown on the same scale in Fig. 1 and the conditions under which they were obtained are listed in Table I. The diameter of the 13-cm long Pyrex cylinder was 4.6 cm for *A*, *B*, *C* and *E*, and 3.4 cm for *D*. On these curves, which can be reproduced with a fidelity of about 5 percent, the pulsating character of the glow is easily recognized. In spite of the considerable changes introduced by varying the experimental conditions, the following features are always observed: a sharp initial rise is followed by two, and sometimes more maxima and a gradual decay. True periodicity is not evident. In ether-oxygen mixtures, the induction period is of the order of a few tenths of a second above 200°C.

Flames of octane, acetaldehyde, diethylether and diethylperoxide were examined. The curves show that the intensities of the first three are comparable, although the flames of octane *A* and acetaldehyde *B* tend to be shorter than those of ether, *C*, *D* (1) and *E* (1). The total amounts of light emitted are in the ratios of the areas under the curves. Comparison of *C* and *E* (1) shows the influence of changing the total pressure from 48 mm to 66 mm: both maxima are enhanced, brought nearer to each other and the total duration and emission are increased. Changing the diameter of the vessel introduces considerable distortion, as shown by *D* (1), which was obtained in the 3.4-cm vessel. We have prepared some diethylperoxide and examined the glow which accompanies its decomposition[2] at 215°C and 10–20 mm, both alone and in the presence of 50-mm oxygen. The oscillograms, not shown here, indicate a flash lasting about 0.01 second and at least ten times as intense as the average cool flame of ether.

Addition of H_2, H_2O or CO_2 to the ether-oxygen mixture produces a mere inert-gas effect comparable to that of N_2 shown by *E* (2), in which the second maximum is slightly favored at the expense of the first one, the total emission being increased by 10 percent. The flame is delayed several seconds and quenched by 5 percent HCHO. With 2 percent NO, the induction period is increased a thousandfold but the flame which takes place after about 100 seconds at 215°C seems normal, as far as could be ascertained by visual observations of the oscillograms. These retarded events cannot be recorded with our present set-up. An ether-oxygen mixture containing tetraethyllead at its vapor pressure at room temperature gave the quenched flame shown by

TABLE I. Key to oscillograms shown in Fig. 1.

Curve	Temperature	Partial pressures of reactants
A	257°C	4 mm C_3H_{18}+166 mm O_2
B	250	37 mm CH_3CHO+37 mm O_2
C	215	24 mm $C_2H_5OC_2H_5$+24 mm O_2
D (1)	215	47 mm $C_2H_5OC_2H_5$+47 mm O_2
D (2)	215	Same+trace of $Pb(C_2H_5)_4$
E (1)	215	33 mm $C_2H_5OC_2H_5$+33 mm O_2
E (2)	215	Same+72 mm N_2

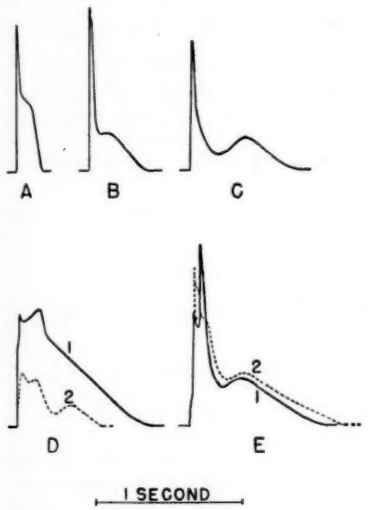

FIG. 1. Intensity of luminescence (on arbitrary scale) against time, for various cool flames identified in Table I.

curve *D* (2), but the induction period was not affected. When this compound was introduced alone a few seconds before a normal mixture, only the second maximum was depressed. In a series of alternate runs, the undoped mixtures continued to give normal flames until a deposit was visible on the walls, causing a screening effect and possibly also some inhibition.[3,4] These peculiarities will require more detailed investigation. Cleaning the reaction vessel or coating it with KCl made no appreciable difference.

The facts suggest that an intermediate builds up through a free-radical chain reaction, sensitive to inhibition by NO or HCHO, and suffers a homogeneous thermal explosion (similar to that of diethylperoxide)[2] responsible for the sharp initial peak. The subsequent, rounder maximum, which vanishes at pressures below 20 mm, may be due either to a smoother recurrence of the same process, or to some further step in the reaction.

We express our thanks to the National Research Council of Canada for a grant in support of this research and to Ethyl Corporation for a sample of tetraethyllead.

[1] Ouellet, Leger, and Ouellet, J. Chem. Phys. (in press).
[2] E. J. Harris and A. C. Egerton, Proc. Roy. Soc. **A168**, 1 (1938).
[3] R. O. King, Can. J. Research **F26**, 125 (1948).
[4] G. H. N. Chamberlain and A. D. Walsh, Abstracts of Symposium on Combustion, Flame and Explosion Phenomena (University of Wisconsin Press, Madison, September 1948), p. 109.

The Infra-Red Spectrum of $C^{14}O_2$*

R. K. SHELINE AND J. W. WEIGL
Department of Chemistry and Radiation Laboratory, University of California, Berkeley, California
June 20, 1949

RECENTLY radio-carbon dioxide containing about 30 percent $C^{14}O_2$ has become available. We have used a Perkin-Elmer automatic infra-red spectrometer with a NaCl prism to obtain the spectrum of this CO_2 in the region 2–16 microns. The measurements were made at room temperature in a 9.4-cm glass cell fitted with KBr windows. The total CO_2 pressure was 9.6 mm. The absorption curves are shown in Fig. 1.

TABLE I. Isotope shift of band centers.

	ν_2	ν_3	Ratio $(\nu_i/\nu)_2$	Ratio $(\nu_i/\nu)_3$
$C^{13}O_2$ obs	667.3	2349.3	1.0000	1.0000
calc.	—	—	1.0000	1.0000
$C^{13}O_2$ obs. (2)	—	2284.5	—	0.97242
calc.	648.3	2282.4	0.97154	0.97154
$C^{14}O_2$ obs.	632±2	2220±5	0.94710	0.94496
calc.	631.6	2223.7	0.94656	0.94656

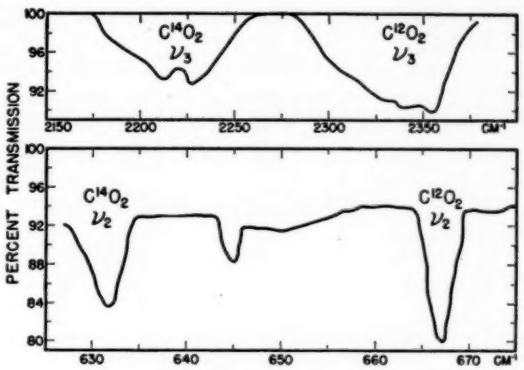

FIG. 1. Fundamental bands of $C^{12}O_2$ and $C^{14}O_2$.

The calibration function of McKinney and Friedel,[1] which gives a straight line when plotted against drum reading, permitted a more accurate determination of frequencies than the usual curve of ν itself *vs.* drum reading. This was important because the precision with which it was possible to determine the band centers limited the accuracy of the product rule check.

Table I shows our experimental results, as well as those of A. H. Nielsen for $C^{13}O_2$.[2] These data are compared to the frequencies calculated from the infra-red active fundamentals of $C^{12}O_2$ by the Redlich-Teller product rule.[3] The agreement between the observed and calculated quantities is well within the precision of our measurements. The product rule applies strictly only to zero-order bands; however, the difference in ratio between the zero-order bands and the fundamentals for CO_2 is so small as to be negligible, unless one has the accuracy of a grating spectrograph.

In view of recent interest in the isotope effect on bond energies we hope to locate these band centers with a grating spectrometer, with the purpose of determining differences in the potential functions of the isotopic molecules. The authors are indebted to Professor M. Calvin for his interest in this work.

* This work was supported by the AEC.
[1] D. S. McKinney and R. A. Friedel, J. Opt. Soc. Am. **38**, 222 (1948).
[2] A. H. Nielsen, Phys. Rev. **53**, 983 (1938).
[3] G. Herzberg, *Infrared and Raman Spectra of Polyatomic Molecules* (D. Van Nostrand Company, Inc., New York, 1947), p. 230.

Bond Energies and Bond Distances of the Normal Paraffins

GEORGE GLOCKLER
Department of Chemistry and Chemical Engineering, State University of Iowa, Iowa City, Iowa
June 28, 1949

FROM the known relations between bond energies and bond distances of carbon-carbon and carbon hydrogen bonds,[1] the following quantities for ethane can be derived:

CC bond energy $=B(\text{CC in } C_2H_6)=2.938$ ev,
CC bond distance $=R(\text{CC in } C_2H_6)=1.552$A,
CH bond energy $=\overline{B}(\text{CH in } C_2H_6)=3.831$ ev,
CH bond distance $=R(\text{CH in } C_2H_6)=1.0965$A.

TABLE I. Estimated bond energies (B, ev) and bond distances (R, A) of normal paraffins

H_3C—(I)—(CH_2)—(I II)—(II)—(CH_2)—(II III)—(III)

	B(CH I) R(CH I)	B(CH I II) R(CH I II)	B(CH II III) R(CH II III)	$Q_0{}^0a$ (expt.) $Q_0{}^0a$ (calc.)
CH_4	3.884 1.092	—	—	15.537
C_2H_6	3.831 1.0965	—	—	25.925 (25.924)
C_3H_8	3.825 1.097	3.810 1.098	—	36.419 36.436
C_4H_{10}	3.825 1.097	3.804 1.0985	—	46.952 46.959
C_5H_{12}	3.825 1.097	3.804 1.0985	3.799 1.099	57.488 57.490
C_6H_{14}	3.825 1.097	3.804 1.0985	3.799 1.099	68.015 (68.015)
	B(CC I) R(CC I)	B(CC II) R(CC II)	B(CC III) R(CC III)	
C_2H_6	2.938 1.552	—	—	
C_3H_8	2.933 1.558	—	—	
C_4H_{10}	2.932 1.559	2.929 1.564	—	
C_5H_{12}	2.932 1.559	2.928 1.566	—	
C_6H_{14}	2.932 1.559	2.928 1.566	2.927 1.567	

They are based on the heat of formation of ethane ($Q_0{}^0f=16.517$ kcal),[2] the heat of sublimation of carbon ($L_0=5.888$ ev)[3] and the heat of dissociation of hydrogen ($D_0{}^0(H_2)=4.4776$ ev),[2] yielding for the atomic heat of formation of ethane: $Q_0{}^0a(C_2H_6)=25.925$ ev. The latter value equals six CH bonds and one CC bond. The bond energies and bond distances given above have been obtained from B(CC):R(CC) and B(CH):R(CH) graphs.[1] Smith[4] finds R(CC)=1.55A from band spectroscopy. Assuming R(CH) =1.098A he calculates $\measuredangle$HCH=109° 7′. The above-mentioned distances give $\measuredangle$HCH=110° 4′. The present considerations permit the calculation of interatomic distances and moment of inertia from heat of formation and vice versa.

The normal paraffins, beyond butane, show a constant increment in heat of formation ($\Delta Q_0{}^0f=3.673$ kcal at 0°K)[2] which in terms of atomic heat of formation is

$$\Delta Q_0{}^0a(C_nH_{2n+2})=0.1593+5.888+4.4776=10.5249 \text{ ev}$$
$$=B(CC)+2\bar{B}(CH)(\text{in } CH_2 \text{ in a paraffin}, n\geqslant 5)$$

or

$$C(^3P)+2H(^2S)\rightarrow CH_2(\text{as in a paraffin}); \quad \Delta Q_0{}^0a=10.5249 \text{ ev}.$$

From the B(CC):R(CC) and B(CH):R(CH) graphs[1] it is found

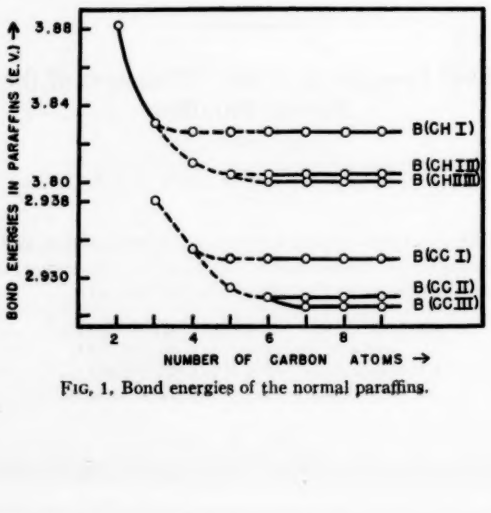

FIG. 1. Bond energies of the normal paraffins.

that

$$B(\text{CC in } CH_2, p)=2.927 \text{ ev at } 1.567\text{A},$$
$$\bar{B}(\text{CH in } CH_2, p)=3.799 \text{ ev at } 1.099\text{A}.$$

If all the bonds were alike (for example, in hexane), then $Q_0{}^0a$(calc.) =67.821 ev, while $Q_0{}^0a$(expt.)=68.015 ev.[2] Hence the bonds in the methyl groups must be stronger. The bond energies given in Table I and shown in Fig. 1 form a consistent set of estimates. These values will reproduce the atomic heats of formation of any normal paraffin above n-butane. From them the general formula

$$Q_0{}^0a(C_nH_{2n+2})=4.8654+10.5249n; \quad n\geqslant 5$$

can be obtained. Propane and n-butane are neither "ethane-like" nor are they "paraffin-like" in their bond energies. Atomic heats of formation calculated on either basis do not check the experimental values. However, estimates can be made for these two molecules by interpolation (between ethane and pentane) as shown in Fig. 1.

The atomic heats of formation are based on Hagstrum's value for the heat of sublimation of carbon[3]

$$C(\text{solid})\rightarrow C(^3P); \quad L_0(C)=5.888 \text{ ev},$$

and they refer to the formation of the paraffins from the elements in their normal gaseous states:

$$nC(^3P)+(2n+2)H(^2S)\rightarrow C_nH_{2n+2}; \quad Q_0{}^0a(C_nH_{2n+2})$$

There is no advantage to refer these energy quantities to the ^5S state of the carbon atom,[5] as Voge[6] pointed out.

From Table I it is seen that *strong and hence short aliphatic carbon-carbon bonds associate with strong and therefore short carbon-hydrogen bonds.*

[1] G. Glockler, J. Chem. Phys. **16**, 842 (1948).
[2] Selected values of properties of hydrocarbons, National Bureau of Standards Circular C461 (1947).
[3] H. D. Hagstrum, Phys. Rev. **72**, 947 (1947).
[4] L. G. Smith, J. Chem. Phys. **17**, 139 (1949).
[5] L. Gerö, J. Chem. Phys. **16**, 1011 (1948).
[6] H. H. Voge, J. Chem. Phys. **16**, 984 (1948).

Bond Energies and Bond Distances of Branched Paraffins

GEORGE GLOCKLER
Department of Chemistry and Chemical Engineering, State University of Iowa, Iowa City, Iowa

June 21, 1949

BOND energies (B) and bond distances (R) have been derived for the normal paraffins[1] from considerations of atomic heat of formation ($Q_0{}^0a$) based on relations between bond energies and bond distances of carbon-carbon and carbon-hydrogen bonds.[2] In applying similar calculations to the branched paraffins, it is necessary to remember the remarks made by Rossini and coworkers[3, 4] and Platt,[5] namely that neighboring bonds affect the properties of a given bond. In the present case these *"near-bond-effects"* have been evaluated as *"near-group-effects"* and include all features of interaction such as hyperconjugation,[6] Van der Waals, London, dipole and induction effects, etc. These interactions are referred to *ideal*, single carbon-carbon and carbon-hydrogen bonds. The ideal carbon-carbon single bond is here defined as the bond to which a free CH-radical (D(CH)=3.47 ev)[7] could be attached and remain unchanged, so that the resulting structure (H−C−C) would fit onto the B(CC):R(CC) and B(CH):R(CH) graphs.[2] From these graphs B(C−C, ideal) would be 2.85 ev at R(C−C, ideal)=1.76A, while Mulliken[6] estimates this distance to be 1.58A. From the B(CC):R(CC) curves B(CC, 1.58A) would be 2.92 ev. Hence B(CC, ideal) is assumed to be 2.88 ev at 1.65A. The ideal CH bond is taken to be the bond in $CH(^2\Pi_r)$ radical; B(CH, ideal)=3.47 ev at 1.1305A.[7]

TABLE I. Atomic heats of formation ($Q_0{}^0a$) of branched paraffins.

	$Q_0{}^0a$ (ev) expt.	calc.	% error
Methane	15.537	—	—
Ethane	25.925	—	—
Propane	36.419	36.440	0.06
n-Butane	46.952	46.965	0.03
i-Butane	47.007	47.005	−0.004
n-Pentane	57.488	57.490	0.004
2-Methylbutane	0.549	0.546	−0.002
2,2-Dimethylpropane	0.663	0.668	0.01
n-Hexane	68.015	(68.015)	—
3-Methylpentane	0.038	0.059	0.03
2-Methylpentane	0.063	0.068	0.008
2,3-Dimethylbutane	0.097	0.084	−0.02
2,2-Dimethylbutane	0.172	0.163	−0.01
3-Ethylpentane	78.516	78.593	0.1
n-Heptane	0.540	0.540	0.0
3-Methylhexane	0.553	0.594	0.05
2-Methylhexane	0.588	0.595	0.01
2,3-Dimethylpentane	0.611	0.633	0.03
3,3-Dimethylpentane	0.638	0.691	0.07
2,4-Dimethylpentane	0.641	0.639	−0.002
2,2,3-Trimethylbutane	0.666	0.708	0.05
2,2-Dimethylpentane	0.685	0.682	−0.003
3-Ethylhexane	89.038	89.118	0.09
2-Methyl-3-Ethylpentane	0.047	0.162	0.13
n-Octane	0.065	0.065	0.0
4-Methylheptane	0.069	0.113	0.05
3,4-Dimethylhexane	0.073	0.162	0.1
3-Methylheptane	0.078	0.119	0.04
3-Methyl-3-Ethylpentane	0.080	0.203	0.13
2,3-Dimethylhexane	0.083	0.158	0.08
2,3,3-Trimethylpentane	0.094	0.261	0.18
2,3,4-Trimethylpentane	0.099	0.202	0.11
2-Methylheptane	0.112	0.109	−0.003
2,4-Dimethylhexane	0.126	0.159	0.03
2,2,3-Trimethylpentane	0.127	0.230	0.11
3,3-Dimethylhexane	0.133	0.208	0.09
2,5-Dimethylhexane	0.164	0.153	−0.01
2,2,4-Trimethylpentane	0.169	0.246	0.08
2,2,3,3-Tetramethylbutane	0.184	0.306	0.13
2,2-Dimethylhexane	0.191	0.207	0.02
	Average		0.05

From B(CC, C_2H_6) = 2.938 ev and B(CC, ideal) it follows that the near-group-effect of the six hydrogen atoms is 2.938 − 2.880 = 0.058 ev or the average effect of one CH-bond on the CC-bond is 0.01 ev. From B(CC, propane) = 2.933 ev the near-bond effect [(CH_3, 5H) on C−C] is 0.053 ev. Assuming that [H−C on C−C] is the same in all paraffins, then [CH_3 on C−C] is 0.005 ev. The constant increment $\Delta Q_0{}^0a$ for the normal paraffins (10.5249 ev)[1] yields B(CC, p) = 2.927 ev whence 2[(R+2H) on CC] = 2.927 − 2.88 and [R on CC] = 0.004 ev where $R = C_nH_{2n+1}$, $n \geqslant 2$ (straight or branched).

The near-group-effect of carbon-hydrogen bonds can be estimated from the relations:

$$B(\text{CH}, C_2H_6) - B(\text{CH, ideal}) = 2[\text{H on CH}] + [CH_3 \text{ on CH}] = 3.831 - 3.470 = 0.361,$$

$$B(\text{CH}(m), C_3H_8) - B(\text{CH, ideal}) = [\text{H on CH}] + 2[CH_3 \text{ on CH}],$$

$$B(\text{CH, paraffin}) - B(\text{CH, ideal}) = 2[R, \text{ paraffin on CH}] + [\text{H on CH}] = 3.799 - 3.470 = 0.329.$$

The solutions of these equations which also fit $Q_0{}^0a$(n-C_6H_{14}) are: [H on CH] = 0.1273 ev; [CH_3 on CH] = 0.1064 ev; [R(n-paraffin) on CH] = 0.101 ev; B(CH(m)C_3H_8) = 3.810 ev; B(CH I, hexane) = 3.826 ev and B(CH I II, hexane) = 3.805 ev[1] CH_3-, $(CH_3)_2$:CH·CH_2-, $(CH_3)_3$:C·CH_2-, $(CH_3)_2$:Ċ·CH_2·CH_3, $(CH_3)_2$:Ċ$(CH_2)_2$·CH_3, C_2H_5·Ċ(CH_3)·C_2H_5 and $(CH_3)_2$:CH·Ċ$(CH_3)_2$ exert a near-group effect of 0.1064 ev, while all other propyl, butyl, pentyl, hexyl, and heptyl radicals influence a C−H bond to the extent of 0.101 ev. With these assumptions the values of $Q_0{}^0a$(paraffins) have been calculated (Table I).[8]

It can be seen that the influence of the compactness of the carbon skeleton is brought out, but that the order of the calculated $Q_0{}^0a$-values is not the same as of the experimental ones in the heptanes and octanes. If compactness were the only influence, 2,2,3,3-tetramethylbutane would be expected to be the most stable of octanes and 2,2,3-trimethylpentane of the heptanes. The effect of Van der Waals attraction between hydrogen atoms on adjacent carbon atoms probably accounts for the difference in calculated and experimental values.

The calculations are shown for 3-methylpentane. The end C−C bonds are numbered III, the next two C−C bonds are II and the C−C bond from the third carbon atom to the methyl group is labeled I:

(CC I) = 2.880 + [(4H, 2C_2H_5) on C−C] = 2.924 ev at 1.570A.

(CC II) = 2.880 + [(3H, 2CH_3, C_2H_5) on C−C] = 2.924 ev at 1.570A.

(CC III) = 2.880 + [(5H, (CH_3·CH_2·ĊH(CH_3))) on C−C] = 2.934 ev at 1.556A.

(CH I) = 3.470 + [(2H, ((C_2H_5)$_2$·CH-)) on C−H] = 3.825 ev at 1.097A.

(CH I II) = 3.470 + [(CH_3, 2C_2H_5) on C−H] = 3.778 ev at 1.101A.

(CH II III) = 3.470 + [H, CH_3(C_2H_5·ĊH·CH_3) on C−H] = 3.804 ev at 1.099A.

(CH III) = 3.470 + [(2H, (n-C_3H_7·CH(CH_3)·CH_2-)) on C−H] = 3.825 ev at 1.097A.

$Q_0{}^0a$(3-Methylpentane) = 3×2.924 + 2×2.934 + 9×3.825 + 3.778 + 4×3.804,
= 68.059 ev (calc.),
= $Q_0{}^0f$ + 6L(C) + 7D(H_2),
= 1.367 + 35.328 + 31.343,
= 68.038 ev (expt.).

The calculated value is 0.03 percent too high. Considering the relative simplicity of these calculations, it appears that these considerations furnish at least a beginning toward an empirical understanding of these energy relations. A more detailed theoretical analysis of the various factors of interaction between the atoms of these molecules will likely result in a smaller error of such estimates of the atomic heats of formation. Since sufficiently accurate theoretical calculations covering all the factors of interaction cannot be made at the present time, these empirical considerations are of value.

[1] G. Glockler, J. Chem. Phys. **17**, 747 (1949).
[2] G. Glockler, J. Chem. Phys. **16**, 842 (1948).
[3] E. J. R. Prosen and F. D. Rossini, J. Res. Nat. B. St. **27**, 519 (1941).
[4] Taylor, Pignocco, and Rossini, J. Res. Nat. B. St. **34**, 413 (1945).
[5] J. R. Platt, J. Chem. Phys. **15**, 419 (1947).
[6] Mulliken, Riecke, and Brown, J. Am. Chem. Soc. **63**, 41 (1941).
[7] G. Herzberg, *Molecular Spectra and Molecular Structure, I. Diatomic Molecules* (Prentice-Hall, Inc., New York, 1939).
[8] F. D. Rossini *et. al.*, "Selected values of properties of hydrocarbons," National Bureau of Standards, Circular C461 (1947).

Dissociation Energies of Carbon-Hydrogen Bonds in Paraffins from Bond-Energies

GEORGE GLOCKLER
Department of Chemistry and Chemical Engineering, State University of Iowa, Iowa City, Iowa
June 21, 1949

FROM the *near-group-effects*[1] the bond-energies and bond distances of hydrocarbon radicals can be estimated and their atomic heats of formation ($Q_0{}^0a$) can be calculated. The difference between $Q_0{}^0a$ of the corresponding paraffin gives the dissociation energy of the paraffin (D) in respect to the removal of the first hydrogen atom:

$$\begin{array}{l} C_nH_{2n+2} \rightarrow nC + (2n+2)H - Q_0{}^0a(\text{paraffin}) \\ nC + (2n+1)H \rightarrow C_nH_{2n+1} + Q_0{}^0a(\text{radical}) \\ \hline C_nH_{2n+2} \rightarrow C_nH_{2n+1} + H - D(\text{paraffin}). \end{array}$$

The data for CH_4 to C_4H_{10} are:

Near-Group-Effects (ev):

B(C−C ideal) = 2.880; [H on C−C] = 0.01;
[CH_3 on C−C] = 0.005;

TABLE I. Dissociation energies of some paraffins (kcals).

Reaction	Bond energies	Activation energies [a]		Resonance and conjugation energies [e]
$CH_4 \rightarrow CH_3 + H$	100.4	103.6	100.8[b] 102.9[c]	—
$CH_3 \rightarrow CH_2 + H$	92.2	—	—	—
$CH_2 \rightarrow CH + H$	85.7	—	—	—
$C_2H_6 \rightarrow C_2H_5 + H$	96.9	96.4	98 ± 2[d]	97.5
$n\text{-}C_3H_8 \rightarrow n\text{-}C_3H_7 + H$	95.9	95.5	—	—
$C_3H_8 \rightarrow i\text{-}C_3H_7 + H$	90.7	91.0	—	92.6
$n\text{-}C_4H_{10} \rightarrow n\text{-}C_4H_9 + H$	96.1	—	—	—
$i\text{-}C_4H_{10} \rightarrow i\text{-}C_4H_9 + H$	88.1	86.9	—	90.0

[a] Baughan, Evans, and Polanyi, Trans. Faraday Soc. **37**, 377 (1941).
[b] G. B. Kistiakowsky and E. R. Van Artsdalen, J. Chem. Phys. **12**, 469 (1944).
[c] M. Szwarc, J. Chem. Phys. **17**, 431 (1949).
[d] H. C. Anderson and E. R. Van Artsdalen, J. Chem. Phys. **12**, 479 (1944).
[e] J. S. Roberts and H. A. Skinner, Trans. Faraday Soc. **45**, 339 (1949).

$[CH_2$ on $C-C] = \frac{2}{3}[CH_3$ on $C-C] = 0.003$;
$[C_2H_5$ on $C-C] = 0.004$; $B(C-H$ ideal$) = 3.47$;
$[H$ on $C-H] = 0.127$; $[CH_3$ on $C-H] = 0.106$;
$[CH_2$ on $C-H] = 0.106$; $[CH_2$ on $C-H] \doteq \frac{2}{3}[CH_3$ on $C-H] = 0.07$;
$[C_2H_5$ on $C-H] = 0.101$;
$[-CH_2 \cdot CH_2-$ on $C-H] \doteq [n\text{-}C_3H_7$ on $C-H]$
$= [i\text{-}C_3H_7$ on $C-H] = [-CH_2 \cdot CH_2 \cdot CH_2-$ on $C-H] \doteq 0.101$.

Bond energies (B in ev) and bond distances (R in A):

Methane: $Q_0{}^0a = 15.537$; $\bar{B}(CH) = 3.884$; $R(CH) = 1.0921$.

Methyl radical: $Q_0{}^0a = 11.184$; $\bar{B}(CH) = 3.728$; $R(CH) = 1.105$.

Methylene radical: $Q_0{}^0a = 7.186$; $\bar{B}(CH) = 3.593$; $R(CH) = 1.118$.

CH, $^2\Pi_r$: $Q_0{}^0a = B = 3.47$; $R(CH) = 1.1305$.

Ethane: $Q_0{}^0a = 25.925$; $B(CC) = 2.938$; $R(CC) = 1.552$;
$\bar{B}(CH) = 3.831$; $R(CH) = 1.096$.

Ethyl radical: $Q_0{}^0a = 21.722$; $B(CC) = 2.928$; $R(CC) = 1.565$;
$\bar{B}(CH$ of $CH_3) = 3.796$; $R(CH$ of $CH_3) = 1.099$;
$\bar{B}(CH$ of $CH_2) = 3.704$; $R(CH$ of $CH_2) = 1.107$.

Propane: $Q_0{}^0a = 36.419$; $\bar{B}(CC) = 2.933$; $R(CC) = 1.558$;
$\bar{B}(CH$ of $CH_3) = 3.825$; $R(CH$ of $CH_3) = 1.097$;
$\bar{B}(CH$ of $CH_2) = 3.810$; $R(CH$ of $CH_2) = 1.098$.

n-Propyl radical: $Q_0{}^0a = 32.258$; $B(CC$ of $CH_3) = 2.932$;
$R(CC$ of $CH_3) = 1.559$; $B(CC$ of $CH_2) = 2.904$;
$R(CC$ of $CH_2) = 1.602$; $\bar{B}(CH$ of $CH_3) = 3.825$;
$R(CH$ of $CH_3) = 1.097$; $\bar{B}(CH$ of mid-$CH_2) = 3.775$;
$R(CH$ of mid-$CH_2) = 1.101$; $\bar{B}(CH$ of end-$CH_2) = 3.698$;
$R(CH$ of end-$CH_2) = 1.108$.

i-Propyl radical: $Q_0{}^0a = 32.483$; $\bar{B}(CC$ of $CH_3) = 2.924$;
$R(CC$ of $CH_3) = 1.570$; $\bar{B}(CH$ of $CH_3) = 3.825$;
$R(CH$ of $CH_3) = 1.097$; $B(CH$ of mid-C$) = 3.683$;
$R(CH$ of mid-C$) = 1.109$.

n-Butane: $Q_0{}^0a = 46.952$; $\bar{B}(CC$ of $CH_3) = 2.932$;
$R(CC$ of $CH_3) = 1.559$; $B(CC$, center$) = 2.929$;
$R(CC$, center$) = 1.564$; $\bar{B}(CH$ of $CH_3) = 3.825$;
$R(CH$ of $CH_3) = 1.097$; $\bar{B}(CH$ of mid-C$) = 3.804$;
$R(CH$ of mid-C$) = 1.099$.

n-Butyl radical: $Q_0{}^0a = 42.784$; $B(CC$ of $CH_3) = 2.932$;
$R(CC$ of $CH_3) = 1.559$; $B(CC$, center$) = 2.927$;
$R(CC$, center$) = 1.566$; $B(CC$ of end $CH_2) = 2.903$;
$R(CC$ of end $CH_2) = 1.604$; $\bar{B}(CH$ of $CH_3) = 3.825$;
$R(CH$ of $CH_3) = 1.097$; $\bar{B}(CH$, I II$) = 3.804$; $R(CH$, I II$) = 1.099$;
$\bar{B}(CH$, II III$) = 3.769$; $R(CH$, II III$) = 1.101$;
$\bar{B}(CH$, end $CH_2) = 3.698$; $R(CH$, end $CH_2) = 1.108$.

i-Butane: $Q_0{}^0a = 47.007$; $\bar{B}(CC) = 2.929$; $R(CC) = 1.564$;
$\bar{B}(CH$ of $CH_3) = 3.825$; $R(CH$ in $CH_3) = 1.097$;
$B(CH$ of mid-C$) = 3.789$; $R(CH$ of mid-C$) = 1.100$.

i-Butyl radical: $Q_0{}^0a = 43.165$; $\bar{B}(CC) = 2.919$; $R(CC) = 1.576$;
$\bar{B}(CH) = 3.823$; $R(CH) = 1.097$.

From Table I it is seen that the estimates of the heats of dissociation of these paraffins, derived from bond energies based on the heat of sublimation of carbon L(C) = 5.888 ev check results obtained by other methods.

[1] G. Glockler, J. Chem. Phys. **17**, 748 (1949).